Roles of TRPM8 and TRPM3 in sensory transduction

Quallo, Talisia Esme

Awarding institution:
King's College London

Roles of TRPM8 and TRPM3 in sensory transduction

Thesis submitted for the degree of

Doctor of Philosophy

King's College London

Talisia Esme Quallo

Wolfson Centre for Age-Related Diseases

School of Biomedical Health Sciences

King's College London

2010-2014

Abstract

Primary afferent neurons are equipped with sensory transduction channels which allow the conversion of physical and chemical stimuli into electrical signals. TRP channels are a heterogeneous superfamily of largely non-selective cation channels, which have been implicated in a myriad of sensory transduction mechanisms from the detection of temperature to the sensation of touch. Many TRP channels are key targets for the study of pain physiology due to their polymodal activation and expression in small diameter, unmyelinated sensory fibres. The aim of my project was to examine the roles of TRP channels in sensory transduction mechanisms. Three results chapters focusing on three different TRP channels are presented.

A novel role for the established cold thermosensor, TRPM8, as a cellular osmosensor was determined. The studies presented establish that TRPM8 is activated by increases in extracellular osmolality and is partially activated at normal physiological osmolalities. Cool temperatures increase the sensitivity of TRPM8 to osmotic stimuli and activation of phospholipase enzymes modulates activation of TRPM8 by hyperosmotic solutions. TRPM8 is expressed within sensory neurons where it functions as the chief detector of increased osmolality in addition to a molecular sensor of cold sensations.

The role of TRPM3 as a candidate heat transduction channel is examined. The findings presented demonstrate that recombinantly expressed TRPM3 channels are heat-sensitive and mice lacking functional TRPM3 channels lose a population of heat-activated neurons and have impaired behavioural responses to noxious heat. Moreover, modulation of TRPM3 by intracellular pathways downstream of G-protein coupled receptor activation has been determined. Activation of TRPM3 in sensory neurons is shown to be robustly inhibited by morphine in a predominantly mu-opioid receptor and G_i dependent mechanism. Additionally the role of TRPM3 in several pain states is examined.

Finally, this thesis reports on the characterisation of a medium-throughput CGRP release assay for examining activation of TRPA1 natively expressed on the central terminals of dorsal root ganglion neurons. Activation of TRPA1 expressed on spinal cord synaptosomes by a selection of agonists evokes a concentration-dependent release of CGRP which is inhibited by TRPA1 antagonists. The VGCC subtypes important for TRPA1 and depolarisation-induced CGRP release are examined.

Acknowledgements

I would like to thank Stuart, my primary supervisor for offering me this PhD studentship four years ago and for being such a consistently supportive and encouraging supervisor. I have enjoyed being part of the Bevan lab so much and feel very lucky to have been a member of such a great research team. I would also like to thank David for being an incredible mentor and for always being there to answer my many, many questions. It has been so reassuring to have such expert guidance on tap at all times! I would also like to thank Clive, firstly for his help with behavioural techniques and dissections and secondly for being great company and a fountain of knowledge! I would also like to thank Adrian and Lisa for their help and guidance during my time spent at Lilly.

I would like to thank my good friend and fellow lab member, Nisha, for her ability to instil calm and for all of her help both inside and outside of the lab. Thank you for brightening up long lab days and for your unrelenting kindness. I am not sure whether I could have done it without all of your pep talks! I would like to thank Liz, Jack, Julie, Chancie, Emma, Byron and Dave for welcoming me into the Wolfson CARD and for all of those much needed dancing sessions! I would also like to thank Clare and Ed for the essential office tea and biscuit breaks, and discussions on important matters, like the bizarre television programmes of our childhoods. Clare, I can't believe our four years together has flown by so quickly. Best of luck in your new job, I can't wait to hear all about it!

I would like to thank all of my friends for keeping me sane over the last four years; I couldn't have done it without you all. I would like to thank my Mum, Dad and sister, Marsha, for their unwavering encouragement and love. I certainly wouldn't be where I am now without it. Lastly, I would like to thank Neil, for being my best friend and for putting up with me for so long.

Table of Contents

Table of Figures

Table of Tables

Abbreviations and Acronyms

1-(6-((17β-3-methoxyestra-1,3,5(10)-trien-17-yl)amino)hexyl)-1*H*-pyrrole-2,5-dione (U73122)

15-deoxy-Δ12,14-prostaglandin J2 (15d-PGJ2)

2,4,6-trimethyl-N-(meta-3-trifluoromethyl-phenyl)-benzenesulfonamide (*m*-3M3FBS)

3'-5'-cyclic adenosine monophosphate (cAMP)

3-isobutyl-1-methylxanthine (IBMX)

4-Hydroxynonenal (4-HNE)

5-hydroxytryptamine (5-HT)

Adenosine triphosphate (ATP)

Allyl-isothiocyanate (AITC)

Amino (N)

Anoctamin 1 (ANO1)

Bovine adrenal medulla peptide 8–22 (BAM8–22)

Bromoenol lactone (BEL)

Ca^{2+} activated chloride channel (CaCC)

Calcitonin gene related peptide (CGRP)

Cannabinoid receptor type 1 (CB1)

Carboxy (C)

Chinese hamster ovary (CHO)

D-erythro-sphingosine (DeSPH)

Diacyl glycerol (DAG)

dihydro-D-erythro-sphingosine (DHS)

Diphtheria toxin (DTx)

Dorsal root ganglion (DRG)

Enzyme-linked immunosorbent assay (ELISA)

G protein coupled receptor (GPCR)

Glyceraldehyde-3-phosphate dehydrogenase (GAPDH)

Green fluorescent protein (GFP)

HEPES-buffered Tyrode's solution (HEPES)

Human embryonic kidney (HEK)

Inositol 1,4,5-trisphosphate (IP_3)

Interleukin-6 (IL-6)

Magnocellular neurosecretory cells (MNCs)

Mas-related G protein coupled receptor (Mrgpr)

Miniature excitatory postsynaptic current (mEPSC)

N-(4-*tert*-butylphenyl)-4-(3-chloropyridin-2-yl)piperazine-1-carboxamide (BCTC)

N-(p-amylcinnamoyl) anthranilic acid (ACA)

N,N-dimethyl-D-erythro-sphingosine (DMS)

N-methyl-D-aspartate (NMDA)

Organum vasculosum lamina terminalis (OVLT)

4-Oxo-2-nonenal (4-ONE)

Pertussis toxin (PTX)

Phorbol 12,13-dibutyrate (PDBu)

Phorbol 12-myristate 13-acetate (PMA)

Phosphatidylinositol 4,5-bisphosphate (PIP_2)

Pregnenolone sulphate (PS)

Proteinase-activated receptor (PAR)

Ser-Leu-Ile-Gly-Arg-Leu (SLIGRL)

Small interfering RNA (siRNA)

Substance P (SP)

Supraoptic nucleus (SON)

Δ^9-Tetrahydrocannabinol (THC)

Trigeminal ganglion (TG)

Voltage-gated calcium channel (VGCC)

α-Amino-3-hydroxy-5-methyl-4-isoxazolepropionic acid (AMPA)

γ-Aminobutyric acid (GABA)

Chapter 1. General introduction

1.1 Introduction to sensation

The ability to sense and respond to stimuli present within the local environment is crucial for organism survival. Humans are thought to have five traditional exteroceptive senses which allow them to perceive their outside surroundings. These five senses were first defined by Aristotle in *De Anima*, book II, and include the senses of sight, hearing, smell, taste and touch (Damann et al., 2008). In addition to sensing the outside world using exteroceptive senses, humans are also able to perceive sensations which arise internally through interoceptive senses.

1.2 The somatosensory nervous system

Sensory nerves continuously survey the internal and external environments and convey a plethora of sensory information to the central nervous system (CNS) concerning multiple sensory modalities. Mechanical sensations such as touch, pressure and vibration, in addition to the sensations of temperature and pain are processed by the somatosensory nervous system.

Anatomically, the somatosensory nervous system consists of a pathway of three neurons. The first order neuron or primary afferent neuron innervates target organs in the periphery. The second order neuron is located within the spinal cord or brainstem and relays information to a third order neuron within the brain. The dorsal column-medial lemniscal pathway and the spinothalamic tract are distinct neuronal pathways which carry information relating to innocuous mechanical sensation and temperature/pain, respectively.

1.3 The primary afferent neuron

Primary afferent neurons of the somatosensory system are pseudounipolar and are composed of two axonal branches (see Figure 1-1), a peripheral branch which provides innervation of target tissues and a central branch which terminates onto second order neurons located within the dorsal horn of the spinal cord or the sensory nucleus in the brain (Mosso and Kruger, 1973; Wall, 1967). The cell bodies of primary afferent neurons which carry information from the body are contained within the dorsal root ganglia (DRG). In contrast, the cell bodies of sensory neurons carrying information from the face, head and neck regions are contained within the trigeminal ganglia (TG).

1.3.1 Sensory nerve modalities

The nineteenth century Scottish physician, Charles Bell (1774-1842), was one of the first to convey the idea that sensory nerves were modality-specific. This concept was shared by the German physiologist Johannes Müller (1801-1858) who formulated the 'law of specific nerve energies' which stated that the perception of a sense was reliant upon the pathway which carried it and not the stimulus which evoked it (Norrsell et al., 1999).

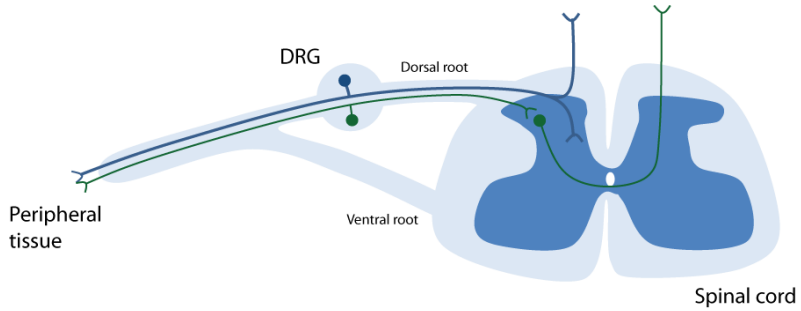

Figure 1-1 Primary afferent nerves of the somatosensory system

Primary afferent nerves which have their cell bodies in the DRG terminate onto second order neurons in the dorsal horn of the spinal cord. These spinal neurons carry sensory information to third order neurons in the brain, Adapted from (Mantyh, 2006).

Consistent with this concept, three researchers, Magnus Blix, Alfred Goldscheider and Henry Donaldson independently published papers in the early 1880's which detailed the existence of distinct cutaneous spots which were selective for specific sensory modalities i.e. cool, warm, touch and pain (Norrsell et al., 1999). These findings were supported by the work of Austrian-German physiologist Max von Frey (1852-1932), who studied cutaneous sensation in detail and confirmed the existence of punctate cold, warm, tactile and pain spots on the skin (Kruger, 1996). It is now known that different primary afferent neurons possess sensitivity to one or more specific sensory modalities. Nerve fibres are often classified according to the sensory modalities that they transduce and can be broadly categorised as mechanoreceptors, thermoreceptors and nociceptors.

1.3.2 Primary afferent nerve fibre types

Sensory nerve fibres which contribute to different sensations can be categorised according to their diameter size and myelination characteristics (see Figure 1-2). Aα-fibres are very large diameter (15-20mm), thickly-myelinated neurons which are responsible for signalling proprioceptive information. Aβ-fibres are large-diameter (5-15µm), myelinated fibres

which largely signal information about innocuous (harmless/non-painful) mechanical stimuli and have fast conduction velocities of ~50 m/s (Squire et al., 2002).

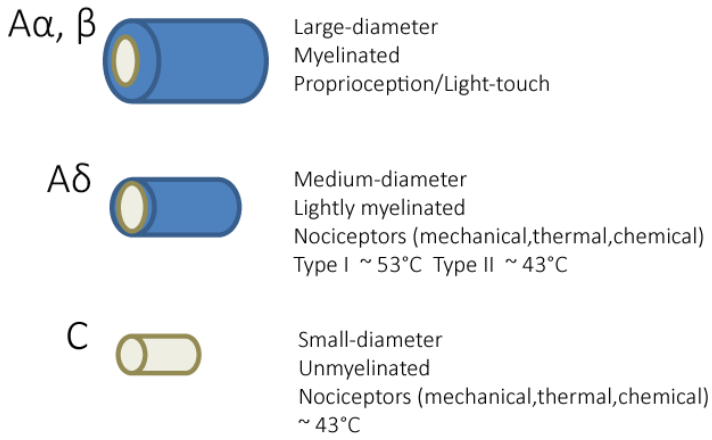

Figure 1-2 Primary afferent nerve fibre types

Diagram illustrating the properties of different classes of primary afferent nerve fibres. Approximate temperature thresholds are listed for heat-sensitive nerve fibres. Adapted from (Julius and Basbaum, 2001).

In contrast to Aβ-fibres, Aδ-fibres are thinly myelinated, medium-diameter (1-5µm) neurons. They have slower conduction velocities than Aβ-fibres and are involved in thermosensing and nociception. This class of fibres can be further divided into two sub-populations, Type I and Type II, based on their heat sensitivity. Type I fibres have high heat thresholds whilst Type II Aδ-fibres have comparatively lower thresholds for heat activation (Basbaum et al., 2009; Dubin and Patapoutian, 2010; Squire et al., 2002).

C-fibres are very small diameter (<1µm) fibres and in contrast to A-fibres, are completely unmyelinated. C-fibres have very slow conduction velocities and similar to Aδ-fibres these neurons are principally involved in the detection of temperature and pain (Basbaum et al., 2009; Squire et al., 2002). The majority of C-fibres are sensitive to mechanical and heat stimuli (CMH), or mechanical and cold stimuli (CMC) or mechanical, cold and heat stimuli (CMHC). Interestingly, a population of C-fibres are insensitive to both heat and mechanical stimuli under physiological conditions but gain sensitivity to these stimuli following inflammatory sensitisation (Dubin and Patapoutian, 2010). A population of C-fibres has also been identified which responds to innocuous light touch stimuli (Olausson et al., 2008).

1.3.3 Nociceptive nerve fibres

Primary afferent neurons which are selectively gated by noxious (painful) stimuli are referred to as 'nociceptors'. This term was coined by the English neurophysiologist, Charles Sherrington (1857-1952) in 1906 (Woolf and Ma, 2007). Evidence of peripheral nerve fibres which are selectively activated by high threshold or 'noxious' stimuli was presented in papers by Edward Perl and colleagues in the late 1960s and early 1970s. Perl *et al* recorded the activities of cutaneous nerve fibres in cats and primates and identified nerves which were activated by noxious stimuli but showed little or no activity to innocuous stimuli (Bessou and Perl, 1969; Burgess and Perl, 1967; Perl, 1968).

Previous to Perl's research, the Austrian-German physiologist Max Von Frey (1852-1932) had sought to associate sensory modalities with different classes of nerve endings by comparing the numbers of specific modality spots present within a cutaneous area with the numbers of different categories of nerve endings (Kruger, 1996). On the basis of these observations von Frey suggested that the sensation of pain was associated with unencapsulated free nerve endings (Norrsell et al., 1999). Charles Sherrington (1857-1952), concurred with von Frey's observation. Sherrington reported from his own research that areas where stimulation lead only to sensations of pain were innervated by free nerve endings which were either unmyelinated or thinly myelinated (Kruger, 1996). The characteristics of nociceptors are now well documented (Basbaum et al., 2009; Woolf and Ma, 2007). Nociceptors are composed of C and Aδ primary afferent nerve fibres which innervate peripheral tissues as free nerve endings.

Noxious stimulation in humans elicits two sensations of pain, the first a sharp, rapid pain and the second a delayed, longer lasting, dull pain (Julius and Basbaum, 2001). It is widely assumed that the difference in conduction velocities between Aδ (~6-25 m s^{-1}) and C fibres (~ 1 m s^{-1}) accounts for these two distinct pain sensations (see Figure 1-3).

1.3.3.1 Neurochemical characterisation of nociceptors

Unmyelinated, nociceptive, C-fibres can be divided into two neurochemical classes based on their neuropeptide content: peptidergic and non-peptidergic nociceptors (Basbaum et al., 2009; Woolf and Ma, 2007). Peptidergic nociceptors can be distinguished from the non-peptidergic population by their expression of the peptide neurotransmitters substance P (SP) and calcitonin-gene related peptide (CGRP). The non-peptidergic nociceptors are characterised by an ability to bind isolectin B4 (IB4) and have been found to express

receptors belonging to the Mrg family of G protein coupled receptors (Dong et al., 2001; Snider and McMahon, 1998).

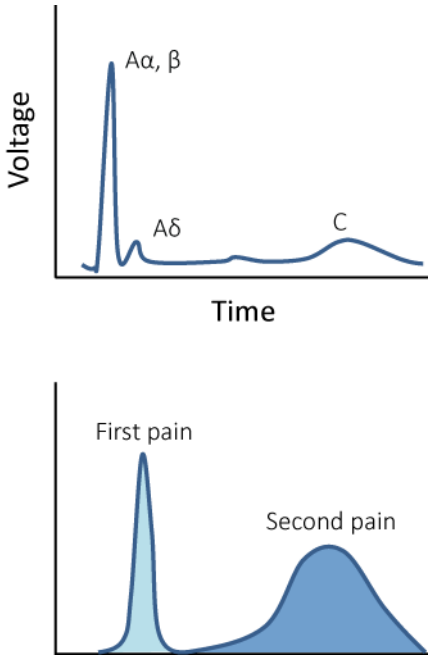

Figure 1-3 Pain sensations associated with different nociceptor fibre types

The sharp, first pain elicited by noxious stimuli can be attributed to activation of medium-diameter, lightly myelinated Aδ-fibres and the activation of the more slowly-conducting, small-diameter, unmyelinated C-fibres is responsible for the second, dull, aching pain. Activation of large-diameter, myelinated, fast-conducting Aα and Aβ fibres does not evoke painful sensations. Adapted from (Julius and Basbaum, 2001).

All embryonic nociceptive neurons express the TrkA receptor for nerve growth factor (NGF), however, studies have shown that in early postnatal life a population of nociceptive nerve fibres stops expressing TrkA and starts to express a component of the glial cell line-derived neurotrophic factor (GDNF) receptor, RET. It is these RET-expressing fibres which become the non-peptidergic population of nociceptors (Bennett et al., 1996; Molliver et al., 1997; Snider and McMahon, 1998). The peptidergic nociceptor sub-population is formed from the remaining nerve fibres which continue to express the TrkA NGF receptor (Snider and McMahon, 1998).

1.3.4 Central projections of primary afferent neurons

The central terminals of primary afferent nerve fibres (from the body) innervate the dorsal horn of the spinal cord (Basbaum et al., 2009). The different categories of nerve fibre types discussed earlier, project to different locations within the dorsal horn (see Figure 1-4). The large, myelinated Aβ fibres terminate deep within the dorsal horn (laminae III-V) whereas,

the small-diameter, nociceptive C -fibres, terminate within the superficial layers of the dorsal horn (laminae I and II). The medium diameter, nociceptive, Aδ-fibres terminate within superficial laminae I and deep laminae V (Basbaum et al., 2009).

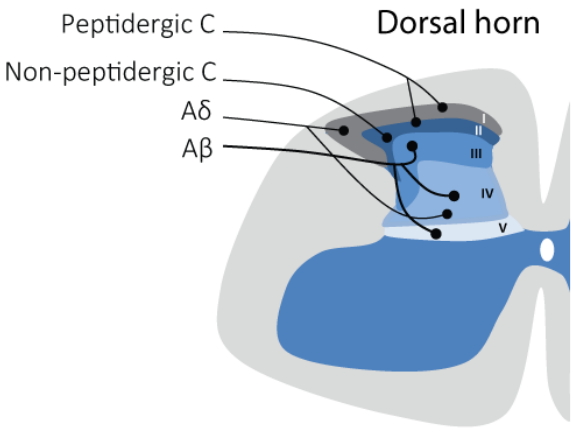

Figure 1-4 Central projection patterns of primary afferent fibres

Different classes of primary afferent neurons project to distinct areas of the dorsal horn. Nociceptive nerve-fibres (Aδ- and C-fibres) terminate within the superficial layers (lamina I-II) of the dorsal horn of the spinal cord. In contrast nerve-fibres carrying information about innocuous touch (Aβ-fibres) terminate deeper within the dorsal horn (lamina III-IV).

Projection patterns of C-fibre nociceptor subpopulations have been even further dissected; peptidergic, TrkA-expressing nerve fibres appear to mostly terminate in lamina I and the outer layer of lamina II, in contrast, the IB4-binding nociceptor population project to the inner layer of lamina II (Snider and McMahon, 1998).

1.4 TRP Channels

Primary afferent neurons are equipped with sensory transduction channels which allow the conversion of physical and chemical stimuli into electrical signals. Over the past two decades, extensive research into the transient receptor potential (TRP) family of ion channels has revealed a role for TRP channels in the transduction of a diverse range of stimuli (Damann et al., 2008; Eijkelkamp et al., 2013; Sexton et al., 2014; Vriens et al., 2014a).

TRP channels are a heterogeneous superfamily of largely non-selective cation channels, members have been found in both invertebrate and vertebrate animal species, and have even been found in yeast (Nilius and Owsianik, 2011).

1.4.1 Discovery

The first TRP channel was discovered through the finding of a mutation in the visual system of the fruit fly, *Drosophila melanogaster* (Cosens and Manning, 1969). In this system, rhodopsin is coupled to phospholipase C (PLC) activation which, in turn, opens cationic channels to evoke a depolarising membrane current (Pedersen et al., 2005). In contrast to the wildtype, sustained receptor potential, the *Drosophila* TRP mutant exhibited a transient response to a continuous light stimulus (Cosens and Manning, 1969). The gene responsible for this transient receptor potential was accordingly named the *trp* gene and was cloned in 1989 (Montell and Rubin, 1989).

1.4.2 Sub-families

Members of the TRP channel family can be separated into seven sub-families (TRPC, TRPV, TRPM, TRPA, TRPML, TRPP and TRPN) based on protein homology (Nilius and Owsianik, 2011). Members of the TRPN sub-family are not present in mammals and have only been identified in lower vertebrates and invertebrates. At present, the mammalian TRP channel family consists of 28 members belonging to six TRP sub-families, 27 of which are expressed in humans (as human TRPC2 has been identified as a pseudogene).

1.4.3 Structure

TRP channels assemble into tetramers to form an ion permeable pore. Some studies have reported the formation of functional heteromultimeric TRP channels however most TRP channels are thought to function as homotetramers (Nilius and Owsianik, 2011). Each TRP channel subunit or monomer is characterised by six transmembrane (TM) domains, intracellular amino (N) and carboxy (C) termini, and a pore region which is located between TM5 and TM6 (see Figure 1-5).

The intracellular termini of TRP channels contain a wide range of domains and can vary in length (Hellmich and Gaudet, 2014; Nilius and Owsianik, 2011). Notably, some members of the TRPM sub-family, namely TRPM2, TRPM6 and TRPM7, feature enzyme domains within their intracellular C-termini (Perraud et al., 2001; Runnels et al., 2001; Schlingmann et al., 2002). Another structural characteristic of many TRP channels is the presence of ankyrin repeat domains (ARDs). Ankyrin repeats are motifs of ~33-34 amino acids which form two α-helices connected to a β-hairpin loop (Hellmich and Gaudet, 2014). ARDs have been identified in the intracellular N-termini of channels belonging to the TRPA, TRPV, TRPC and TRPN sub-families. The number of repeats present within a domain vary, ranging from 29

predicted repeats in TRPNs, to 17 in TRPAs, 6 in TRPVs and 4 in TRPCs (Hellmich and Gaudet, 2014). In the context of TRPV channels, ARDs have been suggested to be important for channel assembly and appear to exert an inhibitory role on channel sensitivity (Hellmich and Gaudet, 2014).

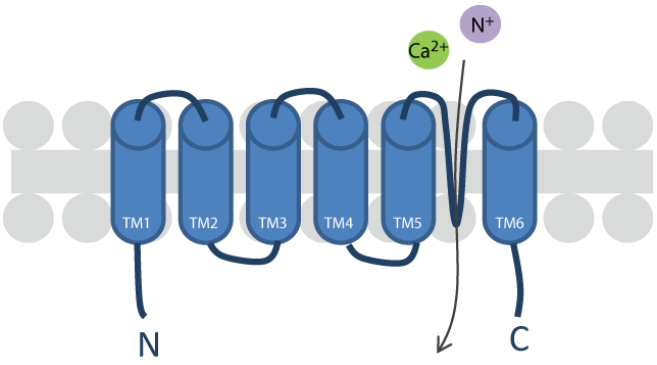

Figure 1-5 TRP channel structure

TRP channel subunits feature six membrane-spanning domains (TM1-6) with a pore region located between the fifth and sixth transmembrane domains. The majority of TRP channels are non-selective cation channels and are permeable to both monovalent and divalent cations.

Many TRP channels also contain motifs which are important for regulation of channel function; these include, binding domains for the calmodulin (CaM) protein and sites for phosphorylation and lipid interaction (Nilius and Owsianik, 2011). Members of some TRP subfamilies also contain coiled-coil domains which have been demonstrated to be important for channel assembly (Hellmich and Gaudet, 2014; Tsuruda et al., 2006).

1.4.4 Mammalian TRP channels

1.4.4.1 TRPC

Members of the TRPC or 'canonical' subfamily of TRP channels are the closest mammalian relatives to the *D.melanogaster* TRP channel. TRPC1 was the first identified mammalian TRP channel and was cloned in 1995 (Petersen et al., 1995; Wes et al., 1995). There are seven mammalian TRPC channels in total and these can be organised into four subsets based on function and sequence homology (see Figure 1-6): TRPC1, TRPC2, TRPC3/6/7 and TRPC4/5 (Pedersen et al., 2005). Notably, TRPC channels can form heteromultimeric channels both within and between subsets which possess distinct properties that differ from those of homotetramers (Pedersen et al., 2005). In general, TRPC channel activity is stimulated by receptors which are coupled to PLC activation. TRPC1 is widely expressed and is reported to have important functions within the brain (Clapham, 2003). Additionally, it

has also been identified as a mechanosensitive component of the stretch-activated cation channel in vertebrate cells and has been implicated in the transduction of innocuous mechanical stimuli (Garrison et al., 2012; Maroto et al., 2005). As mentioned previously TRPC2 is a pseudogene in humans, however in rats it is important for pheromone detection as well as sexual and social behaviours (Pedersen et al., 2005). TRPC3, 6 and 7 are highly expressed in cardiac and smooth muscle cells and their activity can be increased by DAG (Clapham, 2003). Moreover, TRPC3 and TRPC6 are expressed in a subset of small-diameter sensory neurons where they are thought to function as components of a mechanically-activated complex (Eijkelkamp et al., 2013; Quick et al., 2012). TRPC4 and 5 are both widely expressed. TRPC4 appears to play roles in a wide range of biological processes including axon regeneration and myotube formation (Freichel et al., 2014). TRPC5 is also implicated in a diverse array of biological functions. Interestingly, TRPC5 has been implicated in the transduction of innocuous cold and mechanical/osmotic stimuli (Gomis et al., 2008; Zimmermann et al., 2011).

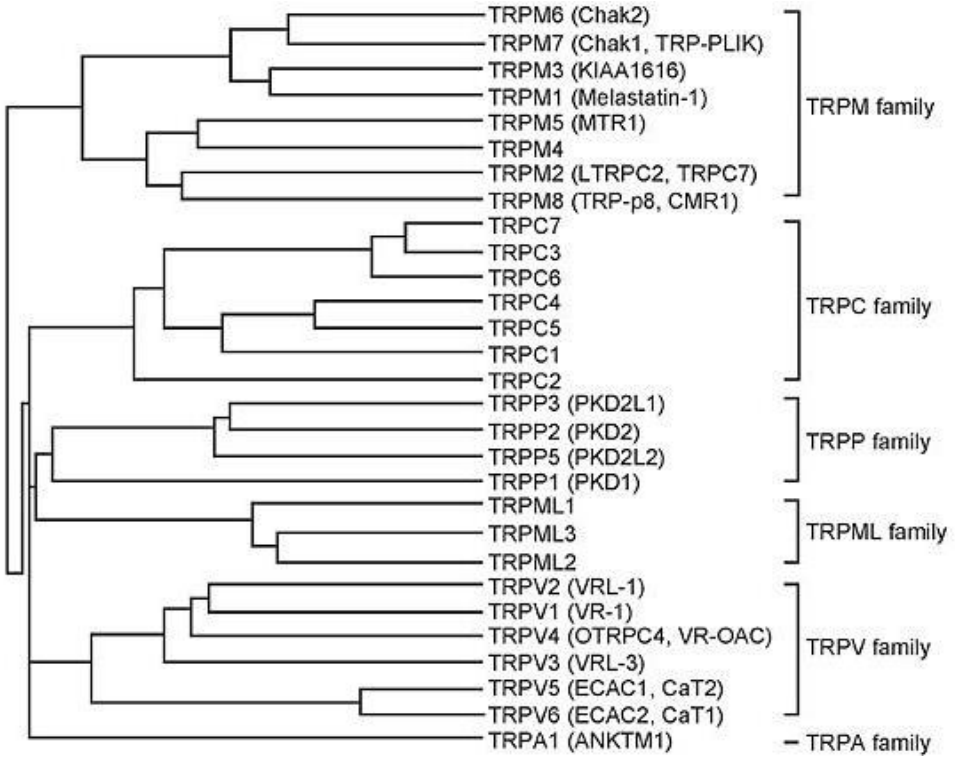

Figure 1-6 Phylogenetic tree of mammalian TRP channels

A phylogenetic tree of the mammalian TRP channel family based on homology. Taken from (Takahashi et al., 2012).

1.4.4.2 TRPV

The TRPV or 'vanilloid' subfamily of TRP channels is named after its founding member, TRPV1, a vanilloid and heat-sensitive channel (Caterina et al., 1997). TRPV1 was cloned in 1997 and has since been found to be important for regulation of body temperature, behavioural responses to acute noxious heat and hyperalgesia following tissue injury (Caterina et al., 2000; Davis et al., 2000; Romanovsky et al., 2009). TRPV1 is expressed in sensory neurons as well as non-neuronal cells and in addition to being activated by vanilloid compounds, TRPV1 is also activated by protons, anandamide and the lipid products, 12- and 15-(S)-HPETE, 5-(S)-HETE, and leukotriene B_4 (for review see Bevan et al., 2014). Many members of the TRPV subfamily have been identified as molecular transducers of thermal stimuli. For example, TRPV2, which is 50% identical to TRPV1, is also expressed in sensory neurons and is activated by painfully hot temperatures with a higher temperature threshold than TRPV1 (Caterina et al., 1999). TRPV2 is also sensitive to hypotonic stimulation and cell stretch, and has been implicated in the hypotonicity-induced responses of mouse vascular myocytes (Muraki et al., 2003). TRPV3 and TRPV4 have been identified as heat-sensitive ion channels which are activated by 'warm' temperatures (Peier et al., 2002a; Smith et al., 2002; Xu et al., 2002). In addition, to being heat-sensitive TRPV4 is also sensitive to decreases in osmolarity and has been implicated in mechanisms controlling water intake (Liedtke and Friedman, 2003; Liedtke et al., 2000, 2003). TRPV5 and TRPV6 are the most Ca^{2+} selective TRP channels and are highly expressed in the kidney and intestine where they play important roles in Ca^{2+} reabsorption (den Dekker et al., 2003). TRPV5 and TRPV6 can form either homotetramers or heteromultimeric channels with each other (Pedersen et al., 2005).

1.4.4.3 TRPM

The TRPM or melastatin subfamily of TRP channels consists of eight identified channels, TRPM1-8, which can be separated into four pairs due to their amino acid identity; TRPM1 and TRPM3, TRPM2 and TRPM8, TRPM4 and TRPM5, and TRPM6 and TRPM7 (Grimm et al., 2003). The first identified member of this subfamily, TRPM1 (or melastatin), is thought to be a tumour suppressor protein, it was found to be poorly expressed in a highly metastatic cell line and highly expressed in weakly metastatic cell line (Duncan et al., 1998). In addition to this role, TRPM1 has also been implicated in the responses of mouse retinal ON-bipolar cells to light (Irie and Furukawa, 2014). The TRPM3 channel shares 57% sequence identity with TRPM1 and is widely expressed, but has not been extensively characterised. Multiple

splice variants for TRPM3 exist, one variant has been shown to be activated by hypotonicity and another has been implicated in noxious heat-sensing (Grimm et al., 2003; Vriens et al., 2011). In addition, TRPM3 is activated by the neurosteroid pregnenolone sulphate, D-erytho-sphingosine and nifedipine (Grimm et al., 2005; Wagner et al., 2008).

Interestingly, the TRPM2 channel contains a Nudix hydrolase domain in its intracellular C-terminal which is able to function as an ADP-ribose pyrophosphatase (Perraud et al., 2001). TRPM2 is activated ADP-ribose and Ca^{2+}, in addition to reactive oxygen and nitrogen species (Faouzi and Penner, 2014). TRPM8 has ~42% sequence identity with TRPM2 and was originally identified in prostate tissue (Pedersen et al., 2005; Tsavaler et al., 2001). Expression of TRPM8 has been shown to be upregulated in tumours (Almaraz et al., 2014). Notably, TRPM8 is expressed in a subpopulation of small diameter sensory neurons which are sensitive to cold and is implicated in mammalian cold-sensing mechanisms (Bautista et al., 2007; Colburn et al., 2007; Dhaka et al., 2007; McKemy et al., 2002; Peier et al., 2002b). Activators of TRPM8 include: cool temperatures, the naturally-occurring cooling compound from the mint plant, menthol, and the synthetic cooling agent, icilin (McKemy et al., 2002; Peier et al., 2002b).

In contrast to other members of the TRP family, TRPM4 and TRPM5 are selective for monovalent ions and are directly gated by Ca^{2+} (Guinamard et al., 2011; Pedersen et al., 2005). TRPM4 is widely expressed and has been implicated in pressure-induced vascular smooth muscle depolarisation, insulin secretion from pancreatic β-cells and mechanisms of cardiac hypertrophy (Mathar et al., 2014). In contrast, TRPM5 functions within taste cells to mediate bitter, sweet and umami taste sensations (Liman, 2014; Zhang et al., 2003). Activation of TRPM5 in taste cells occurs downstream of GPCR-mediated activation of PLCβ2. The final pair of TRPM members, TRPM6 and TRPM7, share 50% sequence identity and both contain an atypical α-kinase domain in their intracellular C-termini (Runnels et al., 2001; Schlingmann et al., 2002). TRPM6 is highly expressed in epithelial cells of the kidney and intestine, whilst TRPM7 appears to be ubiquitously expressed. Both channels are important for Mg^{+} homeostasis (Chubanov and Gudermann, 2014; Fleig and Chubanov, 2014).

1.4.4.4 TRPA

The TRPA1 channel is the sole member of the mammalian TRPA family, it is expressed in a subpopulation of small to medium diameter sensory neurons and can also been found in

non-neuronal cells such as epithelial cells, enterochromaffin cells and pancreatic β cells (Story et al., 2003a; Zygmunt and Högestätt, 2014). TRPA1 is activated by pungent food compounds such as cinnamaldehyde (cinnamon), allyl isothiocyanate (mustard oil), and allicin (garlic). It can also be activated by environmental irritants such as acrolein and products of oxidative stress (Andersson et al., 2008; Bautista et al., 2006). TRPA1 has also been reported to be activated by cold temperatures and has been implicated in the transduction of noxious cold (Fajardo et al., 2008a; Karashima et al., 2009; Kwan et al., 2006) however activation of TRPA1 by cold is controversial (Bautista et al., 2006; Jordt et al., 2004). Moreover, various reports have suggested a role for TRPA1 in mechanotransduction (Brierley et al., 2011; Corey et al., 2004; Kwan et al., 2006, 2009).

1.4.4.5 TRPP + TRPML

The TRPP or 'polycystin' subfamily of TRP channels consists of three members: TRPP2, TRPP3 and TRPP5. TRPP channels are thought to form functional complexes with members of the polycystin-1 family, which are larger 11 transmembrane domain (TMD) proteins (Semmo et al., 2014). Mutations in the TRPP2 channel gene result in polycystic kidney disease a form of inherited kidney failure (Nilius and Owsianik, 2011). TRPP2 is also required for vertebrate left-right asymmetry (Semmo et al., 2014). Heteromeric complexes of TRPP3 and a PKD1L3 (a member of the polycystin-1 family) have been implicated in sour taste transduction (Semmo et al., 2014).

The TRPML or 'mucolipin' subfamily of TRP channels also has three members: TRPML1-3 (Nilius and Owsianik, 2011). A mutation in the founding member of this family, TRPML1, causes the lysosomal storage disease, mucolipidosis type IV (MLIV). TRPML1 is predominantly expressed on late endosomes/lysosomes where it is thought to mediate divalent cation release into the cytosol of cells (Wang et al., 2014). Similar to TRPML1, TRPML2 and TRPML3 are also localised to the membranes of endosomes and lysosomes (García-Añoveros and Wiwatpanit, 2014; Grimm et al., 2014).

1.5 The molecular basis of sensation

Primary afferent neurons are sensitive to changes in temperature, mechanical perturbations, fluctuations in extracellular osmolarity and exposure to certain chemicals. The sensitivity of individual nerve fibres to these stimuli is dependent on the selection of sensory ion channels and receptors expressed at the peripheral nerve terminal.

1.5.1 Thermosensation

1.5.1.1 Heat

Sensory neurons respond to both innocuous warmth and noxious heat, with a distinct threshold for the latter which lies around 43°C (Basbaum et al., 2009). The search for the molecular receptor for capsaicin, the pungent ingredient found in chilli peppers which was known to cause activation of nociceptive sensory neurons and a sensation of 'burning pain', lead to the discovery of TRPV1 (Caterina et al., 1997; Szolcsányi, 1977). TRPV1, in addition to being the receptor for capsaicin, was also shown to be a thermosensitive channel activated by 'hot' temperatures (Caterina et al., 1997, 2000). Interestingly, the temperature activation threshold for TRPV1 (~43°C) mirrored the temperature at which heat becomes painful in humans (Basbaum et al., 2009; Caterina et al., 2000). This finding combined with the expression of TRPV1 in the majority of heat-sensitive sensory neurons, strongly suggested a role for TRPV1 as the molecular sensor for noxious heat (Basbaum et al., 2009; Caterina et al., 1997, 2000). However, studies examining mice lacking functional TRPV1 channels (*Trpv1*$^{-/-}$) reported limited effects on acute noxious heat sensitivity *in vivo*. In one study *Trpv1*$^{-/-}$ mice displayed longer latencies to paw and tail withdrawal from a plate or water bath set at noxious high temperatures (>50°C) respectively, but showed little to no difference in latency to paw withdrawal from radiant hot temperatures, suggesting that mice without TRPV1 channels are still sensitive to noxious heat (Caterina et al., 2000). Another study reported that there were no significant differences in the paw withdrawal responses of *Trpv1*$^{+/+}$, *Trpv1*$^{-/+}$ and *Trpv1*$^{-/-}$ mice to a plate heated to noxious temperatures or radiant noxious heat (Davis et al., 2000). Interestingly, a study which examined mice which had been given a high dose of intrathecal capsaicin to ablate TRPV1-expressing central nerve terminals, did report profound deficits in noxious heat sensing to both hot-plate and radiant heat tests, suggesting a requirement of TRPV1-expressing nociceptors for noxious heat sensitivity (Cavanaugh et al., 2009). These studies indicate that whilst TRPV1 is likely to play a role in sensing noxious heat, other sensors of acute noxious heat are still to be identified.

Other ion channels belonging to the TRPV subfamily have since been implicated as potential heat transducers which function alongside TRPV1 (see Figure 1-7). TRPV2, a capsaicin-insensitive TRPV1 homologue expressed in medium to large diameter sensory neurons, is activated by hot temperatures with a temperature activation threshold of ~52°C (Caterina et al., 1999). However, studies examining the acute nociceptive responses of

Trpv2$^{-/-}$ mice revealed that mice lacking functional TRPV2 channels display normal responses to acute noxious heat even above temperatures required to activate the channel, suggesting that TRPV2 is not essential for sensing noxious hot temperatures (Park et al., 2011). Further experiments demonstrated that the lack of effect from TRPV2 deletion was not due to compensation by TRPV1, as double TRPV1/TRPV2 knockouts did not differ in their responses to acute noxious heat from TRPV1 null mice (Park et al., 2011). These findings were consistent with an earlier study, which reported that 11 out of 12 heat-sensitive *Trpv1*$^{-/-}$ C-fibres sampled did not express TRPV2 (Woodbury et al., 2004).

TRPV3 and TRPV4 have been identified as sensors of 'warm' innocuous temperatures. Temperature thresholds between 31-39°C have been reported for TRPV3 (Peier et al., 2002a; Smith et al., 2002; Xu et al., 2002). TRPV3 is predominantly expressed by keratinocytes, however some studies have reported expression by sensory nerve ganglia with an overlap with TRPV1 expression (Chung et al., 2004; Peier et al., 2002a; Smith et al., 2002; Xu et al., 2002). Reports have shown that mice lacking functional TRPV3 channels display a reduced preference for innocuous warm temperatures on the two plate preference test compared to their wildtype counterparts (Moqrich et al., 2005). Although heat-evoked TRPV3 currents occur at innocuous temperatures, currents continue to increase when temperatures are raised to within the noxious range (Peier et al., 2002a). Consistent with this finding, *Trpv3*$^{-/-}$ mice were shown in one study, to display impaired behavioural responses to acute nociceptive thermal stimuli. *Trpv3*$^{-/-}$ mice displayed increased latencies to tail flick-evoked by a 50°C and 52°C water bath, and to paw withdrawal from a 55°C hot plate (Moqrich et al., 2005). However, a study examining *Trpv3*$^{-/-}$ mice on C57Bl/6 and 129S6 backgrounds (in contrast to the 129S6/C57BL6 mixed background of mice studied in the report by Moqrich and colleagues) has disputed the importance of TRPV3 for heat sensation, reporting no significant changes in behaviour in thermal preference or nociceptive heat tests between *Trpv3*$^{-/-}$ and wildtype mice (Huang et al., 2011).

TRPV4 is also activated by ambient temperatures with a temperature activation threshold of 25-34°C (Güler et al., 2002; Watanabe et al., 2002). The TRPV4 channel is sensitive to hypotonic stimuli and, consistent with this finding, hypoosmotic solutions potentiate heat-evoked responses whilst hyperosmotic solutions inhibit them (Güler et al., 2002). Similar to TRPV3, TRPV4 channels are expressed by skin keratinocytes, where they are postulated to be responsible for the majority of heat-evoked currents (Chung et al., 2004). Primary

mouse keratinocytes exhibit two currents in response to innocuous warming, one which is weakly rectifying and desensitises, and another which is outwardly rectifying and sensitises (Chung et al., 2004). The former is attributed to TRPV4 and is the current most commonly observed in keratinocytes: it is diminished in *Trpv4*$^{-/-}$ keratinocytes and is re-established by transfection of wildtype TRPV4 (Chung et al., 2004). These results suggest that TRPV4 is required for a large element of heat sensing in keratinocytes, however examination of *Trpv4*$^{-/-}$ mice determined no differences in their responses to acute nociceptive thermal stimuli compared to the responses of wildtype mice, suggesting that TRPV4 is not required for noxious heat sensing (Liedtke et al., 2003). Furthermore, a study examining TRPV3/TRPV4 double knockouts reported no impairments to noxious or innocuous heat sensing and demonstrated that this was not due to compensatory heat-sensing by TRPV1 channels masking a deficit in the double knockout mice, suggesting that neither TRPV3 channels nor TRPV4 channels are required for heat sensing (Huang et al., 2011).

Recently a steroid-sensitive member of the TRP melastatin sub-family, TRPM3, has been implicated in the mechanisms of noxious heat detection (Vriens et al., 2011), see Chapter 4 for a full discussion.

Ion channels which do not belong to the TRP channel family have also been implicated in heat-sensing mechanisms. A Ca^{2+} activated chloride channel (CaCC), named anoctamin 1 (ANO1), has been reported to be activated by heat with a threshold temperature of ~44°C (Cho et al., 2012). ANO1 is expressed within the nociceptive subpopulation of sensory neurons with a high level of co-expression with TRPV1 (~80%). Co-treatment of WT DRG neurons with a TRPV1 antagonist and the CaCC blocker, mefloquine, was reported to abolish heat-evoked currents and mefloquine was reported to block heat responses in *Trpv1*$^{-/-}$ neurons (Cho et al., 2012). Consistent with these findings, wildtype and *Trpv1*$^{-/-}$ mice intrathecally injected with small interfering RNA (siRNA) specific for *Ano1* displayed significantly increased tail withdrawal latencies from water heated to noxious temperatures (50-54°C) and paw withdrawal latencies from radiant noxious heat in comparison to mice injected with scrambled siRNA. Similar impairments in noxious heat sensing were reported for ANO1 conditional knockout mice (CKO) where ANO1 expression was knocked down in sensory neurons of the DRG (Cho et al., 2012). These findings implicate ANO1 as a candidate heat sensor in nociceptive sensory neurons.

1.5.1.2 Cold

In humans a sensation of innocuous cooling, which is distinct from cold pain, can be evoked by cool temperatures which are just 1°C lower than basal skin temperature (Erpelding et al., 2012). Cold temperatures are purported to feel painful when they fall below 15°C, however, a wide-range of cold temperatures (0-28°C) can be perceived as painful sensations (Erpelding et al., 2012; McKemy, 2013).

Primary afferent nerve fibres which have their cell bodies in the DRG and TG, respond to cooling within both the innocuous and noxious range. They are typically Aδ or C-fibres and two populations with differing thresholds exist. One population of cold-sensitive nerve fibres is activated by temperatures within the innocuous range (30-15°C). This sub-group of cool-sensitive neurons tends to display spontaneous activity at physiological skin temperature which is increased upon cooling and decreased upon warming. The other population of cold-sensitive nerve fibres begins to fire at noxious cold temperatures (<15°C) and is composed of 'cold nociceptors' which are typically quiescent at normal skin temperature and are only activated when stimulated by noxiously cold temperatures (McKemy, 2013).

Initially, it was theorised that cold sensation was signalled by cold-mediated inhibition of the Na^+/K^+ pump and a resulting depolarisation of the plasma membrane (Pierau et al., 1974). An inhibitor of the sodium-potassium adenosine triphosphatase, oubain, was shown to alter the activity of cold-sensitive nerve fibres (Pierau et al., 1974) however a later study demonstrated that oubain did not evoke depolarisation in the majority of cold-sensitive DRG neurons and, in the small number of neurons where oubain did evoke depolarisation, it was insufficient to trigger action potential firing (Reid and Flonta, 2001a). This later finding demonstrated that inhibition of the Na^+/K^+ pump was not the chief mechanism for cold transduction.

Other background ion channels have also been implicated in cold transduction mechanisms (McKemy, 2013). One study suggested that cold-induced activation of cold-insensitive neurons is prevented by a K^+ current (IK_D) and demonstrated that inhibition of this current by 4-aminopyridine was able to induce cold-sensitivity (Viana et al., 2002). Background K^+ channels belonging to the K_{2P} family, TREK-1 and TRAAK, have also been implicated in the mechanisms of cold sensation (Noël et al., 2009). Deletion of TREK-1 and TRAAK increases the number of cold-sensitive neurons and shifts the temperature threshold of neurons

which normally respond to noxious cold temperatures to higher temperatures, therefore resulting in the activation of cold nociceptors at warmer temperatures (Noël et al., 2009). Consistent with these findings TREK-1 and TRAAK double knockout mice experience cold hypersensitivity (Noël et al., 2009). It is postulated that the opening of both TREK-1 and TRAAK reduces the excitability of the neurons on which they are expressed and when these channels are absent or closed, cold-sensitive neurons become more easily excitable (Noël et al., 2009).

A study by Suto and Gutoh (1999) examining activation of rat DRG neurons by a cool stimulus (20°C) demonstrated that cooling could evoke the influx of calcium ions. The authors of this study demonstrated this process was not secondary to Na^+ mediated depolarisation as removal of external Na^+ had no effect on the response (Suto and Gotoh, 1999). This finding demonstrated the existence of a cold-sensitive channel which allowed the influx of calcium in response to cooling. An overlap between the cold sensitivity of neurons and activation by the naturally-occurring cooling compound from the mint plant, menthol (Reid and Flonta, 2001b), suggested a common transduction process for these stimuli and lead to the discovery of TRPM8, a receptor for menthol and cold and a relative of the noxious heat sensor, TRPV1 (McKemy et al., 2002; Peier et al., 2002b). TRPM8 is expressed in 5-10% of primary afferent neurons of the DRG and at slightly higher levels in the TG and is activated by cooling with a threshold temperature of ~25°C (McKemy et al., 2002; Peier et al., 2002b). Studies examining cold sensation in mice lacking functional TRPM8 channels have shown that dissociated sensory neurons and nerve fibres from *Trpm8*$^{-/-}$ mice lose sensitivity to menthol and cold (Bautista et al., 2007; Colburn et al., 2007). Moreover, *Trpm8*$^{-/-}$ mice have impaired thermal discrimination behaviour in comparison to their wildtype counterparts and display decreased behavioural responses to application of acetone to the paw, which evokes evaporative cooling (Bautista et al., 2007; Colburn et al., 2007; Dhaka et al., 2007).

Although TRPM8 was shown to contribute to the sensation of innocuous cold temperatures, it was difficult to ascertain whether TRPM8 played a role in noxious cold sensing (Sexton et al., 2014). One temperature discrimination study reported that *Trpm8*$^{-/-}$ mice (unlike *Trpm8*$^{+/+}$ mice) did not avoid the cool plates in preference to a plate at an innocuous warm temperature until temperatures of the cold plate dropped below 15°C: at these lower temperatures the mice began to show avoidance behaviour, suggesting that *Trpm8*$^{-/-}$ mice can sense noxious cold temperatures (Bautista et al., 2007). Indeed, the same

study reported that the number of cold-sensitive TG neurons with a temperature activation threshold of 12°C was unchanged in *Trpm8*$^{-/-}$ mice. In addition, early studies reported contradictory data on noxious cold-plate evoked behaviour. One study found that *Trpm8*$^{-/-}$ mice placed on a 0°C cold plate displayed longer latencies to a hind paw response in comparison to wildtype animals (Colburn et al., 2007). In contrast, two other studies showed that hind paw withdrawal latency responses to a 10, 0, -1 and -5°C cold plate did not differ between *Trpm8*$^{-/-}$ and *Trpm8*$^{+/+}$ mice (Bautista et al., 2007; Dhaka et al., 2007). However, a later study by Knowlton and colleagues (2013) examining mice with ablated TRPM8 neurons (DTx-injected *Trpm8*^{DTR} mice/ *ablated*) and *Trpm8*$^{-/-}$ mice, attributed this discrepancy to the huge variability of hind-paw responses in this assay. Knowlton *et al* reported significant increases in the latencies to forepaw responses by *ablated* and *Trpm8*$^{-/-}$ mice, to a 0°C cold plate, in comparison to control mice. The study measured two different forepaw behaviours, forepaw flinching and forepaw licking, which were described by the authors as robust and repeatable (Knowlton et al., 2013). These findings suggest that TRPM8 is also a transducer of noxious cold temperatures although a residual capability for sensing noxious cold is present in *Trpm8*$^{-/-}$ mice.

The sensation of noxious cold has been attributed to activation of TRPA1, a TRP channel expressed in a subpopulation of nociceptive sensory neurons which usually co-express the noxious heat sensor TRPV1 (Story et al., 2003a). Activation of TRPA1 was reported to occur at noxious cold temperatures which were much lower than required for activation of TRPM8, with a threshold temperature of ~17°C (Story et al., 2003a). However, the contribution of TRPA1 to cold sensation is a subject of much debate (Basbaum et al., 2009; McKemy, 2005, 2013; Sexton et al., 2014). TRPA1 has been identified as the receptor for a selection pungent food irritants including cinnamaldehyde, allyl isothiocyanate (AITC) and allicin (Bandell et al., 2004; Bautista et al., 2006; Jordt et al., 2004). One study using AITC as a probe for TRPA1 expressing TG neurons, demonstrated that 96% of AITC-sensitive neurons were insensitive to a noxious cold stimulus (Jordt et al., 2004). Interestingly, the same study demonstrated that cooling (22-6°C) lead to a reduction in the AITC-evoked responses of TRPA1-expressing oocytes. Furthermore, one study examining TRPA1 knockout mice found that the number of neurons responding to a cold stimulus and the amplitudes of cold-evoked responses were unchanged in TG neurons from *Trpa1*$^{-/-}$ mice (Bautista et al., 2006). These findings suggested that TRPA1 is not involved in the mechanisms of noxious cold sensation and is not inherently sensitive to cooling. However, a separate study disputed these findings, demonstrating that there was a significant

reduction in the number of cold-sensitive TG neurons from *Trpa1*$^{-/-}$ mice compared to wildtype mice and a shift in the thresholds of the remaining neurons to higher temperatures (Karashima et al., 2009). Moreover, TRPA1 activity has been demonstrated to be required for the cold-evoked responses of vagal sensory neurons (Fajardo et al., 2008a). The findings of Karashima *et al* (2009) and Fajardo *et al* (2008) implicate TRPA1 channels in cellular cold transduction mechanisms. In contrast to the findings by Jordt and colleagues (2004), one study reported that cold (25-10°C) potentiated AITC-induced currents in TRPA1-expressing HEK293 cells and isolated DRG neurons suggesting that cold could potentiate tonic activation of TRPA1 (del Camino et al., 2010).

The role played by TRPA1 in cold sensation at the behavioural level has also proved difficult to determine. Bautista and colleagues (2006) reported that *Trpa1*$^{-/-}$ animals display normal behavioural responses to noxious cold stimuli (cold-plate tests: latency to hindpaw lift/shivering and acetone-evoked cooling: number of flinches/licks per min) suggesting that mice lacking functional TRPA1 channels retain their ability to sense noxious cold temperatures. However, the findings of a separate study reported that female *Trpa1*$^{-/-}$ mice exhibit reduced responses to a 0°C noxious cold plate (number of paw lifts) and acetone-evoked cooling (number of paw shakes) suggesting that TRPA1 is required in part for sensing intensely cold temperatures (Kwan et al., 2006). Interestingly, male *Trpa1*$^{-/-}$ mice did not display significantly impaired responses compared to their wildtype counterparts ; suggesting that for male mice TRPA1 does not play an important role in noxious cold detection (Kwan et al., 2006). Another study found no difference in the latency to shivering or paw rubbing in response to a 0°C cold plate but did report a difference in nocifensive jumping between *Trpa1*$^{-/-}$ and *Trpa1*$^{+/+}$ mice (Karashima et al., 2009). The authors of this study reported that both male and female *Trpa1*$^{-/-}$ mice jump significantly less when placed on a the noxious cold plate. Moreover, *Trpa1*$^{-/-}$ mice displayed significantly longer latencies to tail withdrawal from a -10°C solution in comparison to wildtype mice (Karashima et al., 2009). A study examining mice with ablated TRPV1-expressing central nerve terminals established that cold-sensitivity was normal in these mice. Ablated mice avoided innocuous cold for a warmer environment and displayed normal responses to a noxious cold plate (Cavanaugh et al., 2009). Due to the fact that TRPA1 expression is restricted to the TRPV1-expressing nerve population (Kobayashi et al., 2005), this data supports the proposition that TRPA1 is not involved in cold transduction mechanisms.

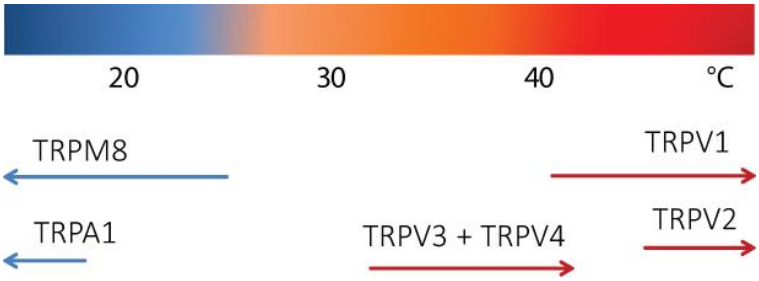

Figure 1-7 Thermosensitive TRP channels

Temperature activation ranges for TRPM8, TRPA1, TRPV1, TRPV2, TRPV3 and TRPV4. Adapted from (Tominaga, 2007).

Interestingly, a member of the TRPC family has also been implicated in cold transduction. TRPC5 was found in one study to be cold-sensitive when expressed in a recombinant cell line, TRPC5 currents increased as temperatures were decreased below 37°C achieving maximum responses at 25°C (Zimmermann et al., 2011). TRPC5-cold activated currents were potentiated by Gq-coupled receptor activation. Despite the ability of TRPC5 channels to confer cold sensitivity to a cell line, animals lacking functional TRPC5 channels did not display deficits in behavioural responses to cool temperatures (Zimmermann et al., 2011). However, TRPC5 may contribute to innocuous cold sensation alongside TRPM8.

1.5.2 Mechanosensation

A diverse array of mechanical sensations are signalled by mechanosensitive nerve fibres which innervate the skin, viscera, tendons, muscles and joints (Delmas et al., 2011).

Mechanosensitive neurons which innervate the skin terminate as encapsulated or free nerve endings (Lewin and Moshourab, 2004). Innocuous mechanical stimuli such as vibration and stretch are detected by encapsulated Aβ nerve-endings (Meissner, Pacinian and Ruffini corpuscles) which are present in dermis of the skin. Additionally, innocuous mechanical stimuli are detected by Merkel cell-neurite complexes coupled to Aβ fibres and low-threshold C-fibre free nerve-endings. Moreover, light brush mechanical sensations are transduced by Aβ and Aδ fibres which are connected to guard hairs (G-hair follicle) and down hairs (D-hair follicle), respectively (Delmas et al., 2011). Noxious mechanical stimuli are transduced by free nerve endings belonging to the C and Aδ neuronal subtypes (Basbaum et al., 2009).

Little is known about mammalian mechanotransducer channels, on which the entire process of mechanotransduction is dependent. It is thought that mechanical force causes

the opening of excitatory, cation permeable channels which leads to the depolarisation of the nerve terminal and generation of an action potential (Delmas et al., 2011).

Candidate mechanotransduction channels include members of the acid sensing ion channel (ASIC) sub-family of degenerin–epithelial Na^+ channels (DEG/ENaCs). ASICs were first implicated in the transduction of mechanical stimuli after invertebrate homologues of these channels (MEC subunits) were found to be required for the transduction of touch in *Caenorhabditis elegans* (*C.elegans*). ASIC1, 2 and 3 are expressed by sensory neurons of the DRG and nodose ganglia (Page et al., 2005). Interestingly, studies have shown that deletion of ASIC1 results in increased mechanosensitivity of gastrointestinal nerve fibres but has no effect on cutaneous mechanoreceptor sensitivity (Page et al., 2004, 2005). Similar to the findings with ASIC1, studies have shown that the mechanosensitivity of cutaneous afferents is unchanged in ASIC2 knockout mice (Roza et al., 2004). Other studies have found that ASIC2 deletion has mixed effects on the mechanosensitivity of gastrointestinal fibres (Page et al., 2005). In ASIC3 null-mice, mechanosensitivity of the majority of afferent fibres innervating the gut is decreased (Page et al., 2005). Furthermore, in the absence of ASIC3 the mechanosensitivity of A-fibre mechanonociceptors is decreased (Price et al., 2001). However, a study examining DRG neuron mechanosensitivity demonstrated that neither ASIC2 nor ASIC3 play roles in mechanically activated currents in sensory neuron ganglia (Drew et al., 2004). The precise functions of ASICs in mechanotransduction are still unclear.

Other promising candidates for the mammalian mechanotransduction channel belong to the TRP channel family. Invertebrate TRPN channels have been reported to play important roles in mechanotransduction. In *Drosophila* mechanosensory organs, NOMPC appears to act as a primary mechanotransducer channel (Lee et al., 2010a; Walker et al., 2000). In the nematode, *C.elegans*, a TRPN homologue has a role in mediating proprioceptive behaviour (Li et al., 2006) and interestingly zebrafish require a TRPN orthologue to sense vibration and after knockdown of the channel with a morpholino antisense oligonucleotide the zebrafish do not respond to acoustic stimuli (Sidi et al., 2003).

TRPA1 has also been suggested to play a mechanosensory role. Ion channels located at the tips of sensory hair bundles in the inner ear open in response to mechanical deflection allowing the perception of sound. TRPA1 expression is localised to the tips of hair cell stereocilia and TRPA1 was initially thought to function here as a hair cell mechanosensitive transduction channel (Corey et al., 2004). However, a subsequent study demonstrated that TRPA1 KO mice did not display hearing deficits, suggesting that TRPA1 is not required for

hair cell transduction (Kwan et al., 2006). Interestingly, findings from this study implicated TRPA1 in cutaneous mechanotransduction, mice lacking functional TRPA1 channels were shown to display deficits in their response to punctate mechanical stimuli (Kwan et al., 2006). However, a separate study reported that mechanical paw withdrawal thresholds of wildtype and *Trpa1*$^{-/-}$ mice are not significantly different; suggesting that TRPA1 does not play a role in acute mechanosensation (Bautista et al., 2006).

Notably, a study examining the properties of cutaneous mechanosensitive nerve fibres in a skin-nerve preparation, found that C and Aδ mechanonociceptors from *Trpa1*$^{-/-}$ mice exhibited decreased mechanically evoked action potential firing in comparison to wildtype fibres suggesting an involvement of TRPA1 in the transduction of noxious mechanical stimuli (Kwan et al., 2009). Interestingly, mixed effects (increases and decreases) were reported on the firing rates of different sub-types of mechanosensitive Aβ fibres (Kwan et al., 2009). The findings of a separate study demonstrated that within a subset of small diameter sensory neurons TRPA1 contributes to intermediately adapting mechanically-activated currents (Brierley et al., 2011). These findings suggest that whilst TRPA1 might be important for some mechanosensing activity it is not the principal transducer of mechanical stimuli.

Members of the TRPC family have also been implicated in mechanotransduction. TRPC3 and TRPC6 are expressed in a subpopulation of small-diameter sensory neurons and deletion of these channels leads to deficits in mechanosensitivity (Quick et al., 2012). A study reported that TRPC3/C6 double, but not single, knockout mice displayed a reduced sensitivity to innocuous mechanical stimuli (von Frey hairs and a cotton bud) but did not exhibit impaired behavioural responses in a test of noxious mechanosensitivity. Notably, in small-diameter neurons from TRPC3/C6 double KO mice, the number of neurons displaying a rapidly adapting current was halved and this was accompanied by an increase in the number of neurons which were not mechanically-sensitive (Quick et al., 2012). Expression of TRPC3 and TRPC6 has also been identified in cochlear hair cells and deletion of both of these channels leads to a deficit in hearing in addition to vestibular impairments (Quick et al., 2012). Surprisingly, expression of TRPC3 and TRPC6 in CHO or HEK-293 cell lines was not able to confer mechanosensitivity, however expression of either TRPC3 alone or TRPC3 and TRPC6 together conferred sensitivity to a sensory neuron cell line (ND-C cells). These findings suggest that TRPC3 and TRPC6 are components of a mechanically-activated transduction complex.

Another member of the TRPC family, TRPC1, is also expressed in sensory neurons and has been implicated in mechanotransduction. One study demonstrated that TRPC1 was able to confer mechanosensitivity to a CHO cell line and found that injection of *Xenopus* oocytes with a human TRPC1 cRNA attenuated endogenous mechanosensitive ion channel activity (Maroto et al., 2005). Another study has demonstrated that TRPC1 KO mice display reduced behavioural responses to 'light' mechanical stimuli ('puffed out' cotton bud and 0.68mN von Frey hair) in comparison to their wildtype counterparts (Garrison et al., 2012). The same study reported that rapidly adapting (RA) Aδ down-hair and slowly adapting (SA) Aβ mechanosensitive fibres from TRPC1 KO mice display reduced firing in response to mechanical stimuli in comparison to fibres from wildtype animals. These findings suggest that TRPC1 plays a role in the transduction of light touch. TRPC5 has also been suggested to function as a mechanosensitive channel. The findings of one study demonstrated that TRPC5 is activated by hypo-osmotic stimuli and cell stretch in a PIP_2 dependent-manner, suggesting that TRPC5 channels expressed in sensory neurons may contribute to mechanosensation (Gomis et al., 2008).

The large transmembrane proteins Piezo1 and Piezo2 have been identified as mechanosensing proteins which can assemble into homo-multimers and function as non-selective cation channels (Coste et al., 2010, 2012; Volkers et al., 2014; Woo et al., 2014). Both Piezo1 and Piezo2 have been found to confer mechanosensitivity when expressed in heterologous systems (Coste et al., 2010). Piezo2 is expressed in 20% of DRG neurons and has been shown to be required for a sub-group of mechanically-activated currents (Coste et al., 2010). Notably, a recent study has shown that Piezo2 proteins are required for Merkel cell mechanotransduction; specific deletion of Piezo2 proteins expressed in Merkel cells resulted in significantly longer paw withdrawal latencies at low forces in the von Frey filament test (Woo et al., 2014). These findings suggest that Piezo proteins contribute to the transduction of innocuous mechanical stimuli.

1.5.3 Osmosensation

Subpopulations of sensory neurons which innervate peripheral tissues such as the airways, gastrointestinal tract, liver and cornea are sensitive to increases and decreases in extracellular fluid osmolality (Fox et al., 1995; Hirata and Meng, 2010; Lechner et al., 2011; Pedersen et al., 1998; Zhu et al., 2001). Members of the TRP family of ion channels have been suggested as molecular transducers of hypotonicity. The thermosensitive TRPV4 channel has been reported to confer hypo-osmosensitivity to a HEK293 cell line (Liedtke et

al., 2000). Moreover, hypotonic solutions have been found to activate neurons expressing TRPV4 and deletion of TRPV4 results in the loss of hypotonicity-activated hepatic sensory neurons (Alessandri-Haber et al., 2003; Lechner et al., 2011). The TRPV2 channel is also sensitive to decreases in osmolality and can be activated by cell stretch (Muraki et al., 2003; Shibasaki et al., 2010). In addition to members of the vanilloid subfamily, TRPC1 and TRPC5 are also gated by cell-stretch and a human splice variant of TRPM3 has also been reported to be activated by hypotonic stimuli (Gomis et al., 2008; Grimm et al., 2003; Maroto et al., 2005).

A molecular transducer of hyperosmotic stimuli in peripheral sensory neurons has not yet been identified. An N-terminal splice variant of TRPV1 has been purported to act as an osmosensory channel within osmosensitive areas of the mammalian central nervous system (Ciura and Bourque, 2006; Naeini et al., 2006; Sharif-Naeini et al., 2008). However, one study reported that the TRPV1 variant is not directly osmosensitive when expressed in Xenopus oocytes suggesting that it does not act as a transducer of hypertonic stimuli (Eilers et al., 2007). The findings of one further study suggest that TRPA1 can be activated by hyper-osmotic stimuli (Zhang et al., 2008). Please see section 3.1 for a more detailed discussion on TRP channels and osmosensation.

1.1.1 Chemosensation

In addition to being sensitive to thermal, mechanical and osmotic stimulation, primary afferent nerve fibres are also chemosensitive and can be activated by an array of chemical mediators such as purines, amino acids and pungent food compounds (Wood and Docherty, 1997).

Between 40 and 96% of cultured DRG neurons have been shown to respond to the purine, ATP, by an increase in $[Ca^{2+}]_i$ or depolarisation (Burnstock, 2000). ATP is able to activate sensory neurons by binding to ionotropic P2X receptors which exist as homo- or heteromultimeric channel complexes. Currently, seven P2X receptor subtypes have been identified, $P2X_{1\text{-}7}$ (Burnstock, 2009). $P2X_{1\text{-}6}$ have been reported to be expressed in sensory neurons of the DRG, TG and nodose ganglia (North, 1996). However, only $P2X_3$ is selectively expressed by nociceptive sensory neurons (Burnstock, 2001; Chen et al., 1995; Wood and Docherty, 1997). The major purinergic ionotropic responses in sensory neurons are mediated by $P2X_2$ and $P2X_3$ homomers or heteromers (Burnstock, 2009; Cockayne et al., 2005).

Sensory neurons are also activated by the neurotransmitter 5-HT, ~40% of cultured DRG neurons have been reported to be activated by 5-HT (Robertson and Bevan, 1991). The direct activation of the primary afferent nerve terminal by 5-HT occurs primarily through activation of the ionotropic 5-HT_3 receptor, although, it is worth noting that activation of other 5-HT receptor subtypes, which are GPCRs, can lead to an increase in neuronal sensitivity via modulation of intracellular pathways (Wood and Docherty, 1997). Nicotinic and muscarinic receptors for the neurotransmitter acetylcholine are also expressed on sensory nerves and cholinergic agonists have been reported to excite peripheral nerve terminals and dorsal root ganglion neurons (Genzen et al., 2001; Nandigama et al., 2010; Smith et al., 2013; Steen and Reeh, 1993; Wood and Docherty, 1997).

Primary afferent sensory neurons also express receptors for excitatory amino acids and metabotropic and ionotropic receptors for the excitatory neurotransmitter glutamate have been reported (Carlton and Hargett, 2007; Sato et al., 1993; Willcockson and Valtschanoff, 2008).

In addition, sensory neurons express Mrgprs, a family of GPCRs which was discovered in 2001 (Dong et al., 2001). Members of the human (MrgprX1) and mouse (MrgprA3) Mrgpr families are activated by the pruritic, antimalarial drug, chloroquine (Liu et al., 2009; McNeil and Dong, 2014). Chloroquine excites DRG neurons resulting in increases in $[Ca^{2+}]_i$ and action potential generation and this process is reliant upon expression of functional Mrgprs but has also been shown to be blocked by the non-selective TRP channel inhibitor, ruthenium red, suggesting an involvement of TRP channels in this pathway (Liu et al., 2009). DRG neurons are activated by the endogenous pruritogen/pruritic peptide, BAM8-22, which is a cleaved product of proenkephalin A, in a Mrgpr dependent manner (Liu et al., 2009). Interestingly, a member of the Mrgpr family (MrgprC11) is activated by the synthetic activating peptide for proteinase-activated receptor 2 (PAR2), SLIGRL. Surprisingly, MrgprC11 and not PAR2, is responsible for SLIGRL-induced activation of DRG neurons and behavioural itch responses (Liu et al., 2011).

As mentioned previously, sensory neurons can be activated by pungent compounds found in food and some of these molecules have been of central importance for studies of sensory neuron transduction mechanisms. Capsaicin from chilli peppers and piperine from black pepper activates TRPV1 expressed on sensory neurons (Caterina et al., 1997; McNamara et al., 2005). Compounds found in cinnamon, mustard oil and garlic activate sensory neurons in a TRPA1-dependent manner and the cooling compound from the mint

plant, menthol, activates sensory neurons predominantly through activation of TRPM8 (Bautista et al., 2006; Jordt et al., 2004; McKemy et al., 2002; Peier et al., 2002b).

Sensory neurons expressing TRPA1 can also be activated by environmental irritants such as acrolein and by oxidants and products of oxidative stress, such as H_2O_2, 4-HNE and 4-ONE (Andersson et al., 2008; Bautista et al., 2006). Additionally, hydrogen sulphide (H_2S), 15d-PGJ2 and methylglyoxal activate sensory neurons in a TRPA1-dependent manner (Andersson et al., 2008, 2012; Eberhardt et al., 2014, 2012; Taylor-Clark et al., 2008a).Moreover, TRPV1 channels can be activated by the endogenous cannabinoid lipid, anandamide (Zygmunt et al., 1999) as well as the related lipid, 2-acylglycerol (Zygmunt et al., 2013). TRPA1 is activated by THC, the active principle in cannabis, and several other cannabinoids (Jordt et al., 2004; De Petrocellis et al., 2008; Zygmunt et al., 2002).

1.6 Pain and inflammatory sensitisation

High threshold 'painful' stimuli activate sensory transduction channels expressed on nociceptive nerve fibres resulting in the sensation of pain. Acute pain serves as a useful warning signal to the alert the body to environmental stimuli which could cause tissue damage (Basbaum et al., 2009). However, in some circumstances the pain pathway becomes sensitised leading to pain hypersensitivity (Basbaum et al., 2009). In this hypersensitive state pain is no longer serving as a useful warning signal. Stimuli which do not usually evoke sensations of pain become painful (allodynia) and the pain evoked by noxious stimuli is exaggerated (hyperalgesia). Pain hypersensitivity develops secondary to tissue injury and inflammation (inflammatory pain) or following sensory nerve damage (neuropathic pain).

Tissue injury, and the resulting inflammatory response, leads to sensitisation of peripheral sensory nerve afferents. At the site of tissue injury, the area surrounding the terminals of sensory nerves is flooded with pro-inflammatory agents (Basbaum et al., 2009). These chemicals are released from cells which have been disrupted by injury, or are secreted from immune cells which have infiltrated the injury site or produced by the activity of inflammatory enzymes (Woolf and Ma, 2007). The resulting mixture of inflammatory compounds is commonly referred to as the 'inflammatory soup' and includes peptides (CGRP, SP, bradykinin), lipid mediators (prostaglandins, thromboxanes, leukotrienes, endocannabinoids), cytokines, chemokines, growth factors, protons and ATP (Basbaum et al., 2009; Woolf and Ma, 2007). These inflammatory agents act on peripheral sensory nerve

terminals to increase their sensitivity and in some cases may depolarise sensory afferents directly.

Inflammatory mediators are able to increase the sensitivity of sensory nerve terminals by interacting with specific receptors. Some constituents of the inflammatory soup, for example protons and ATP, directly activate ion channels expressed at the peripheral nerve terminal (Dawes et al., 2013). The resulting influx of cations caused by opening of the ion channel evokes a depolarisation of the membrane and an increase in action potential firing. Other inflammatory agents such as prostaglandins, bradykinin, histamine and chemokines, bind to G-protein coupled receptors (GPCRs) to exert their effects (Ji et al., 2014). Activation of a GPCR by an inflammatory mediator results in activation of a heterotrimeric G protein and induction of a biochemical signalling cascade which is dependent on the class of G-protein activated. Activation of Gq stimulates phospholipase C (PLC) which cleaves the membrane phospholipid, phosphatidylinositol 4,5-bisphosphate (PIP_2), into diacyl glycerol (DAG) and inositol 1,4,5-trisphosphate (IP_3). Activation of Gs stimulates the activity of the membrane associated enzyme, adenylyl cyclase which synthesises the intracellular messenger, cAMP, from molecules of ATP (Dawes et al., 2013; Gilman, 1987). Induction of these signalling pathways typically culminates in activation of protein kinases (PKC, PKA) which are able to modulate the activity of transduction channels, including TRPA1 and TRPV1, and ion channels which are important for excitability and conduction (Nav1.7-1.9, HCN2) via phosphorylation thereby lowering their threshold for action potential generation and promoting increased neuronal firing (Emery et al., 2011; Ji et al., 2014; Schnorr et al., 2014).

Neurotrophic factors such as NGF, GDNF, brain-derived neurotrophic factor (BDNF) and artemin, elicit effects by binding to receptor tyrosine kinases (Chao, 2003). Upon activation the receptor monomers dimerise and activate downstream signalling pathways which can affect the transcription of pain and inflammation-related proteins and can also acutely modulate the activity of ion channels expressed at the nerve terminal (Basbaum et al., 2009). Pro-inflammatory cytokines such as TNFα and IL-1 bind to cytokine receptors which also induce signalling cascades which are capable of modulating neuronal function (Dawes et al., 2013).

In summary, inflammatory mediators sensitise nociceptive afferents to incoming stimuli by post-translational modification of receptors and ion channels and by altering gene expression; increasing the likelihood of neuronal excitation.

Chapter 2. General material and methods

The methods listed here are the general materials and methods used, specific methods and variations to the general methodology are presented in the individual chapters.

2.1 Cell Culture

2.1.1 Chinese hamster ovary cells

Untransfected Chinese hamster ovary (CHO) cells were grown in MEM AQ supplemented with penicillin (100 U/ml), streptomycin (100 µg/ml) and foetal bovine serum (10%). CHO cells expressing mouse or human TRPM8, mouse TRPV3 or mouse TRPA1 were grown in the additional presence of hygromycin (200 µg/ml). TRPA1 expression was under the control of a tetracycline inducible promoter to avoid cell death due to constitutive TRPA1 activity and expression was induced by addition of tetracycline 12-18 hours before experimentation. CHO cells expressing mouse TRPM3 or rat TRPV1 were grown in MEM AQ supplemented with penicillin (100 U/ml), streptomycin (100 µg/ml), foetal bovine serum (10%) and G418 (0.5mg/ml). 12-24 hours before experimentation cells were plated onto either 96 well black-walled plates (Costar) or poly-D-lysine coated (10µg.ml^{-1}) glass 13mm cover slips at a high density (~80%). Cultures were maintained at 37°C in a humidified incubator gassed with 5% CO_2 and cells were studied 12-24 hours after plating.

2.1.2 Dorsal root and trigeminal ganglion neurons

Dorsal root and trigeminal ganglion neurons were prepared from adult Wistar rats or C57Bl6 mice. Animals were killed by cervical dislocation, as approved by the United Kingdom Home Office, and spinal ganglia were removed from all levels of the spinal cord using aseptic methods. Ganglia were incubated in 0.25% collagenase in serum-free MEM (Invitrogen, Paisley, UK) containing 1% penicillin and streptomycin for 3 hours at 37°C in a humidified incubator gassed with 5% CO_2 in air. This was followed by 20 minute incubation with 0.25% trypsin in MEM. The ganglia were then dissociated mechanically via trituration with flame polished Pasteur pipettes to obtain a suspension of single cells. Trypsin was removed by addition of 10ml MEM (containing 10% FBS) followed by centrifugation at ~168 x g (1000 revolutions min^{-1}) for 10 minutes. The pellet, containing the ganglia, was re-suspended in MEM containing 1% penicillin and streptomycin, 10% FBS and 0.05% DNase. The cell suspension was then centrifuged through a 2ml cushion of sterile 15% bovine albumin in MEM at ~168 x g (1000 revolutions min^{-1}) for 10 minutes. The pellet, containing the neurons, was then re-suspended in an appropriate volume of MEM containing 10% FBS, 50ng.ml^{-1} NGF and 10µM cytosine arabinoside to prevent/reduce the growth of non-neuronal cells. The neurons were then plated at a high density (~80%) onto the centre of sterile 13mm glass coverslips previously coated with 10µg.ml^{-1} poly-D-lysine. Cultures were

maintained at 37°C in a humidified incubator gassed with 5% CO_2 and cells were studied 12- 24 hours after dissociation.

2.2 Imaging of intracellular calcium levels

2.2.1 Fura-2

Fura-2 (Invitrogen), a UV excitable ratiometric calcium indicator dye was used to measure changes in $[Ca^{2+}]_i$. The excitation spectrum for Fura-2 changes upon binding calcium, emission measured at >510nm increases when the dye is excited at 340nm and decreases at 380nm excitation.

Cells were loaded with the acetoxymethyl (AM) ester version of the dye which allows Fura-2 to pass across cell membranes by passive diffusion. Intracellular esterases then cleave the ester bonds once the dye is inside the cell, yielding a relatively membrane-impermeant acidic form of the dye. For all calcium imaging experiments the cells or neurons were loaded with Fura-2 for 1-2 hour/s prior to experimentation. Fura-2 was loaded in physiological extracellular solution supplemented with 0.01% pluronic acid and 1mM probenecid. Pluronic acid promotes permeation of Fura-2 through the cell membrane, and probenecid helps to prevent Fura-2 from being exported from the cell by inhibiting organic-anion transporters in the plasma membrane.

2.2.2 Microscope-based imaging of intracellular calcium levels

Cells or neurons were plated onto 13mm glass cover slips which formed the base of the perfusion chamber (volume~1ml). The chamber was mounted on to the stage of an inverted microscope (Nikon Diaphot) and cells were viewed using a 10x Fluor objective with a numerical aperture of 0.5.

Test solutions were applied to cells by local microperfusion of solution through a fine tube placed very close to the cells being studied. The temperature of the superfusate was controlled using a Peltier device connected to a power supply (Marlow Industries, model SE5010) with the temperature measured at the orifice of the inflow tube. Cells and neurons were perfused with solutions supplied from one of 8 reservoirs. In experiments using neuronal preparations, neurons were distinguished from non-neuronal cells by a final depolarising challenge with a solution containing 50mM KCl, which evoked a calcium influx through voltage gated calcium channels.

Fura-2 signals were measured using RatioMaster Fluorescence Microscopy System (PTI). Cells were excited by light generated by a xenon-arc lamp which was passed alternately through one of two monochromonators (DeltaRam high speed monochromator, PTI) to transmit light of the pre-selected wavelengths (340nm and 380nm, ± 2nm). The emitted light was filtered by a long pass optical filter (>510nm) and captured by a cooled CCD camera (PTI CoolOne). Exposure length was equal for each excitation wavelength and determined by the user to ensure adequate signal without saturation of the camera (typically 100-400msec).

PTI ImageMaster software served as the user interface during the experiments to monitor the fluorescence emission intensity ratios at 340nm/380nm excitation and was also used to select individual cells/neurons of interest for analysis. The intensity time-base data was exported into Microsoft Excel (Microsoft) for further analysis and then into Origin (Origin Pro, version 9.1) for graphical representation of the results.

In experimental chapters, *n* is presented as n= X, Y, Z; where X refers to the total number of cells studied, Y refers to the number of coverslips studied and Z refers to the number of individual passages (recombinant cell line) or animals (neuronal preparations) studied.

2.2.3 Fluorimeter measurement of intracellular calcium levels

A FlexStation 3 (Molecular Devices, Sunnyvale, CA) a bench-top scanning fluorimeter and integrated fluid-transfer workstation was used to measure Fura-2 responses for 96-well plate experiments. Experiments were performed using triplicate columns so that 4 experiments were carried out per 96-well plate. FlexStation experiments were performed using a cell line which was plated directly into the 96-well plate 12 to 24 hours before experimentation; cell confluency was typically greater than 80% at the time of experimentation.

SoftMax Pro (Molecular Devices, version 5.1) software served as the user interface during the experiments and was also used to produce the fluorescence intensity time-base data. The intensity time-base data was exported into Microsoft Excel (Microsoft) for further analysis and then into Origin (Origin Pro, version 9.1) for graphical representation of the results. The 96-well plate experiments had duration of 180s, baseline signals were collected for the first 20s of the experiment, and at the 20s time-point of the experiment cells were challenged with a test solution. All experiments were conducted at 25°C unless stated otherwise.

In experimental chapters, *n* refers to the number of independent experiments performed (each from different cell passages). In each individual experiment a minimum of 3 replicate samples per treatment were used.

Chapter 3. TRPM8 is an osmosensor modulated by temperature

3.1 Introduction

Primary afferent neurons innervate the skin and organs and provide feedback about internal and external sensory environments. Individual sensory neurons possess sensitivity to one or more modalities, and together they are able to detect a myriad of stimuli including mechanical perturbations, temperature fluctuations and exposure to chemicals.

Sensory neurons innervating the airways, gastrointestinal tract, liver and cornea are activated by changes in extracellular osmolality; however the identity of neurons excited by increases in osmolality are unknown (Fox et al., 1995; Hirata and Meng, 2010; Lechner et al., 2011; Pedersen et al., 1998; Zhu et al., 2001).

The molecular mechanism by which an osmotic stimulus evokes neuronal excitation is not clear, but it is thought to be either a mechanical process whereby membrane deformation physically gates ion channel activity or a process which is reliant upon osmotic activation of an intracellular pathway (Bourque, 2008; Zhang et al., 2007).

3.1.1 TRP Channels and osmosensation

Members of the transient receptor potential (TRP) family of ion channels act as cellular sensors for a diverse range of stimuli including temperature, pH, pungent chemicals and osmotic pressure (see section 1.4 for a full discussion).

3.1.2 OSM-9

The first study to provide evidence of TRP channel involvement in osmosensing processes was examining a TRPV orthologue, OSM-9, expressed in *Caenorhabditis elegans* (*C.elegans*) (Colbert et al., 1997). The OSM-9 gene encodes a 6 transmembrane domain channel which is expressed on sensory nerve endings and has a high resemblance to other TRP channels around the sixth transmembrane domain; a highly conserved area in the TRP family (Colbert et al., 1997).

ASH sensory neurons are responsible for initiating backward movement of the nematode in response to high osmotic strength and gentle touch of the nose. OSM-9 expression was identified in a subset of sensory neurons and mutations in the OSM-9 channel gene lead to deficits in nematode avoidance behaviours (Colbert et al., 1997). In addition to these defects OSM-9 mutant strains also had olfactory deficits (Colbert et al., 1997).

3.1.3 TRPV4

TRPV4 is a mammalian orthologue of OSM-9 and shares a 26% amino acid identity (44% identity or conservative change) with the channel (Liedtke et al., 2003). When TRPV4 was expressed in the OSM-9 mutant nematodes it was able to rescue osmotic and nose touch avoidance behaviours but not olfactory deficits; this suggests a divergence of roles between vertebrate and invertebrate TRP channels (Liedtke et al., 2003). Odorant sensation in *C. elegans* requires GPCR signalling and it has been suggested that TRPV4 might fail to interact with the required component of the GPCR pathway (Liedtke et al., 2003).

TRPV4, when expressed in a recombinant system is sensitive to decreases in osmolarity. Chinese hamster ovary (CHO) cells transfected with rat and chicken TRPV4 but not untransfected cells, displayed $[Ca^{2+}]_i$ responses when isotonic extracellular solution (295 mmol kg^{-1}) was replaced with a hypotonic solution (245 mmol kg^{-1}) (Liedtke et al., 2000). TRPV4 has been identified in areas known to be sensitive to fluctuations in osmolality such as the neurons of two sensory circumventricular organs the subfornical organ (SFO) and the organum vasculosum lamina terminalis (OVLT) (Liedtke et al., 2000). TRPV4 was also expressed in other sensory areas of the body such as the inner ear and the trigeminal ganglia; this suggests that TRPV4 might also be associated with other sensory processes which are independent of osmosensation (Liedtke et al., 2000).

Trpv4$^{-/-}$ mice were found to have deficits in fluid homeostasis. *Trpv4*$^{-/-}$ mice drank less water than their wildtype counterparts, both spontaneously and when deprived of water for 48hrs (Liedtke and Friedman, 2003). In addition this study found that TRPV4 null animals have higher blood osmolality levels and lower levels of the antidiuretic hormone, ADH (Liedtke and Friedman, 2003). These results directly contrast with the results of another study which reported that disruption of the mouse TRPV4 gene did not affect plasma osmolality and found that water deprivation lead to an increased ADH level (Mizuno et al., 2003).

Exposure to hypotonic solutions (219 mOsm) has been shown to depolarise DRG neurons expressing TRPV4 and to evoke an increase in intracellular calcium concentration in nociceptive neurons (Alessandri-Haber et al., 2003). Exposure to a hypotonic solution activated 54% of C fibres from the saphenous nerve and the number of action potentials evoked was increased when the nerve fibres were pre-sensitised by PGE_2. Application of a

hypotonic stimulus to skin sensitised by PGE_2 caused pain-related behaviour (flinching) in rats, and this behaviour was reduced when rats were treated with a TRPV4 antisense solution (Alessandri-Haber et al., 2003).

Xu and colleagues discovered that a pronounced tyrosine phosphorylation of heterologously expressed TRPV4 occurred when cells were exposed to hypotonic stress (150 mosm/kg H_2O) but not hypertonic stress (Xu et al., 2003). This was also evident in a native system; TRPV4 expressed in a mouse distal convoluted tubule cell line underwent a time-dependent tyrosine phosphorylation when exposed to hypotonic stress. This evoked phosphorylation was partially attenuated by the tyrosine kinase inhibitor genistein and completely inhibited by a selective Src family tyrosine kinase inhibitor PP1. In contrast a selective Syk inhibitor had no effect. In the same study, co-immunoprecipitation experiments revealed physical interactions between TRPV4 and Lyn, Src, Fyn, Hck, Lyk and Yes Src family kinases. Furthermore, confocal immunofluorescence studies identified complete co-localisation of TRPV4 with Lyn and a small degree of co-localisation with Src. Importantly, Xu and colleagues (2003) found that hypotonicity-induced phosphorylation of TRPV4 in a recombinant cell line was significantly impaired by a tyrosine-253 to phenylalanine (Y253F) mutation, and in contrast to cells transfected with wildtype (WT) TRPV4, the mutant Y253F TRPV4 failed to respond to hypotonic stimuli. However, these findings could not be replicated by Vriens and colleagues (2004). Vriens *et al* reported that cells expressing the Y253F TRPV4 mutant displayed hypotonicity-induced responses which were identical to the responses evoked in cells expressing WT TRPV4. The authors of the study reported that inhibition of phospholipase-A_2 (PLA_2) enzyme activity by four structurally dissimilar PLA_2 inhibitors attenuated hypotonicity-induced $[Ca^{2+}]_i$ responses (Vriens et al., 2004). Hypotonic responses were also prevented by cytochrome P450 epoxygenase inhibition. The authors of the study suggest that activation of TRPV4 by hypotonicity could be the result of PLA_2-dependent production of arachidonic acid which is metabolised by cytochrome P450 epoxygenase to 5',6'-EET which activates TRPV4 (Vriens et al., 2004; Watanabe et al., 2003).

In addition to the role of TRPV4 as a sensor of hypotonic conditions, it has also been argued that TRPV4 serves as a transducer of hypertonic stimuli during inflammatory states (Alessandri-Haber et al., 2005). Alessandri-Haber and colleagues (2005) observed that injection of a 2% NaCl solution into the rat hind paw elicited nociceptive behaviours which could be amplified by pre-sensitisation of skin with PGE_2. An intrathecal injection of

antisense oligodeoxynucleotides (ODN) for TRPV4 reduced the nociceptive response by 46%.

Parallel studies established that injection of hypertonic solutions into the hind paws of mice also evokes nociceptive behaviours (licking and shaking the affected paw). The nociceptive behaviour was amplified by sensitisation with PGE_2 and was attenuated in *Trpv4*$^{-/-}$ mice. Injection of the mouse paw with PP1 (a Src family tyrosine kinase inhibitor), was able to inhibit the nociceptive behaviours evoked by hypertonic solution to PGE_2 sensitised skin in the *Trpv4*$^{+/+}$ mice but not the *Trpv4*$^{-/-}$ mice (Alessandri-Haber et al., 2005). Interestingly, a hypertonic challenge (mannitol) of up to 646 mOsm induced similar $[Ca^{2+}]_i$ responses in small diameter DRG neurons (both % of neurons responding and increase in fluorescence ratio), from both TRPV4 WT and null mice, even when DRG neurons were pre-sensitised with PGE_2 (Alessandri-Haber et al., 2005).

TRPV4 has also been shown to be expressed on sensory nerve endings innervating hepatic blood vessels where it is suggested to be a sensor and transducer of hypo-osmotic shifts in hepatic osmolality (Lechner et al., 2011). In WT mice, 91.3% of retrogradely labelled hepatic sensory neurons responded to a hypotonic stimulus (260 mOsm), and this percentage was reduced to 31.6% in mice lacking TRPV4 (Lechner et al., 2011).

In summary, TRPV4 is sensitive to decreases in osmolality when expressed heterologously or natively in a kidney tubule cell line, and channel activation could be dependent on either phosphorylation of the channel by Src family kinases or a PLA^2-dependent mechanism. Furthermore, sensory neurons expressing TRPV4 respond to hypotonic stimulation, and *in vivo* nociceptive responses to hypotonic and hypertonic stimuli can be sensitized by prostaglandin treatment and attenuated by TRPV4 silencing with antisense oligonucleotides.

3.1.4 TRPV1

TRPV1 has also been proposed to play a role in osmosensory transduction in the mammalian CNS. An N-terminal splice variant of TRPV1 is expressed by magnocellular neurosecretory cells (MNCs) in the supraoptic nucleus (SON). In these neurons, increases in membrane conductance associated with a hyperosmotically-induced decrease in cell volume were reduced by the promiscuous TRPV antagonist ruthenium red and absent in MNCs from *Trpv1*$^{-/-}$ mice. *Trpv1*$^{-/-}$ mice also had a higher basal serum osmolality compared

to wildtype mice and a reduced ADH response to increased osmolality compared to wildtype mice (Naeini et al., 2006).

A further study examining the intrinsic osmosensitivity of the organum vasculosum lamina terminalis (OVLT) demonstrated that OVLT neurons responded to increases in osmolality by increases in membrane conductance and an increased frequency of action potential discharges (Ciura and Bourque, 2006). This response to a hyperosmotic challenge was ruthenium red sensitive and absent in *Trpv1*$^{-/-}$ mice. In addition *Trpv1*$^{-/-}$ mice consumed significantly less water than wildtype mice in response to a systemic hyperosmotic challenge (30 min water deprivation and intraperitoneal injection of 1M NaCl), suggesting that TRPV1 plays a role in the regulation of water intake (Ciura and Bourque, 2006). However, these findings were disputed by a study which reported that water intake in response to subcutaneous injection of 0.5M or 1.0M NaCl was not impaired in *Trpv1*$^{-/-}$ mice (Taylor et al., 2008). Furthermore, Taylor *et al* reported that water intake in response to chronic hyperosmolality (overnight water deprivation or access to only 2% NaCl solution for 2 days) was not disrupted in *Trpv1*$^{-/-}$ mice. Interestingly, the study also showed that there were no differences in plasma osmolality level between wildtype and *Trpv1*$^{-/-}$ mice at baseline or in response to acute (subcutaneous injection of 1M NaCl) or chronic hyperosmolality (access to only 2% NaCl solution for 2 days). A recent study from the same research group reported that *Trpv1*$^{-/-}$*v4*$^{-/-}$ double knockout (and *Trpv4*$^{-/-}$ single knockout) mice do not display water intake impairments in response to acute (intraperitoneal or subcutaneous injection of 0.5M or 1.0M NaCl) or chronic hyperosmolality (access to only 2% NaCl solution for 2 days). In addition the plasma osmolality levels of *Trpv1*$^{-/-}$*v4*$^{-/-}$ double knockout (and *Trpv4*$^{-/-}$ single knockout) mice were not significantly different from osmolality levels in WT mice (Kinsman et al., 2014). In contrast to the findings by Ciura and Bourque (2006) these findings suggest that TRPV1 is not essential for mechanisms which regulate water intake in response to increased osmolality.

3.1.5 TRPV2

TRPV2, a channel which has ~50% homology with TRPV1 and is expressed in sensory ganglia and other neural tissues, has also been implicated in osmosensory transduction mechanisms (Caterina et al., 1999; Muraki et al., 2003). Hypotonic (227 mosm) stimulation of mouse aortic myocytes evoked a non-selective cation current and elevated intracellular calcium, and this response was inhibited by ruthenium red (Muraki et al., 2003). Expression analysis established the presence of TRPV2 mRNA and protein in mouse vascular myocytes,

and treatment with TRPV2 anti-sense oligodeoxynucleotides impaired the myocyte responses to hypotonic stimulation (Muraki et al., 2003). Furthermore, hypotonic solutions and cell stretch (by application of negative pressure to the patch pipette) evoked membrane currents in CHO cells (cell-attached mode) transiently expressing TRPV2 but not in un-transfected control cells. A study by Shibasaki and colleagues (2011) reported that TRPV2 channels are activated by membrane stretch during development and promote axon outgrowth (Shibasaki et al., 2010).

3.1.6 Nanchung and water witch

A Drosophila protein, nanchung, which is a TRPV channel orthologue, together with a protein from the TRPA family, water witch, have been identified as important sensors of environmental humidity. Nanchung expression is required for detection of dry air whilst water witch is needed in order to sense moisture. Hygrosensing behaviour was examined by placing flies between two tubes, one in which air flowing into the tube was at ~100% humidity and one where air was at ~0% humidity. Both proteins are required for behavioural responses to humidity. The number of flies locating to the humid tube was increased in experiments examining flies with a nanchung deletion or flies driving water witch^{RNAi} expression (with a promoter expressed in neurons or a waterwitch promoter) compared to wildtype flies (Liu et al., 2007). The authors established two distinct populations of antennal hygrosensing neurons, one population which responded to dry air and another which responded to moist air (Liu et al., 2007). Nanchung deletion abolished the dry air responses and water witch disruption reduced responses to moist air.

3.1.7 TRPC1

Outside of the TRPV family, members of other TRP subfamilies have been implicated in the transduction of membrane-stretch, TRPC1, a member of the canonical family, has been identified as a component of the stretch-activated cation channel in vertebrate cells (Maroto et al., 2005). Cell-attached membrane patches from CHO cells heterologously expressing human TRPC1 were reported to display greater mechanosensitive channel activity than patches from untransfected cells in response to pipette applied membrane pressure (increasing steps of suction).

3.1.8 TRPA1

A member of the ankyrin subfamily of TRP channels has also been identified as an osmotically-activated channel. In one study TRPA1 was found to respond to stimulation by

hypertonic solutions (Zhang et al., 2008). Rat TRPA1 expressed in human embryonic kidney 293 (HEK293) cells responded to hyperosmotic solutions with an increase in $[Ca^{2+}]_i$. Ruthenium red (non-selective TRPA1 inhibitor) and camphor blocked the whole-cell currents induced by hypertonic solutions. In addition, hypertonically-evoked channel activity was only achieved in membrane patches that were also responsive to the TRPA1 agonist AITC (Zhang et al., 2008). In contrast to the results presented in the study by Zhang and colleagues, previously unpublished data (S. Bevan) has shown that hyperosmotic activation (up to ~500 mosm kg^{-1}) failed to evoke any significant increases in $[Ca^{2+}]_i$ in a CHO cell line heterologously expressing mouse TRPA1.

3.1.9 TRPM3

In addition to members of the vanilloid, ankyrin and canonical sub-families of TRP channels, a member of the melastatin family has also been shown to be activated by changes in osmolality. Grimm and colleagues (2003) identified a splice variant of the human TRPM3 channel, $TRPM3_{1325}$, which was expressed in the human kidney, brain, ovaria and pancreas. Exposure of HEK293 cells transfected with $TRPM3_{1325}$, but not un-transfected HEK293 cells, to a hypotonic solution (200 mosmol $liter^{-1}$) resulted in a rise in $[Ca^{2+}]_i$ (Grimm et al., 2003). Furthermore application of a hypertonic solution (400 mosmol $liter^{-1}$) caused a decrease in $[Ca^{2+}]_i$ but not in cells transfected with YFP (Grimm et al., 2003).

3.1.10 What is the mammalian osmosensor for increased osmolality?

Whilst TRPV4 appears to play a role in the detection of osmotic variation below the homeostatic set-point, a mammalian sensory neuron equivalent for detection of raised osmolality has not been identified. The N-terminal splice variant of TRPV1 which has been purported to act as an osmosensory channel within the mammalian central nervous system was found not to be directly osmosensitive when expressed in Xenopus oocytes (Eilers et al., 2007). Therefore the existence of a transduction channel expressed in sensory neurons which is sensitive to hypertonicity still remains to be found (see Table 3-1).

Table 3-1 Summary of the established roles of TRP channels in osmosensation

Table detailing TRP channel family members which have been reported to play a role in the osmosensory mechanisms of different species.

Channel	TRP Family	Species	Osmosensitivity
OSM-9	Vanilloid	*Caenorhabditis elegans*	Sensitive to hypertonic stimuli. Responsible for nematode responses to some olfactory and osmotic stimuli, and mechanosensory nose touch responses (Colbert et al., 1997).
Nanchung	Vanilloid	*Drosophila melanogaster*	Required for sensation of environmental humidity. Sensitive to dry air (Liu et al., 2007).
TRPV4	Vanilloid	Mammalian	Sensitive to hypotonic stimuli when heterologously or natively expressed. Expressed on osmosensitive neurons. Rescues osmotic and nose-touch responses in OSM-9 deficient nematodes (Lechner et al., 2011; Liedtke et al., 2000, 2003; Xu et al., 2003).
TRPV1	Vanilloid	Mammalian	N-terminal splice variant of TRPV1 expressed on MNC, SON and OVLT neurons. Sensitive to increases in osmolality and may play a role in regulation of water intake (Ciura and Bourque, 2006; Naeini et al., 2006).
TRPV2	Vanilloid	Mammalian	Sensitive to hypotonic solutions and cell stretch when heterologously expressed. Important for cardiac myocyte responses to hypotonic stimulation and cell stretch (Muraki et al., 2003).
TRPC1	Canonical	Mammalian	Component of the stretch-activated cation channel in vertebrate cells (Maroto et al., 2005).
Water witch	Ankyrin	*Drosophila melanogaster*	Required for sensation of environmental humidity. Sensitive to moist air. (Liu et al., 2007)

TRPA1	Ankyrin	Mammalian	Sensitive to hypertonic stimulation when heterologously expressed (Zhang et al., 2008).
TRPM3	Melastatin	Mammalian	Human TRPM3 variant activated by hypotonic stimulation and inhibited by hypertonic solutions when expressed in a recombinant cell line (Grimm et al., 2003).

3.2 Aim of the present study

The aim of the research presented in this chapter was to examine whether TRPM8 is a cellular osmosensor. A further aim was to investigate how activation or inhibition of intracellular pathways, which have been previously shown to modify TRPM8 activity and which have been linked with hypertonic conditions, modulate the osmosensitivity of TRPM8. Finally as TRPM8 is an established thermosensitive channel, the present study also investigated the interaction between osmotic responses and temperature. These experimental aims were investigated using single cell and cell population Ca^{2+} measurements of CHO cells heterologously expressing the TRPM8 channel and rat DRG neurons natively expressing TRPM8.

3.3 Materials and Methods

3.3.1 Solutions

The compositions of the physiological and slightly hypotonic (267 mosm kg^{-1}) extracellular solutions used in these experiments are shown in Table 3-2 and Table 3-3. The osmolality of the slightly hypotonic solution (267 mosm kg^{-1}) was varied by addition of either sucrose or NaCl. Osmolality was measured by freezing point depression using an osmometer (Roebling 13). For Ca^{2+}-free experiments $CaCl_2$ was omitted from the buffer and 1mM EGTA was added. All solutions were buffered to pH 7.4 (NaOH).

Table 3-2 Composition of physiological extracellular solution

	Concentration (mM)
NaCl	140
KCl	5
Glucose	10
HEPES	10
$CaCl_2$	2
$MgCl_2$	1

Table 3-3 Composition of slightly hypotonic extracellular solution

	Concentration (mM)
NaCl	120
KCl	5
Glucose	10
HEPES	10
$CaCl_2$	2
$MgCl_2$	1

3.3.2 Reagents

Master stock solutions of icilin (Biomol; Exeter, UK) capsaicin (Sigma-Aldrich; St Louis, MO) and menthol (Sigma-Aldrich; St Louis, MO) were made in DMSO (Calbiochem; Darmstadt, Germany). Master stock solutions of m-3M3FBS, U73122, ACA, BEL (Sigma-Aldrich; St Louis, MO), AMTB (kindly synthesized and provided by Dr Simon Lewis; Bath University) and PP2 (Tocris Bioscience; Bristol, UK) were also made in DMSO (Calbiochem; Darmstadt, Germany). All master stock solutions were aliquotted and stored at -20°C. Dilutions from these aliquots into physiological solution were made daily for their use in experiments.

3.3.3 Osmosensitivity studies

In microscope based imaging experiments investigating the osmosensitivity of mouse dorsal root and trigeminal ganglion neurons (background studies), solutions were made hyperosmotic by addition of NaCl to a physiological or slightly hypotonic extracellular solution (267 mosm kg^{-1}) unless stated otherwise. These experiments were conducted at 28°C using calcium imaging methods described in section 2.2.2. Neuronal responses to osmotic or agonist solutions were determined by direct observation of Fura-2 intensity changes in individual neurons. Additionally, neurons were screened visually for a discontinuity in the Fura-2 ratio time-course indicative of a response.

In 96-well plate experiments investigating the osmosensitivity of TRP channel transfected CHO cell lines, solutions were made hyperosmotic by addition of sucrose to a slightly hypotonic extracellular solution (267 mosm kg^{-1}) unless stated otherwise. All assays were carried out at 25°C, except where stated otherwise, using calcium imaging methods described in section 2.2.3.

3.3.4 Temperature activation threshold studies

Microscope-based imaging experiments investigating the effect of osmolality on temperature activation thresholds were conducted on mouse TRPM8 transfected CHO cells and rat dorsal root ganglion (DRG) neurons (using calcium imaging experiment methods described in section 2.2.2).

3.3.4.1 Heterologously expressed TRPM8

Mouse TRPM8 CHO cells were exposed to a linear cooling temperature ramp (~37-21°C) and time-points of temperature decrease at 2°C intervals were recorded. For each population of cells tested a mean temperature activation threshold was determined.

The impact of osmolality on the temperature thresholds of cells was measured by controlling the osmolality of the perfusing solution. Perfusing solutions had an osmolality of either: 227, 267, 287, 307, 327, 367, 517 or 767 mosm kg^{-1}. A solution with a reduced osmolality of 227 mosm kg^{-1} was made using 100mM NaCl, 5mM KCL, 10mM glucose, 10mM HEPES, 2mM $CaCl_2$, and 1mM $MgCl_2$. Other solutions were made hyperosmotic by addition of sucrose to a slightly hypotonic extracellular solution (267 mosm kg^{-1}).

Solutions were applied to cells 3 minutes prior to the beginning of the cooling temperature ramp. Before and after exposure to a cooling temperature ramp the temperature of the perfusate was held at a constant temperature (~38°C).

3.3.4.2 Natively expressed TRPM8

In rat DRG neuron experiments, two cooling temperature ramps (~37-18°C) were conducted. All neurons were perfused with a slightly hypotonic extracellular solution (267 mosm kg^{-1}) before being exposed to a first cooling temperature ramp. In control experiments there was no change to the perfusate solution before exposing the neurons to a second cooling temperature ramp. In other experiments the slightly hypotonic extracellular solution was replaced with a hyperosmotic solution (either 367 or 517 mosm kg^{-1}) before exposure (3 minutes prior) to a second cooling temperature ramp. Temperature activation thresholds for the first and second cold challenges were compared in individual rat DRG neurons. Before and after exposure to a cooling temperature ramps the temperature of the perfusate was held at a constant temperature (~38°C). After exposure to the cooling ramps, neurons were exposed to a maximally-effective concentration of the TRPM8 agonist Icilin (1μM) in order to identify TRPM8-expressing

neurons. Neurons were distinguished from non-neuronal cells by a final depolarising challenge with a solution containing 50mM KCl.

Neuronal responses to cold and icilin application were determined by direct observation of Fura-2 intensity changes in individual neurons. Additionally, neurons were screened visually for a discontinuity in the Fura-2 ratio time-course indicative of a temperature threshold or agonist-induced response.

3.3.4.3 Activation thresholds

To determine the temperature activation thresholds, time-points of temperature decrease at 2°C intervals were recorded during cooling temperature ramps. The rate of cooling was linear over most of the temperature range used. The Fura-2 ratios for cold-sensitive cells were exported into Microsoft Excel (Microsoft). The time-points were then converted into temperatures and were plotted against log Fura-2 ratios using Origin (Origin Lab, version 7.5). The temperature at which the log ratio deviated from baseline, identified as the point of intersection between two lines fitted to the 2 phases of the Fura-2 ratio, was used as the temperature activation threshold.

3.3.5 Statistics

Normality of data was tested using the Shapiro-Wilk Test and homogeneity of variances was tested using Levene's test. Differences in normally distributed data means between two groups were analysed using an independent samples t-test. Differences in normally distributed data means between three groups or more were analysed using a one-way ANOVA, followed by a Tukey's HSD post-hoc test (for datasets with equal variances) or a Dunnett's T3 post-hoc test (for datasets with unequal variances). Differences in non-normally distributed data means between two groups were analysed using a Mann-Whitney U test. Differences in non-normally distributed data means between three groups or more were analysed using a Kruskal-Wallis test, followed by a Dunn-Bonferroni's pairwise post-hoc test. All statistical analyses were made using IBM SPSS statistics, version 22.

3.4 Background

Microscope-based imaging experiments (performed by N. Vastani and E. Horridge) examining the $[Ca^{2+}]_i$ responses of dorsal root and trigeminal ganglion neurons to hypertonic stimuli led to the identification of TRPM8 as a candidate transduction channel for increased osmolality. The data presented in this section provides the experimental backdrop to the characterisation of TRPM8 as a cellular osmosensor.

3.4.1 Sensory neurons are activated by hyperosmotic solutions

Changes in $[Ca^{2+}]_i$ within isolated DRG and TG neurons were monitored using the calcium indicator dye Fura-2, to identify the presence of osmosensitive neurons. This technique was suitable to detect calcium influx mechanisms as well as mechanisms involving release of Ca^{2+} from intracellular stores.

Increasing the osmolality of the extracellular solution from 307 to 367 mosm kg^{-1} evoked an increase in $[Ca^{2+}]_i$ in a small percentage of DRG neurons (1.65%; n= 19/1154 neurons, 4, 1). Interestingly, some neurons displayed oscillatory baseline $[Ca^{2+}]_i$ responses at physiological osmolality (307 mosm kg^{-1}) which were attenuated upon reduction of the extracellular osmolality (267 mosm kg^{-1}). In order to avoid these responses, experiments starting at a slightly hypotonic osmolality (267 mosm kg^{-1}) were conducted.

In experiments where neurons were exposed to an increase in osmolality from 267 to 367 mosm kg^{-1} $[Ca^{2+}]_i$ responses were observed in 3.6% (n= 81/2240 neurons, 13, 2) of DRG neurons and 4.1% (n= 35/846, 5, 1) of TG neurons. These responses were the result of a Ca^{2+} entry pathway, as shown by the absence of the responses when experiments were performed in Ca^{2+} free conditions (in the presence of 1mM EGTA in the external solution). These responses exhibited little desensitisation with repeated hyperosmotic challenges.

3.4.2 Hyperosmotically activated neurons express TRPM8

In order to identify whether there was any correlation between the osmosensitivity of a neuron and TRP channel expression, isolated DRG and TG neurons were exposed to a series of TRP channel agonists following a hyperosmotic challenge. This approach examined whether the osmosensitive neurons displayed characteristics of a particular functional class of neuron. The TRP channel agonists were used to identify some of the possible neuronal sub-populations (cold activated, nociceptors, non-nociceptors). The panel of agonists included icilin for TRPM8, allyl isothiocyanate (AITC) for TRPA1, and capsaicin for TRPV1.

Remarkably 69.1% (n= 56/81 neurons, 13, 2) of DRG neurons and 86% (n= 30/35 neurons, 5, 1) of trigeminal neurons that showed an increase in $[Ca^{2+}]_i$ when exposed to a 367 mosm kg^{-1} hyperosmotic solution (from 267 mosm kg^{-1}) subsequently responded to icilin, suggesting that these osmosensitive neurons also express TRPM8 (see Figure 3-1a). In order to investigate whether TRPM8 was acting as a transducer of increased osmolality, the effect of a TRPM8 antagonist was investigated. Sensory neurons were exposed to consecutive hyperosmotic challenges, first in the absence and then in the presence of the TRPM8 antagonist, AMTB (30µM). AMTB completely inhibited the hyperosmotic responses in over 75% of DRG neurons (n= 62/81 neurons, 13, 2) and 80% of TG neurons (n= 28/35 neurons, 5, 1) and reduced the mean amplitude of the Fura-2 responses by 92% in DRG neurons (from 35.5 ±1.6% to 2.8 ±0.9% of the KCl evoked amplitude, n=62) and 91% (from 36.8 ±3.5% to 3.4 ±1.2%, n= 28) in TG neurons. This is in contrast to the similar sized responses (1^{st} response 35.6 ±2.6%, 2^{nd} response 39.5 ±3.9% n= 29) evoked by two sequential hyperosmotic stimuli in control conditions (Figure 3-1b). Next, neurons isolated from animals lacking functional TRPM8 channels (*Trpm8*$^{-/-}$ mice) were investigated. Hyperosmotic stimuli (367 mosm kg^{-1}) did not evoke responses in neurons from *Trpm8*$^{-/-}$ mice (0.3%, n= 4/1453 responsive DRG neurons, 6, 2; 0%, n= 0/460 responsive TG neurons, 7, 1, Figure 3-1c) in contrast to neurons from wildtype littermates (2.8%, n= 52/1843 responsive DRG neurons, 7, 2; 4.1%, n= 35/846 responsive TG neurons, 5, 1).

In summary, only TRPM8 expressing DRG and TG neurons responded to small elevations in extracellular osmolality. These hyperosmotic responses could be inhibited by a TRPM8 antagonist, AMTB, and were absent from sensory neurons isolated from animals lacking functional TRPM8 channels (*Trpm8*$^{-/-}$ mice).

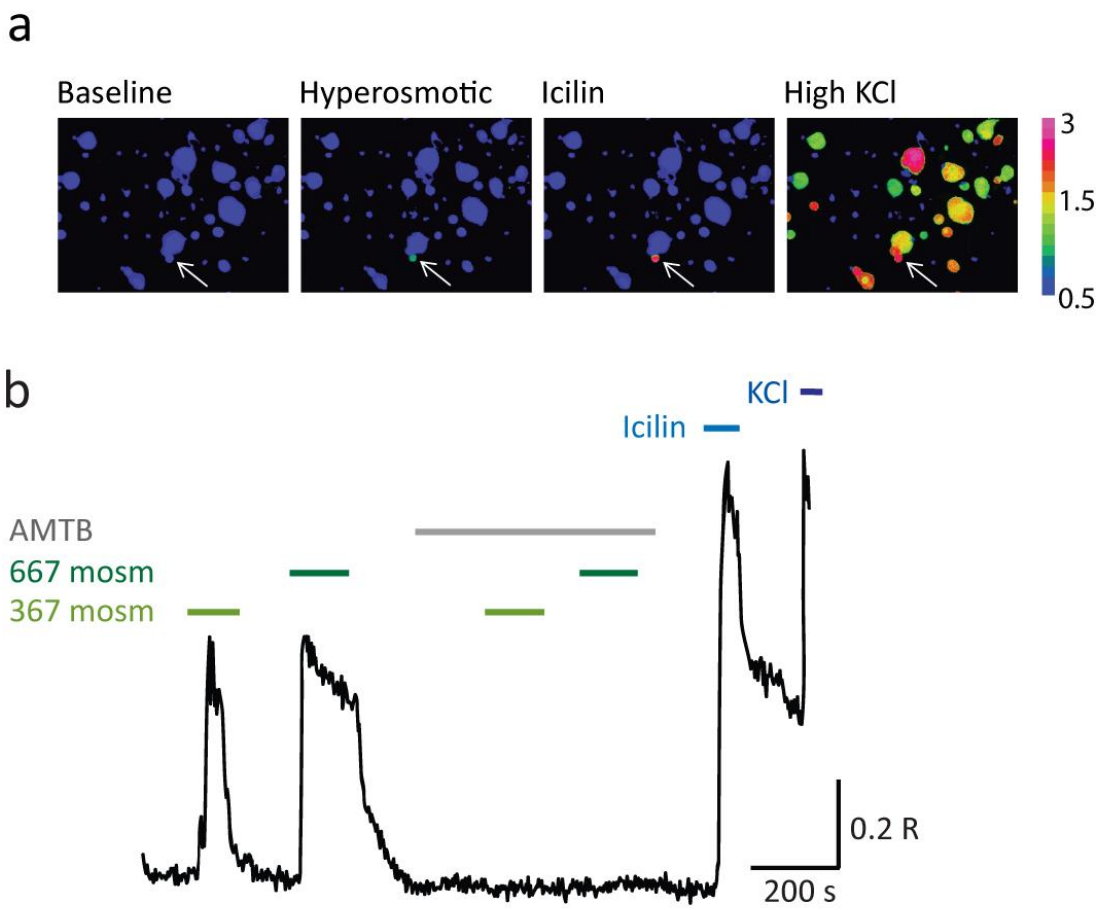
a
Baseline
Hyperosmotic
Icilin
High KCl
3
1.5
0.5
b
KCl
Icilin
AMTB
667 mosm
367 mosm
0.2 R
200 s
c
Trpm8+/+
Trpm8-/-
Responding neurons (%)
4
3
2
1
0
DRG
TG
DRG
TG

Figure 3-1 Hyperosmotically activated sensory neurons express TRPM8

(**a**) Pseudocoloured images illustrating the Fura-2 responses of DRG neurons to a sequential challenge with a hyperosmotic solution (517 mosm kg^{-1}) followed by icilin and depolarisation with a high KCl concentration (50mM). The white arrow highlights a small, icilin-sensitive neuron which was activated by the hyperosmotic stimulus. (**b**) $[Ca^{2+}]_i$ responses monitored by Fura-2 in an icilin-sensitive neuron. AMTB (30μM) completely inhibited responses evoked by hyperosmotic solutions. AMTB application indicated by the grey bar. Note that the reversible TRPM8 antagonist AMTB was removed before the challenge with icilin. Neurons were identified by a final depolarising challenge with a solution containing 50mM KCl. (**c**) Percentage of mouse DRG and TG neurons from *Trpm8*$^{+/+}$ and *Trpm8*$^{-/-}$ mice responsive to a hypertonic stimulus (367 mosm kg^{-1}). Absence of TRPM8 reduced the percentage of hyperosmotically activated DRG neurons from 2.6% (n=52/1843 neurons, 7, 2) to 0.3% (n=4/1453 neurons, 6, 2) and TG neurons from 4.1% (n=86/846 neurons, 5, 1) to 0% (n=0/460 neurons, 7, 1).

3.5 Results

3.5.1 Osmotic sensitivity of TRPM8

In order to examine whether the TRPM8 channel is sufficient to confer osmosensitivity or whether some element(s) present in the sensory neuron environment are required, the responses of CHO cells heterologously expressing TRPM8 to increases in osmolality were examined. In the experiments described changes in $[Ca^{2+}]_i$ were monitored using the calcium indicator dye Fura-2 using a 96-well plate assay format.

An extracellular saline solution with a slightly reduced osmolality was used to reduce the level of constitutive TRPM8 activity observed at physiological osmolalities (see Table 3-3). Figure 3-2 shows the responses of mouse TRPM8 CHO cells to increases in osmolality (addition of 10-200 mosm kg^{-1}) from a baseline osmolality of 267 mosm kg^{-1}. Solutions were made hyperosmotic by addition of sucrose to the extracellular solution.

Hyperosmotic stimuli evoked a concentration-dependent increase in $[Ca^{2+}]_i$ with a mean EC_{50} value of 318 ± 5 mosm kg^{-1} (mean ± SEM; n= 9 independent experiments). The physiological osmolality for mouse extracellular fluid (311 mosm kg^{-1}) lies on the steep part of the curve indicating that TRPM8 is highly sensitive to changes around the physiological set-point (Bourque, 2008). The osmolality-response relationship reached a plateau at final osmolalities above 367 mosm kg^{-1} (see Figure 3-2b). Smaller increases in osmolality evoked slower responses which took longer to reach their maximum response amplitude (see Figure 3-2a).

Experiments were conducted to determine whether the hyperosmotically evoked responses were independent of the agent added to the extracellular solution. Similar $[Ca^{2+}]_i$ responses were observed when solutions were made hyperosmotic by addition of sucrose (Figure 3-2) and NaCl (Figure 3-3, EC_{50} value - 313 ±8 mosm kg^{-1}; mean ± SEM; n= 5 independent experiments). The relationship between the increase in $[Ca^{2+}]_i$ and the final osmolality was similar to that observed with sucrose. The osmolality-response relationship reached a plateau at final osmolalities above 367 mosm kg^{-1} and responses evoked by lower osmolalities took longer to reach their maximum response amplitude (see Figure 3-3). However, in experiments where NaCl was added to increase the osmolality of the extracellular solution, the maximum amplitudes of the $[Ca^{2+}]_i$ responses evoked were consistently lower than in experiments using sucrose. This could be due to the increased extracellular Na^+ ion concentration when NaCl is used as the hyperosmotic agent. As

TRPM8 is a non-selective cation channel, Na^+ ions will also flow through the activated TRPM8 channel and these ions will compete with Ca^{2+} ions for entry into the cell thus resulting in a lower influx of Ca^{2+} at higher external Na^+ concentrations. These findings demonstrate that TRPM8 is sensitive to modest increases in osmolality around the homeostatic set-point, regardless of the agent used.

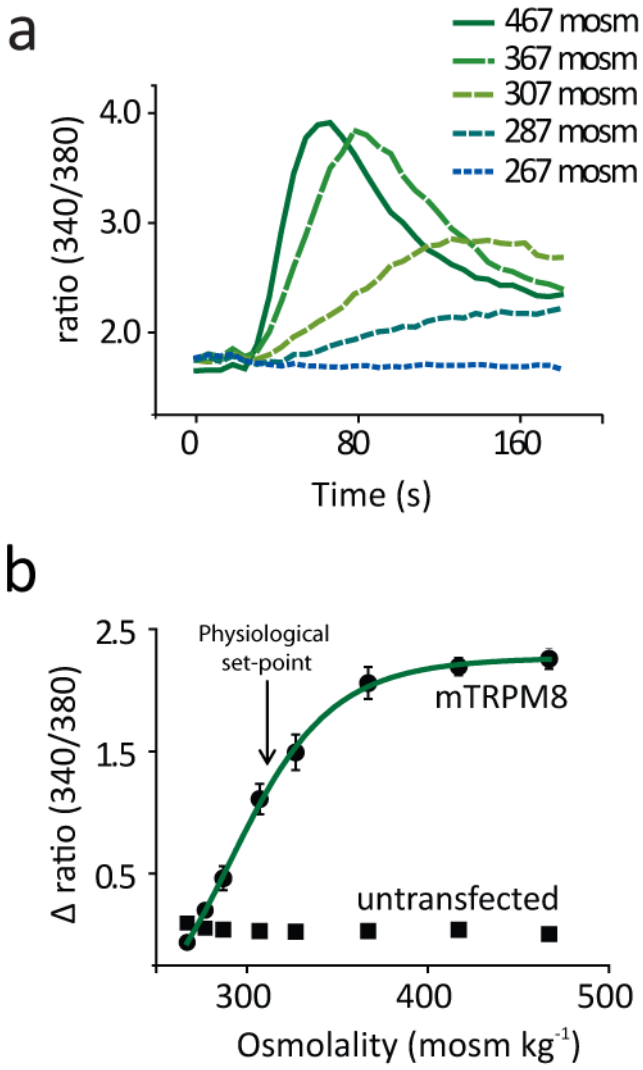

Figure 3-2 Mouse TRPM8 is activated by increases in osmolality

(**a**) Time courses of $[Ca^{2+}]_i$ responses elicited by challenges with different osmolalities (osmolality altered by addition of sucrose) in CHO cells transfected with mouse TRPM8 (mTRPM8) in a 96-well plate experiment. Baseline signals were collected before cells were challenged with osmotic solutions at 20 seconds. Traces shown are mean ratios from triplicate wells from a representative experiment (**b**) Increases in osmolality evoked $[Ca^{2+}]_i$ (Δ Fura-2 340/380) responses in mTRPM8-expressing CHO cells with an EC_{50} of 318 ± 5 mosm kg^{-1} (mean ± SEM; n=9 independent experiments) in 96-well plate experiments. Hyperosmotic (sucrose) solutions failed to increase $[Ca^{2+}]_i$ in untransfected CHO cells. Representative plots shown, data points are the mean ratio of triplicate wells ± SEM. The arrow on the graph points to the physiological osmolality of mouse extracellular solution (311 mosm kg^{-1}). Hyperosmotic (sucrose) solutions failed to increase $[Ca^{2+}]_i$ in untransfected control CHO cells.

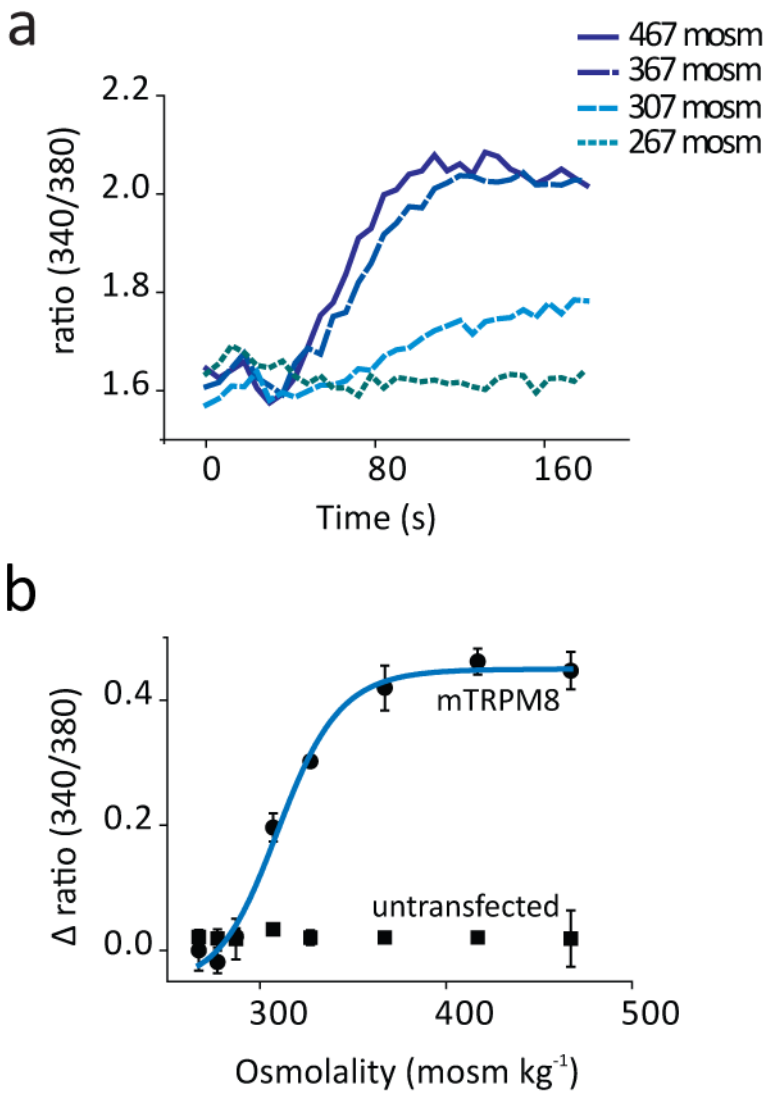

Figure 3-3 NaCl-induced increases in osmolality activate TRPM8

(**a**) Time courses of $[Ca^{2+}]_i$ increases evoked by challenges with different osmolalities (osmolality altered by addition of NaCl) in CHO cells transfected with mTRPM8 in a 96-well plate experiment. Baseline signals were collected before cells were challenged with osmotic solutions at 20 seconds. Traces shown are mean ratios from triplicate wells from a representative experiment (**b**) Increases in osmolality evoked $[Ca^{2+}]_i$ (Δ Fura-2 340/380) responses in mTRPM8-expressing CHO cells with an EC_{50} of 313 ±8 mosm kg^{-1} (mean ±SEM; n=5 independent experiments) in 96-well plate experiments. Hyperosmotic (NaCl) solutions failed to increase $[Ca^{2+}]_i$ in untransfected CHO cells. Representative plots shown, data points are the mean ratio of triplicate wells ± SEM.

3.5.2 TRPM8 is required for osmotic sensitivity

The $[Ca^{2+}]_i$ responses of untransfected CHO cells exposed to hyperosmotic solutions, over the range that activated TRPM8 CHO cells (up to 467 mosm kg^{-1} final concentration), were examined to test whether expression of TRPM8 is required for osmosensitivity. Hyperosmotic solutions did not evoke $[Ca^{2+}]_i$ responses in Fura-2 loaded untransfected CHO cells; suggesting that expression of TRPM8 is necessary for osmotic sensitivity (Figure 3-2b, Figure 3-3b).

In order to investigate whether functional TRPM8 channels are required for the hyperosmotic responses, the effect of a TRPM8 antagonist, AMTB, was investigated. AMTB inhibits the activation of TRPM8 by the prototypical TRPM8 agonist menthol with an IC_{50} value of 3.18 ± 0.33μM (mean ± SEM; n=3 independent experiments; Figure 3-4c). TRPM8 CHO cells were exposed to a hyperosmotic stimulus (367 mosm kg^{-1}) in the presence of increasing concentrations of AMTB (0.5-50μM). AMTB inhibited the hyperosmotic responses of TRPM8 CHO cells in a concentration dependent manner with an IC_{50} value of 3.98 ± 0.25μM (mean ± SEM; n=3 independent experiments; Figure 3-5b). Furthermore, in the presence of a maximal concentration of AMTB (20μM) responses to hyperosmotic solutions (267-367 mosm kg^{-1}) were abolished (reduction in average maximum amplitude from 1.86 ± 0.21 to 0.17 ± 0.04; mean ± SEM; n=3 independent experiments; Figure 3-5b).

These findings demonstrate that functional TRPM8 expression is necessary for CHO cell sensitivity to increases in extracellular osmolality.

3.5.3 Osmosensitivity is conserved between species

Sensitivity to increases in osmolality were found not to be dependent on the species of TRPM8 channel expressed, CHO cells expressing human TRPM8 evoked similar $[Ca^{2+}]_i$ responses to those expressing mouse TRPM8 with responses reaching a plateau at final osmolalties above 367 mosm kg^{-1} (Figure 3-6, EC_{50} 291 ± 16 mosm kg-1, n=3 independent experiments).

3.5.4 Other sensory neuron TRP channels are not activated by hyperosmotic solutions

Significant proportions of sensory neurons express other TRP channels (TRPV1, TRPV2, TRPA1, TRPM3, TRPC3/6, and TRPC1), some of which have been suggested to mediate responses to osmotic or mechanical stimulation (Ciura and Bourque, 2006; Corey et al., 2004; Grimm et al., 2003; Maroto et al., 2005; Muraki et al., 2003; Quick et al., 2012; Zhang et al., 2008). To determine the osmosensitivity for some of these channels, experiments were performed on CHO cells expressing TRPA1, TRPV1, TRPV3 or TRPM3.

Measurement of Ca^{2+} influx in TRPV3 assay systems is complicated by Ca^{2+} mediated inactivation of the channel (Peier et al., 2002a; Xiao et al., 2008). In order to circumvent Ca^{2+} mediated inhibition of TRPV3 an extracellular solution containing $BaCl_2$ as a replacement for $CaCl_2$ (120 mM NaCl, 5 mM KCL, 10 mM glucose, 10 mM HEPES, 2 mM $BaCl_2$, and 1 mM $MgCl_2$) was used in experiments examining CHO cells stably transfected with mTRPV3; and $[Ba^{2+}]_i$ responses were measured.

Increasing the osmolality (by addition of sucrose or NaCl) up to ~467 mosm kg^{-1} failed to evoke any significant increases in $[Ca^{2+}]_i$ or $[Ba^{2+}]_i$ in these cell lines (Figure 3-7). However activation of the channels by their respective agonists induced robust $[Ca^{2+}]_i$ or $[Ba^{2+}]_i$ responses. The maximum amplitudes for responses evoked by hyperosmotic stimulation were below 12.5% of the maximum response amplitude evoked by the respective channel agonists.

These findings suggest that other sensory neuron TRP channels (TRPA1, TRPV1, TRPV3, or TRPM3), unlike TRPM8, are not responsible for mediating neuronal responses to modest increases in osmolality at physiologically relevant levels.

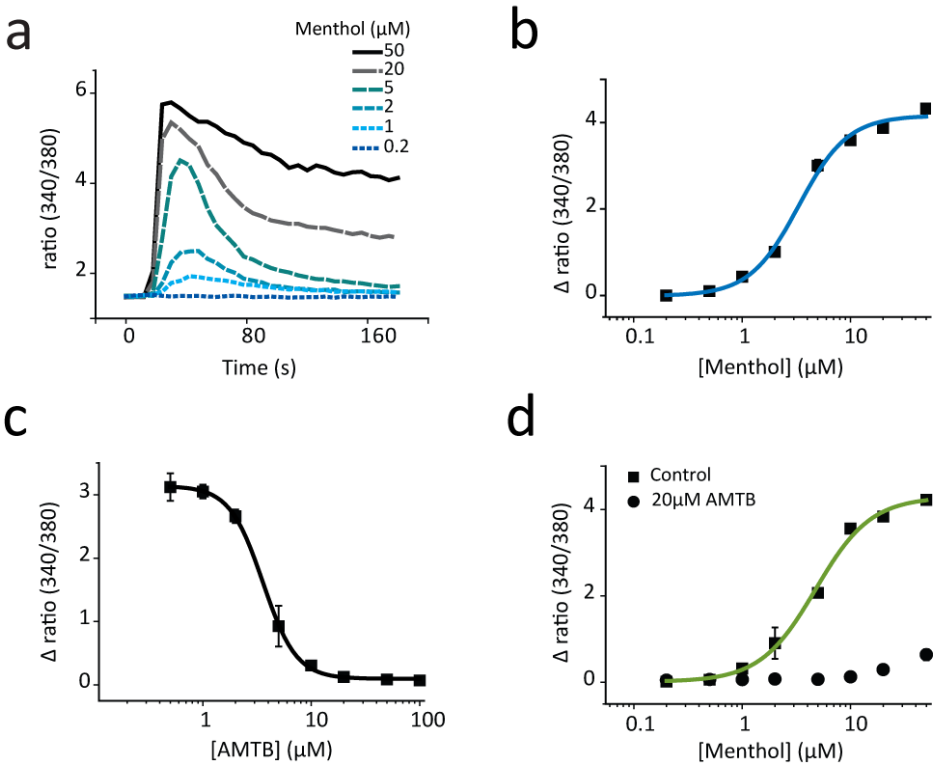

Figure 3-4 Menthol evoked $[Ca^{2+}]_i$ responses are inhibited by AMTB

(**a**) Time courses of $[Ca^{2+}]_i$ increases evoked by different concentrations of menthol (0.2-50μM) in CHO cells transfected with mTRPM8 in a 96-well plate experiment. Baseline signals were collected before cells were challenged with osmotic solutions at 20 seconds. (**b**) Menthol evoked concentration-dependent $[Ca^{2+}]_i$ (Δ Fura-2 340/380) responses in mTRPM8-expressing CHO cells with an EC_{50} of 4.28 ± 0.47μM (n=3 independent experiments) in 96-well plate experiments. Representative plot shown, data points are the mean ratio of triplicate wells ± SEM. (**c**) Activation of TRPM8 by menthol (5μM) was inhibited by AMTB in a concentration dependent manner, IC_{50} - 3.18 ± 0.33μM (n=3 independent experiments). Representative plot shown, data points are the mean ratio of triplicate wells ± SEM. (**d**) AMTB (20μM) suppressed menthol (0.2-50μM) evoked $[Ca^{2+}]_i$ (Δ Fura-2 340/380) responses. Representative plots shown, data points are the mean ratio of triplicate wells ± SEM.

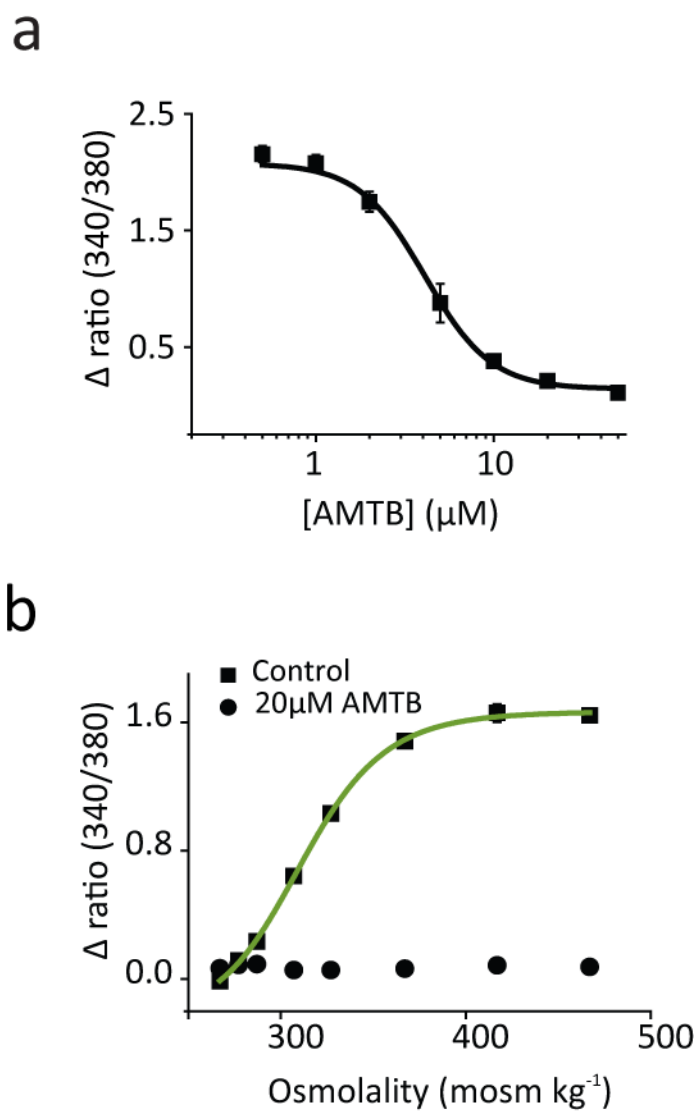

Figure 3-5 Osmolality evoked $[Ca^{2+}]_i$ responses are inhibited by AMTB

(**a**) $[Ca^{2+}]_i$ responses of mTRPM8 CHO cells to a hyperosmotic stimulus (367 mosm kg^{-1}) in the presence of increasing concentrations of a TRPM8 antagonist, AMTB (0.5-50μM). Activation of TRPM8 by a hyperosmotic solution (367 mosm kg^{-1}) was inhibited by AMTB in a concentration dependent manner, IC_{50} – 3.98± 0.25μM (n=3 independent experiments). Representative plot shown, data points are the mean ratio of triplicate wells ± SEM (**b**) AMTB (20μM) abolished hyperosmotic evoked $[Ca^{2+}]_i$ (Δ Fura-2 340/380) responses (267-367 mosm kg^{-1}). Representative plots shown, data points are the mean ratio of triplicate wells ± SEM.

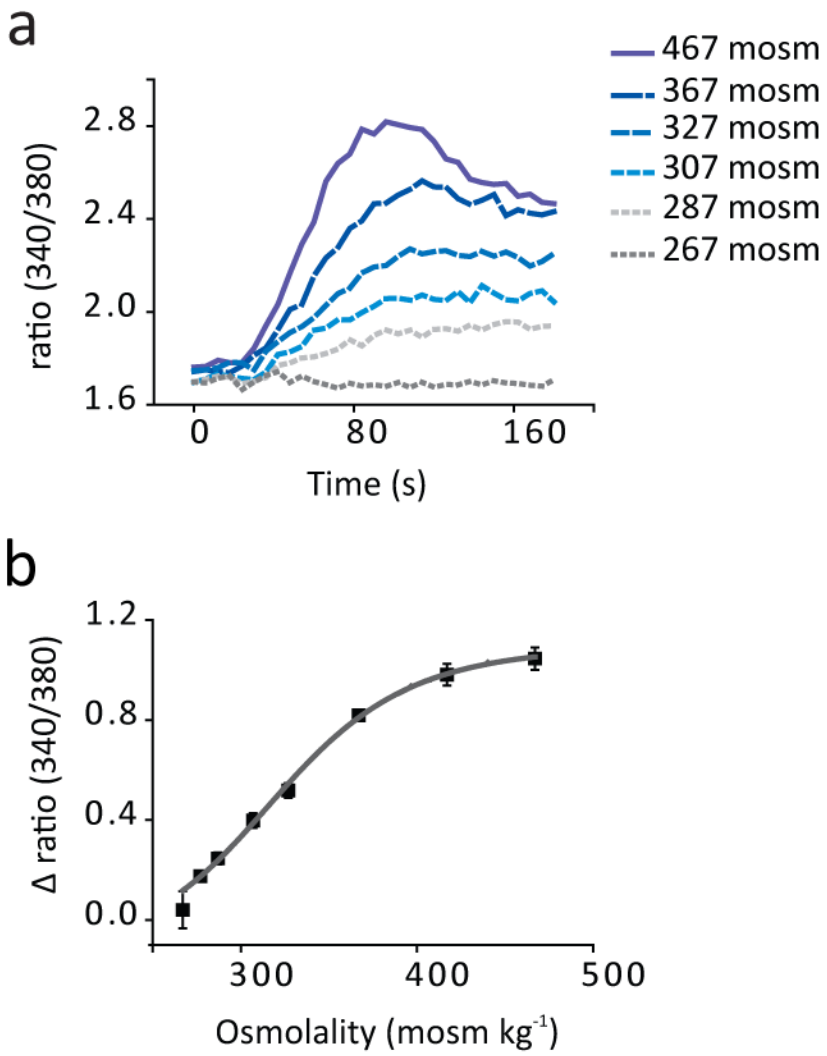

Figure 3-6 Human TRPM8 is activated by increases in osmolality

(**a**) Time courses of $[Ca^{2+}]_i$ responses elicited by challenges with different osmolalities (osmolality altered by addition of sucrose) in CHO cells transfected with human TRPM8 (hTRPM8). Baseline signals were collected before cells were challenged with osmotic solutions at 20 seconds. Traces shown are mean ratios from triplicate wells from a representative experiment (**b**) Increases in osmolality evoked $[Ca^{2+}]_i$ (Δ Fura-2 340/380) responses in hTRPM8-expressing CHO cells with an EC_{50} - 291 ± 16 mosm kg^{-1} (n=3 independent experiments). Representative plot shown, data points are the mean ratio of triplicate wells ± SEM.

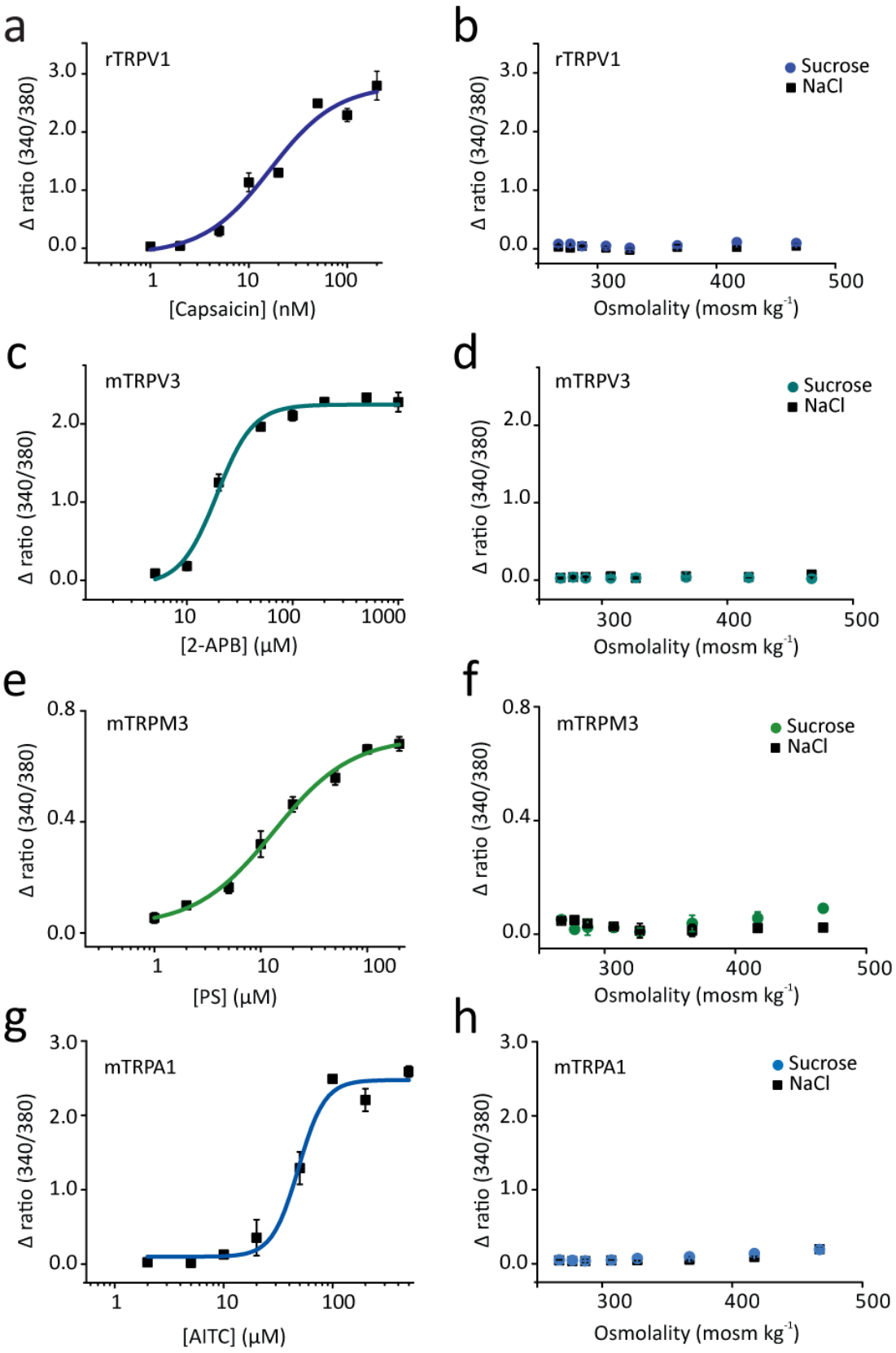
a
rTRPV1
Δ ratio (340/380)
3.0
2.0
1.0
0.0
1
10
100
[Capsaicin] (nM)
b
rTRPV1
Sucrose
NaCl
Δ ratio (340/380)
300
400
500
Osmolality (mosm kg-1)
c
mTRPV3
Δ ratio (340/380)
10
100
1000
[2-APB] (μM)
d
mTRPV3
Sucrose
NaCl
Osmolality (mosm kg-1)
e
mTRPM3
0.8
0.4
[PS] (μM)
f
mTRPM3
g
mTRPA1
[AITC] (μM)
h
mTRPA1

Figure 3-7 Other sensory neuron TRP channels are not activated by hyperosmotic solutions

Δ Fura-2 (340/380) responses of CHO cells stably transfected with (**a,b**) rat TRPV1, (**c,d**) mouse TRPV3*, (**e,f**) mouse TRPM3 (**g,h**) or mouse TRPA1. (**a-h**) Robust $[Ca^{2+}]_i/[Ba^{2+}]_i$ responses were evoked by channel agonists (Capsaicin – TRPV1, 2-APB – TRPV3, Pregnenolone Sulphate – TRPM3, Allyl isothiocyanate – TRPA1) but not by hyperosmotic solutions (made by addition of sucrose or NaCl) in 96-well plate experiments n=3 independent experiments for each cell line and treatment. Representative plots shown, data points are the mean ratio of triplicate wells ± SEM.

* In experiments examining CHO cells stably transfected with mTRPV3 (**c,d**), extracellular solutions containing $BaCl_2$ were used as a substitute for $CaCl_2$ and the $[Ba^{2+}]_i$ responses were measured.

3.5.5 Regulation of osmotic responses

3.5.5.1 Regulation by lysophospholipids and polyunsaturated fatty acids

Lysophospholipids (LPLs) and polyunsaturated fatty acids (PUFAs) are endogenous lipids liberated downstream of phospholipase A_2 (PLA_2) activation which have been shown to modulate TRPM8 channel activity. Application of LPLs has been shown to activate the TRPM8 channel whereas application of PUFAs inhibits TRPM8 channel activation by cold, and TRPM8 agonists, icilin and menthol (Abeele et al., 2006; Andersson et al., 2007). The net effect of PLA_2 inhibition has previously been observed to be inhibition of channel activity suggesting the potentiating effect of LPLs is more powerful than the inhibitory effect of PUFAs (see Figure 3-8).

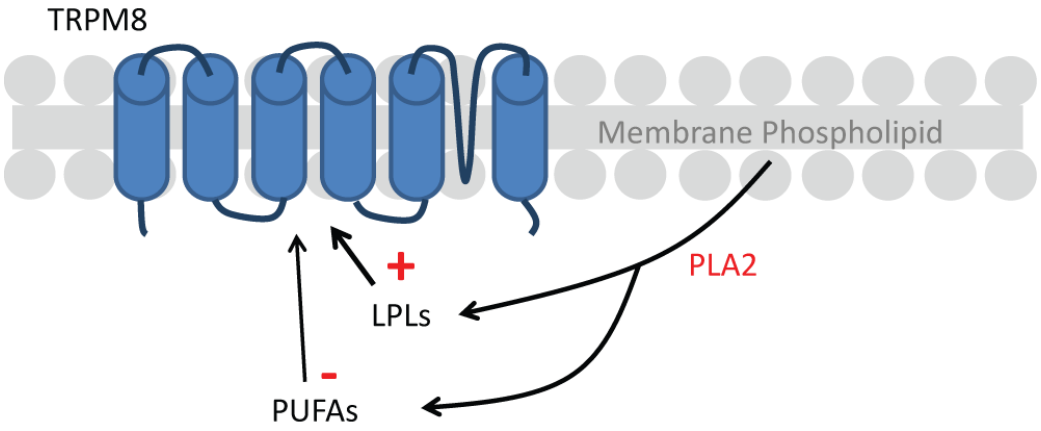

Figure 3-8 Modulation of TRPM8 by products of PLA_2

Phospholipase A_2 (PLA_2) enzymes hydrolyse the sn-2 acyl bond of membrane phospholipids releasing lysophospholipids (LPLs) and polyunsaturated fatty acids (PUFAs). Arachidonic acid (AA) is an example of PUFA which is released by PLA_2 activity. Both LPLs and PUFAs can modulate TRPM8 activity (red + indicates positive modulation of TRPM8 activity and – represents negative modulation). Observation of the effects of PLA_2 inhibition on TRPM8 activation has suggested that the potentiating effect of LPLs outweighs the negative effect exerted by PUFAs (Andersson et al., 2007).

Two main groups of intracellular PLA_2 enzyme exist, namely cytosolic PLA_2 ($cPLA_2$/group IV PLA_2) and calcium insensitive PLA_2 ($iPLA_2$/group VI PLA_2). The former is selective for phospholipids which contain arachidonic acid (AA) in the sn-2 position whilst the latter will release other fatty acids in addition to AA (Balsinde and Balboa, 2005; Six and Dennis, 2000).

In order to examine the effects of PLA_2 activation on the hyperosmotic activation of TRPM8, mouse TRPM8 CHO cells were exposed to hyperosmotic stimuli (267-467 mosm kg^{-1}) in the presence and absence of a cell permeable, non-selective PLA_2 inhibitor (N-(p-amylcinnamoyl)anthranilic acid, ACA, 1.5 hour pre-incubation) (Figure 3-9a). Hyperosmotic-evoked $[Ca^{2+}]_i$ responses were consistently reduced in cells which were treated with 10µM ACA in comparison to untreated cells, with an average reduction in maximum amplitude of 75% from 2.16 ± 0.06 Δ Fura-2 ratio to 0.53 ± 0.11 Δ Fura-2 ratio (mean ± SEM; P<0.001, t-test; n=4 independent experiments). However there was no significant change in the EC_{50} values for activation by hyperosmotic stimuli (mean ± SEM; control, 311 ± 1 mosm kg^{-1}; ACA, 400 ± 35 mosm kg^{-1}; NS, t-test; n=4 independent experiments).

To identify any regulation by lipids generated by the $iPLA_2$ isoform the effects of a cell permeable $iPLA_2$ inhibitor, bromoenol lactone (BEL), were investigated. Treatment with 20µM BEL (1.5 hour pre-incubation) resulted in a modest reduction of hyperosmotic evoked responses with an average reduction in maximal response amplitude of 27% when compared to the responses of untreated cells (from 2.16 ± 0.06 Δ Fura-2 ratio to 1.57 ± 0.07 Δ Fura-2 ratio; mean ± SEM; P<0.01, t-test; n=4 independent experiments; Figure 3-9b) and no change in the EC_{50} values for activation (mean ± SEM, control - 311 ± 1 mosm kg^{-1}; BEL – 296 ± 16 mosm kg^{-1}; NS, t-test; n=4 independent experiments).

These results demonstrate that hyperosmotic activation of TRPM8 can be modulated by intracellular lipids downstream of PLA_2 activation. These results suggest that increased PLA_2 activity and the consequential increased production of LPLs (and PUFAs) could lead to activation of TRPM8 at lower osmolalities than under normal conditions.

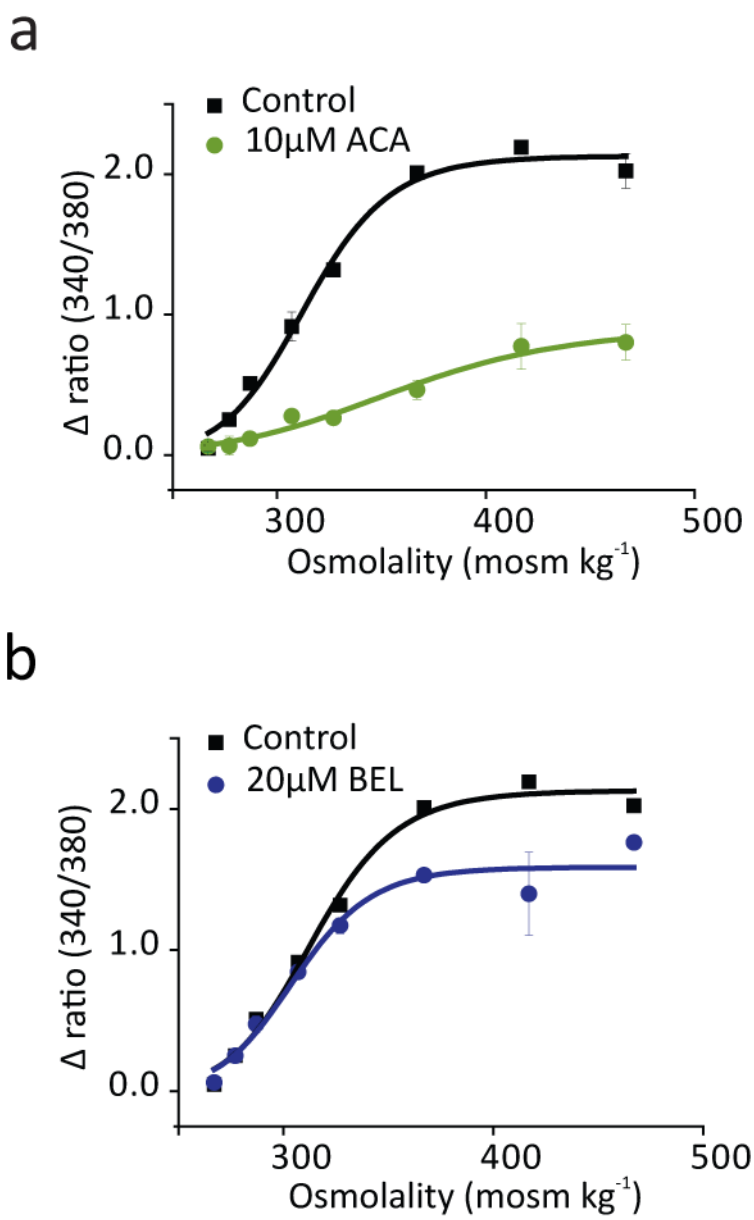

Figure 3-9 PLA_2 modulates osmotic responses

(**a**) The non-selective PLA_2 inhibitor, ACA (1.5 hour pre-incubation) supressed $[Ca^{2+}]_i$ responses evoked by hyperosmotic solutions (267-367 mosm kg^{-1}) in CHO cells transfected with mTRPM8 (n=4 independent experiments). Representative plots shown, data points are the mean ratio of triplicate wells ± SEM (**b**) Treatment with the selective $iPLA_2$ inhibitor, BEL (1.5 hour pre-incubation) lead to a modest reduction in the hyperosmotic evoked $[Ca^{2+}]_i$ responses (267-367 mosm kg^{-1}) of mTRPM8 CHO cells (n=4 independent experiments). Representative plots shown, data points are the mean ratio of triplicate wells ± SEM.

3.5.5.2 Regulation by pathways downstream of PLC activation

Activation of receptors coupled to Gαq proteins, by mediators such as bradykinin and histamine, has been shown to inhibit TRPM8 activity (Zhang et al., 2012). Receptor activation triggers phospholipase C (PLC)-mediated hydrolysis of the membrane phospholipid phosphatidylinositol 4,5-bisphosphate (PIP_2) releasing the second messengers; diacyl-glycerol (DAG) and inositol 1,4,5-trisphosphate (IP_3) as hydrolysis products (Figure 3-10). Previous reports have demonstrated that PIP_2 can activate the TRPM8 channel in the absence of chemical or thermal stimuli and that in the presence of menthol or cold PIP_2 acts as a positive modulator of TRPM8 activation (Liu and Qin, 2005; Rohács et al., 2005).

In order to investigate the relationship between PIP_2 hydrolysis and hyperosmotic activation of TRPM8, the hyperosmotic-evoked $[Ca^{2+}]_i$ responses of mouse TRPM8 CHO cells treated with an activator of PLC, *m*-3M3FBS (10µM, 15 minute pre-incubation) were examined and compared to the $[Ca^{2+}]_i$ responses of untreated cells. *m*-3M3FBS treated cells exhibited a significantly reduced $[Ca^{2+}]_i$ response to hyperosmotic stimuli in comparison to untreated cells, with an average reduction in maximum amplitude of 68% from 1.73 ± 0.16 Δ Fura-2 ratio to 0.55 ± 0.06 Δ Fura-2 ratio (mean ± SEM; P<0.01, t-test; n=3 independent experiments; Figure 3-11a). Furthermore the EC_{50} value for activation was shifted to significantly higher osmolalities in the presence of *m*-3M3FBS (mean ± SEM; control, 297 ± 4 mosm kg^{-1}; *m*-3M3FBS, 355 ± 6 mosm kg^{-1}; p<0.01, t-test; n=3 independent experiments; Figure 3-11a). These findings demonstrate that the breakdown of PIP_2 negatively modulates hyperosmotic activation of TRPM8, and are consistent with reports on the effects of PIP_2 on other modes of TRPM8 activation.

Next the effects of *m*-3M3FBS on osmotic responses were examined in mouse TRPM8 CHO cells co-treated with a PLC inhibitor, U71322 (5µM, 15 minute pre-incubation). The presence of a PLC inhibitor was not able to reverse the inhibition achieved with *m*-3M3FBS treatment. Remarkably the inhibition was exacerbated and the $[Ca^{2+}]_i$ responses to hyperosmotic stimuli were completely abolished (average reduction of 82% from 1.73 ± 0.16 Δ Fura-2 ratio to 0.32 ± 0.10 Δ Fura-2 ratio; mean ± SEM; P<0.01, t-test; n=3 independent experiments; Figure 3-11b).

In order to ascertain whether U73122 treatment alone was having an effect on the hyperosmotic responses of the cells, the hyperosmotic-evoked $[Ca^{2+}]_i$ responses of mouse

TRPM8 CHO cells treated with U73122 alone (5µM, 15 minute pre-incubation) were examined and compared to the $[Ca^{2+}]_i$ responses of untreated cells. Interestingly, treatment with U73122 lead to a reduction in the hyperosmotic evoked $[Ca^{2+}]_i$ responses (average reduction of 25% from 1.73 ± 0.16 Δ Fura-2 ratio to 1.29 ± 0.77 Δ Fura-2 ratio; mean ± SEM; NS, t-test; n=3 independent experiments Figure 3-11c). However there was no significant change in the EC_{50} values for activation (control - 297 ± 4 mosm kg^{-1}; *m*-3M3FBS – 314 ± 12 mosm kg^{-1}; mean ± SEM; NS, t-test; n=3 independent experiments; Figure 3-11c).

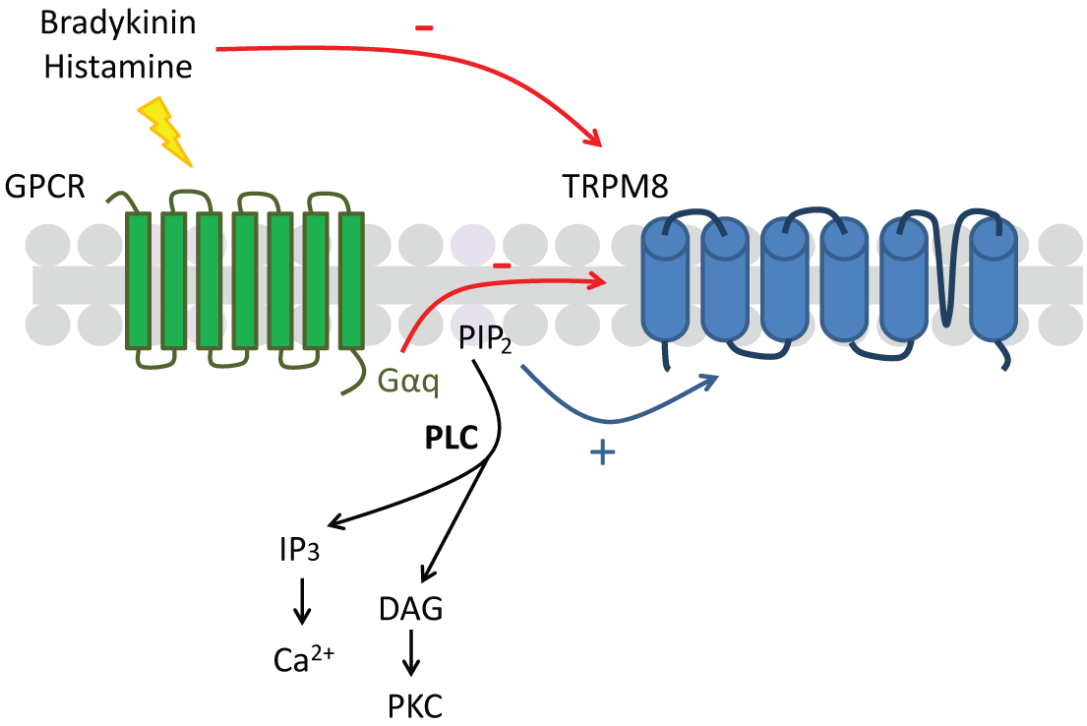

Figure 3-10 Modulation of TRPM8 by Gαq-coupled GPCRs and PLC

Activation of Gαq coupled receptors by agonists such as bradykinin and histamine results in activation of the G protein by allowing the exchange of a molecule of GDP for GTP at the Gα subunit (which is inactive when bound to GDP). The activated Gαq-GTP monomer and a βγ dimer (not shown) dissociate from the receptor, allowing Gαq to activate phospholipase C (PLC). PLC cleaves phosphatidylinositol 4,5-bisphosphate (PIP_2) into diacyl glycerol (DAG) and inositol 1,4,5-trisphosphate (IP_3). IP_3 releases Ca^{2+} from intracellular stores and DAG activates protein kinase C (PKC). Activation of Gαq coupled receptors by agonists has been shown to negatively modulate (red arrow) TRPM8 activity whilst PIP_2 has been shown to positively modulate (blue arrow) TRPM8 activity (Rohács et al., 2005; Zhang et al., 2012). Activated Gαq proteins (GTP bound) have also been shown to have a direct inhibitory effect on TRPM8 activity (Zhang et al., 2012).

a

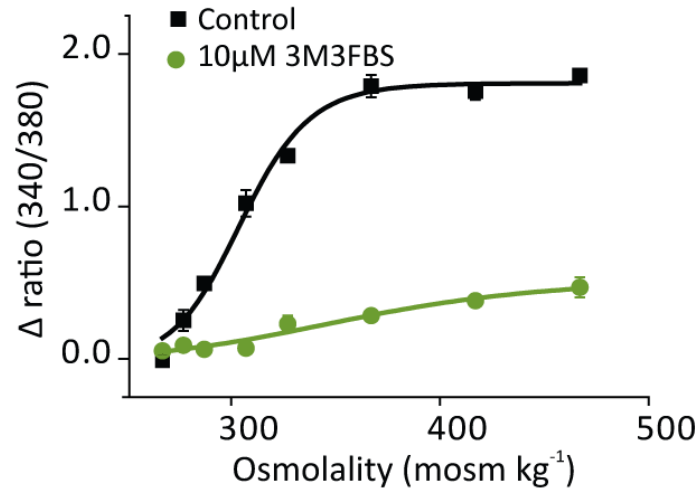
Control
10µM 3M3FBS
2.0
1.0
0.0
Δ ratio (340/380)
300
400
500
Osmolality (mosm kg-1)

b

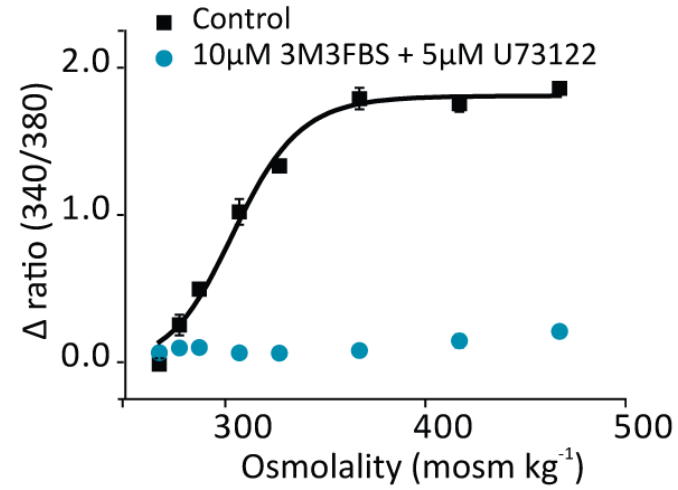
Control
10µM 3M3FBS + 5µM U73122
2.0
1.0
0.0
Δ ratio (340/380)
300
400
500
Osmolality (mosm kg-1)

c

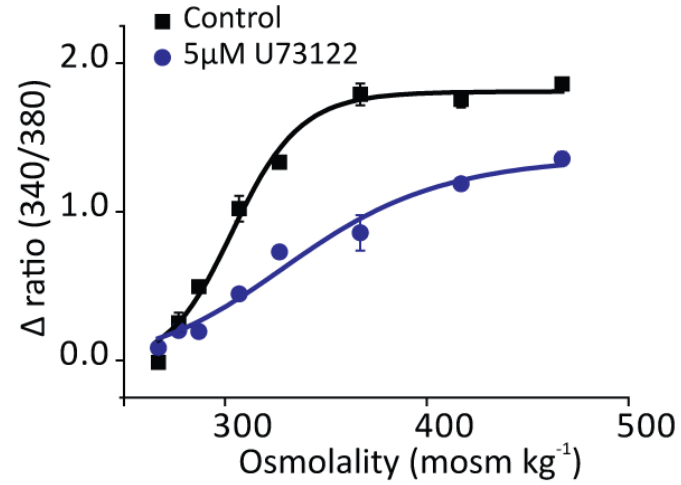
Control
5µM U73122
2.0
1.0
0.0
Δ ratio (340/380)
300
400
500
Osmolality (mosm kg-1)

Figure 3-11 PLC modulates osmotic responses

(**a**) The effects of a PLC activator *m*-3M3FBS on hyperosmotically evoked $[Ca^{2+}]_i$ responses of mTRPM8-transfected CHO cells. *m*-3M3FBS (10µM, 15 minute pre-incubation) inhibited responses evoked by hyperosmotic solutions (267-467 mosm kg^{-1}) in mTRPM8 CHO cells (mean reduction in maximum amplitude of 68% from 1.73 ± 0.16 Δ Fura-2 ratio to 0.55 ± 0.06 Δ Fura-2 ratio; mean ± SEM; P<0.01, t-test; n=3 independent experiments). Representative plot shown, data points are the mean ratio of triplicate wells ± SEM (**b**) The effects of co-treatment with *m*-3M3FBS (10µM) and a PLC inhibitor, U73122 (5µM, 15 minute pre-incubation) on hyperosmotic activation of mTRPM8 CHO cells. Co-treatment of cells with *m*-3M3FBS and U71322 abolished $[Ca^{2+}]_i$ responses evoked by hyperosmotic solutions (mean reduction in maximum amplitude of 82% from 1.73 ± 0.16 Δ Fura-2 ratio to 0.32 ± 0.10 Δ Fura-2 ratio; mean ± SEM; P<0.01, t-test; n=3 independent experiments). Representative plot shown, data points are the mean ratio of triplicate wells ± SEM (**c**) The effects of U71322 alone on hyperosmotically-induced $[Ca^{2+}]_i$ mTRPM8 CHO cells. Treatment of cells with U73122 (5µM, 10 minute pre-incubation) alone lead to a reduction in the hyperosmotic evoked $[Ca^{2+}]_i$ responses (mean reduction in maximum amplitude of 25% from 1.73 ± 0.16 Δ Fura-2 ratio to 1.29 ± 0.77 Δ Fura-2 ratio; mean ± SEM; NS, t-test; n=3 independent experiments). Representative plot shown, data points are the mean ratio of triplicate wells ± SEM.

3.5.5.3 Regulation by pathways downstream of Src family tyrosine kinase activation

Hypo- and hypertonic conditions have been associated with tyrosine kinase activation (Alessandri-Haber et al., 2003; Junger et al., 1997; Xu et al., 2003). Tyrosine phosphorylation of TRPV4 channels by Src family tyrosine kinases was observed to be crucial for cellular transduction of hypotonic stimuli and nociceptive responses to hypertonic saline injection mediated by TRPV4 (Alessandri-Haber et al., 2005; Xu et al., 2003).

In order to examine whether inhibition of Src family tyrosine kinases modulates TRPM8 activity, the responses of mouse TRPM8 CHO cells treated with a selective inhibitor of Src family tyrosine kinases, PP2 (10µM, 15 minute pre-incubation) to menthol (0.2-50µM) were studied. PP2 treatment had no effect on the menthol-evoked $[Ca^{2+}]_i$ responses of mouse TRPM8 CHO cells (Figure 3-12a). The maximum amplitudes of the $[Ca^{2+}]_i$ responses of the PP2 treated cells were not significantly different from the maximum amplitudes of untreated cells (control – 4.21 ± 0.07 Δ Fura-2 ratio; PP2 – 3.97 ± 0.20 Δ Fura-2 ratio; mean ± SEM; NS, t-test; n=3 independent experiments). Furthermore there was no change in EC_{50} values for activation (control – 4.28 ± 0.47µM; PP2 – 5.61 ± 1.73µM; mean ± SEM; NS, Mann-Whitney U test; n=3 independent experiments).

Next the effect of PP2 treatment on the hyperosmotic induced responses of mouse TRPM8 CHO cells was tested. Hyperosmotic stimuli evoked similar responses in untreated and PP2 treated mouse TRPM8 CHO cells (Figure 3-12b). The maximum amplitudes of the $[Ca^{2+}]_i$ responses of the untreated and treated cells were not significantly different (control, 1.86 ± 0.21 Δ Fura-2 ratio; PP2, 1.64 ± 0.12 Δ Fura-2 ratio; mean ± SEM; NS, Mann-Whitney U test; n=3 independent experiments) and there was no change in EC_{50} values for activation (control, 307 ± 6 mosm kg^{-1}; PP2, 311 ± 2 mosm kg^{-1}; mean ± SEM; NS, t-test; n=3 independent experiments).

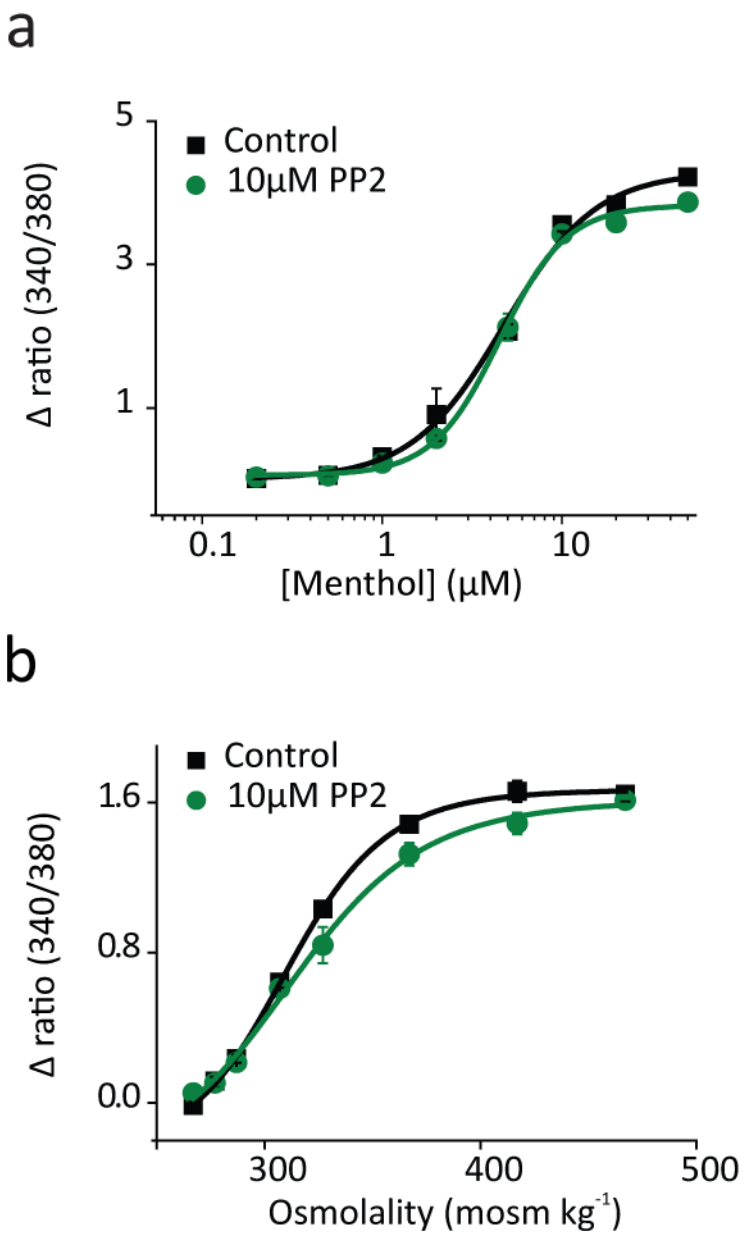

Figure 3-12 Src family tyrosine kinases do not modulate TRPM8 activity

(**a**) The effect of a selective Src family tyrosine kinase inhibitor PP2 on menthol-evoked $[Ca^{2+}]_i$ responses of mTRPM8 CHO cells. PP2 (10µM, 15 minute pre-incubation) had no effect on the $[Ca^{2+}]_i$ responses evoked by menthol (0.2-50µM) in mouse TRPM8 CHO cells. Representative plot shown, data points are the mean ratio of triplicate wells ± SEM (**b**) The effect of PP2 (10µM, 15 minute pre-incubation) on hyperosmotic activation of mTRPM8 CHO cells. Mouse TRPM8 CHO cells treated with PP2 displayed similar hyperosmotic-evoked $[Ca^{2+}]_i$ responses to untreated cells. Representative plot shown, data points are the mean ratio of triplicate wells ± SEM.

3.5.6 Interactions between cold and osmolality

3.5.6.1 Osmolality modulates temperature activation of heterologously expressed TRPM8

TRPM8 is an established cold-transduction channel and cool temperatures can modulate voltage- and menthol-dependent activation of TRPM8. In order to investigate the relationship between osmotic activation of TRPM8 and temperature, the hyperosmotically-evoked $[Ca^{2+}]_i$ responses of TRPM8 CHO cells were examined at different temperatures. A clear temperature sensitivity was noted as the relationship between osmolality and the evoked $[Ca^{2+}]_i$ responses was increasingly shifted to the right as the temperature was increased towards 37°C, resulting in significantly raised EC_{50} values for activation (25°C, 318 ± 5 mosm kg^{-1}; 29°C, 345 ± 6 mosm kg^{-1}; 33°C, 362 ± 6 mosm kg^{-1}; 37°C, 365 ± 8 mosm kg^{-1}; mean ± SEM; n=9 independent experiments; Figure 3-13). As temperature increased there was also an accompanying decrease in maximum amplitude of the osmotic responses (25°C, 1.16 ± 0.09 Δ Fura-2 ratio; 29°C, 0.95 ± 0.06 Δ Fura-2 ratio; 33°C, 0.72 ± 0.07 Δ Fura-2 ratio; 37°C, 0.52 ± 0.07 Δ Fura-2 ratio; mean ± SEM; n=9 independent experiments; Figure 3-13a).

Next the effects of osmolality on the temperature threshold for TRPM8 activation were examined. Microscope-based imaging experiments were conducted which allowed the temperature of the perfusate to be changed in a controlled manner. Populations of mouse TRPM8 CHO cells were exposed to cooling temperature ramps (~37-20°C) at different osmolalities and the thresholds of their responses were determined by plotting the log mean Fura-2 (340/380) ratio against temperature (Figure 3-14b).

In an extracellular solution with a physiologically normal osmolality (~307 mosm kg^{-1}), TRPM8 CHO cells responded to a cooling ramp with an increase in $[Ca^{2+}]_i$ at an average threshold temperature of 27.2 ± 1.0°C, (mean ± SEM, n=4 coverslips). Reducing the osmolality of the external solution to 227 mosm kg^{-1} lowered the average threshold temperature to 25.9 ± 0.1°C (mean ± SEM; n=4 coverslips) while increasing osmolality (517 mosm kg^{-1}) elevated the average threshold temperature to 31.9 ± 0.1°C (mean ± SEM; NS; comparison to 307 mosm kg^{-1}; ANOVA followed by Dunnett's T3 test; n= 4-5 coverslips; Figure 3-15a).

A relationship between osmolality of the extracellular solution and temperature activation thresholds can be seen clearly when observing pseudocoloured images of experiments examining cell temperature thresholds at two different osmolalities (Figure 3-15b). In a

population of mouse TRPM8 CHO cells perfused with a 367 mosm kg^{-1} solution, many cells are activated at 27°C in comparison to only a small fraction of cells in a population perfused with a 267 mosm kg^{-1} solution. These experiments demonstrate that increasing the extracellular osmolality raises the threshold for TRPM8 activation towards more physiologically relevant temperatures.

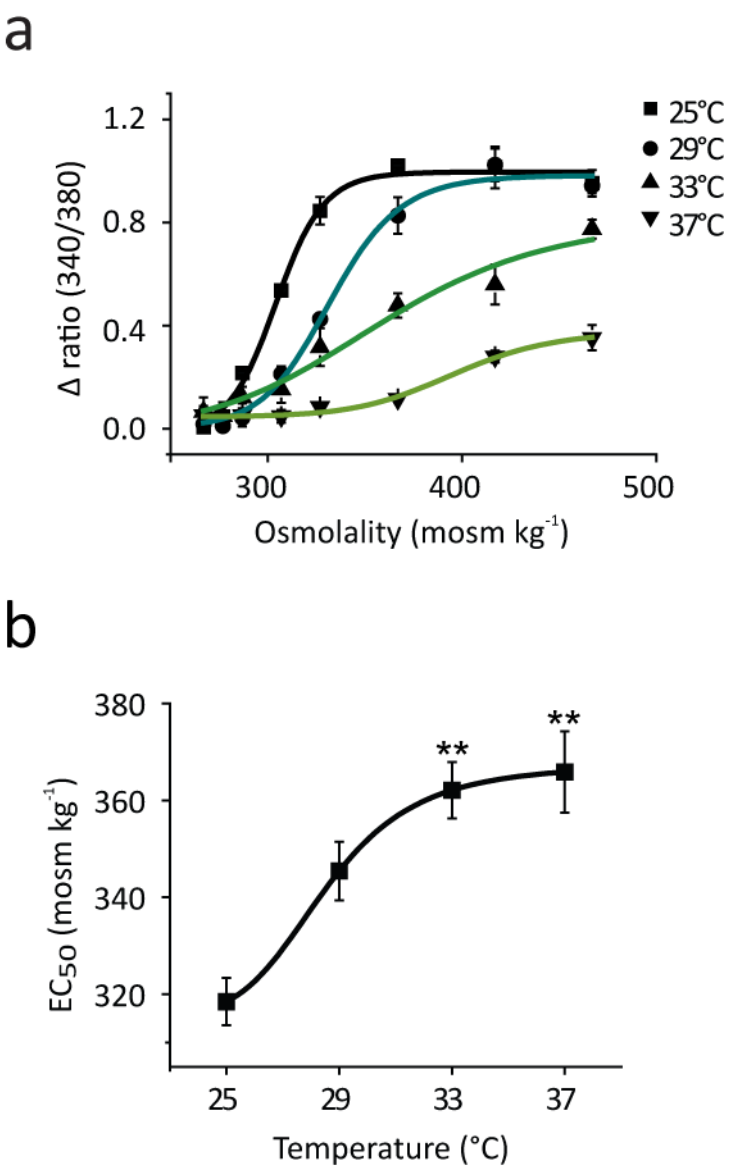

Figure 3-13 Cool temperatures potentiate osmotic activation of TRPM8

(**a**) $[Ca^{2+}]_i$ Responses of mTRPM8 CHO cells to hyperosmotic stimuli (267-467 mosm kg^{-1}) at increasing temperatures (25-37°C). Osmolality-evoked $[Ca^{2+}]_i$ responses were shifted to the right as the temperature was increased with an accompanying depression in maximum amplitude (25°C, 1.16 ± 0.09 Δ Fura-2 ratio; 29°C, 0.95 ± 0.06 Δ Fura-2 ratio; 33°C, 0.72 ± 0.07 Δ Fura-2 ratio**; 37°C, 0.52 ± 0.07 Δ Fura-2 ratio***; mean ± SEM; P values represent comparison to 25°C.** P < 0.01, *** P <0.001; ANOVA followed by Tukey's HSD test; n=9 independent experiments). (**b**) The EC_{50} for activation of mTRPM8 CHO cells by hyperosmotic solutions was increased as the temperature was elevated (mean ± SEM; P values represent comparison to 25°C.** P < 0.01; Kruskal-Wallis followed by Dunn-Bonferroni's pairwise post-hoc test; n=9 independent experiments).

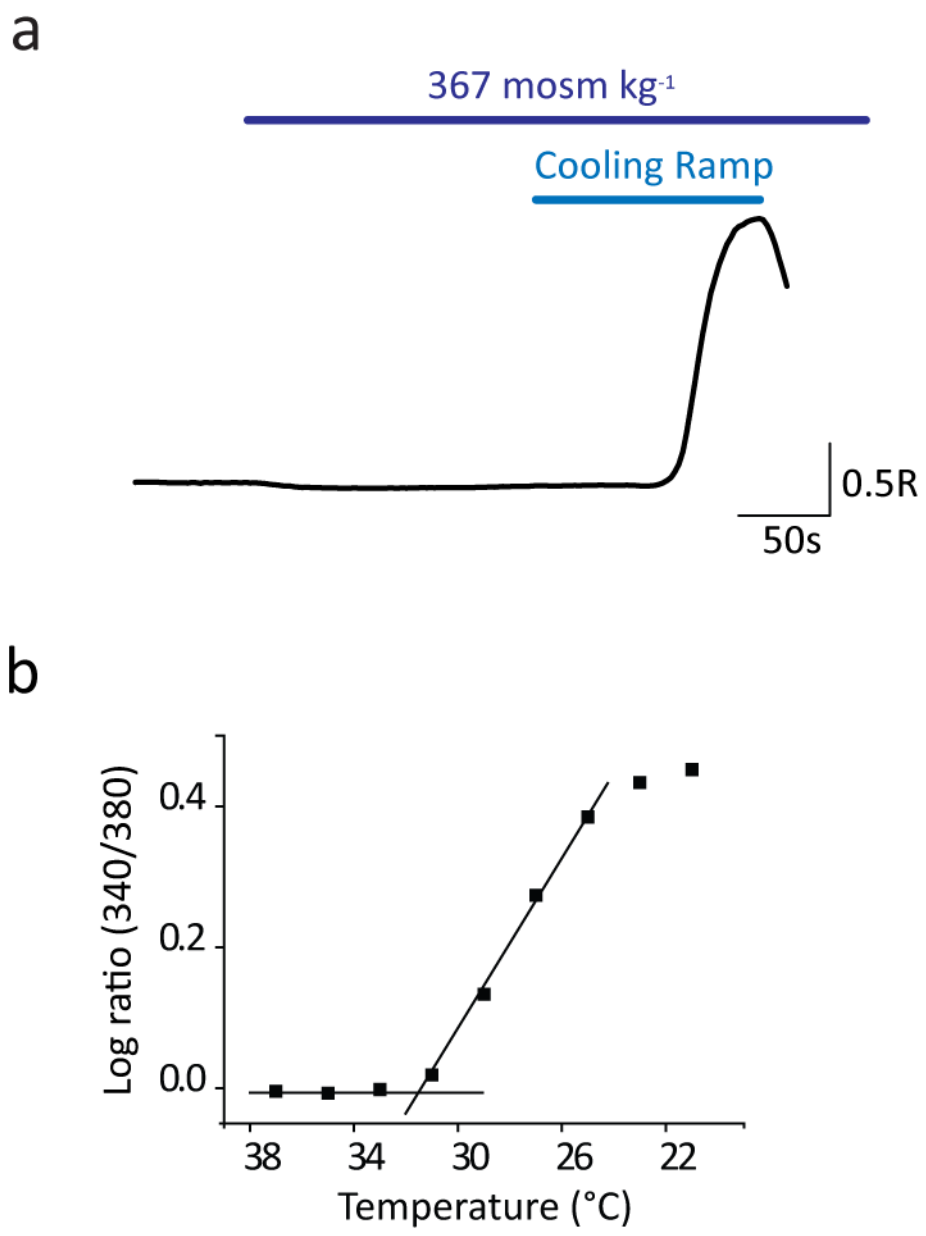

Figure 3-14 Cooling activates mouse TRPM8 CHO cells

(**a**) Trace illustrating a $[Ca^{2+}]_i$ response evoked by a cooling temperature ramp (37-21°C) in a mTRPM8 CHO cell population. In this experiment the osmolality of perfusate was changed from 267 mosm kg^{-1} to 367 mosm kg^{-1} 3 minutes prior to the cold ramp (**b**) Temperature activation thresholds were determined by plotting the log Fura-2 (340/380) ratio against temperature. The temperature at which the log ratio begins to deviate from baseline is used as the temperature activation threshold. The graph illustrates the threshold determination for the population of mouse TRPM8 CHO cells shown in (a).

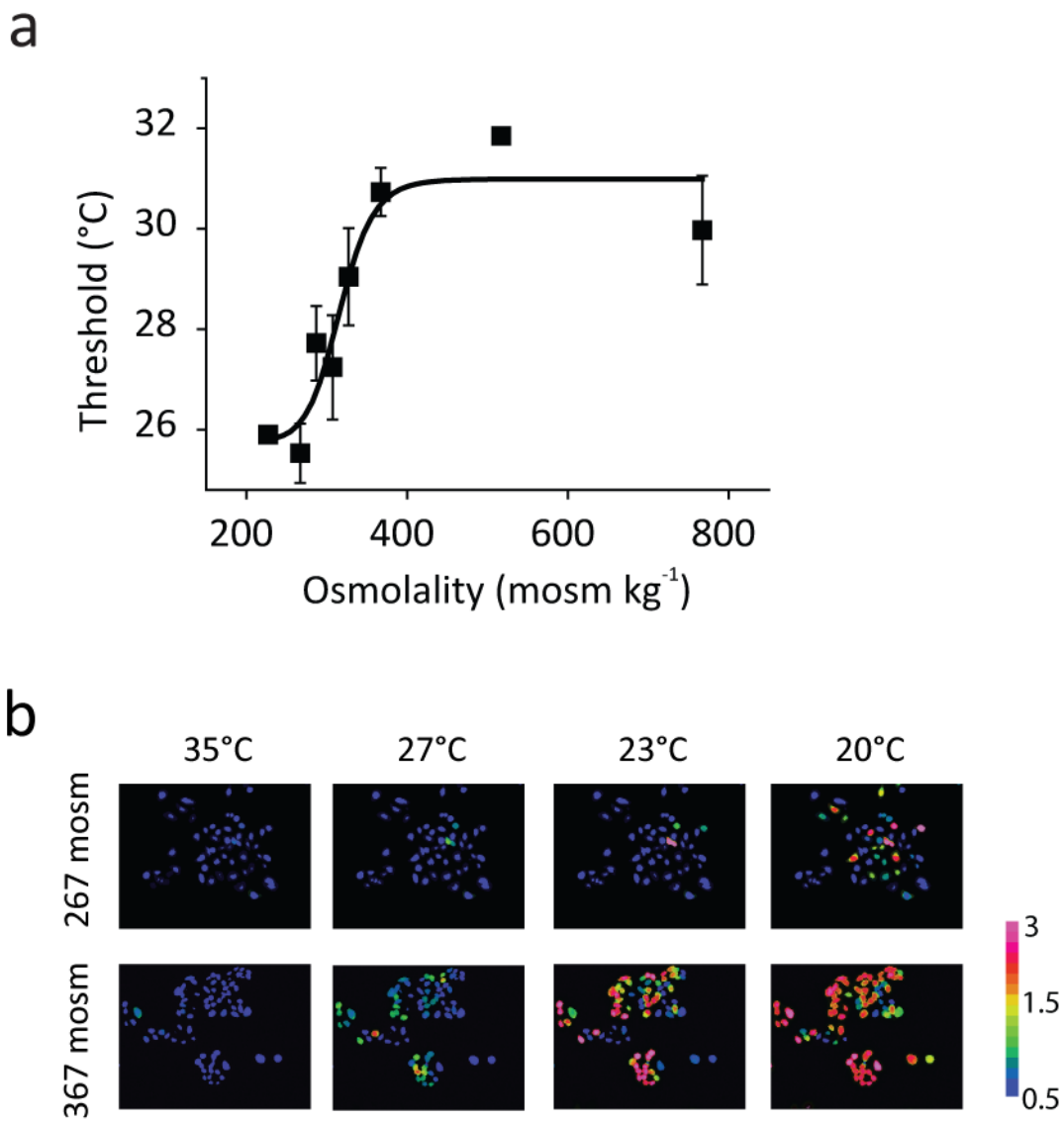

Figure 3-15 Osmolality influences temperature thresholds of heterologously expressed TRPM8

(**a**) Temperature thresholds of mTRPM8 CHO cells were determined at different osmolalities. Activation thresholds of mTRPM8 CHO cells were increased when cells were challenged with solutions of higher osmolalities (mean ± SEM; NS; comparison to 307 mosm kg^{1}; ANOVA followed by Dunnett's T3 test; n= 4-5 coverslips, 2-3) (**b**) Pseudocoloured images illustrating the Fura-2 responses of mouse TRPM8 CHO cell populations to 35, 27, 23 and 20°C; the upper and lower panels represent cell populations which were perfused with 267 and 367 mosm kg^{-1} solutions, respectively.

3.5.6.2 Osmolality modulates temperature activation of DRG neurons

An interaction between osmolality and temperature thresholds for cold activation was also seen in sensory neurons. TRPM8 is natively expressed in 5-10% of DRG neurons (McKemy et al., 2002; Peier et al., 2002b), so microscope-based imaging experiments similar in nature to the experiments conducted on heterologously expressed TRPM8 were conducted on preparations of rat DRG neurons to allow $[Ca^{2+}]_i$ to be monitored in individual neurons

Isolated rat DRG neuron cultures were exposed to two consecutive cooling ramps (~37-18°C) and the temperature thresholds of individual cold-sensitive neurons for both cooling ramps were determined using the method previously described (Figure 3-16b). In control experiments cells were superfused with a 267 mosm kg^{-1} solution during both cooling ramps, while in other experiments cells were perfused with a 267 mosm kg^{-1} solution during the first cooling ramp before being perfused with a solution of a higher osmolality (367 or 517 mosm kg^{-1}) and exposed to the second cooling temperature ramp (Figure 3-16a).

Under control conditions, without a change in osmolality, it was noted that temperature thresholds of neurons were shifted to lower temperatures for the second cold ramp, suggesting some degree of desensitization (average reduction in temperature threshold of 1.3 ± 0.3°C; mean ± SEM; n= 38 neurons; Figure 3-16c). However, under conditions where osmolality was increased to 367 mosm kg^{-1} for the second cold challenge no reduction was evident and temperature thresholds of both cold-evoked responses were similar (average increase in temperature threshold of 0.1 ± 0.2°C; mean ± SEM; n= 85 neurons; Figure 3-16c). In experiments where the osmolality during the second cold challenge was increased even further (517 mosm kg^{-1}), the activation thresholds were elevated towards warmer temperatures (average increase in temperature threshold of 1.6 ± 0.4°C; mean ± SEM; n=55 neurons; Figure 3-16c).

A subsequent application of a maximally effective concentration of the TRPM8 agonist Icilin (1μM) caused an increase in $[Ca^{2+}]_i$ in the majority (57%, n=115/178) of cold sensitive neurons; consistent with expression of TRPM8 in this neuronal subset. These data demonstrate that osmolality can influence temperature sensitivity in sensory neurons in addition to recombinant cells.

a

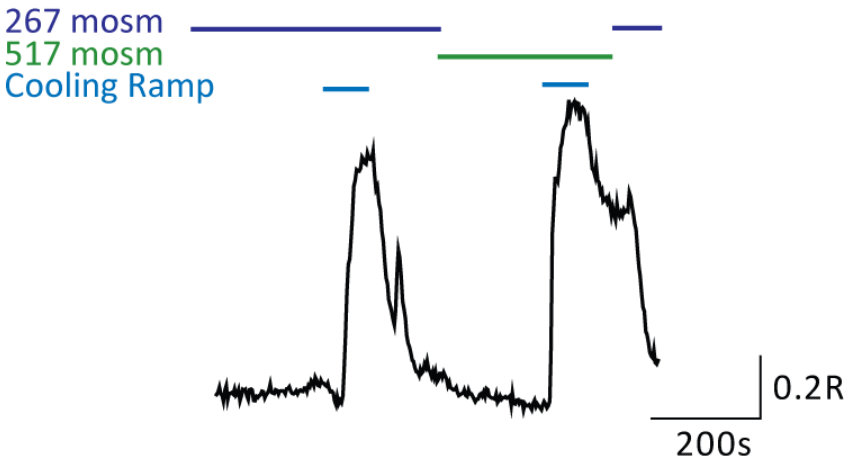
267 mosm
517 mosm
Cooling Ramp
0.2R
200s

b

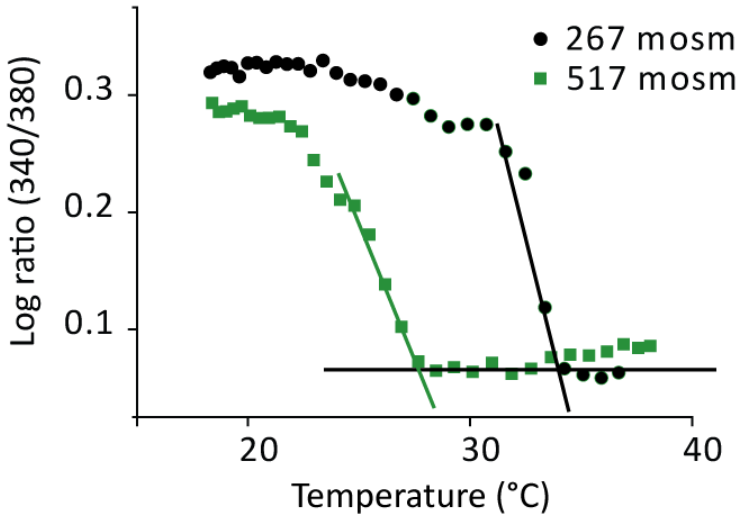
267 mosm
517 mosm
Log ratio (340/380)
0.3
0.2
0.1
20
30
40
Temperature (°C)

c

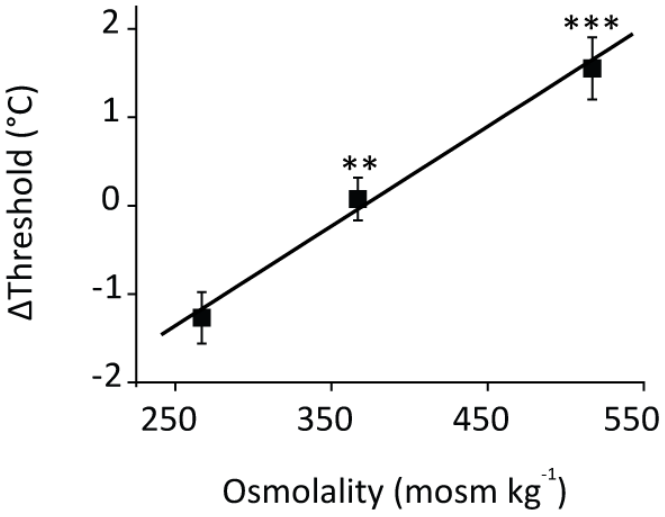
ΔThreshold (°C)
2
1
0
-1
-2
**
***
250
350
450
550
Osmolality (mosm kg-1)

Figure 3-16 Osmolality influences temperature thresholds of TRPM8-expressing DRG neurons

(**a**) Trace illustrating the $[Ca^{2+}]_i$ (Fura-2 340/380) response of a rat DRG neuron to two consecutive cooling ramps (~37-18°C). The neuron was perfused with a 267 mosm kg^{-1} solution during the first cold challenge and this solution was replaced with a solution of higher osmolality (567 mosm kg^{-1}) 3 minutes prior to the second cold challenge (**b**) Graph depicting the threshold analysis for the cooling-evoked responses. Increasing the osmolality of the perfusate from 267 to 517 mosm kg^{-1} shifted the neuron activation threshold to a warmer temperature. (**c**) Graph showing temperature threshold changes (from first temperature threshold to second temperature threshold) at different osmolalities. Negative values represent a shift in temperature threshold towards colder temperatures and positive values represent a shift to warmer temperature thresholds. Neurons exposed to hyperosmotic solutions prior to a second cold challenge exhibited shifts in activation thresholds to warmer temperatures (mean ± SEM; P values represent comparison to 267 mosm kg^{-1}; ** $P < 0.01$, *** $P < 0.001$; Kruskal-Wallis followed by Dunn-Bonferroni's pairwise post-hoc test; 267 mosm kg^{-1}, n= 38 neurons, 10, 2; 367 mosm kg^{-1}, n= 85 neurons, 13, 7; 517 mosm kg^{-1}, n= 55 neurons, 10, 6).

3.6 Discussion

3.6.1 TRPM8 is a cellular osmosensor functioning at physiologically relevant osmolalities

The studies presented in this chapter have established a role for TRPM8 as a mammalian cellular osmosensor. TRPM8 is expressed in a population of osmosensitive neurons and functional TRPM8 channels are required for neuronal responses to hyperosmotic stimuli as the responses of cultured DRG and TG neurons to hyperosmotic stimulation were inhibited by AMTB and were absent in neurons from *Trpm8*$^{-/-}$ mice. In addition, the studies presented here have shown that the sensory neuron environment is not required for osmotic activation of TRPM8. The expression of TRPM8 in a recombinant cell line resulted in robust $[Ca^{2+}]_i$ responses to hyperosmotic solutions which were blocked by a TRPM8 antagonist, and absent in untransfected cells, strongly suggesting that TRPM8 expression is sufficient to confer osmosensitivity.

TRPM8 is sensitive to changes in osmolality and the increases in osmolality required to induce responses are modest. The average EC_{50} for activation of mouse TRPM8 (318 ± 5 mosm kg^{-1}) is close to the physiological set point for the extracellular fluid of mice which lies around 311 mosm kg^{-1} (Bourque, 2008). For human TRPM8 the EC_{50} for activation was slightly lower (291 ± 16 mosm kg^{-1}) and this correlates well with a lower physiological osmolality in humans of around 288 mosm kg^{-1} (Bourque, 2008). These data demonstrate that TRPM8 is highly sensitive to increases in osmolality in the physiological range, making its osmosensing capabilities highly relevant in a physiological setting.

Activation of TRPM8 by hyperosmotic solutions was independent of the solute used to alter extracellular osmolality. Hyperosmotic solutions made with sucrose and NaCl activated TRPM8 with a similar potency. This demonstrates that the $[Ca^{2+}]_i$ responses evoked by hyperosmotic solutions are not due to an agonist action of a sugar or NaCl on the TRPM8 expressing cells. Instead the responses are a reaction of the TRPM8 channel to an increased concentration of extracellular solutes.

In experiments where NaCl was added to increase the osmolality of the extracellular solution, the maximum amplitudes of the $[Ca^{2+}]_i$ responses evoked were consistently lower than in experiments using sucrose. It is likely that this is due to the increased extracellular Na^+ ion concentration when NaCl is used as the hyperosmotic agent. TRPM8 is a non-selective cation channel and both Na^+ and Ca^{2+} ions will flow through activated channels.

The Na^+ ions will compete with Ca^{2+} ions for entry into the cell thus resulting in a lower influx of Ca^{2+} at higher external Na^+ concentrations. As well as a difference in the maximum amplitude of the responses induced by hyperosmotic NaCl solutions, the time-course profiles of the $[Ca^{2+}]_i$ responses induced by sucrose and NaCl were also different. The Fura-2 (340/380) responses evoked by high osmolality sucrose solutions (367 and 467 mosm kg^{-1}) began to decline after reaching a maximum peak response. However, this pattern was not observed in the Fura-2 (340/380) responses evoked by high osmolality NaCl solutions, where responses began to plateau after reaching a maximum peak response. This could be explained by the fact that sucrose solutions evoked larger $[Ca^{2+}]_i$ responses than NaCl solutions. High $[Ca^{2+}]_i$ concentration reached in sucrose experiments may have led to Ca^{2+} dependent desensitisation of TRPM8 (Ca^{2+} mediated activation of PLC and subsequent PIP_2 depletion) which is not evident with reduced influxes of Ca^{2+} (Almaraz et al., 2014).

3.6.2 Other sensory neuron TRP channels are insensitive to increases in osmolality

Deviations in extracellular osmolality above the physiological set-point (up to 467 mosm kg^{-1}) did not evoke responses in cell lines transfected with other sensory neuron TRP channels. An N-terminal splice variant of TRPV1 has been implicated in the responses of central osmosensory neurons to increases in osmolality and *Trpv1*$^{-/-}$ mice have been shown to have impaired physiological (vasopressin release) and behavioural (water consumption) responses to hyperosmotic conditions (Ciura and Bourque, 2006; Naeini et al., 2006). Furthermore, a study by Nishihara and colleagues examining HEK293 cells transfected with full-length TRPV1, reported that TRPV1 was sensitive to hyperosmotic stimulation (330-350 mosm kg^{-1}) at 36°C (Nishihara et al., 2011). The osmosensitivity of TRPV1 was temperature-dependent and hyperosmotic stimulation (350 mosm kg^{-1}) of TRPV1 at 24°C did not evoke $[Ca^{2+}]_i$ responses (Nishihara et al., 2011). The hyperosmotic responses described in the report by Nishihara and colleagues (2011) were slow in onset, beginning ~2 minutes after stimulus application and are therefore likely not to be the result of direct channel activation but rather activation of a second messenger pathway. In contrast activation of TRPM8 induces rapid elevations in $[Ca^{2+}]_i$ which are evident seconds after application of a hyperosmotic stimulus.

Interestingly, TRPV1 heterologously expressed in a CHO cell line was not sensitive to increases in extracellular osmolality over the range which activated TRPM8. Moreover, it has been reported that osmotic activation of the TRPV1 N-terminal splice variant (expressed in *Xenopus* oocytes) does not generate inward currents and a role of the splice

variant as an inhibitory modulator of TRPV1 responses to noxious heat, protons, capsaicin and resiniferatoxin (RTX) has been suggested (Eilers et al., 2007).

A study by Zhang and colleagues (2008) reported that hyperosmotic solutions (330-600 mosm kg^{-1}) induced $[Ca^{2+}]_i$ responses in HEK293 cells heterologously expressing rat TRPA1 but did not evoke responses in mock-transfected cells. However, solutions with an osmolality greater than 600 mosm kg^{-1} would have been needed to determine a maximal response and these could not be used due to non-specific effects; therefore an EC_{50} for activation could not be determined (Zhang et al., 2012). The findings presented in this chapter demonstrate that mouse TRPA1 heterologously expressed in a CHO cell line is not sensitive to increases in osmolality over the range which activates TRPM8. Furthermore the sensitivity of TRPM8 to hyperosmotic stimuli is greater than that demonstrated for TRPA1 in the study by Zhang *et al*, as TRPM8 is maximally activated by osmolalities just over 367 mosm kg^{-1}.

A human variant of TRPM3 has previously been reported to be sensitive to changes in extracellular osmolality (Grimm et al., 2003). Grimm and colleagues (2003) reported that TRPM3 was activated by decreases in osmolality and inhibited by increases in osmolality. In the current study, no changes in $[Ca^{2+}]_i$ levels were noted in CHO cells transfected with mouse TRPM3 when extracellular osmolality was increased, consistent with a channel which is insensitive to hyperosmotic stimuli. Furthermore, expression of another sensory neuron TRP channel, TRPV3, in a CHO cell line had no effect on osmosensitivity. Moreover, although TRPV4 has been implicated in PGE_2 sensitised responses to hypertonic stimuli, studies (not presented here) have shown that TRPV4 expressed in a HEK293 cell line is activated by the TRPV4 agonist, GSK1016790A, but not by hyperosmotic stimuli (N. Vastani).

It is also important to note that neurons from animals lacking functional TRPM8 channels do not respond to hyperosmotic stimulation, suggesting that at the sensory neuron level TRPM8 is the predominant sensor of hyperosmotic stimuli.

3.6.3 Osmotic responses are modulated by PLA_2 and PLC but not Src family tyrosine kinases

3.6.3.1 Modulation by PLA_2

Inhibition of PLA_2 activity reduced $[Ca^{2+}]_i$ responses evoked by hyperosmotic stimuli in cells transfected with mouse TRPM8. These findings suggest that, as found for activation of TRPM8 by cold, icilin and menthol (Abeele et al., 2006; Andersson et al., 2007), PLA_2 activity is needed for maximal activation of the channel.

It is possible that a product liberated by PLA_2 activation is required for this potentiating effect. Lysophospholipids produced by activation of PLA_2 enzymes have previously been shown to stimulate TRPM8 activity (Abeele et al., 2006; Andersson et al., 2007). The actions of lysophospholipids on TRPM8 have been shown to depend on the length of the fatty acyl chain and the properties of the head group. These lipid products could bind to the TRPM8 channel directly to exert an effect or they could interfere with other proteins or the plasma membrane indirectly affecting TRPM8.

Targeting both the cytosolic ($cPLA_2$) and calcium-insensitive PLA_2 ($iPLA_2$) enzyme subtypes led to a greater reduction in hyperosmotically-evoked responses than targeting the $iPLA_2$ subtype alone, suggesting that hyperosmotic activation of TRPM8 can be regulated by both enzyme subsets; or that block of $iPLA_2$ by the selective inhibitor, BEL, is not as effective as the block achieved with the non-selective inhibitor, ACA. The findings presented in this chapter demonstrate that PLA_2 is tonically active and this tonic activity is required for full activation of TRPM8 by hyperosmotic stimuli. Furthermore the results shown are consistent with a more powerful positive modulatory role of lysophospholipids over the negative modulatory role of PUFAs on TRPM8 activity evoked by cold, icilin and menthol.

It has been argued that the effect of ACA on the activity of TRPM8 and other TRP channels is due to a direct effect of the compound on the channels rather than a result of PLA_2 activation and downstream signalling effects. In a study by Kraft and colleagues, investigating the effects of ACA on a closely related channel, TRPM2, block of TRPM2 by ACA could only be achieved when the compound was applied extracellularly and not when the compound was applied to the cytoplasmic side (Kraft et al., 2006). Furthermore the authors showed that although ACA was able to inhibit TRPM2 and TRPM8 channels this inhibition was not achieved with structurally unrelated blockers of PLA_2. In contrast, a study by Andersson and colleagues (2007) found that PLA2 inhibitors which are structurally

unrelated to ACA (e.g. ETYA and BEL) inhibit TRPM8 activation by cold and icilin. Consistent with these findings, both BEL and ACA inhibited hyperosmotic activation of TRPM8, suggesting that the inhibitory effects seen are at least in part PLA_2 dependent.

3.6.3.2 Modulation by PLC

Activation of TRPM8 by hyperosmotic stimuli was significantly inhibited by the PLC activator *m*-3M3FBS suggesting that the PIP_2 concentration modulated the TRPM8 osmotic response. This finding is consistent with studies which have reported that TRPM8 sensitivity is regulated/controlled by PIP_2 availability (Liu and Qin, 2005; Rohács et al., 2005). Stimulation of receptors which activate the PLCγ isoform and therefore induce PIP_2 hydrolysis, such as the TrkA receptor and the platelet-derived growth factor (PDGF) β-receptor, reduced menthol-induced currents in TRPM8 expressing cells (Liu and Qin, 2005; Rohács et al., 2005). Moreover, stimulation of a Gq-coupled GPCR receptor, M1, which results in PIP_2 depletion via activation of the PLCβ isoform, also significantly inhibited menthol-induced currents in TRPM8 expressing cells (Rohács et al., 2005). Studies have also shown that application of purified PIP_2 or a PIP_2 analogue to the cytosolic side of TRPM8-expressing oocytes reverses the rundown of menthol-induced channel activity which occurs after establishment of an inside-out patch configuration (Liu and Qin, 2005; Rohács et al., 2005). In addition exposure of the cytosolic membrane of TRPM8-expressing cells to purified PIP_2 or a PIP_2 analogue caused channel activity in the absence of any other stimuli. Furthermore, the second messengers DAG and IP_3 which are liberated by PLC have been reported to have no effect on TRPM8 channel activity (Almaraz et al., 2014; Rohács et al., 2005).

Notably, in the current study, the effects of 3M3FBS-induced PLC activation could not be reversed by the PLC inhibitor U73122 which caused inhibition of the hyperosmotic responses when applied alone. In a study by Zhang and colleagues (2012) it was reported that activation of TRPM8 could be inhibited by the Gαq linked GPCR agonist bradykinin. This inhibition was not reversed by U73122 leading the authors to conclude that the process was PLC-independent (Zhang et al., 2012). This effect of bradykinin was explained by a direct inhibitory effect of Gαq on TRPM8 (Zhang et al., 2012).

There are three main subfamilies of PLC enzymes: PLCβ, PLCγ and PLCδ. Gαq linked GPCRs are coupled to the PLCβ subfamily of enzymes, whilst activation of the PLCγ subfamily is coupled to receptor tyrosine kinases, and it is likely that Ca^{2+} influx/high intracellular Ca^{2+}

activates the PLCδ subfamily of enzymes (Rohacs, 2009). The PLC-activating compound, *m*-3M3FBS, used in the experiments described in the results section stimulates the β2, β3, γ1, γ2, and δ1 isoforms of PLC (Bae et al., 2003).

Surprisingly, a study examining the effects of the U73122 on human PLC isoforms discovered that U73122 (10µM) increased the activity of hPLCβ3, hPLCβ2 and hPLCγ1 isoenzymes (Klein et al., 2011). Furthermore U73122 had no action on PLCδ1. Activation of a PLC isozyme by U73122 with a consequent hydrolysis of PIP_2 could explain the increased inhibition of hyperosmotic responses when cells were pre-treated with *m*-3M3FBS and U73122, and the inhibitory effects of U73122 alone.

Alternatively, a direct action of U73122 on TRPM8 or another protein involved in the osmosensory transduction pathway, could be responsible for the inhibitory effects with U73122. U73122 contains an electrophilic maleimide group which reacts with thiol-containing nucleophiles such as cysteine (Wilsher et al., 2007). U73122 could thus modify TRPM8 activity or the activity of other proteins involved in the TRPM8 osmotransduction pathway by covalently modifying cysteine residues.

3.6.3.3 Src family tyrosine kinases have no effect on osmotic activation of TRPM8

Hypo- and hypertonicity can result in the activation of Src kinases (Evans, 2008). Moreover, phosphorylation of TRPV4 by Src kinases has been suggested to be required for hypotonicity-induced activation of TRPV4 expressed in HEK293 cells (Xu et al., 2003).

The Src family of tyrosine kinases comprises a group of 9 tyrosine kinase enzymes: Src, Yes, Fyn, Fgr, Blk, Lck, Hck, Lyn, and Yrk; three of which are ubiquitously expressed (Src, Fyn and Yes) (Cohen, 2005). Incubation of cells expressing TRPM8 with a non-selective Src family tyrosine kinase inhibitor, PP2, was unable to modulate TRPM8 activation by hyperosmotic stimulation or by the prototypical TRPM8 agonist menthol. These findings suggest that hyperosmotic activation of TRPM8 does not occur through and is not reliant upon tyrosine phosphorylation by Src family kinases.

In contrast to the findings presented in this chapter, a recently published study showed that increases in $[Ca^{2+}]_i$ in human TRPM8 expressing SH-SY5Y cells evoked by a TRPM8 agonist (WS-12) could be inhibited by PP2 (Morgan et al., 2014). Notably, the effects of PP2 on TRPM8-expressing HEK293 cells could not be studied due to TRPM8-independent increases in $[Ca^{2+}]_i$. These findings suggest that the effects of PP2 are dependent on the cell line being used and this could explain the discrepancy between the findings presented in

the report by Morgan and colleagues and the results discussed in this chapter (the findings reported in this chapter are based on experiments using CHO cells). Alternatively, the difference in results could be due to the use of a different species of TRPM8 or the different mode of activation used to stimulate TRPM8 channels. Moreover, Morgan and colleagues reported half maximal inhibition of WS-12 responses by PP2 at 24μM. At such high concentrations it is possible that PP2 is beginning to inhibit non-Src tyrosine kinases (Hanke et al., 1996).

3.6.4 How does a hyperosmotic stimulus activate TRPM8?

TRPM8 is activated by increases in extracellular osmolality, but precisely how the channel is stimulated by changes in osmotic pressure is not clear. During hyperosmotic stimulation cell shrinkage occurs with deformation of the membrane and cell volume is decreased. For this reason, hyperosmotic solutions are often used to probe for mechanosensitive channels (Delmas et al., 2011). Activation of TRPM8 by hyperosmotic stimulation could be a mechanical process. Scaffolds within the phospholipid bilayer which are tethered to TRPM8, could pull the channel into an open conformation during cell shrinkage and cause the channel to close when physiological osmolality is restored. Studies examining centrally-located osmosensitive neurons have found that in contrast to non-osmosensitive neurons, the membrane surface area does not change with fluctuations in cell volume (Zhang and Bourque, 2003). This finding indicates that changes in cell volume are accompanied by transformations in membrane shape, and it has been suggested that these changes could be involved in the mechanical gating of osmosensory channels (Bourque, 2008). A recent study demonstrated that disruption of microtubules by nocodazole abolished hyperosmotically-induced and mechanosensory-induced (negative pressure to the recording pipette) increases in membrane conductance and action potential firing in centrally-located osmosensory neurons (Prager-Khoutorsky et al., 2014). Tubulin was found to interact with TRPV1 channels (purported to be an osmosensory transduction channel in centrally located osmosensitive neurons) on the surface of osmosensory neurons and treatment with nocodazole decreased the number of sights of interaction. Furthermore, proteins which blocked presumptive TRPV1 binding domains for tubulin (located within the C terminal), diminished mechanically-evoked increases in membrane conductance and action potential firing in isolated osmosensory neurons (Prager-Khoutorsky et al., 2014). The authors of the study suggest that microtubules cause activation of TRPV1 via a pushing force which is exerted during cell shrinkage.

The opening of TRPM8 channels could be secondary to activation of a separate mechanosensitive/osmosensitive protein or an intracellular pathway. A study examining mechanosensory responses of TRPC6, established that TRPC6 channels are not directly mechanosensitive and that responses mediated by TRPC6 require an interaction with GPCRs (Mederos y Schnitzler et al., 2008). These authors showed that mechanical stimulation (hypotonic solutions, positive pipette pressure) causes caused ligand-independent activation of mechanosensitive Gq-linked GPCRs which are coupled to TRPC6 channels in a G-protein and PLC-dependent manner. A multimeric protein complex could exist for TRPM8, whereby a mechanosensitive or osmosensitive protein gates the TRPM8 channel.

Studies using a HeLa cell line have shown that during hyperosmotic conditions (high extracellular NaCl or sucrose), phosphatidylinositol 4-phosphate 5-kinase β isoform (PIP5KIβ) is recruited to the plasma membrane and activated (by serine/threonine dephosphorylation) (Yamamoto et al., 2006). PIP5KIβ phosphorylates PI4P leading to increased levels of PIP_2. Interestingly, this increase in PIP_2 levels is not observed when a cell-permeable reagent which raises osmolality but does not induce cell shrinkage is used (Yamamoto et al., 2006). As previously discussed PIP_2 is a positive modulator of TRPM8 activity and can activate the channel in the absence of other stimuli (Liu and Qin, 2005; Rohacs, 2009). PIP_2 could be a component of an osmosensory transduction pathway which results in activation of TRPM8. The findings presented in this chapter have shown that activation of PLC causes an almost complete inhibition of hyperosmotically induced TRPM8 responses. These results establish a relationship between PLC linked breakdown of PIP_2 and hyperosmotic activation of TRPM8 which could be consistent with an osmosensory transduction pathway involving PIP_2. Alternatively, PIP_2 could be essential for TRPM8 channel function and activation of TRPM8 might be prevented by low levels of PIP_2.

3.6.5 A relationship exists between cold and osmotic responses

TRPM8 is well characterised as a thermosensitive channel which is activated by cool temperatures (Almaraz et al., 2014; McKemy et al., 2002; Peier et al., 2002b). Activation of TRPM8 by hyperosmotic stimuli is positively modulated by decreases in temperature. Cool temperatures shifted the EC_{50} for activation to lower osmolalities and increased the maximum amplitudes of hyperosmotic responses. Moreover, osmotic activation of TRPM8 was associated with warmer temperature activation thresholds. Hyperosmotic stimuli raised temperature thresholds closer to estimates for physiological temperatures of the

skin and cornea, organs which are innervated with TRPM8-expressing nerve afferents (Dhaka et al., 2008; Parra et al., 2010; Takashima et al., 2007). Furthermore, activation thresholds of cold-sensitive sensory neurons were also increased to warmer temperatures in hyperosmotic conditions, suggesting a similar interaction between cold and osmotic responses for natively expressed TRPM8 channels.

Although the majority of cold-sensitive sensory neurons responded to the TRPM8 agonist icilin, not all did. This discrepancy could be due false-negative identification of icilin responders. Icilin responses are typically slow oscillations in $[Ca^{2+}]_i$ that occur with a variable latency which can sometimes hamper the identification of responding neurons during the limited observation period. Furthermore, all neurons were exposed to two prior cold challenges before being exposed to icilin and previous studies have shown that icilin responses are prone to desensitisation (Chuang et al., 2004).

A previous study has identified expression of TRPM8 channels on sensory nerves innervating the superficial epithelial layers of the cornea (Parra et al., 2010). The report proposed that TRPM8 channels expressed on cold-sensing neurons in the cornea can regulate lacrimation by detecting the decreases in temperature which occur at the ocular surface due to evaporative cooling during inter-blink periods. The study found that *Trpm8*$^{-/-}$ mice had a significantly lower basal tearing rate than WT mice and that increases in corneal temperature lead to significantly decreased tear production in WT but not *Trpm8*$^{-/-}$ mice (Parra et al., 2010).

During inter-blink periods a decrease in temperature will also be accompanied by an increase in extracellular osmolality. This change will be exacerbated in conditions where the osmolality of the ocular fluid is already higher, for example in patients with dry-eye syndrome. Therefore it is possible that combined activation of TRPM8 by decreased temperature and increased osmolality is required for excitation of corneal afferent neurons during evaporation of the ocular film. A study by Hirata and Oshinsky (2012) confirmed that the responses (increase in firing rate) of rat corneal afferents to 'dry' stimuli (removal of a well containing artificial tears enclosing an entire anterior eye and removal of excess artificial tears using filter paper in anesthetised rats) could not be entirely accounted for by corneal temperature fluctuations (Hirata and Oshinsky, 2012). Furthermore, they found that application of the TRPM8 antagonist BCTC (20µM) significantly inhibited corneal afferent 'dry' responses; suggesting a key role for TRPM8 in corneal responses to 'dry' sensations.

3.7 Conclusion

TRPM8 functions as a cellular osmosensor in addition to its already established roles as a thermosensor and receptor for cooling compounds. It is able to detect subtle fluctuations in extracellular osmolality around the physiological norm. Hyperosmotic responses mediated by TRPM8 can be modulated by activation of phospholipase enzymes and temperature. This novel role for TRPM8 as an osmosensory transduction channel could have implications for TRPM8 channels expressed in areas which are exposed to variations in both osmolality and temperature.

Chapter 4. TRPM3 is a sensory-neuron expressed, heat-sensitive channel which is modulated by activation of GPCRs

4.1 Introduction

4.1.1 Introduction to TRPM3

TRPM3 is one member of the melastatin TRP family which has not been extensively studied. Proteins encoded by the TRPM3 gene form non-selective cation channels which are widely expressed in mammalian tissues. TRPM3 is activated by the endogenous neurosteroid pregnenolone sulphate (PS), which has been utilised as a pharmacological tool for channel characterisation and as a probe for TRPM3 expression (Wagner et al., 2008). Expression of TRPM3 has been observed in the mammalian central nervous system and sensory neuron ganglia, and studies have suggested roles for TRPM3 in thermosensing and nociception (Jang et al., 2012; Kunert-Keil et al., 2006; Lee et al., 2003; Oberwinkler et al., 2005; Staaf et al., 2010; Vandewauw et al., 2013; Vriens et al., 2011).

4.1.2 TRPM3 gene

The TRPM3 gene transcript encodes a large number of isoforms which occur predominantly through alternative splicing (Oberwinkler and Philipp, 2014). Six different splice variants (a-f) of the human TRPM3 gene were identified by Lee and colleagues (2003). The TRPM3a variant was found to localise to the plasmalemmal compartment of HEK293 cells overexpressing the channel, as well as to intracellular compartments (Lee et al., 2003). Grimm and colleagues (2003) described another human TRPM3 variant, composed of 1325 amino acid residues (later referred to as $TRPM3_{1325}$ variant), which possessed a shorter carboxyl terminus and longer amino terminus than the variants previously described and was activated by cell swelling (Grimm et al., 2003).

A further 5 splice variants, TRPM3α1-5, from the mouse TRPM3 gene were described by Oberwinkler and colleagues (2005). The sequences were between 1699-1721 amino acids long and were encoded by exons 1, 3-7, and 9-28 (Oberwinkler et al., 2005). Similar to the human a-f variants, the described mouse splice variants lack an amino terminal sequence encoded by exon 2 which is present in the $hTRPM3_{1325}$ variant; however, they contain a novel amino terminal sequence encoded by exon 1 which is not present in any of the previously discovered TRPM3 variants (Oberwinkler et al., 2005). A high amino acid identity (~97%) exists between the mouse TRPM3 proteins (α1-5) described by Oberwinkler and colleagues (from residue 156 onwards), and the human TRPM3 (a-f) proteins described by Lee and colleagues. Each mouse variant corresponds to an analogous human variant (mouse TRPM3α1- TRPM3c, mTRPM3α2- hTRPM3a, mTRPM3α3- hTRPM3b, mTRPM3α4-

hTRPM3e and mTRPMα5- hTRPM3d). These findings demonstrate that splice events are highly conserved between mice and humans (Oberwinkler et al., 2005).

4.1.3 Expression of TRPM3

Analysis of TRPM3 RNA and protein levels has revealed expression of TRPM3 in a wide range of mammalian tissues (see Table 4-1 and Table 4-2 for summaries). The human TRPM3a variant is predominately expressed in the human kidney but is also present in the brain, spinal cord and testis (Lee et al., 2003). Further analysis of TRPM3a expression in the human kidney established expression in the collecting tubular epithelium in the medulla, medullary rays, and periglomerular regions (Lee et al., 2003). More detailed analysis of expression within the brain revealed the highest levels of TRPM3a transcripts were present in the cerebellum, locus coeruleus, posterior hypothalamus and substantia nigra.

Expression of the $TRPM3_{1325}$ transcript was also found in the human kidney and brain, and additionally in human ovaries and pancreas (Grimm et al., 2003). $TRPM3_{1325}$ RNA was also present in the mouse brain but not in the mouse kidney (Grimm et al., 2003). Further examination of TRPM3 expression in immunoblotting studies found bands of 160 kDa (calculated mass of TRPM3 is 157 kDa) in human kidney and brain, and bovine kidney. In the mouse brain samples, bands were detected around 130 and 220 kDa which were attributed to alternatively spliced variants of the gene (Grimm et al., 2003). Expression of TRPM3 in the human brain, pancreas and kidney was confirmed in a study by Fonfria and colleagues (2006). This study also identified high levels of TRPM3 expression in the pituitary and lower levels of expression in adipose tissue, prostate and bone.

One study examining expression of TRPM3 mRNA in mice, established expression of TRPM3 transcripts at multiple brain sites including; the dentate gyrus, the intermediate lateral septal nuclei, the indusium griseum and the tenia tecta (Oberwinkler et al., 2005). However, the strongest expression of TRPM3 was present in the epithelial cells of the choroid plexus. In addition to TRPM3 expression in the central nervous system, TRPM3 transcripts were also found in the mouse eye (Oberwinkler et al., 2005).

A separate study confirmed expression of TRPM3 in the mouse brain with high expression levels in the cerebrum, cerebellum, basal ganglia and hippocampus of C57Bl/10 mice (Kunert-Keil et al., 2006). Interestingly, analysis of TRPM3 expression in other mouse strains revealed that the high expression levels of TRPM3 observed in the cerebrums of C57Bl/10 mice were not seen in tissue from NOD or Balb/c mice (Kunert-Keil et al., 2006). In

corroboration with findings from Grimm and colleagues, extensive expression of TRPM3 was not found in the mouse kidney (Kunert-Keil et al., 2006).

TRPM3 has been found to be expressed at glutamatergic synapses in neonatal Purkinje cells (Zamudio-Bulcock et al., 2011). Activation of TRPM3 by a TRPM3 agonist (pregnenolone sulphate) was reported to increase glutamate release and this effect was found to be inhibited by a TRPM3 antagonist (mefenamic acid). TRPM3 expression has also been identified in pancreatic β cells and treatment of these cells with a TRPM3 agonist (pregnenolone sulphate) resulted in intracellular Ca^{2+} signals and was found to potentiate glucose-induced insulin secretion (Wagner et al., 2008)

TRPM3 expression has been identified in the rodent aorta and pulmonary artery, and has been reported to modulate contraction of the mouse aorta (Naylor et al., 2010; Yang et al., 2006). In the vascular smooth muscle cells of the human saphenous vein, TRPM3 has been reported to mediate a Ca^{2+} entry pathway. In proliferating vascular smooth muscle cells, inhibition of TRPM3 (by a TRPM3-blocking antibody) resulted in increased IL-6 secretion suggesting that TRPM3 activity is negatively coupled to secretion of some cytokines (Naylor et al., 2010). Furthermore, TRPM3 expression has been identified in fibroblast-like synoviocytes of rheumatoid arthritis patients; here TRPM3 activity has been reported to be negatively coupled to the secretion of hyaluronan (Ciurtin et al., 2010). TRPM3 expression has also been reported in oligodendrocytes (Hoffmann et al., 2010).

Importantly for the current study, TRPM3 expression has also been identified in rodent sensory neurons in the dorsal root, trigeminal and nodose ganglia (Jang et al., 2012; Nealen et al., 2003; Staaf et al., 2010; Vandewauw et al., 2013; Vriens et al., 2011).

Table 4-1 Human tissues expressing TRPM3

Tissue	Detection Method	Reference
Brain	RT-qPCR/Western blot + Northern blot + RT-PCR/ RT-qPCR	(Fonfria et al., 2006; Grimm et al., 2003; Lee et al., 2003)
- ***Cerebellum***	RT-qPCR	(Lee et al., 2003)
- ***Locus coeruleus***	RT-qPCR	(Lee et al., 2003)
- ***Posterior hypothalamus***	RT-qPCR	(Lee et al., 2003)
- ***Substantia nigra***	RT-qPCR	(Lee et al., 2003)
Spinal Cord	RT-qPCR	(Lee et al., 2003)
Kidney	RT-qPCR/ Western blot + Northern blot + RT-PCR /RT-qPCR	(Fonfria et al., 2006; Grimm et al., 2003; Lee et al., 2003)
- ***Collecting tubule epithelium***	RT-qPCR	(Lee et al., 2003)
- ***Medullary rays***	RT-qPCR	(Lee et al., 2003)
- ***Periglomerular regions***	RT-qPCR	(Lee et al., 2003)
Pancreas	RT-qPCR/ RT-PCR	(Fonfria et al., 2006; Grimm et al., 2003)
Pituitary gland	RT-qPCR	(Fonfria et al., 2006)
Ovaria	RT-PCR	(Grimm et al., 2003)
Testis	RT-qPCR	(Lee et al., 2003)
Prostate	RT-qPCR	(Fonfria et al., 2006)
Bone	RT-qPCR	(Fonfria et al., 2006)
Adipose tissue	RT-qPCR	(Fonfria et al., 2006)
Saphenous vein	RT-PCR + Function	(Naylor et al., 2010)

Table 4-2 Mouse/rat tissues expressing TRPM3

Tissue	Detection Method	Reference
Brain	Western blot + Northern blot + RT-PCR/RT-PCR/RT-qPCR/Northern blot	(Grimm et al., 2003; Jang et al., 2012; Kunert-Keil et al., 2006; Oberwinkler et al., 2005)
- ***Forebrain***	RT-qPCR/ISH	(Kunert-Keil et al., 2006; Oberwinkler et al., 2005)
○ ***Cerebrum***	RT-qPCR	(Kunert-Keil et al., 2006)
▪ ***Basal ganglia***	RT-qPCR	(Kunert-Keil et al., 2006)
▪ ***Hippocampus***	RT-qPCR	(Kunert-Keil et al., 2006)
• ***Dentate gyrus***	ISH	(Oberwinkler et al., 2005)
▪ ***Septal nuclei***	ISH	(Oberwinkler et al., 2005)
▪ ***Indusium griseum***	ISH	(Oberwinkler et al., 2005)
▪ ***Tenia tecta***	ISH	(Oberwinkler et al., 2005)
- ***Cerebellum***	RT-qPCR	(Kunert-Keil et al., 2006)
- ***Choroid plexus***	ISH	(Oberwinkler et al., 2005)
DRG	RT-PCR/RT-qPCR/ RT-qPCR + ISH + Western blot + Function	(Jang et al., 2012; Vandewauw et al., 2013; Vriens et al., 2011)
TG	RT-PCR/ RT-PCR/ RT-qPCR/ RT-qPCR + ISH + Western blot + Function	(Jang et al., 2012; Nealen et al., 2003; Vandewauw et al., 2013; Vriens et al., 2011)
NG	RT-qPCR	(Staaf et al., 2010)
Eye	Northern blot	(Oberwinkler et al., 2005)
Testis	RT-qPCR	(Jang et al., 2012)
Aorta	RT-PCR + Function/ RT-qPCR	(Naylor et al., 2010; Yang et al., 2006)
Pulmonary artery	RT-qPCR	(Yang et al., 2006)

4.1.4 Activation of TRPM3

4.1.4.1 D-erytho-sphingosine

TRPM3 has been shown to be activated by the sphingolipid, D-erytho-sphingosine (DeSPH). DeSPH evoked large increases in $[Ca^{2+}]_i$ in TRPM3-transfected HEK293 cells, but not untransfected cells, with an EC_{50} value of 12μM (Grimm et al., 2005). Other sphingolipids, namely dihydro-D-erythro-sphingosine (DHS) and *N,N*-dimethyl-D-erythro-sphingosine (DMS), also lead to activation of TRPM3 expressed in HEK293 cells, although the responses evoked by these compounds were smaller than those induced by DeSPH (Grimm et al., 2005).

In contrast to these findings, Wagner et al., (2008) found that a one minute application of DeSPH did not activate INS1 cells endogenously expressing TRPM3 or TRPM3-transfected HEK293 cells. Although prolonged exposure to DeSPH resulted in large currents in INS1 cells and TRPM3-transfected HEK293 cells, this response was also observed in untransfected HEK293 cells; suggesting a TRPM3-independent mechanism (Wagner et al., 2008). However, before the onset of the large non-specific current, a small outwardly rectifying current was observed in TRPM3-transfected HEK293 cells, which was not seen in untransfected cells (Wagner et al., 2008). Although it is likely that this small current was due to activation of TRPM3, the authors of the study proposed that the non-specific effects of DeSPH limit its use for functional identification of TRPM3 channels.

4.1.4.2 Pregnenolone sulphate and structurally related compounds

The neuroactive steroid pregnenolone sulphate (PS) has been identified as a TRPM3 agonist that is active within the micromolar range (Wagner et al., 2008). Application of PS induced concentration-dependent activation of outwardly rectifying currents and increases in $[Ca^{2+}]_i$ in TRPM3 expressing HEK293 cells, which were reliant on extracellular calcium and absent in untransfected cells (Wagner et al., 2008). PS activates TRPM3 with an EC_{50} value of 12-23μM and is able to activate TRPM3 channels in <100ms. The binding site for PS is thought to be located on extracellular side of the channel due to a lack of effect when PS is applied to the cytosolic surface of inside-out membrane patches (Wagner et al., 2008). PS also evoked responses in INS1 cells and pancreatic islet cells endogenously expressing TRPM3 (Wagner et al., 2008). Interestingly, PS can reversibly insert into the plasma membrane thereby altering membrane capacitance (Mennerick et al., 2008). In order to test whether PS activates TRPM3 via a receptor operated mechanism or indirectly via membrane

interactions, experiments were conducted assessing activation of TRPM3 by a synthetic enantiomer of PS, ent-PS, which causes the same change in membrane capacitance as the naturally occurring enantiomer of PS. Ent-PS was much less effective at evoking $[Ca^{2+}]_i$ responses and whole cell currents than the naturally occurring enantiomer of PS (in TRPM3-transfected cells), suggesting a direct, chirally-selective, PS binding site (Drews et al., 2014). PS has also been shown to be an activator of recombinantly-expressed TRPM1 channels. PS (35μM) induced inward and outward currents in HEK293 cells overexpressing TRPM1, however due to variability in PS responses between transfections and small current amplitudes the authors of the study were not able to provide a full characterisation of activation (Lambert et al., 2011).

Structurally related compounds such as pregnenolone, DHEA and DHEA sulphate, were also shown by Wagner *et al* to be activators of TRPM3 channels, albeit less efficacious than PS (Wagner et al., 2008). A later study by Majeed and colleagues (2010) determined that pregnenolone, DHEA and DHEA sulphate are partial agonists of TRPM3 (Majeed et al., 2010).

Other steroids which are closely related to PS have also been identified as agonists of TRPM3: these include epipregnanolone sulphate, epiallopregnanolone sulphate, pregnenolone glucuronidate and pregnenolone hemisuccinate (Drews et al., 2014). Activation of TRPM3 by epipregnanolone sulphate indicates that the double bond between C5-C6 present in PS is not required for activation of TRPM3. However, the β-orientation of the sulphate group at the C3 position has been shown to be important for activation of TRPM3 as a compound which lacks the C5-C6 double bond and has the sulphate group in α-orientation (pregnanolone sulphate) was ineffective at activating TRPM3 channels (Drews et al., 2014). In addition to being in the β-orientation, it is also important for the group at the C3 position to carry a negative charge, as compounds which have an uncharged group at the C3 position such as pregnenolone acetate and pregnenolone methyl ether were unable to effectively stimulate TRPM3. In contrast, compounds containing glucuronidate and hemisuccinate in the C3 position were able to activate TRPM3 transfected cells (Drews et al., 2014).

4.1.4.3 Nifedipine

The dihydropyridine calcium channel blocker, nifedipine is also an agonist at TRPM3 channels. Application of nifedipine induced concentration-dependent increases in $[Ca^{2+}]_i$

and outwardly rectifying currents, in TRPM3 expressing HEK293 cells which were absent in untransfected cells (Wagner et al., 2008). Similar to PS, nifedipine also evoked responses in INS1 cells and pancreatic islet cells endogenously expressing TRPM3. Combined application of PS (maximally effective concentration) and nifedipine to TRPM3 transfected CHO cells caused a supra-additive effect indicating that these two substances cause activation of TRPM3 by interaction at different binding sites (Drews et al., 2014).

4.1.4.4 Hypotonicity

In addition to chemical activation of TRPM3, decreases in osmolarity have also been shown to activate TRPM3 channels. Exposure of TRPM3-transfected, but not un-transfected HEK293 cells, to a hypotonic solution (200 mosmol liter^{-1}) resulted in a rise of $[Ca^{2+}]_i$ (Grimm et al., 2003). This hypotonic response was inhibited in Ca^{2+} free conditions and was reversed by washing with an isotonic solution.

4.1.5 Inhibition of TRPM3

4.1.5.1 Dihydropyridines

Although nifedipine has been found to activate TRPM3, other dihydropyridines can inhibit TRPM3 channel activity. Joint application of nimodipine with PS caused an inhibition of PS-induced $[Ca^{2+}]_i$ responses and a reduction in PS-induced current amplitude (Drews et al., 2014). Similar inhibitory effects were observed with nicardipine and nitrendipine (Drews et al., 2014).

4.1.5.2 Non-selective TRP inhibitors

The promiscuous TRP channel antagonist, 2-APB as well as Gd^{3+} and La^{3+} ions have also been shown to inhibit TRPM3 activity (Grimm et al., 2003; Lee et al., 2003; Xu et al., 2005).

4.1.5.3 Divalent and monovalent cations

Physiological concentrations of Mg^{2+} ions have also been shown to inhibit the activity of TRPM3 channels (Oberwinkler et al., 2005). Furthermore, extracellular Na^+ and K^+ ions inhibit currents through channels composed of the TRPM3α2 variant but not the TRPM3α1 variant (Oberwinkler et al., 2005).

4.1.5.4 Fenamates

The fenamate, non-steroidal anti-inflammatory (NSAID) drug, mefenamic acid has been identified as a potent, selective inhibitor of TRPM3 (Klose et al., 2011). Mefenamic acid inhibits TRPM3 in a pH-dependent manner by interacting with an extracellular site on the channel. It has been shown to inhibit PS evoked activation of TRPM3 channels expressed by HEK293 cells with an IC_{50} value of 6.6 ± 1.8μM (Klose et al., 2011). Experiments with INS-1E cells showed that mefenamic acid was able to inhibit PS-induced Ca^{2+} influx and insulin secretion (Klose et al., 2011). In addition to mefenamic acid, other fenamate drugs such as: DCDPC, tolfenamic acid, meclofenamic acid, flufenamic acid and niflumic acid, act as less potent, non-selective inhibitors of TRPM3 (Klose et al., 2011).

4.1.5.5 Progesterone and structurally related compounds

TRPM3 activity can also be inhibited by the endogenous steroid progesterone, progesterone metabolites and 17β-oestradiol (Majeed et al., 2012). Progesterone (0.01-10μM) inhibited PS- and nifedipine-evoked $[Ca^{2+}]_i$ responses of TRPM3 transfected HEK293 cells, while dihydrotestosterone (50μM) inhibited PS-induced responses but only caused a small inhibition of nifedipine-induced responses (Majeed et al., 2012). Furthermore, progesterone but not dihydrotestosterone, was able to inhibit constitutive activity of TRPM3 (in a Ca^{2+} add back protocol). Progesterone inhibited PS-induced responses in the presence of a progesterone receptor antagonist, indicating that inhibition of TRPM3 by progesterone does not involve the progesterone receptor and suggesting a direct effect of progesterone on either TRPM3 or a protein which is closely associated with TRPM3 (Majeed et al., 2012).

4.1.5.6 Thiazolidinediones

Rosiglitazone, a PPAR-γ agonist has also been shown to inhibit TRPM3 activity evoked by both PS and nifedipine, with IC_{50} values (calcium assay) of 4.6μM and 9.5μM respectively (Majeed et al., 2011). This inhibition was not affected by PPAR-γ antagonist suggesting it is not PPAR-γ-mediated. The inhibitory effects of rosiglitazone were mirrored by troglitazone and pioglitazone, which also belong to the thiazolidinedione class of drugs (Majeed et al., 2011). However, TRPM3 was not inhibited by the endogenous PPAR-γ agonist, 15d-PGJ_2 again suggesting a lack of PPAR-γ involvement in rosiglitazone inhibition of TRPM3 (Majeed et al., 2011).

4.1.5.7 Flavonoids and ononetin

The flavonoids naringenin, hesperetin and eriodictyol which are found in citrus fruits have also been identified as inhibitors of TRPM3, alongside the deoxybenzoin compound, ononetin (Straub et al., 2013a). Naringenin, hesperetin, eriodictyol and ononetin potently inhibited PS activation of TRPM3 expressed in HEK293 cells in a calcium flux assay, with IC_{50} values of 0.5 ± 0.07µM, 2.0 ± 0.1µM, 1.0 ± 0.07µM and 0.3 ± 0.03µM, respectively (Straub et al., 2013a). More detailed electrophysiological examination of the inhibition by naringenin and ononetin concluded that the inhibition was reversible. In addition to block of PS-induced currents, naringenin and ononetin also inhibited nifedipine-induced currents and caused partial block of heat-evoked currents (Straub et al., 2013a). Similar to mefenamic acid, naringenin and ononetin are thought to interact with TRPM3 channels via an extracellular binding site. Naringenin and ononetin were not able to inhibit PS-induced currents when applied intracellularly (Straub et al., 2013a). Interestingly, the IC_{50} value observed with ononetin, but not with naringenin, could be shifted according to the concentration of PS used to activate TRPM3; a higher concentration of PS resulted in a higher IC_{50} value. This suggests that ononetin is acting as a competitive inhibitor of PS in contrast to naringenin which appears to be acting as a non-competitive inhibitor.

Naringenin also exerted effects on TRPV1, TRPM7 and TRPM8; causing partial inhibition of capsaicin-induced activation of TRPV1 expressing HEK293 cells, partial block of TRPM7-mediated currents and both activation and inhibition of TRPM8 (Straub et al., 2013a). Furthermore, ononetin inhibited PS-induced TRPM1 activation and activated TRPA1 (Straub et al., 2013a).

Another citrus fruit product, isosakuranetin, has been identified as a potent TRPM3 antagonist (Straub et al., 2013b). Isosakuranetin, a flavanone present in blood oranges and grapefruits, inhibited activation of TRPM3 transfected HEK293 cells by PS with an IC_{50} value of 50 ± 6nM (calcium assay). Isosakuranetin also blocked inward and outward currents induced by PS in TRPM3 HEK293 cells and partially inhibited TRPM3 mediated heat-evoked currents (Straub et al., 2013b). In contrast to PS, mefenamic acid, ononetin and naringenin, which are all thought to interact with TRPM3 through an extracellular binding site, isosakuranetin is thought to bind to TRPM3 intracellularly (Klose et al., 2011; Straub et al., 2013a, 2013b; Wagner et al., 2008). Another flavanone, liquiritigenin, was identified as a TRPM3 inhibitor with a lower potency than isosakuranetin (Straub et al., 2013b). When tested for selectivity liquiritigenin had no effect on PS-induced TRPM1 activation, however

isosakuranetin caused a small inhibition of TRPM1-mediated PS responses. Neither compound inhibited TRPM8 or TRPV1, but both isosakuranetin and liquiritigenin caused partial activation of TRPA1 at low micromolar concentrations (Straub et al., 2013b).

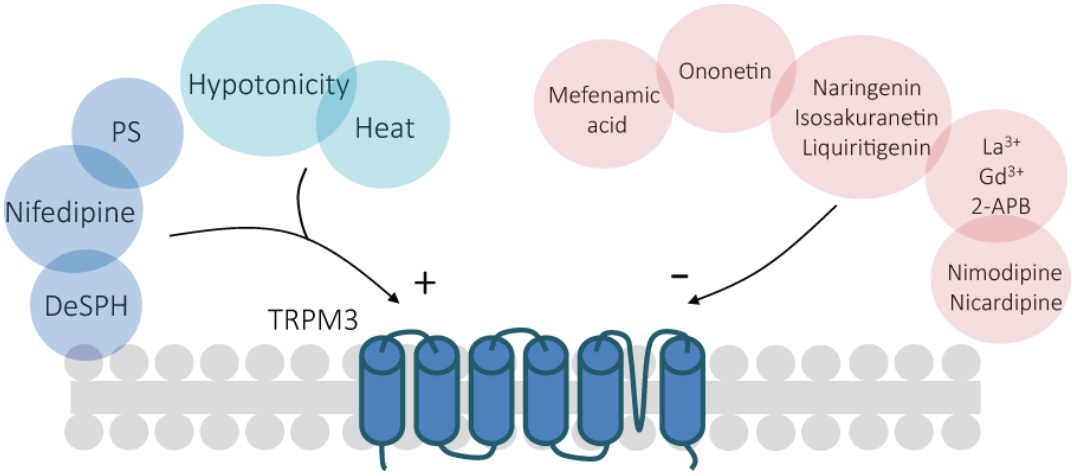

Figure 4-1 Activators and inhibitors of TRPM3

TRPM3 channels can be activated by the sphingolipid, D-erytho-sphingosine (DeSPH) and the dihydropyridine, nifedipine. The most potent and selective activator of TRPM3 is the endogenous neurosteroid, pregnenolone sulphate (PS) which is a useful pharmacological tool for the study of TRPM3. TRPM3 channel activity is purportedly increased by heat and hypotonic solutions. TRPM3 can be inhibited by many different compounds; including the fenamate NSAID drug, mefenamic acid and the deoxybenzoin compound, ononetin. In addition some citrus fruit flavonoids (naringenin, isosakuranetin, liquiritigenin) are inhibitors of TRPM3. The non-selective TRP channel blockers, La^{3+}, Gd^{3+} and 2-APB also block TRPM3 as do the dihyrdropyridines, nimodipine and nicardipine.

4.1.6 Permeation of TRPM3

Grimm and colleagues (2003) established that the human $TRPM3_{1325}$ variant has a greater permeability for Ca^{2+} ions over both Na^{+} ions (permeability ratio of 1.57 ± 0.31 for P_{Ca}/P_{Na}) and Cs^{+} ions (1.14 ± 0.10 for P_{Ca}/P_{Cs}). The TRPM3α2 variant was also shown to have a higher permeability for divalent cations over monovalent cations and the order of conductivity for divalent cations was found to be Ca^{2+} > Zn^{2+} > Mg^{2+} > Ni^{2+} (Wagner et al., 2010). Interestingly, channels formed from the mouse TRPM3α2 variant are much more permeable to Ca^{2+} and Mg^{2+} ions in comparison to channels formed from the TRPM3α1 variant, which are poorly permeable to these divalent cations (Oberwinkler et al., 2005). Alternative splicing in exon 24, results in an extra amino acid domain (containing 12 amino acids) in mouse TRPM3α1 variants which is located between the postulated fifth and sixth transmembrane domains (predicted pore-region). In addition, an alanine residue is replaced with a proline residue. This amino acid domain is absent in the mouse TRPM3α2

variant and all other variants excluding the hTRPM3c variant (Oberwinkler et al., 2005). Oberwinkler *et al* (2005) suggest that the introduction of this amino acid domain, which contains positively charged amino acid residues, to TRPM3α1 variants might lead to a decreased Ca^{2+} permeability due to increased electrostatic repulsion.

Vriens and colleagues (2014) established that ions could flow through TRPM3 channels via two pathways, the first through a centrally located pore and the second through an alternative pore located partly in the TM4 region of the channel (Vriens et al., 2014b). This alternative pathway could be opened by combined application of PS and clotrimazole (an anti-fungal medication) or clotrimazole structural analogues. Influx through this alternative permeation pathway resulted in an inwardly rectifying current which is insensitive to La^{2+} block and could be abolished by a mutation in the TM4 domain which swapped tryptophan for arginine (W982R) (Vriens et al., 2014b).

4.1.7 Modulation of TRPM3 activity

Despite a large array of agonists and antagonists described for TRPM3 there has been little study into the mechanisms which regulate or sensitise the channel. Many TRP channels are regulated by signalling pathways associated with activation of G-protein coupled receptors (GPCRs). However, the activity of the human $TRPM3_{1325}$ variant expressed in HEK293 cells was not modulated by activation of the histamine H1 receptor or by activation of endogenously expressed muscarinic receptors by carbachol (Grimm et al., 2003). In addition, the emptying of intracellular stores induced by the Ca^{2+}-ATPase inhibitor, thapsigargin, did not affect the activity of $TRPM3_{1325}$ (Grimm et al., 2003). In contrast, application of both thapsigargin and carbachol to HEK293 cells expressing the human TRPM3a variant stimulated Ca^{2+} entry (Lee et al., 2003). These findings suggest that different splice variants of the human TRPM3 gene can be differently modulated.

4.1.8 Role of TRPM3 in thermosensation

TRPM3 channels have been reported to be heat-sensitive, one study showed that heat (40°C) evoked increases in $[Ca^{2+}]_i$ in HEK293 cells transiently expressing TRPM3 and repetitive applications of heat resulted in desensitisation of the $[Ca^{2+}]_i$ responses (Vriens et al., 2011). Furthermore, heating activated an outwardly rectifying current in TRPM3 HEK293 cells with a Q_{10} value of 7.2 (Vriens et al., 2011). In addition, a synergistic effect was observed between chemical and thermal activation of TRPM3. The TRPM3 agonist, PS (10μM), shifted the activation of TRPM3 by heat to lower temperatures and increased

temperatures potentiated PS responses so that sub-threshold concentrations of PS at room temperature evoked responses at 37°C (Vriens et al., 2011).

Vriens and colleagues (2011) also found that 82% of *Trpm3*$^{+/+}$ DRG neurons were heat-sensitive and responded to a 43°C heat stimulus and 53% of those neurons were sensitive to both PS and the prototypical TRPV1 agonist, capsaicin. A further 41% of DRG neurons were PS-sensitive but not capsaicin-sensitive and 4% were sensitive to capsaicin but not PS, leaving 3% of neurons which were insensitive to both agonists. Despite a large overlap in heat and PS sensitivity, the number of neurons from *Trpm3*$^{-/-}$ mice responding to a 43°C heat stimulus was only modestly reduced, from 82% of WT DRG neurons to 59% of KO DRG neurons, and from 79% of WT TG neurons to 63% of KO TG neurons (Vriens et al., 2011). A similar percentage of heat-responsive neurons were noted in preparations from *Trpv1*$^{-/-}$ and *Trpm3*$^{-/-}$ mice. Interestingly, a TRPV1 antagonist only partially reduced the percentage of heat sensitive neurons remaining in *Trpm3*$^{-/-}$ DRG cultures. The authors concluded an involvement of both TRPM3 and TRPV1 in heat sensing but also note the existence of other heat sensing mechanisms independent of TRPM3 and TRPV1 (Vriens et al., 2011).

TRPM3 appears to a play a role in heat sensing *in vivo*. Vriens *et al* (2011) stated that *Trpm3*$^{-/-}$ mice showed a reduced preference for a 30°C plate over warmer plates (38°C or 45°C), in comparison to their wildtype counterparts. However, this statement is contradicted by graphical representation of these results which suggest that *Trpm3*$^{-/-}$ mice had a greater preference for the 30°C plate over the 38°C plate in comparison to wildtype counterparts.

4.1.9 Role of TRPM3 in pain

Activation of TRPM3 channels *in vivo* has been shown to evoke nociceptive behaviour and mice without functional TRPM3 channels exhibited compromised responses to noxious heat and failed to develop heat hyperalgesia associated with inflammation (Vriens et al., 2011). Injection of the TRPM3 agonist, PS (2.5 and 5 nmol/paw) into the plantar skin of the hindpaws of *Trpm3*$^{+/+}$ and *Trpv1*$^{-/-}$*/Trpa1*$^{-/-}$ mice evoked paw licking and lifting. However, this nocifensive behaviour was absent when PS was injected into the hindpaws of *Trpm3*$^{-/-}$ mice (Vriens et al., 2011). A later study showed that nocifensive behaviour induced by intraplantar injection of PS (5 nmol/paw) in wildtype mice could be inhibited by the TRPM3 antagonist isosakuranetin (Straub et al., 2013b). Furthermore, Vriens and colleagues (2014)

showed that clotrimazole was able to potentiate PS-evoked nocifensive responses in *Trpv1*$^{-/-}$ mice (Vriens et al., 2014b).

TRPM3 has also been implicated in mechanisms of trigeminal nociception. Supplementing drinking water with PS (750µM), resulted in a small but significant aversion to water consumption in *Trpm3*$^{+/+}$ mice that was absent in *Trpm3*$^{-/-}$ mice (Vriens et al., 2011).

Trpm3$^{-/-}$ mice exhibit normal responses in the tail clip assay and respond to intense tail pinch with a similar latency to their WT counterparts (Vriens et al., 2011) demonstrating that they retain normal mechanical sensitivities. *Trpm3*$^{-/-}$ mice have increased tail flick latencies between the temperatures of 45-57°C and increased response latencies in comparison to WT mice in the hot plate test (temperatures 52-58°C) (Vriens et al., 2011). Straub and colleagues (2013) also showed that response latencies of WT mice to a 52°C hot plate stimulus could be significantly increased by treatment with the TRPM3 antagonists, hesperetin and isosakuranetin (Straub et al., 2013b).

Furthermore *Trpm3*$^{-/-}$ mice, unlike *Trpm3*$^{+/+}$ mice, do not experience heat-hyperalgesia which characteristically appears after injection of Freund's adjuvant (CFA) into the hindpaw, whilst cold hyperalgesia remained unaffected in these mice (Vriens et al., 2011). These behavioural results are consistent with a role for TRPM3 in noxious temperature sensing.

4.1.10 How is the activity of TRPM3 regulated?

Research examining the impact of intracellular signalling pathways on the activity of TRP channels has revealed that their activity can be adjusted to reflect changes in the physiological environment (Wang and Woolf, 2005). For example, during periods of inflammation, mediators are able to indirectly sensitise TRP channels by binding to receptors that activate signalling pathways. This can result in decreased thresholds for nociceptor activation leading to pain hypersensitivity (Schaible, 2007). In order to understand how the activity of TRPM3 can be altered by changes in the local environment it is important to explore how intracellular signalling pathways modulate TRPM3-mediated activity; an area which has not yet been explored in detail.

4.2 Aims of the present study

i) One aim of the study was to characterise TRPM3 expressed in a cell line, examining its responsiveness to heat and known agonists and antagonists, and to determine if TRPM3 plays an important role in the detection of heat.

ii) A second aim was to investigate the mechanisms of TRPM3 channel modulation. In particular, to investigate how activation or inhibition of intracellular pathways can either positively or negatively modulate TRPM3 channel activity and to determine the effects of CB1 and opioid receptor activation on the activity of TRPM3 channels in sensory neurons.

iii) A third aim was to investigate the role played by TRPM3 as a mediator of persistent and visceral pain.

These three experimental aims were investigated using single cell and cell population Ca^{2+} measurements of CHO cells heterologously expressing the TRPM3 channel and isolated DRG neurons from *Trpm3*$^{+/+}$ mice endogenously expressing TRPM3 and from *Trpm3*$^{-/-}$ mice lacking functional TRPM3 channels. The behavioural responses of *Trpm3*$^{+/+}$ and *Trpm3*$^{-/-}$ mice were also assessed in order to elucidate the role played by TRPM3 in models of pain.

4.3 Materials and Methods

4.3.1 Solutions and reagents

Unless stated otherwise, experiments were conducted in a physiological extracellular solution (see Table 3-2) buffered to pH 7.4 (NaOH). For Ca^{2+}-free experiments $CaCl_2$ was omitted from the buffer and 1mM EGTA was added.

Master stock solutions of pregnenolone sulphate, capsaicin, mefenamic acid, ononetin, forskolin; IBMX, *m*-3M3FBS, U73122, PMA, PDBu, KT5720 (Sigma-Aldrich; St Louis, MO), staurosporine (Cayman Chemical; Ann Arbour, MI), WIN 55212-2 and AM251 (Tocris Bioscience; Bristol, UK) were made in DMSO (Calbiochem; Darmstadt, Germany). Master stock solutions of morphine, naloxone (Sigma-Aldrich; St Louis, MO) and H-8 (Cayman Chemical; Ann Arbour, MI) were made in H_2O. Master stock solutions of DAMGO, SB205607 and U50488 (Tocris Bioscience; Bristol, UK) were made in physiological extracellular solution. A master stock solution of 8-bromo cAMP (Sigma-Aldrich; St Louis, MO) was made in H_2O titrated with NaOH. Master stock solutions were aliquotted and stored at -20°C. Dilutions from these aliquots into physiological extracellular solution were made daily for their use in experiments.

PTX (lyophilised powder; Sigma-Aldrich; St Louis, MO) was reconstituted in H_2O and was stored at 4°C. PTX was added to cells at a concentration of 200ng/ml.

4.3.2 TRPM3 CHO cell line

A Chinese hamster ovary (CHO) cell line stably expressing the mouse TRPM3α2 variant was made by Dr David Andersson (King's College London). CHO cells were transfected with a TRPM3α2 plasmid (pcDNA3.1) DNA (provided by Dr Stephan Philipp; University of Saarland, Homburg, Germany) using Lipofectamine® 2000 transfection reagent (Invitrogen). The culture medium was supplemented with G418 (0.5mg/ml) 24 hrs after transfection to select for stable transfectants. Single clones were identified by limiting dilution and expansion. Expression of TRPM3 in the clones was assessed functionally (pregnenolone sulphate sensitivity, Fura-2).

Experiments using the TRPM3 transfected CHO cell line were performed using calcium imaging experiments described in section 2.2.

4.3.3 GFP-tagged CB1 receptor experiments

Subcloning Efficiency™ DH5α competent E. coli cells (Invitrogen) were transformed with CB1-GFP DNA. The CB1-GFP plasmid (pcDNA1) was provided by Dr Andrew J. Irving (University of Dundee). The resulting bacterial culture was grown according to Qiagen HiSpeed™ Plasmid Purification handbook guidelines. The CB1-GFP plasmid DNA was then isolated by following maxipreparation guidelines in the Qiagen HiSpeed™ Plasmid Purification handbook and the DNA concentration was measured by UV spectrophotometry at 260 nm. CHO cells expressing mouse TRPM3 were transfected with the purified CB1-GFP DNA using Lipofectamine® 2000 transfection reagent and plated on to glass coverslips for microscope-based imaging experiments. Additionally some coverslips were fixed and mounted onto slides for visualisation of GFP.

4.3.3.1 Cell transformation and plasmid purification

Subcloning Efficiency™ DH5α competent E. coli cells (Invitrogen) were transformed according to Invitrogen protocol guidelines. DH5α cells (50µl) were thawed on ice and CB1-GFP plasmid DNA (1µl) added with gentle mixing. The cells were incubated on ice for 30 minutes and then heat shocked at 42°C for 20 seconds. The cells were then placed on ice for 2 minutes prior to addition of 950µl S.O.C medium. The cells were then incubated for 1 hour at 37°C with shaking (225 rpm). The transformed cells (20µl) were spread onto pre-warmed agar plates containing 100µg/ml ampicillin and incubated overnight at 37°C.

Plasmid purification was carried out according to the guidelines in the HiSpeed™ Plasmid Purification handbook (Qiagen). A single bacterial colony was picked from the streaked agar plate and incubated in LB broth containing 100µg/ml ampicillin (5mls) for 6-8 hours at 37°C with vigorous shaking (~300rpm). 1ml of this culture was added to 250ml of LB broth containing 100µg/ml ampicillin and further incubated for 12-16 hours at 37°C with vigorous shaking (~300rpm). Cells were harvested by centrifugation (6000 x *g*, 15 minutes, 4°C), lysed and the plasmids isolated using a QIAfilter Maxi kit (Qiagen).

The CB1-GFP DNA concentration was determined using UV spectrophotometry at 260 nm (NanoDrop™ spectrophotometer, Thermo Fisher Scientific).

4.3.3.2 Transfection of CHO cells already expressing mouse TRPM3

12-24 hours before transfection CHO cells expressing mouse TRPM3 were plated onto sterile 13mm glass coverslips previously coated with 10µgml^{-1} poly-D-lysine (contained in a

4-well plate). Cells were plated at a high density to ensure 90-95% confluency on the day of transfection.

Transfection was carried out according to the Invitrogen Lipofectamine® 2000 transfection protocol. Opti-MEM (200µl) was combined with CB1-GFP DNA (0.8µg per well) and the mixture incubated for 5 minutes at room temperature. In a separate bottle Opti-MEM (200µl) was combined with Lipofectamine® 2000 reagent (8µl) and the mixture incubated for 5 minutes at room temperature. The diluted DNA mixture was combined with the diluted Lipofectamine® 2000 mixture and incubated for 20 minutes at room temperature. The mixture was then added drop-wise to the surface of the coverslips (100µl per coverslip/well). The cells were incubated at 37°C for 24 hours before the medium was changed to normal growth medium. Transfected cells were used one day after transfection for microscope-based $[Ca^{2+}]_i$ imaging experiments or fixed and mounted onto slides for visualisation.

4.3.3.3 Visualisation of cells expressing CB1-GFP using fluorescence microscopy

CB1-GFP transfected mouse TRPM3 CHO cells were fixed in 10% p-formaldehyde in 0.1M phosphate-buffered saline (PBS – 500µl) for 15 minutes at room temperature. Coverslips were then washed twice with 0.1M PBS (500µl) and incubated with Hoechst 33342 (Sigma-Aldrich; 1:10,000) in 0.1M PBS for 5 minutes at room temperature (for visualisation of cellular nuclei and total cell counts), followed by three washes with 0.1M PBS (500µl). Coverslips were mounted onto slides using Mowiol mounting solution and viewed with an Apotome Zeiss microscope (20x objective with a numerical aperture of 0.75). Images were captured using AxioVision (Carl Zeiss Microscopy) and the number of GFP stained cells counted and expressed as a percentage of total cells (total number of stained nuclei). The exposure used to capture images of GFP-positive cells was kept constant for all fields of view and set to a duration where no fluorescence was observed in mock-transfected cells. Four coverslips were used for analysis and a minimum of 850 cells were counted for each coverslip.

4.3.4 Heat studies

Microscope-based imaging experiments investigating the heat sensitivity of mouse TRPM3 transfected CHO cells and mouse dorsal root ganglion (DRG) neurons were performed using calcium imaging experiment methods described in section 2.2.2.

CHO cells stably expressing mouse TRPM3 and mouse DRG neurons were exposed to a linear heating temperature ramp (~24-51°C). Time-points of temperature increase at 2°C intervals were recorded. Before and after exposure to the heating temperature ramp the temperature of the perfusate was held at a constant temperature (~23.5°C). In these experiments changes in $[Ca^{2+}]_i$ were monitored using the calcium indicator dye Fura-2. In CHO cell experiments activation by PS was used for functional identification of cells expressing mouse TRPM3. In DRG experiments activation by PS and capsaicin was used for functional identification of neurons expressing TRPM3 and TRPV1, respectively. Neurons were distinguished from non-neuronal cells by a final depolarising challenge with a solution containing 50mM KCl.

4.3.4.1 Identification of PS- and capsaicin- sensitive neurons

Neurons were defined as displaying a PS- or capsaicin-induced response if during exposure to the drug they exhibited a change in Δ Fura-2 ratio which was greater than 0.15. Additionally, Fura-2 ratio time courses for individual neurons were screened visually for confirmation of a ratio change consistent with the typical waveform of a response.

4.3.4.2 Identification of heat-sensitive neurons

Neurons were defined as heat-sensitive if they displayed a change in $[Ca^{2+}]_i$ (Δ Fura-2 ratio) which was which was two standard deviations higher than the change in $[Ca^{2+}]_i$ (Δ Fura-2 ratio) exhibited by a group of non-responsive neurons (heat response <15% of maximal response). Additionally, neurons were screened visually for a discontinuity in the Fura-2 ratio time-course indicative of a threshold temperature.

4.3.4.3 Activation thresholds

To determine the temperature activation thresholds, time-points of temperature increase at 2°C intervals were recorded during heating temperature ramps. The observed rate of heating was linear over most of the temperature range used. The Fura-2 ratios of mTRPM3 CHO cells and heat-sensitive DRG neurons were exported into Microsoft Excel. The temperature at which the ratio deviated from the initial rate of increase was used as the

temperature activation threshold, either by visual identification or from the point of intersection between two lines fitted to the 2 phases of the Fura-2 ratio.

4.3.5 RNA extraction and RT-PCR for quantification of TRPM3 mRNA levels in mouse tissues

Tissues (lumbar DRG, dorsal lumbar spinal cord, olfactory bulb, cerebellum, midbrain and kidney) from C57Bl6 mice were dissected by Clive Gentry (King's College London) and flash-frozen. The frozen tissues were then weighed and homogenised. Homogenisation of tissues was achieved using a glass-Teflon hand homogeniser followed by a QIAshredder (Qiagen). RNA was then extracted and purified from homogenised tissue samples using the RNeasy Mini kit (Qiagen) according to the manufacturer's protocol guidelines for purification of total RNA from animal tissues. The RNA concentration of each tissue was determined using UV spectrophotometry at 260 nm (NanoDrop™ spectrophotometer, Thermo Fisher Scientific).

Next, RNA samples were converted to cDNA by reverse transcription (RT). A RT master mix was prepared using reagents from the AB Applied Biosystems high capacity cDNA reverse transcription kit according to kit guidelines. RNA samples (maximum of 1µg) were added to autoclaved 0.2ml tubes containing 10µl RT master mix and the RT reaction was allowed to proceed for 2 hours at 37°C.

PCR was then performed to amplify TRPM3 and GAPDH (reference gene) cDNA transcripts using the LightCycler® Carousel-Based System (Roche). A PCR master mix was prepared using reagents from the LightCycler® TaqMan® Master kit (Roche) and TaqMan® (GAPDH and TRPM3) probes, according to kit guidelines. Next, cDNA (5ng) samples were added to pre-cooled LightCycler® capillaries containing 18µl PCR master mix and centrifuged at 700 × *g* for 5 s. The capillaries were then transferred to the LightCycler® instrument and the reaction was allowed to proceed for 45 cycles.

Relative quantification of TRPM3 transcript in each tissue was performed using the $2^{-\Delta\Delta CT}$ method (Livak and Schmittgen, 2001). TRPM3 C_T values were normalised to GAPDH (see calculation 1), to compensate for differences in the amount of RNA template. $\Delta\Delta C_T$ values were obtained by calculation 2. The relative mRNA levels compared to lumbar DRG were calculated (see calculation 3).

1. Average TRPM3 C_T - Average GAPDH C_T = ΔC_T
2. ΔC_T test tissue - ΔC_T reference tissue (DRG) = $\Delta\Delta C_T$
3. $2^{-\Delta\Delta C}{}_T$ = Normalised TRPM3 amount relative to reference tissue (DRG)

4.3.6 Behavioural tests

All animal behaviour studies were carried out according to the U.K. Home Office Animal Procedures (1986) Act and were approved by the King's College London Ethical Review Panel. Mice were housed in a temperature-controlled environment on a 12-hour light/dark cycle with access to food and water ad libitum. Data shown in this chapter are from female C57BL/6 mice or from male and female homozygote *Trpm3*$^{-/-}$ C57BL/6 mice were obtained from Charles River UK Ltd. *Trpm3*$^{-/-}$ mice were bred from homozygotic mice provided by Dr Stephan Philipp (University of Saarland, Homburg, Germany). All behavioural tests were conducted with Clive Gentry (King's College London).

4.3.6.1 Hot-plate test

Heat sensitivity was assessed using a calibrated hot-plate (Ugo Basile, Milan) at 53°C. Before testing, the mice were kept in their holding cages to acclimatize (10-15 minutes) to the experimental room. Mice were placed onto the hot-plate within a perspex enclosure and the time to ipsilateral paw lift or lick was recorded as the paw withdrawal latency. A maximum, cut-off paw withdrawal latency of 100 seconds was used to prevent unnecessary tissue damage and trauma.

4.3.6.2 Formalin test

Mice were habituated to perspex observation chambers for 15 minutes. Each animal received a 20µl subcutaneous injection of a 2.5% formalin solution into the plantar surface of the left hindpaw. The animals were returned to the observation chamber and total pain related behaviours (paw shaking, licking or biting) were timed in 5 min bins for a period of 45 min.

4.3.6.3 Acetic acid-induced writhing test

Mice were habituated to perspex observation chambers for 15 minutes. Each animal received an intraperitoneal injection of dilute acetic acid (0.6% acetic acid solution) which induced stereotyped nociceptive behaviour (abdominal writhing). The intensity of pain evoked in both mouse genotypes was measured by counting the number of abdominal writhes occurring in 5 minute bins over a 20 min observation period.

4.3.7 Statistics

Normality of data was tested using the Shapiro-Wilk Test and homogeneity of variances was tested using Levene's test. Differences in normally distributed data means between two groups were analysed using an independent samples t-test. Differences in normally distributed data means between three groups or more were analysed using a one-way ANOVA, followed by a Tukey's HSD post-hoc test (for datasets with equal variances) or a Dunnett's T3 post-hoc test (for datasets with unequal variances). Differences in non-normally distributed data means between two groups were analysed using a Mann-Whitney U test. Differences in non-normally distributed data means between three groups or more were analysed using a Kruskal-Wallis test, followed by a Dunn-Bonferroni's pairwise post-hoc test. Differences in the frequencies of a specific effect between different groups were assessed by a Pearson Chi-Square test or Fisher's exact test. All statistical analyses were made using IBM SPSS statistics, version 22.

4.4 Results

4.4.1 Characterisation of heterologously-expressed TRPM3

In order to study the pharmacological properties of TRPM3 channels, a CHO cell line heterologously expressing mouse TRPM3α2 splice variant was created. The aim of the current study was to fully characterise this newly-established cell line.

4.4.1.1 Activation of TRPM3 by pregnenolone sulphate

The $[Ca^{2+}]_i$ responses of CHO cells heterologously expressing mouse TRPM3α2 (will be referred to as TRPM3) were examined. Channels formed from the TRPM3α2 variant are permeable to divalent cations making it well suited to investigation using fluorometric Ca^{2+} measurements (Oberwinkler et al., 2005). In the experiments described in this section changes in $[Ca^{2+}]_i$ were monitored using the calcium indicator dye Fura-2 using a 96-well plate assay.

It has previously been reported that the endogenous neurosteroid, pregnenolone sulphate (PS), acts as an agonist at TRPM3 channels (Wagner et al., 2008). In order to test whether PS causes opening of recombinantly expressed TRPM3 channels resulting in Ca^{2+} influx, PS (1-200μM) was applied to mouse TRPM3 CHO cells and changes in $[Ca^{2+}]_i$ were measured. Application of PS evoked a concentration-dependent increase in $[Ca^{2+}]_i$ with a mean EC_{50} value of 9.65 ± 1.97 μM (mean ± SEM; n= 3 independent experiments; Figure 4-2). The concentration response relationship for PS reached a plateau at concentrations above 100μM.

In contrast, application of PS (1-200μM) to untransfected CHO cells did not evoke an increase in $[Ca^{2+}]_i$, demonstrating that TRPM3 channels are required for PS-evoked $[Ca^{2+}]_i$ responses (maximum amplitude of PS response for TRPM3 transfected cells, 0.80 ± 0.18 Δ Fura-2 ratio compared to untransfected cells, 0.08 ± 0.01 Δ Fura-2 ratio; Figure 4-2b). Furthermore, PS did not evoke increases in $[Ca^{2+}]_i$ in Ca^{2+} free conditions (in the presence of 1mM EGTA in the external solution) indicating that the increases in $[Ca^{2+}]_i$ observed in TRPM3 transfected CHO cells are the result of Ca^{2+} influx (see Figure 4-2c).

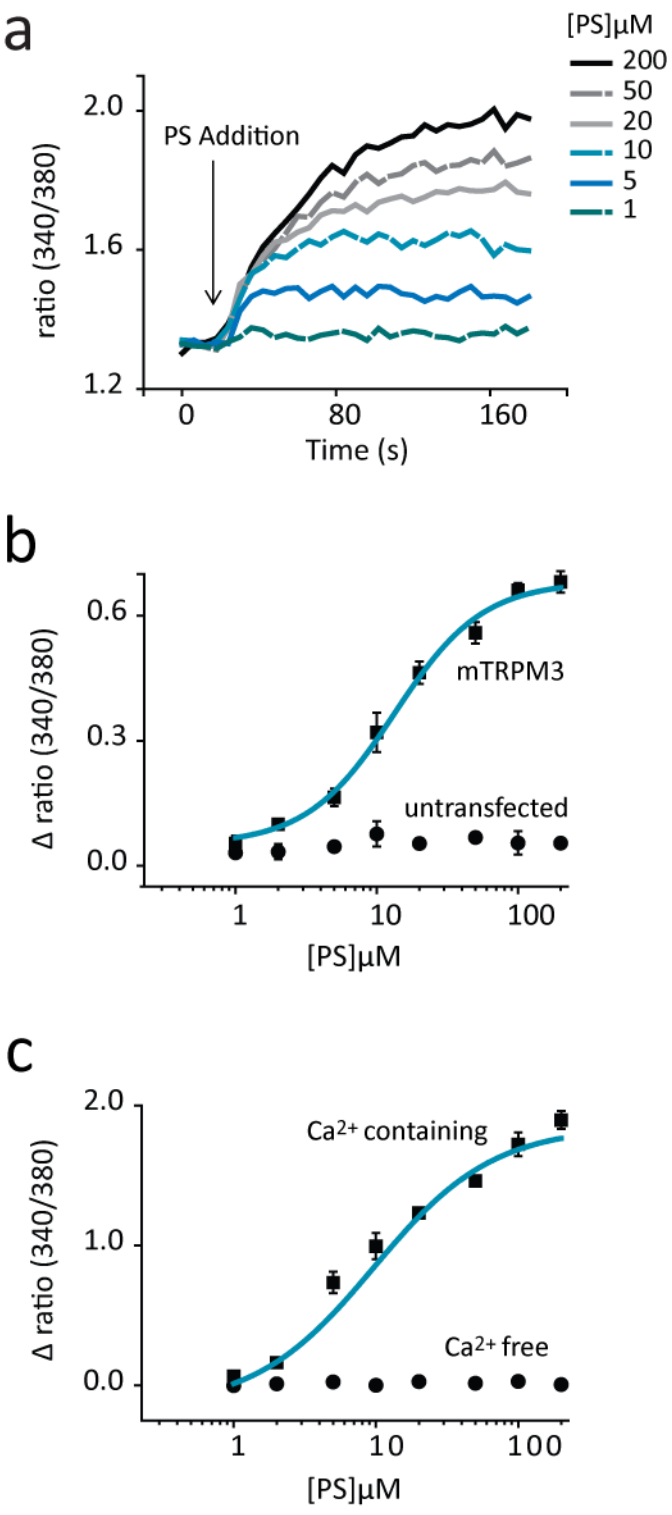
a
[PS]µM
200
50
20
10
5
1
PS Addition
ratio (340/380)
2.0
1.6
1.2
0
80
160
Time (s)
b
Δ ratio (340/380)
0.6
0.3
0.0
mTRPM3
untransfected
1
10
100
[PS]µM
c
Δ ratio (340/380)
2.0
1.0
0.0
Ca2+ containing
Ca2+ free
1
10
100
[PS]µM

Figure 4-2 Pregnenolone sulphate is a TRPM3 agonist

(**a**) Time courses of $[Ca^{2+}]_i$ increases evoked by different pregnenolone sulphate concentrations in Fura-2 loaded CHO cells stably transfected with mouse TRPM3 (mTRPM3). Baseline signals were collected before cells were challenged with PS at 20 seconds. Traces shown are mean ratios from triplicate wells from a representative experiment (**b**) PS evoked a concentration dependent increase in $[Ca^{2+}]_i$ (Δ Fura-2 340/380) in mTRPM3-expressing CHO cells with an EC_{50} of 9.65 ± 1.97 μM (mean ± SEM; n= 3 independent experiments). PS failed to increase $[Ca^{2+}]_i$ in untransfected CHO cells. Representative plots shown, data points are the mean ratio of triplicate wells ± SEM. (**c**) PS evoked a concentration dependent increase in $[Ca^{2+}]_i$ (Δ Fura-2 340/380) in extracellular solutions containing Ca^{2+} but not in Ca^{2+}-free solutions. Representative plots shown, data points are the mean ratio of triplicate wells ± SEM.

4.4.2 Inhibition of TRPM3

Mefenamic acid is a non-steroidal anti-inflammatory, fenamate, drug which has been reported as a potent inhibitor of TRPM3 (Klose et al., 2011). The characteristics of mefenamic acid antagonism of PS-evoked $[Ca^{2+}]_i$ responses were studied by challenging mouse TRPM3 CHO cells with a sub-maximally effective concentration of PS (20µM) in the presence of increasing concentrations of mefenamic acid (0.03-100µM). Mefenamic acid inhibited PS-evoked responses with an IC_{50} value of 3.41 ± 0.82µM (mean ± SEM; n=3 independent experiments; Figure 4-3a). Concentrations above 30µM mefenamic acid caused complete inhibition of PS-evoked $[Ca^{2+}]_i$ responses (see Figure 4-3a).

PS-evoked $[Ca^{2+}]_i$ responses were also inhibited by ononetin, a structurally unrelated antagonist of TRPM3 (Straub et al., 2013a). Ononetin inhibited PS-evoked responses more potently than mefenamic acid with an IC_{50} value of 0.50 ± 0.10µM (mean ± SEM; n=3 independent experiments; Figure 4-3b). These results are consistent with previously published findings showing that mefenamic acid and ononetin are antagonists of TRPM3 (Klose et al., 2011; Straub et al., 2013a).

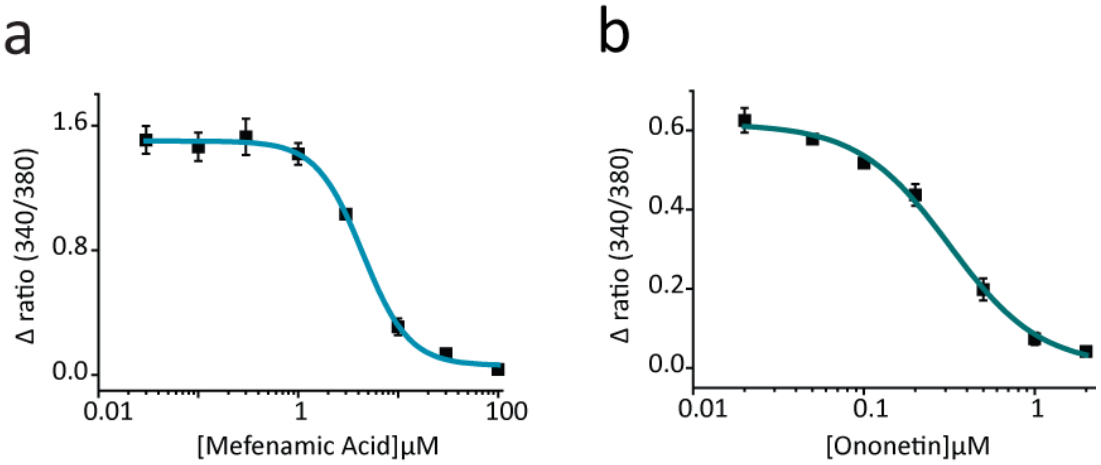

Figure 4-3 Mefenamic acid and ononetin are antagonists of TRPM3

(**a**) $[Ca^{2+}]_i$ (Δ Fura-2 ratio) responses of mTRPM3 CHO cells stimulated with 20µM PS in the presence of increasing concentrations of mefenamic acid (0.03-100µM). Activation of mTRPM3 CHO cells by PS was inhibited by mefenamic acid in a concentration dependent manner, IC_{50} - 3.41 ± 0.82µM (mean ± SEM; n=3 independent experiments). Representative plot shown, data points are the mean ratio of triplicate wells ± SEM. (**b**) $[Ca^{2+}]_i$ (Δ Fura-2 ratio) responses of mTRPM3 CHO cells stimulated with 20µM PS in the presence of increasing concentrations of ononetin (0.01-2µM). Activation of mTRPM3 CHO cells by PS was inhibited by ononetin in a concentration dependent manner, IC_{50} – 0.50 ± 0.1µM (mean ± SEM; n=3 independent experiments). Representative plot shown, data points are the mean ratio of triplicate wells ± SEM.

4.4.3 TRPM3 is expressed in multiple areas of the nervous system

The relative levels of TRPM3 mRNA expression were examined in wildtype DRG, spinal cord, olfactory bulb, cerebellum, midbrain and kidney using RT-qPCR (Figure 4-4).

Robust levels of TRPM3 mRNA transcripts were detected in all of the neural tissues sampled. TRPM3 mRNA was expressed in the DRG consistent with the findings of functional TRPM3 channels in these neurons (Vriens et al., 2011). The highest level of TRPM3 mRNA was found in the spinal cord, where it was on average 3.5-fold higher than the level in the DRG (n= 3 mice). Levels of TRPM3 expression in the olfactory bulb, cerebellum and midbrain were close to that observed in the DRG (n= 3 mice). The levels of TRPM3 mRNA in the mouse kidney were also examined (n = 2 mice) and, consistent with previous findings, revealed very low levels of expression (Kunert-Keil et al., 2006).

These findings confirm expression of TRPM3 mRNA in the mouse peripheral nervous system but also demonstrate expression of TRPM3 transcripts in the central nervous system. The presence of TRPM3 channels in areas such as the olfactory bulb, cerebellum and midbrain indicates the likelihood of other roles for TRPM3 in addition to the ones already described (e.g. sensory transduction channel for noxious heat, modulator of insulin release and vascular smooth muscle contraction).

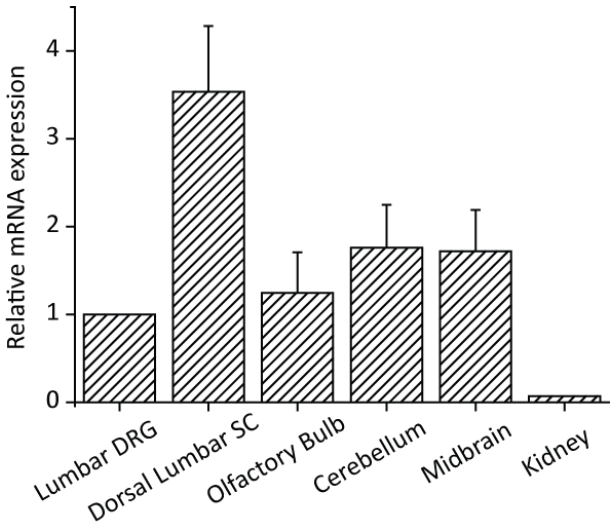

Figure 4-4 TRPM3 is expressed in the brain and spinal cord in addition to sensory neurons

Quantitative RT-PCR was performed on mouse tissues. Relative levels of TRPM3 mRNA expression were quantified using the $2^{-\Delta\Delta C}{}_{T}$ method. Column graph showing normalised TRPM3 mRNA expression (normalised to GAPDH), relative to lumbar DRG expression, in the mouse dorsal lumbar spinal cord, olfactory bulb, cerebellum, midbrain and kidney. Columns represent mean ± SEM (kidney, n= 2 animals; all other tissues, n= 3 animals).

4.4.4 TRPM3 channels are functionally expressed in sensory neurons

The findings of the current study have revealed expression of TRPM3 in DRG neurons and are consistent with previous findings which have identified expression of TRPM3 in rodent sensory neurons (Jang et al., 2012; Nealen et al., 2003; Vandewauw et al., 2013; Vriens et al., 2011). To examine functional expression of TRPM3 channels in sensory neurons, PS-induced changes in $[Ca^{2+}]_i$ within isolated DRG neurons were monitored using the calcium indicator dye Fura-2.

Isolated DRG neurons were exposed to PS at a concentration of 10, 20, 50 or 100µM. Neurons were identified by application of a depolarising concentration of KCl. PS evoked increases in $[Ca^{2+}]_i$ in a large population of DRG neurons as shown in Figure 4-5, which illustrates the responses to sequential application of increasing concentrations of PS. Activation by PS was concentration-dependent; 12% (n= 70/587; 3; 2) of neurons tested were activated by 10µM PS, and this was increased to 27% (n= 106/390; 2; 2) with 20µM PS, 36% (n= 179/492; 3; 2) with 50µM PS and 55% (n= 275/504; 3; 2) with 100µM PS (Figure 4-5c).

In addition to the number of neurons responding, the response amplitudes also followed a concentration-dependent pattern. Lower PS concentrations induced responses with smaller maximum response amplitudes in comparison to responses evoked by higher concentrations of PS (10µM, 43 ± 2%; 20µM, 45 ± 3%; 50µM, 52 ± 2%; 100µM, 62 ± 2%; mean ± SEM; % of KCl response; Figure 4-5b).

However, in experiments using isolated DRG neurons from *Trpm3*$^{-/-}$ animals increases in $[Ca^{2+}]_i$ in response to 50µM PS were only evident in 1% of neurons (9/712). These findings demonstrate that TRPM3 channels are functionally expressed in a large population of DRG neurons and are consistent with previous findings (Vriens et al., 2011). Furthermore, these findings show that PS-evoked DRG responses are dependent on expression of functional TRPM3 channels and demonstrate that PS is a selective pharmacological tool in this preparation.

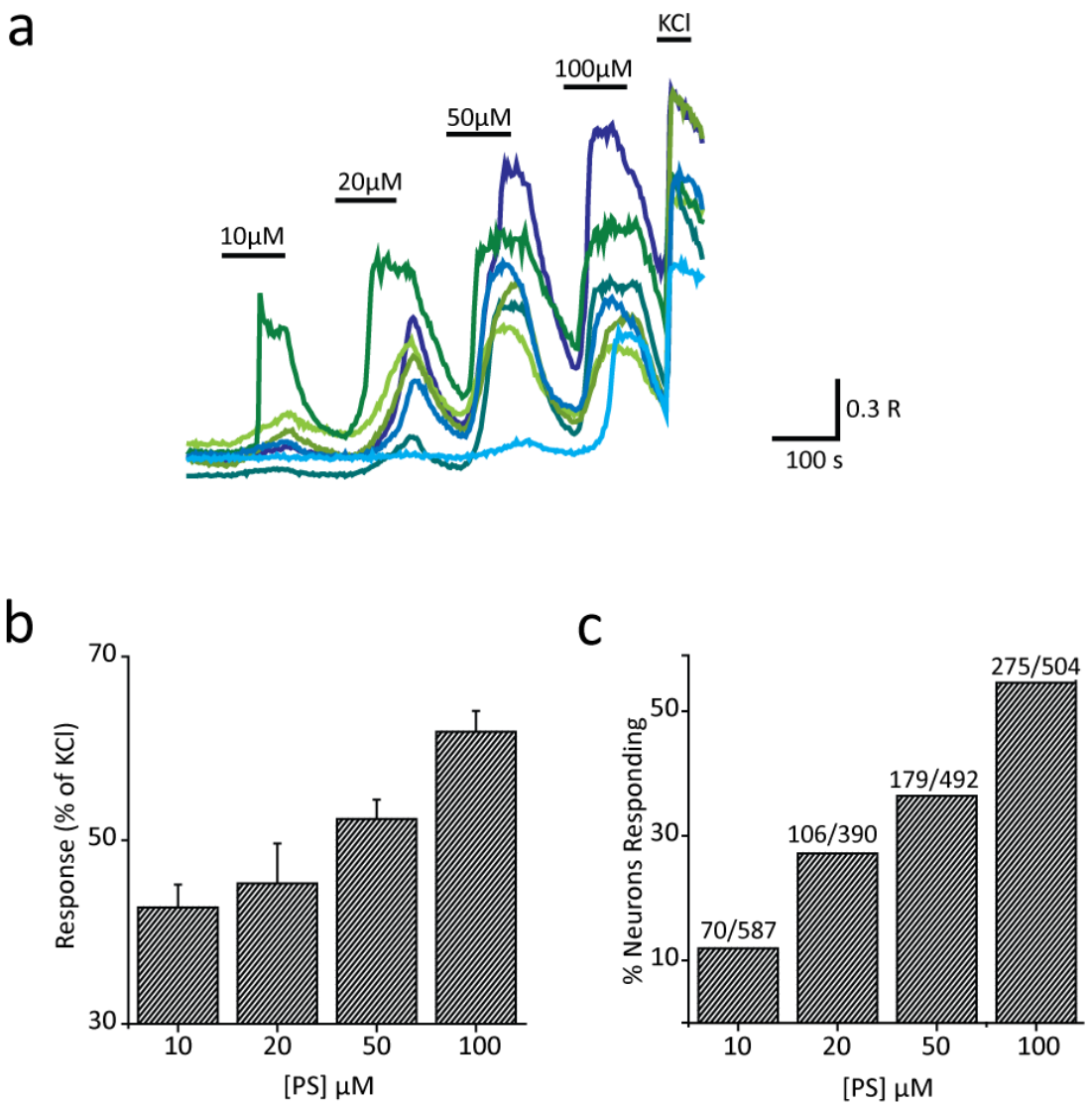

Figure 4-5 Pregnenolone sulphate activates DRG neurons in a concentration-dependent manner

(**a**) $[Ca^{2+}]_i$ responses monitored by Fura-2 (R denotes Fura-2 ratio) in PS-sensitive DRG neurons using microscope-based imaging. Representative traces displaying neuronal $[Ca^{2+}]_i$ responses to sequential PS challenges (10, 20, 50 and 100µM) followed by depolarisation with high K^+ (50mM KCl). (**b**) Column graph displaying the average maximum response amplitudes evoked by different concentrations of PS in responsive DRG neurons. PS response amplitudes were calculated as a % of the KCl-evoked amplitude (10µM PS, n= 70, 3, 2; 20µM PS, n= 106, 2, 2; 50µM PS, n= 179, 3, 2; 100µM PS, n= 275, 3, 2). Columns represent mean ± SEM. (**c**) Column graph displaying the percentage of DRG neurons which responded to PS with an increase in $[Ca^{2+}]_i$. The numbers shown above the columns represent the total number of PS responsive neurons/total number of neurons tested. In the experiments shown in (b) and (c) different PS concentrations were applied to individual coverslips.

4.4.5 Heterologously-expressed TRPM3 is activated by heat

TRPM3 channels have previously been reported to be activated by heat and have been implicated in the heat sensing mechanisms of sensory neurons (Vriens et al., 2011). In order to examine whether TRPM3 channels stably-transfected in a CHO cell line could be activated by heat, microscope-based imaging experiments were conducted. In these experiments, the temperature of the superfusate can be controlled allowing heating temperature ramps to be conducted.

Populations of untransfected and mouse TRPM3 transfected CHO cells were exposed to a heating temperature ramp (24-51°C) which was followed by application of the TRPM3 agonist, PS (50µM). In these experiments changes in $[Ca^{2+}]_i$ were monitored using the calcium indicator dye Fura-2.

PS-sensitive TRPM3 CHO cells exposed to heat (24-51°C) responded with robust, reversible increases in $[Ca^{2+}]_i$ with an average maximum response amplitude of 0.82 ± 0.01 Δ Fura-2 ratio (mean ± SEM; n= 1379 cells, 10, 3; see Figure 4-6) and an average temperature threshold of 44 ± 0.4°C (mean ± SEM; n= 10 coverslips, minimum of 53 cells per coverslip; see Figure 4-7). Heating evoked a much smaller increase in $[Ca^{2+}]_i$ in untransfected CHO cells with a maximum amplitude of 0.43 ± 0.01 Δ Fura-2 ratio (mean ± SEM; n= 2640 cells, 9, 3; Figure 4-6). As shown in the previous 96-well plate experiments untransfected CHO cells displayed no response to PS application (average maximum PS amplitude = 0.00 ± 0.00 Δ Fura-2 ratio; mean ± SEM; n= 895 cells, 3, 1); this was in contrast to mouse TRPM3 CHO cells which displayed large reversible $[Ca^{2+}]_i$ responses upon application of PS (average maximum PS amplitude = 1.39 ± 0.01 Δ Fura-2 ratio; mean ± SEM; n= 1717 cells, 12, 4). The presence of a large $[Ca^{2+}]_i$ response to heat in mouse TRPM3 transfected CHO cells but not untransfected control cells demonstrates that expression of TRPM3 channels confers sensitivity to heat.

In order to determine whether TRPM3 channels are required for the large $[Ca^{2+}]_i$ responses to heat, the effects of two TRPM3 antagonists on the heat-evoked responses of mouse TRPM3 transfected CHO cells were tested using microscope-based imaging. Populations of mouse TRPM3 CHO cells were perfused with either ononetin (10µM) or mefenamic acid (30µM) for 2 ½ minutes, before being exposed to a heating temperature ramp (24-51°C). After washout of the respective antagonist, cells were challenged with PS (50µM) to confirm TRPM3 expression. Cells treated with ononetin (10µM), responded to the heat

ramp with a modest increase in $[Ca^{2+}]_i$ which was similar to the TRPM3-independent heat-evoked responses observed in untransfected cells. The average maximum amplitude of the responses was reduced from 0.77 ± 0.02 Δ Fura-2 ratio in untreated TRPM3 CHO cells (mean ± SEM; n= 819 cells, 8, 3) to 0.41 ± 0.01 Δ Fura-2 ratio in ononetin treated TRPM3 CHO cells (mean ± SEM; n= 642 cells, 6, 3; Figure 4-8). A similar inhibition was observed when cells were perfused with mefenamic acid (30μM). Heating evoked small increases in $[Ca^{2+}]_i$ which were similar in amplitude to untransfected cells (0.33 ± 0.01 Δ Fura-2 ratio in mefenamic acid treated TRPM3 CHO cells (mean ± SEM; n= 689 cells, 7, 3; Figure 4-8).

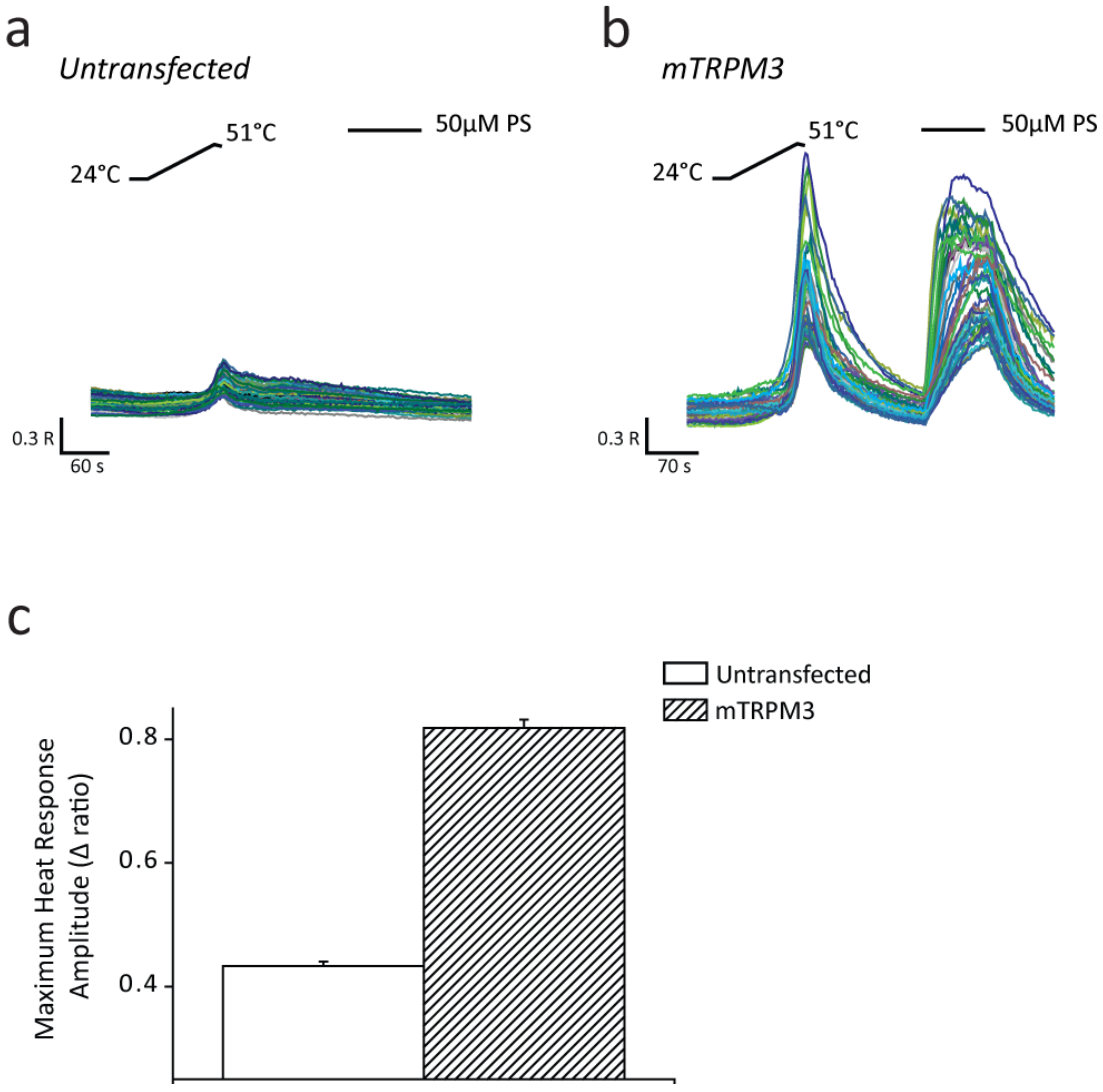

Figure 4-6 Heterologously expressed TRPM3 channels are sensitive to heat

$[Ca^{2+}]_i$ responses were monitored by Fura-2 in untransfected and PS-sensitive TRPM3 transfected CHO cells using microscope-based imaging. Cells were exposed to a heating temperature ramp (24-51°C) followed by the application of PS (50µM). (**a**) Representative traces displaying $[Ca^{2+}]_i$ responses evoked by a heating temperature ramp (24-51°C) in a population of untransfected CHO cells. Heating evoked a modest increase in $[Ca^{2+}]_i$ in untransfected cells however application of PS (50µM) evoked no change in $[Ca^{2+}]_i$. R denotes Fura-2 ratio. (**b**) Representative traces displaying $[Ca^{2+}]_i$ responses evoked by a heating temperature ramp (24-51°C) and 50µM PS in a population of mTRPM3 CHO cells. Both heating and PS (50µM) evoked large reversible $[Ca^{2+}]_i$ increases in a population of mTRPM3 CHO cells. R denotes Fura-2 ratio. (**c**) Column graph showing the average maximum response amplitudes to the heating temperature ramp in untransfected (plain bar) and mTRPM3 transfected CHO cells (striped bar). Columns represent mean ± SEM (untransfected, n= 2640 cells, 9, 3; mTRPM3, n= 1379 cells, 10, 3).

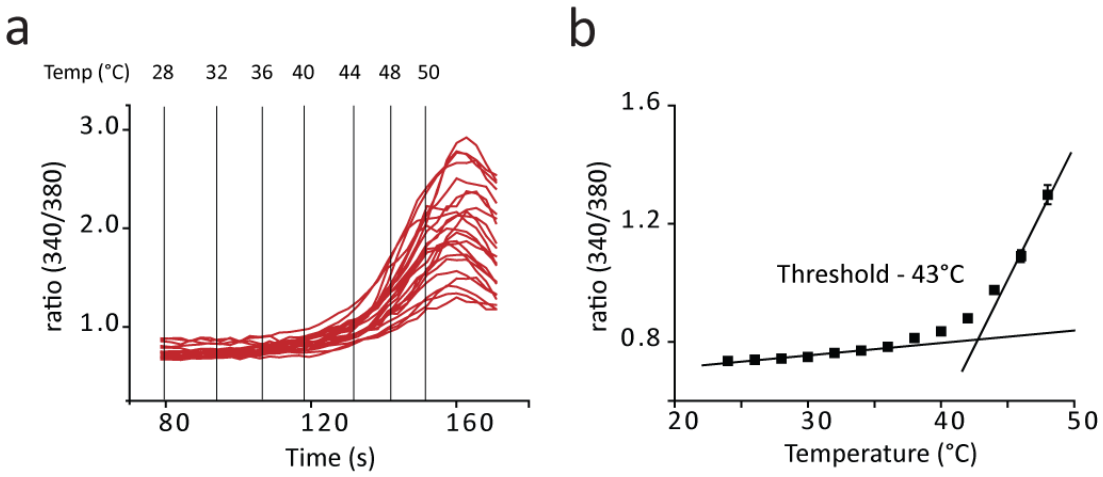

Figure 4-7 Temperature activation thresholds for TRPM3

(**a**) Representative traces displaying $[Ca^{2+}]_i$ responses evoked by heating in mTRPM3 CHO cells . Vertical lines indicate the temperature (°C) of the superfusate at different time points. (**b**) Temperature activation thresholds were determined by plotting the Fura-2 (340/380) ratio against temperature. The temperature at the intersect of the two lines was used as the temperature activation threshold. The graph illustrates the threshold determination for a population of mTRPM3 CHO cells.

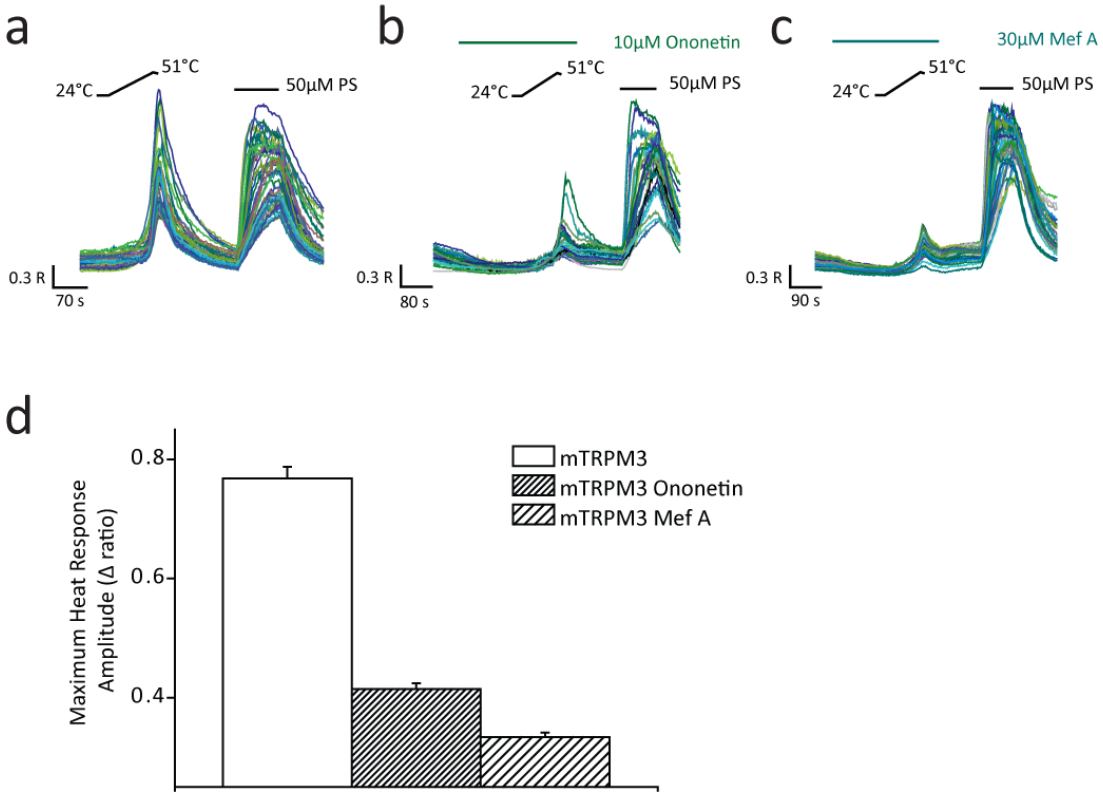

Figure 4-8 TRPM3 heat-evoked responses are inhibited by mefenamic acid and ononetin

$[Ca^{2+}]_i$ responses were monitored by Fura-2 in PS-sensitive TRPM3 transfected CHO cells using microscope-based imaging. Cells were exposed to a heating temperature ramp (24-51°C) followed by the application of PS (50µM). (**a**) Representative traces displaying $[Ca^{2+}]_i$ responses evoked by a heating temperature ramp (24-51°C) and 50µM PS in a population of mTRPM3 CHO cells (same data as shown in Figure 4-6b). Both heating and PS (50µM) evoked large reversible increases $[Ca^{2+}]_i$ in a population of mTRPM3 CHO cells. R denotes Fura-2 ratio. (**b**) Representative traces displaying $[Ca^{2+}]_i$ responses evoked by a heating temperature ramp (24-51°C) and 50µM PS in a population of mTRPM3 CHO. Cells were perfused with ononetin (10µM) 2 ½ minutes prior to and during the heating temperature ramp (green horizontal bar indicates application of ononetin). Ononetin supressed the heat-evoked responses of TRPM3 CHO cells. R denotes Fura-2 ratio. (**c**) Representative traces displaying $[Ca^{2+}]_i$ responses evoked by a heating temperature ramp (24-51°C) and 50µM PS in a population of mTRPM3 CHO. Cells were perfused with mefenamic acid (30µM) 2 ½ minutes prior to and during the heating temperature ramp (blue horizontal bar indicates application of mefenamic acid). Mefenamic acid inhibited the heat-evoked responses of TRPM3 CHO cells. R denotes Fura-2 ratio. (**d**) Column graph showing the average maximum response amplitudes to the heating temperature ramp in untreated mTRPM3 transfected CHO cells and cells treated with ononetin and mefenamic acid. Columns represent mean ± SEM (mTRPM3, n= 819 cells, 8, 3; mTRPM3 ononetin, n= 642 cells, 6, 3; mTRPM3 mefenamic acid, n= 689, 7, 3).

4.4.6 TRPM3 is expressed in heat-sensitive sensory neurons

To examine whether TRPM3 is able to contribute to the heat-sensitivity of sensory neurons, the functional expression of TRPM3 channels on heat-sensitive, mouse, DRG neurons was investigated using microscope-based imaging.

Isolated DRG neurons were first exposed to a heating temperature ramp (24-51°C) in order to establish heat-sensitivity, this was followed by challenges with PS (TRPM3 agonist) and capsaicin (TRPV1 agonist) and a depolarising concentration of KCl (to allow neurons to be identified).

A large population of neurons displayed heat sensitivity, with 42% (n= 719/1701, 12, 4) of neurons responding to the heating temperature ramp (24-51°C) with an increase in $[Ca^{2+}]_i$. Heat-evoked $[Ca^{2+}]_i$ responses had an average temperature threshold of 45 ± 0.4°C (mean ± SEM; n= 89 neurons, 2, 2). Functional expression of TRPM3 and TRPV1 channels on heat-sensitive neurons was assessed by sensitivity to PS and capsaicin, respectively. The majority of heat-sensitive neurons appeared to co-express TRPM3 and TRPV1, with 64% (n= 458/719) of neurons showing sensitivity to both PS and capsaicin (see Figure 4-9 for representative traces). A small population of heat-sensitive neurons appeared to express TRPM3 but not TRPV1, exhibiting PS sensitivity without sensitivity to capsaicin (10%; n= 73/719). Conversely, another population of heat-sensitive neurons did not respond to PS but were sensitive to capsaicin (19%; n= 140/719). In addition to these sub-populations, a small group (7%; n= 48/719) of heat-sensitive neurons displayed no sensitivity to PS or capsaicin, suggesting a lack of both TRPM3 and TRPV1 expression on these neurons (Figure 4-9). The majority (57%, n= 531/925) of PS-sensitive neurons were heat-sensitive. The percentage of capsaicin sensitive neurons which were sensitive to heat was higher (76%, n= 598/788).

The average temperature thresholds of heat-sensitive neurons which were responsive both PS and capsaicin (45 ± 0.5°C; mean ± SEM; n= 51 neurons), to PS but not capsaicin (44 ± 1.4°C; mean ± SEM; n= 10 neurons), to capsaicin but not PS (47 ± 0.4°C; ; mean ± SEM; n= 23 neurons) or to neither agonist (45 ± 0.8°C; mean ± SEM; n= 5 neurons) were similar (NS, Kruskal-Wallis test with Dunn-Bonferroni's pairwise post-hoc test).

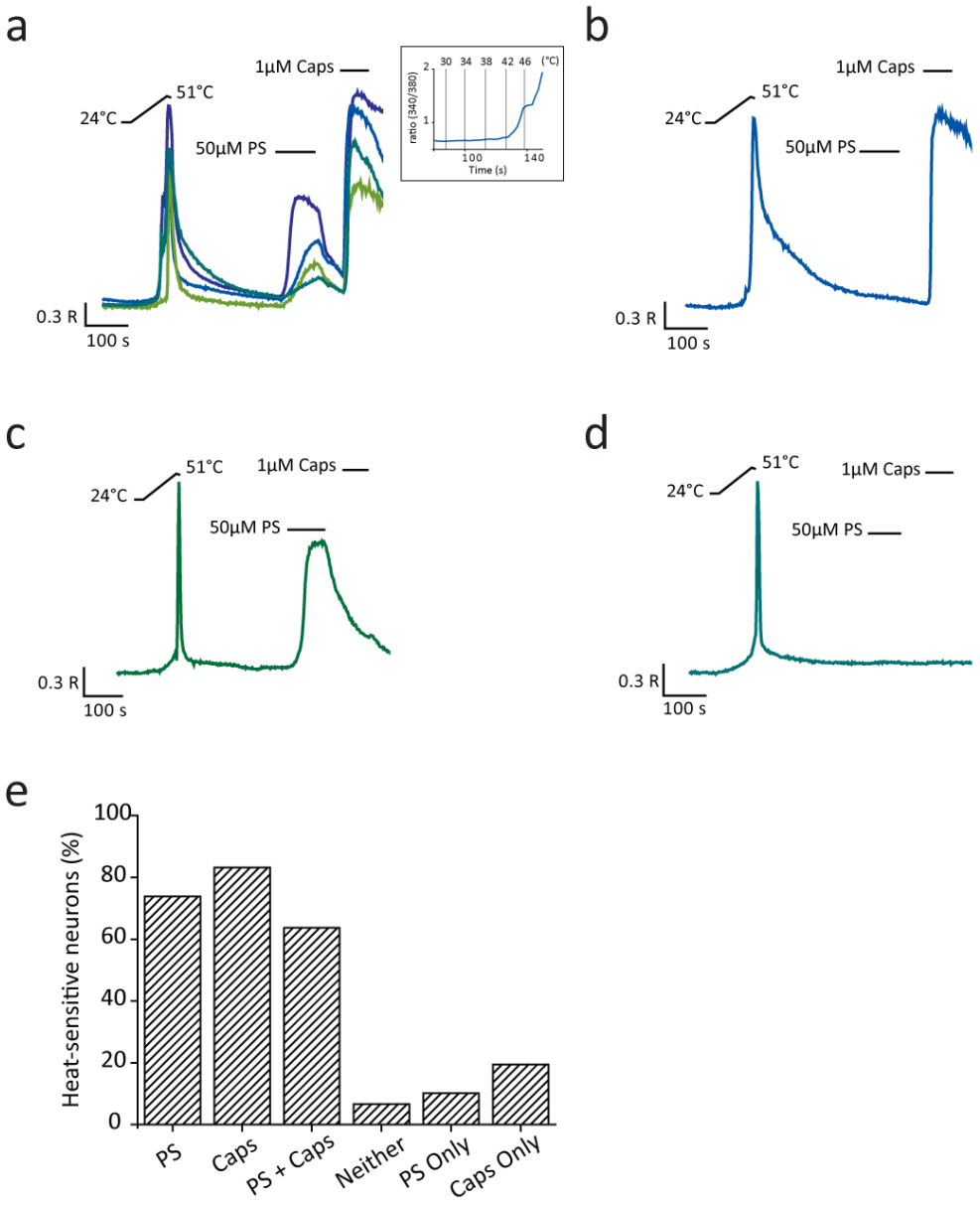

Figure 4-9 Heat-sensitive neurons express TRPM3 alongside TRPV1

Changes in $[Ca^{2+}]_i$ were monitored by Fura-2 in isolated DRG neurons using microscope-based imaging. Neurons were exposed to a heating temperature ramp (24-51°C) followed by challenges with PS (50µM) and capsaicin (1µM) (**a**) Representative traces displaying $[Ca^{2+}]_i$ responses of heat-sensitive DRG neurons which were sensitive to both PS and capsaicin. R denotes Fura-2 ratio. The inset graph displays the $[Ca^{2+}]_i$ response of one of these neurons during the heating temperature ramp. Vertical lines indicate the temperature (°C) of the superfusate at different time points. (**b**) Representative trace displaying the $[Ca^{2+}]_i$ response of a heat-sensitive DRG neuron which was sensitive to capsaicin but not PS. R denotes Fura-2 ratio. (**c**) Representative trace displaying the $[Ca^{2+}]_i$ response of a heat-sensitive DRG neuron which was sensitive to PS but not capsaicin. R denotes Fura-2 ratio. (**d**) Representative trace displaying the $[Ca^{2+}]_i$ response of a heat-sensitive DRG neuron which was not sensitive to PS or capsaicin. R denotes Fura-2 ratio. (**e**) Column graph showing the percentage of heat-sensitive neurons which were sensitive PS, capsaicin, both PS and capsaicin, neither PS nor capsaicin, PS and not capsaicin, and, capsaicin and not PS (n= 719 neurons, 12, 4).

4.4.7 Heat sensitivity of neurons lacking functional TRPM3 channels

In order to examine any role played by TRPM3 in the heat-sensitivity of sensory neurons, the heat-evoked responses of DRG neurons from *Trpm3*$^{-/-}$ mice were examined and compared to the heat-evoked responses of WT mice. As in the previous experiments, isolated DRG neurons were first exposed to a heating temperature ramp (24-51°C) in order to establish heat-sensitivity, this was followed by challenges with PS (TRPM3 agonist) and capsaicin (TRPV1 agonist) and a depolarising concentration of KCl (to identify all neurons).

Isolated DRG neurons from *Trpm3*$^{-/-}$ mice had a smaller percentage of heat-sensitive neurons (34%, n= 243/712 neurons, 4, 2; see Figure 4-10) compared to WT DRG control experiments performed on the same day (44%, n= 472/1072 neurons, 7, 2; P<0.001, Pearson Chi-Square test). The majority of these heat-sensitive neurons were also capsaicin-sensitive (90%, n= 219/243), indicating the expression of TRPV1 in these neurons, similar to WT neurons (81%, n= 383/472).

Notably, the average temperature threshold for activation of heat-sensitive *Trpm3*$^{-/-}$ neurons (45 ± 0.4°C; n= 92 neurons, 2, 2) was the same to that measured for heat-sensitive wildtype neurons (45 ± 0.4°C; n= 89 neurons, 2, 2).

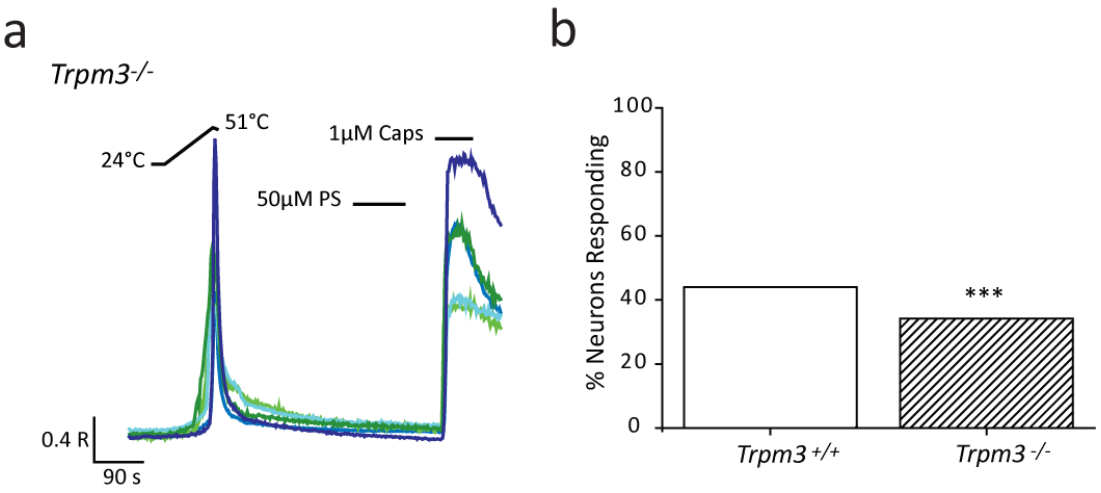

Figure 4-10 Heat sensitivity of *Trpm3*$^{-/-}$ neurons

Changes in $[Ca^{2+}]_i$ were monitored by Fura-2 in isolated DRG neurons using microscope-based imaging. Neurons were exposed to a heating temperature ramp (24-51°C) followed by challenges with PS (50µM) and capsaicin (1µM) (**a**) Representative traces displaying $[Ca^{2+}]_i$ responses of heat-sensitive *Trpm3*$^{-/-}$ DRG neurons which were sensitive to capsaicin but not PS. R denotes Fura-2 ratio. (**b**) Column graph showing the percentage of heat-sensitive neurons isolated from WT and *Trpm3*$^{-/-}$. Columns represent mean ± SEM (*** P <0.001, Pearson Chi-Square test; WT, n= 1072 neurons, 7, 2; *Trpm3*$^{-/-}$, n= 712 neurons, 4, 2)

4.4.8 Mice lacking functional TRPM3 channels exhibit reduced sensitivity to noxious heat

TRPM3 is heat sensitive when heterologously expressed in a recombinant cell line and is expressed in a large proportion of heat-sensitive sensory neurons which co-express the nociceptive thermosensor, TRPV1.

In order to examine whether TRPM3 plays a role in noxious heat sensing *in vivo* the latency to paw withdrawal from a 53°C hot plate was measured in *Trpm3*$^{+/+}$ and *Trpm3*$^{-/-}$ mice (Figure 4-11). Consistent with previous findings (Vriens et al., 2011), *Trpm3*$^{-/-}$ mice displayed significantly longer latencies to paw withdrawal than their wildtype counterparts, removing their paws from the hot plate on average 23.7 ± 1.1 s (n= 9) after exposure, compared to 15.9 ± 0.9 s (n=6) for *Trpm3*$^{+/+}$ mice. This finding demonstrates that mice lacking functional TRPM3 channels are less sensitive to noxious heat.

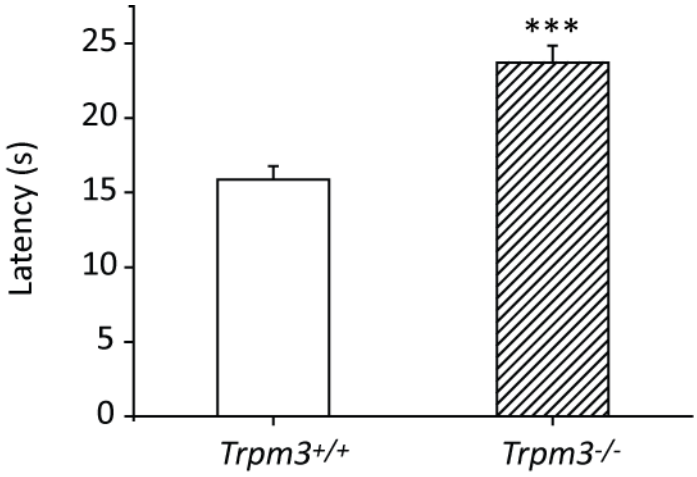

Figure 4-11 *Trpm3*$^{-/-}$ mice are less sensitive to noxious heat

The latency to paw withdrawal from a 53°C hot plate was measured in *Trpm3*$^{+/+}$ and *Trpm3*$^{-/-}$ mice. *Trpm3*$^{-/-}$ mice had significantly longer latencies to paw withdrawal in comparison to their wildtype counterparts. Columns represent mean ± SEM (*** P <0.001; t-test; *Trpm3*$^{+/+}$, n= 6 mice. *Trpm3*$^{-/-}$, n= 9 mice).

4.4.9 Modulation of TRPM3 activity by intracellular signalling pathways

4.4.9.1 Regulation of TRPM3 by cAMP-dependent mechanisms

Many mechanisms exist to regulate ion channel function, and phosphorylation of channel proteins by protein kinases downstream of G protein coupled receptor (GPCR) activation constitutes one of the best characterised forms of regulation.

The activity of one protein kinase subfamily, protein kinase A (PKA) is controlled by cellular levels of cyclic AMP (cAMP). Activation of Gαs linked GPCRs leads to an increase in cellular cAMP levels by stimulating adenylyl cyclase, an enzyme responsible for synthesis of cAMP from its precursor ATP (Berridge, 2012). This increase in cellular cAMP levels leads to activation of PKA (see Figure 4-12 for an illustrated summary of this pathway). Moreover, activation of Gαi/o linked GPCRs leads to a decrease in adenylyl cyclase activity and therefore lower levels of cAMP resulting in reduced PKA activity.

In order to investigate whether cAMP dependent processes are able to regulate the activity of TRPM3, the effects of raised cAMP levels on PS-evoked responses were tested. PS-evoked $[Ca^{2+}]_i$ responses of mouse TRPM3 CHO cells treated with an activator of adenylyl cyclase, forskolin (10μM, 15 minute pre-incubation) and a non-selective phosphodiesterase (PDE) inhibitor, IBMX (100μM, 15 minute pre-incubation), were examined and compared to the $[Ca^{2+}]_i$ responses of untreated cells. The amplitudes of PS-evoked $[Ca^{2+}]_i$ responses were consistently higher in cells treated with forskolin and IBMX than the responses of untreated cells. The average maximum amplitude of PS-evoked responses in untreated cells was 1.69 ± 0.27 Δ Fura-2 ratio and this was increased to 2.32 ± 0.33 Δ Fura-2 ratio, in cells treated with forskolin and IBMX (mean ± SEM; NS, t-test; n=3 independent experiments; Figure 4-13a). However, only a small potentiating shift of the PS EC_{50} value for activation was noted (control, 14.45 ± 3.99μM; forskolin + IBMX, 7.43 ± 1.00μM; NS, t-test; n=3 independent experiments).

Next, the effects of a cAMP analogue, 8-bromo cAMP (1mM, 15 minute pre-incubation), on PS-evoked responses were examined. Similar to the effects of forskolin and IBMX, cells treated with 8-bromo cAMP had consistently larger responses to PS (control, 1.02 ± 0.34 Δ Fura-2 ratio; 8-bromo cAMP, 1.31 ± 0.34 Δ Fura-2 ratio; NS, t-test; n=3 independent experiments; Figure 4-13b). However, 8-bromo cAMP had no effect on PS EC_{50} values (control, 9.36 ± 2.28μM; 8-bromo cAMP, 6.01 ± 0.88μM; NS, t-test; n=3 independent experiments).

In order to test whether the effects observed were due to activation of PKA, cells were treated with 8-bromo cAMP in the presence of either a non-selective protein kinase inhibitor (10µM H8) or a PKA selective inhibitor (1µM KT5720). The increase in PS response amplitude achieved with 8-bromo cAMP treatment was not reversed by incubation with either H8 or KT5720 (see Table 4-3 for values; NS; ANOVA followed by Tukey's HSD test; comparison to 8-bromo cAMP treatment alone). These findings suggest that the effects of raised cAMP levels on TRPM3 activation are PKA independent.

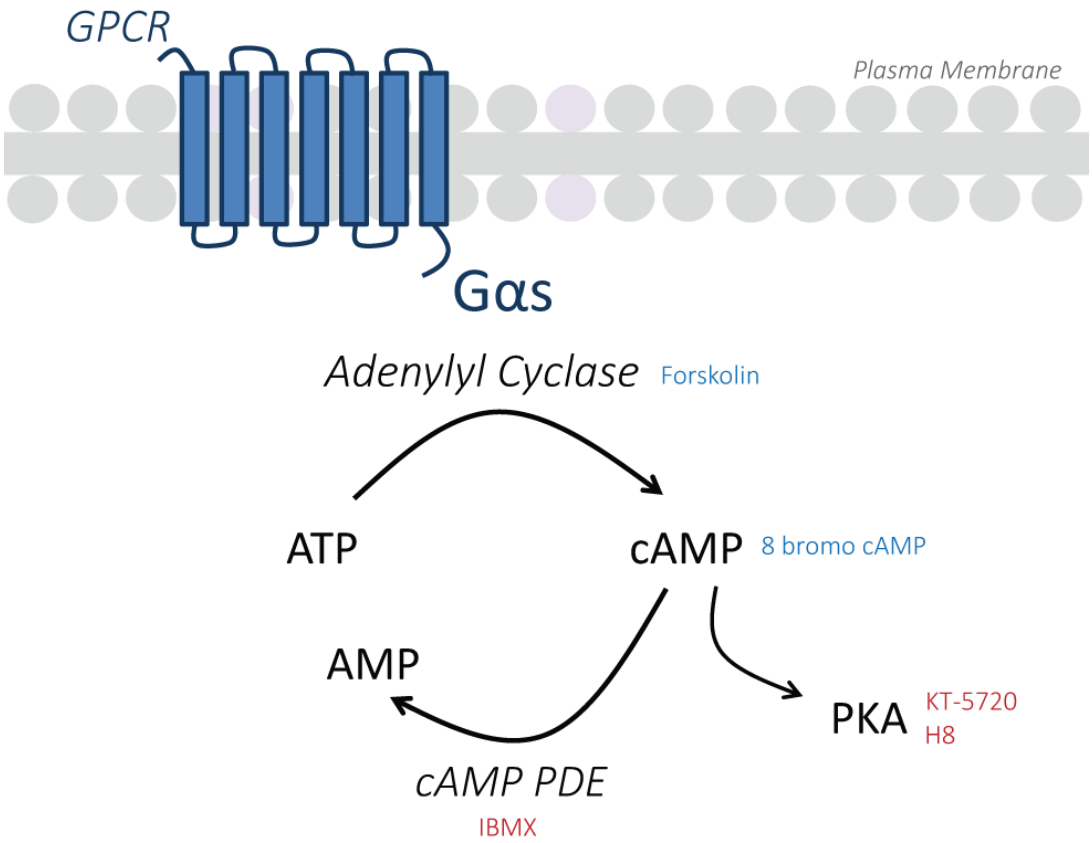

Figure 4-12 Signal transduction pathways downstream of Gαs linked GPCR activation

Activation of Gαs coupled receptors results in activation of the G protein by allowing the exchange of a molecule of GDP for GTP at the Gα subunit (which is inactive when bound to GDP). The activated Gαs-GTP monomer and a βγ dimer (not shown) dissociate from the receptor, allowing Gαs to activate the membrane associated enzyme, adenylyl cyclase. When activated adenylyl cyclase synthesises the intracellular messenger, cAMP, from molecules of ATP, cAMP can bind to and regulate ion channel function, and can also activate PKA. Decomposition of cAMP to AMP is catalysed by cAMP phosphodiesterase (cAMP PDE). Various pharmacological tools can be used to study this pathway and some of which are illustrated on the diagram (compounds which activate targets within the pathway are shown in blue and compounds which inhibit pathway components are shown in red). Forskolin, a diterpene from the Indian plant *Coleus forskohli*, stimulates adenylyl cyclase and can be used in combination with IBMX, a non-selective phosphodiesterase inhibitor, to amplify cellular cAMP levels (Beavo et al., 1971; Calixto et al., 2005). A brominated derivative of cAMP, 8-bromo cAMP which is resistant to degradation by cAMP PDE is also a useful pharmacological tool for studying the effects of cAMP. Furthermore PKA activity can be inhibited by KT-5720 (a potent and selective blocker of PKA) and H8 (a non-selective inhibitor of PKs).

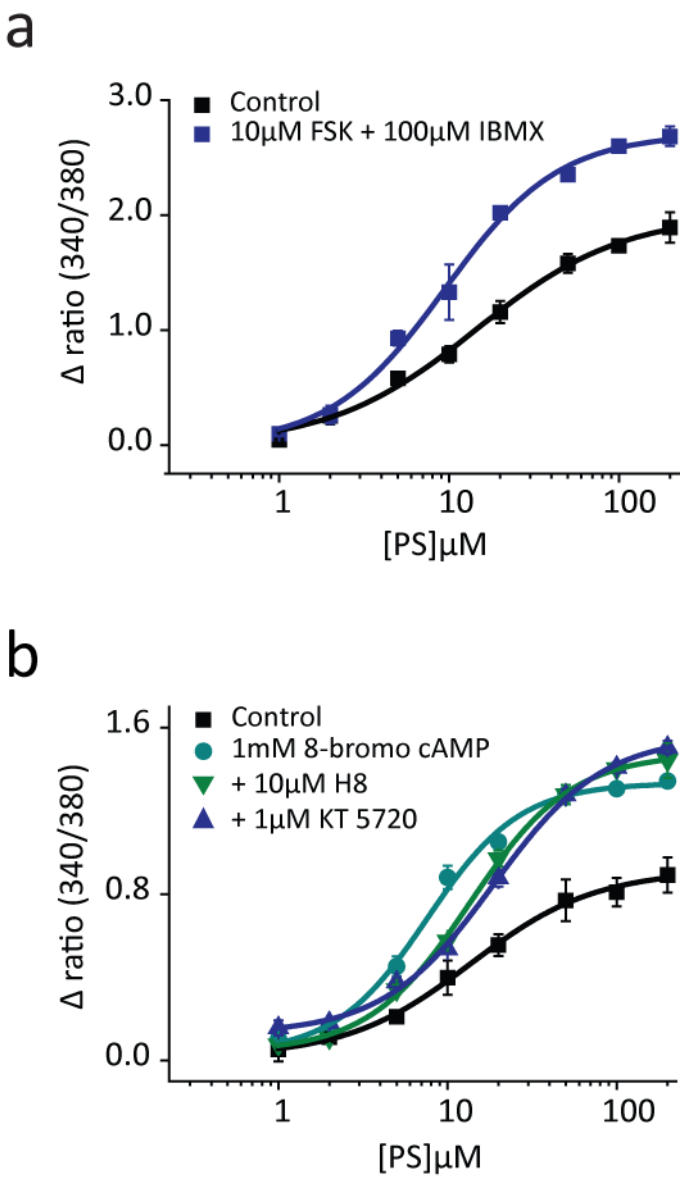

Figure 4-13 Increased levels of cAMP potentiate TRPM3 activity via a PKA-independent mechanism

(**a**) The effects of an adenylyl cyclase activator (10µM forskolin, 15 minute pre-incubation) and a PDE inhibitor (100µM IBMX, 15 minute pre-incubation) on PS-evoked $[Ca^{2+}]_i$ responses of CHO cells stably transfected with mTRPM3. Forskolin and IBMX treatment increased the maximum amplitude of PS-evoked responses (from 1.69 ± 0.27 Δ Fura-2 ratio and to 2.32 ± 0.33 Δ Fura-2 ratio; mean ± SEM; NS, t-test; n=3 independent experiments). Representative plot shown, data points are the mean ratio of triplicate wells ± SEM (**b**) The effects of a cAMP analogue, 8-bromo cAMP (1mM, 15 minute pre-incubation) on PS-evoked $[Ca^{2+}]_i$ responses of CHO cells stably transfected with mTRPM3. 8-bromo cAMP treatment appeared to increase the maximum amplitude of PS-evoked responses (from 1.02 ± 0.34 Δ Fura-2 ratio to 1.31 ± 0.34 Δ Fura-2 ratio; mean ± SEM; NS, t-test; n=3 independent experiments). The effects of 8-bromo cAMP treatment could not be reversed by treatment (15 minute pre-incubation) with a non-selective protein kinase inhibitor (10µM H8) or a selective PKA inhibitor (1µM KT-5720). Representative plot shown, data points are the mean ratio of triplicate wells ± SEM

Table 4-3 Effects of a cAMP analogue on PS evoked $[Ca^{2+}]_i$ responses

Table detailing the average EC_{50} values and maximum amplitudes for PS-evoked $[Ca^{2+}]_i$ responses in the presence and absence of 8-bromo cAMP, 8-bromo cAMP + H8 and 8-bromo cAMP + KT-5720. Values listed are mean ± SEM (n= 3 independent experiments).

	Control	**1mM 8-bromo cAMP**	**1mM 8-bromo cAMP + 10µM H8**	**1mM 8-bromo cAMP + 1µM KT-5720**
Average EC_{50} (µM)	9.36 ± 2.28	6.01 ± 0.88	9.01 ± 2.60	10.65 ± 4.23
Average Maximum Amplitude (Δ Fura-2 ratio)	1.02 ± 0.34	1.31 ± 0.34	1.39 ± 0.35	1.38 ± 0.31

4.4.9.2 Regulation of TRPM3 by pathways downstream of PLC activation

Several TRP channels are regulated by phosphoinositides derived from phosphatidylinositol (PtdIns), which are located within the cytoplasmic leaflet of the plasma membrane (Rohacs, 2007, 2009). Phosphatidylinositol 4,5-bisphosphate (PIP_2) is the most well studied of these lipids within the domain of ion channel regulation (Rohacs, 2009). Activity of TRPV1 has been shown to be both activated and inhibited by PIP_2 (Chuang et al., 2001; Klein et al., 2008; Lukacs et al., 2007; Prescott and Julius, 2003; Ufret-Vincenty et al., 2011; Yao and Qin, 2009) whereas TRPV5, TRPM4, TRPM5, TRPM7 and TRPM8 have all been shown to be activated by PIP_2 (Lee et al., 2005; Liu and Liman, 2003; Liu and Qin, 2005; Nilius et al., 2006; Rohács et al., 2005; Runnels et al., 2002; Zhang et al., 2005).

Breakdown of PIP_2 occurs when PLCβ cleaves the lipid into the second messengers, diacyl glycerol (DAG) and inositol 1,4,5-trisphosphate (IP_3) (Berridge, 2012). PLCβ isoforms are activated by Gαq/11-GTP monomers downstream of GPCR activation (Rohacs, 2013). DAG is the best known activator of the PKC family of serine/threonine kinases and as discussed earlier protein phosphorylation is one of the best characterised forms of ion channel regulation. In addition, DAG has been shown to activate some TRPC channels in a PKC-independent manner (Rohacs, 2013). IP_3 releases Ca^{2+} from intracellular stores by binding to IP_3 receptors present on the endoplasmic reticulum (see Figure 4-14 for an illustrated summary of this pathway).

In order to investigate whether signalling pathways downstream of PLC activation are able to regulate the activity of TRPM3, PS-evoked $[Ca^{2+}]_i$ responses of mouse TRPM3 CHO cells treated with an activator of PLC, *m*-3M3FBS (10μM, 15 minute pre-incubation) were examined and compared to the $[Ca^{2+}]_i$ responses of untreated cells in 96-well plate experiments. Treatment with *m*-3M3FBS consistently elevated the maximum amplitudes of PS-evoked $[Ca^{2+}]_i$ responses. The average maximum amplitude of PS-evoked responses in untreated cells was 1.91 ± 0.20 Δ Fura-2 ratio and this was increased to 2.42 ± 0.30 Δ Fura-2 ratio, in cells treated with *m*-3M3FBS (mean ± SEM; NS, t-test; n=5 independent experiments; Figure 4-15a). However, there was no change in PS EC_{50} values for activation (control, 12.11 ± 2.61μM; *m*-3M3FBS, 12.78 ± 4.02μM; NS, t-test; n=5 independent experiments).

In order to test whether the effects observed could be reversed by a PLC inhibitor, cells were treated with *m*-3M3FBS in the presence of U73122 (5μM, 15 minute pre-incubation).

The increase in PS response amplitude achieved with *m*-3M3FBS treatment was reversed by co-treatment with U73122. Co-treated cells had an average maximum response amplitude of 1.73 ± 0.35 Δ Fura-2 ratio which was even lower than the average maximum amplitude of untreated cells, suggesting some tonic activation of PLC (mean ± SEM; n=3 independent experiments; Figure 4-15a).

Next, the effects of direct PKC stimulation on TRPM3 activation were investigated. The PS-evoked responses of cells treated with a PKC activator (1μM PMA, 15 minute pre-incubation) were examined and compared to untreated cells. Interestingly, PS-evoked responses in cells treated with PMA were consistently inhibited, with the maximal response amplitudes reduced from 1.84 ± 0.30 Δ Fura-2 ratio in untreated cells, to 1.33 ± 0.25 Δ Fura-2 ratio in cells treated with PMA (mean ± SEM; NS, t-test; n=4 independent experiments; Figure 4-15b). However, there was no change in EC_{50} value (control, 13.73 ± 3.32μM; PMA, 15.24 ± 2.31μM; mean ± SEM; n=4 independent experiments).

To confirm whether the reduced activity of TRPM3 was due to PKC activation or a separate action of PMA, the effects of another PKC activator (1μM PDBu, 15 minute pre-incubation) were tested. Similar to PMA treatment, cells treated with PDBu had significantly smaller maximum responses to PS stimulation than untreated cells (control, 1.99 ± 0.08 Δ Fura-2 ratio; PDBu, 1.41 ± 0.02 Δ Fura-2 ratio; mean ± SEM; $P<0.05$, t-test; n=3 independent experiments; Figure 4-15c). Again the EC_{50} values for activation were not affected (control, 10.89 ± 4.19μM; PDBu, 12.34 ± 1.42μM; mean ± SEM; n=3 independent experiments).

In order to test whether the effects of PDBu could be reversed with a protein kinase inhibitor, the PS-evoked responses of cells co-treated with PDBu and staurosporine (3μM) were examined. Unexpectedly, the combination of these compounds resulted in a greater inhibition of TRPM3 PS evoked responses (see Table 4-4 for values; comparison to control; NS, ANOVA followed by Dunnett's T3 test; n= 3 independent experiments; Figure 4-15c). The effect of staurosporine treatment alone was then investigated, cells treated with staurosporine (without PDBu) had significantly inhibited PS-evoked responses, maximum response amplitudes were reduced from 2.12 ± 0.13 in untreated cells to 1.20 ± 0.15 Δ Fura-2 ratio in cells treated with staurosporine (mean ± SEM; $P<0.01$, t-test; n=4 independent experiments; Figure 4-15d). EC_{50} values were slightly lower with staurosporine treatment (control, 11.30 ± 2.99μM; staurosporine, 7.69 ± 1.80μM; mean ± SEM; NS, t-test; n=4 independent experiments).

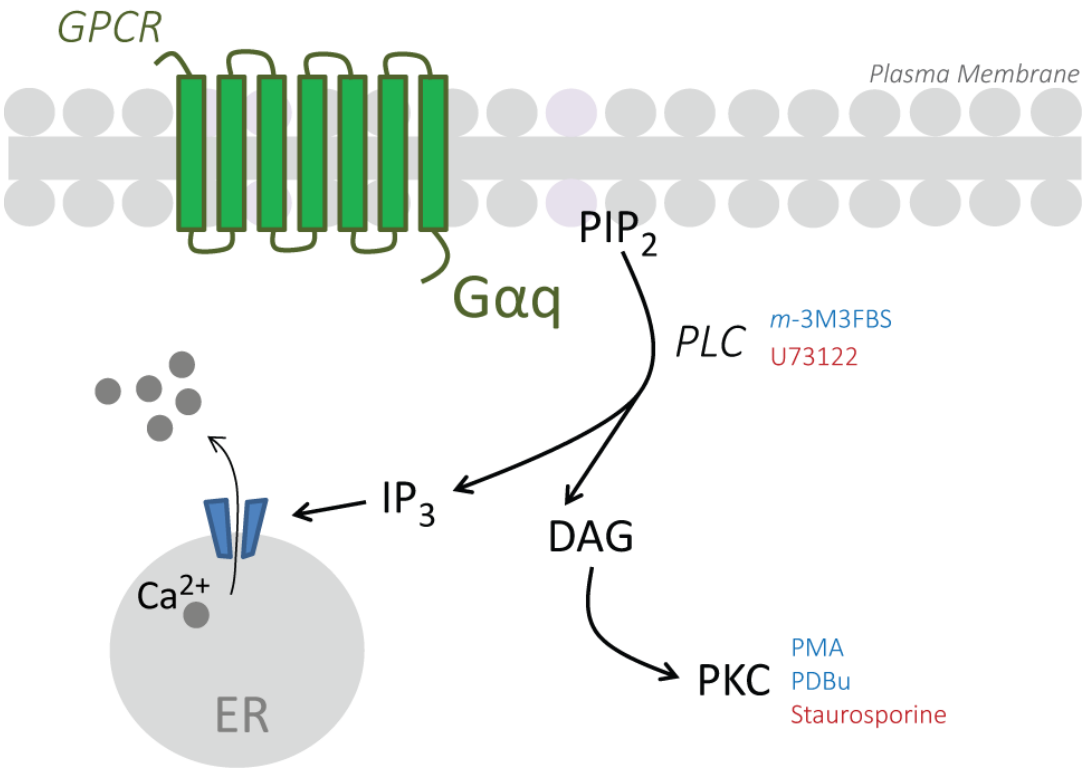

Figure 4-14 Signal transduction pathways downstream of Gαq/11 linked GPCR activation

Activation of Gαq coupled receptors results in activation of the G protein by allowing the exchange of a molecule of GDP for GTP at the Gα subunit (which is inactive when bound to GDP). The activated Gαq-GTP monomer and a βγ dimer (not shown) dissociate from the receptor, allowing Gαq to activate phospholipase C (PLC). PLC cleaves phosphatidylinositol 4,5-bisphosphate (PIP_2) into diacyl glycerol (DAG) and inositol 1,4,5-trisphosphate (IP_3). IP_3 releases Ca^{2+} from intracellular stores (ER/endoplasmic reticulum) and DAG activates protein kinase C (PKC). Various pharmacological tools can be used to study this pathway and some of which are illustrated on the diagram (compounds which activate targets within the pathway are shown in blue and compounds which inhibit pathway components are shown in red). A compound called *m*-3M3FBS can be used to activate PLC and a compound named U73122 can be used as a PLC inhibitor (Bae et al., 2003; Rohacs, 2009). Furthermore PKC activity can be stimulated by PMA or PDBu, and inhibited by staurosporine (Calixto et al., 2005).

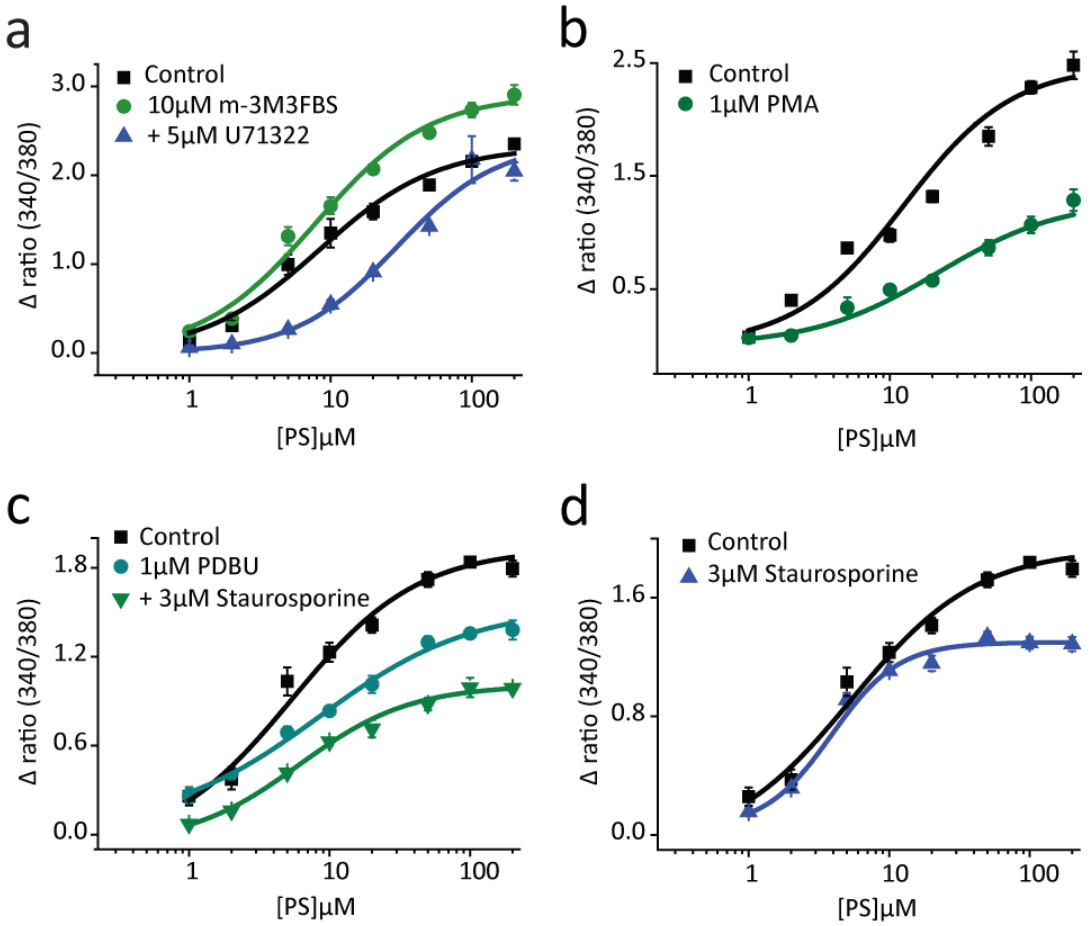

Figure 4-15 Pathways downstream of PLC activation modulate TRPM3

(**a**) The effects of a PLC activator (10µM *m*-3M3FBS, 15 minute pre-incubation) on PS-evoked $[Ca^{2+}]_i$ responses of CHO cells stably transfected with mTRPM3. *M*-3M3FBS treatment increased the maximum amplitude of PS-evoked responses and this effect was reversed by co-treatment with a PLC inhibitor (5µM U73122). Representative plot shown, data points are the mean ratio of triplicate wells ± SEM. (**b**) The effects of a PKC activator, PMA (1µM, 15 minute pre-incubation) on PS-evoked $[Ca^{2+}]_i$ responses of CHO cells stably transfected with mTRPM3. PMA treatment inhibited PS-evoked responses. Representative plot shown, data points are the mean ratio of triplicate wells ± SEM. (**c**) The effects of another PKC activator, PDBu (1µM, 15 minute pre-incubation) on PS-evoked $[Ca^{2+}]_i$ responses of CHO cells stably transfected with mTRPM3. PDBu treatment significantly inhibited PS-evoked responses but this effect was not reversed by co-treatment with a PKC inhibitor, staurosporine (3µM), which caused responses to be inhibited even further. Representative plot shown, data points are the mean ratio of triplicate wells ± SEM. (**d**) The effects of staurosporine (3µM, 15 minute pre-incubation) on PS-evoked $[Ca^{2+}]_i$ responses of mTRPM3 CHO cells. Cells treated with staurosporine had significantly reduced maximum response amplitudes in comparison to untreated cells. Representative plot shown, data points are the mean ratio of triplicate wells ± SEM.

Table 4-4 Effects of a PKC activator on PS evoked $[Ca^{2+}]_i$ responses

Table detailing the average EC_{50} values and maximum amplitudes for PS-evoked $[Ca^{2+}]_i$ responses in the presence and absence of PDBu and PDBu + Staurosporine. Values listed are mean ± SEM (n= 3 independent experiments).

	Control	**1µM PDBu**	**1µM PDBu + 3µM Staurosporine**
Average EC_{50} (µM)	10.89 ± 4.19	12.34 ± 1.42	15.07 ± 4.45
Average Maximum Amplitude (Δ Fura-2 ratio)	1.99 ± 0.08	1.41 ± 0.02	1.09 ± 0.11

4.4.10 Activation of the CB1 receptor inhibits TRPM3

The findings of the previous section demonstrated that manipulation of cAMP levels resulted in modulation of TRPM3 activity: when cAMP levels were raised using pharmacological tools the activity of TRPM3 was potentiated. In order to investigate whether cAMP activity is needed for activation of TRPM3 the effect of decreased cAMP production on PS-induced TRPM3 activation was investigated.

The cannabinoid receptor type 1 or CB1 is a GPCR which is expressed in a large proportion of peripheral sensory neurons (Ahluwalia et al., 2000; Binzen et al., 2006; Khasabova et al., 2002). Activation of CB1 receptors causes inhibition of adenylyl cyclase by a process which is dependent on the activity of Gαi/o proteins, and leads to decreased cellular levels of cAMP (Turu and Hunyady, 2010).

In order to test whether agonist-induced activation of a Gαi/o linked GPCR and the resulting decrease in cAMP levels could inhibit TRPM3; a GFP-tagged CB1 receptor was transiently transfected into CHO cells stably expressing the mouse TRPM3 channel (see

Figure **4-16**). Microscope-based imaging experiments were then used to investigate whether the PS evoked $[Ca^{2+}]_i$ responses of individual cells were modulated by administration of a CB1 receptor agonist (WIN 55212-2) or antagonist (AM251).

The TRPM3-CB1 transfected cells were exposed to two consecutive 20μM PS challenges with the second PS challenge occurring either in the presence or absence of a CB1 agonist or antagonist. A submaximally effective concentration of PS was used because subtle modulation of responses would be difficult to detect if TRPM3 channels were maximally activated.

In control experiments where cells experienced two consecutive PS challenges without exposure to a CB1 agonist/antagonist, PS responses were repeatable and exhibited little desensitisation. On average cells responded to the second PS challenge with a maximum response amplitude which was 0.09 Δ Fura-2 ratio lower (from 0.78 ± 0.02 to 0.69 ± 0.02 Δ Fura-2 ratio) than the first PS response amplitude (mean ± SEM; n= 135 cells, 1, 1; Figure 4-17a). However, in experiments where cells were perfused with a CB1 agonist, WIN 55212-2 (1μM), 1.5 minutes before and during the second PS challenge, many cells displayed an inhibited response to PS (see Figure 4-17b). On average cells treated with WIN 55212-2 responded to the second PS challenge with a maximum response amplitude which was 0.25

Δ Fura-2 ratio lower (from 0.78 ± 0.02 to 0.53 ± 0.02 Δ Fura-2 ratio) than the first PS response amplitude (mean ± SEM; n= 336 cells, 2, 1; Figure 4-17a).

In contrast, in experiments where cells were perfused with a CB1 antagonist, AM251 (0.5μM), many cells exhibited potentiated responses when challenged with a second PS response (Figure 4-17a). In some cases cells that exhibited no response to the first challenge responded to PS in the presence of the CB1 antagonist. However, on average the maximum response amplitude was unchanged (from 0.71 ± 0.02 to 0.70 ± 0.02 Δ Fura-2 ratio; mean ± SEM; n= 307 cells, 2, 1).

It is important to note that the CB1-GFP DNA will not have been successfully incorporated into all TRPM3 CHO cells and this can be seen when observing GFP fluorescence in transfected cells (see

Figure **4-16**). Only a fraction of the cells shown were fluorescent and these are the cells which will contain the GFP-tagged CB1 receptor (9% fluorescent, 388/ 4342). Modulation of responses is easier to observe in a scatterplot displaying the change in PS response amplitudes for cells in each experiment (Figure 4-17b). A trend for cells to have decreased maximum response amplitudes can be seen in cells treated with the CB1 agonist (WIN 55212-2). In contrast a trend for potentiated responses is clear in experiments where cells were treated with a CB1 antagonist (AM251).

Quantitatively, 4% (12/336) of cells exposed to the CB1 receptor agonist, responded to the second PS challenge with a response amplitude that was 1 Δ Fura-2 ratio lower than their first, control response amplitude. However, this was observed in 0% (0/135 cells) of cells in control experiments ($P<0.05$, Fisher's exact test). Conversely, when cells were exposed to the CB1 receptor antagonist 7% (21/307) responded to the second PS challenge with a maximum response amplitude which was 1 Δ Fura-2 ratio higher than their response to the first PS challenge. This large increase in response amplitude was not observed in any cells (0/135 cells) in control experiments ($P<0.001$, Fisher's exact test).

It is highly likely that the cells which demonstrated this behaviour are the cells which contain the GFP-tagged CB1 receptor, and it is therefore possible to conclude that activation of the CB1 receptor inhibits TRPM3 responses whereas inhibition of CB1 potentiates TRPM3 PS responses suggesting a level of constitutive activity at the CB1 receptor.

a *Mock-transfected TRPM3 CHO cells*

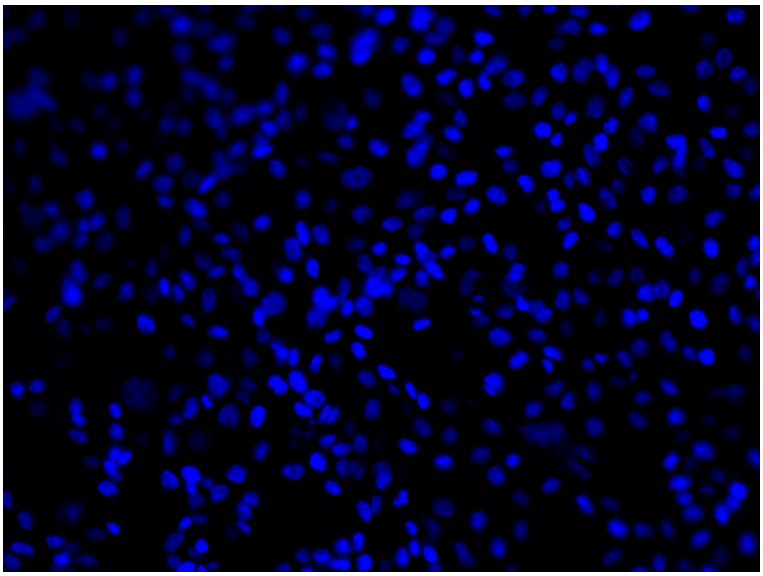

b *CB1-GFP transfected TRPM3 CHO cells*

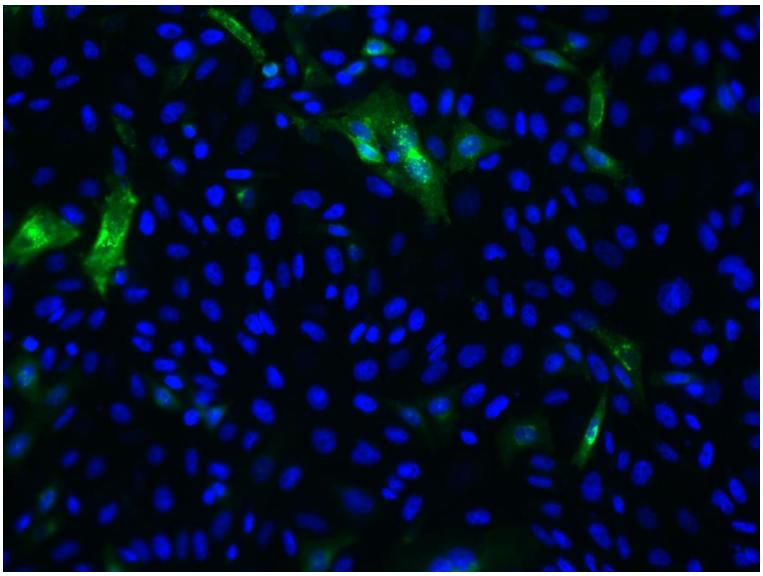

Figure 4-16 Images of mock- and CB1-GFP transfected TRPM3 CHO cells

Verification of CB1-GFP^{+} TRPM3 CHO cells. Combined image demonstrating an overlap of GFP expression (green) with hoescht staining (blue) in CB1-GFP transfected TRPM3 CHO cells (bottom panel) but not mock-transfected cells (upper panel).

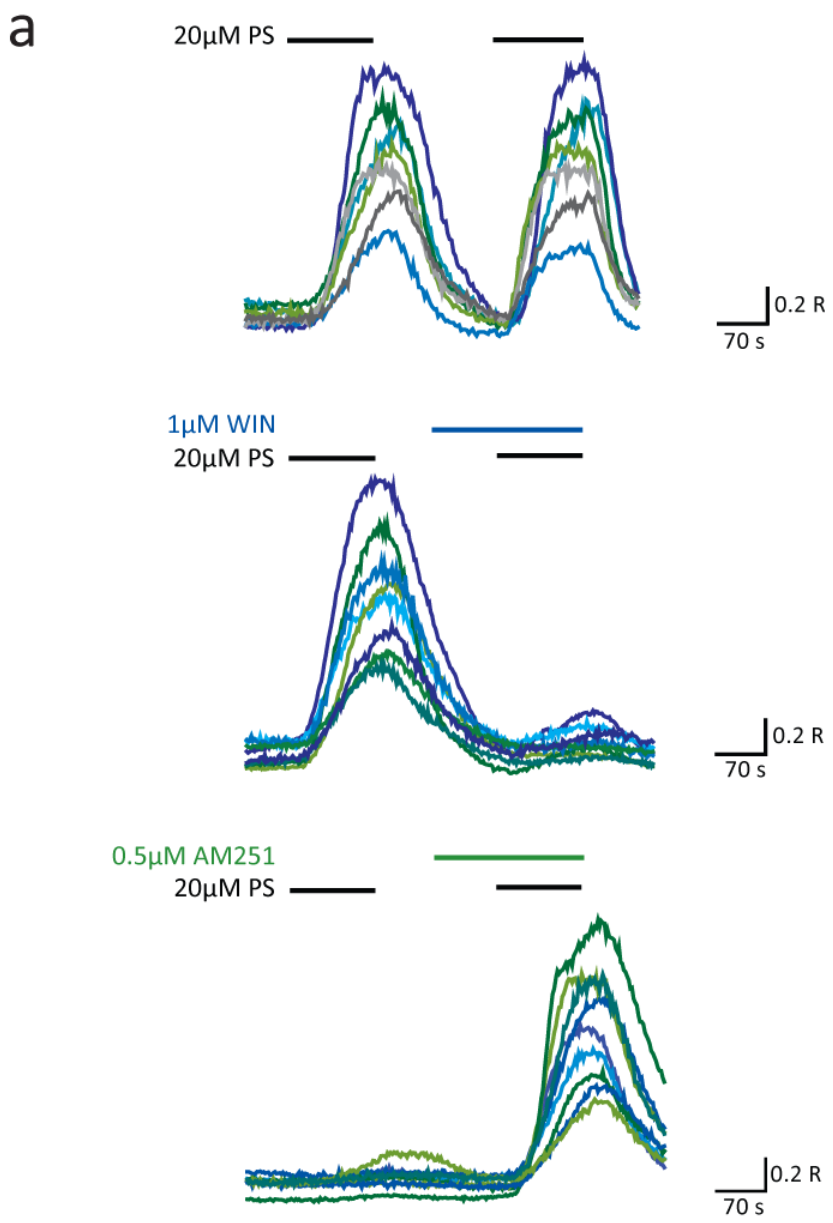
a
20μM PS
0.2 R
70 s
1μM WIN
20μM PS
0.2 R
70 s
0.5μM AM251
20μM PS
0.2 R
70 s
b
NS
***
***
Change in PS Response
Amplitude (Δ ratio)
2
1
0
-1
-2
Control
1μM WIN
0.5μM AM251

Figure 4-17 CB1 modulates activation of recombinantly expressed TRPM3

(**a**) $[Ca^{2+}]_i$ responses monitored by Fura-2 (R denotes Fura-2 ratio) in PS-sensitive GFP-CB1 transfected TRPM3 CHO cells using microscope-based imaging. Cells were exposed to two consecutive 20μM PS challenges. In control experiments (traces in the top panel) cells were not exposed to a CB1 receptor agonist or antagonist. In other experiments cells were perfused with a CB1 receptor agonist (1μM WIN 55212-2) 1.5 minutes before and during the second PS challenge (traces in the middle panel). In some experiments cells were perfused with a CB1 receptor antagonist (0.5μM AM251) 1.5 minutes before and during the second PS challenge (traces in the bottom panel). In control experiments PS responses were repeatable and exhibited little desensitisation. In experiments where cells were exposed to 1μM WIN 55212-2, some cells exhibited dramatically inhibited PS responses. In contrast, some cells exposed to 0.5μM AM251 displayed responses which were greatly potentiated. Selected traces from cells which displayed marked inhibition/potentiation are shown. (**b**) A scatter plot illustrating the change in maximum amplitude between responses to the first and second PS challenges. Negative values indicate cells which exhibited a reduced response to the second PS challenge and positive values indicate cells which displayed a potentiated response to the second PS challenge (Control, n= 135 cells, 1, 1; 1μM WIN, n= 336 cells, 2, 1; 0.5μM AM251, n= 307 cells, 2, 1). Note that some cells treated with 1μM WIN showed large decreases in response amplitudes and exposure to 0.5μM AM251 resulted in large potentiation in some cells. These larger changes were not observed in control experiments. The change in response amplitudes was significantly different between control cells and cells treated with 1μM WIN but was not significantly different between control cells and cells treated with 0.5μM AM251 (*** $P < 0.001$; Kruskal-Wallis test with Dunn-Bonferroni's pairwise post-hoc test).

4.4.11 CB1 modulation of TRPM3 channels expressed on sensory neurons

The CB1 receptor is expressed in ~40-60% of DRG neurons with a high level of co-expression with TRPV1 (Agarwal et al., 2007; Ahluwalia et al., 2000; Binzen et al., 2006; Khasabova et al., 2002). Moreover TRPM3 has also been found to be highly co-expressed with TRPV1 and its expression has been shown by one study to be restricted to small diameter sensory neurons (Vriens et al., 2011). These findings indicate that both CB1 receptors and TRPM3 channels are expressed by the nociceptor subpopulation of sensory neurons. As activation of the CB1 receptor modulated the activity of TRPM3 channels expressed in a recombinant cell line, the effects of CB1 receptor agonists on TRPM3 channels natively expressed in mouse DRG neurons were investigated.

Isolated DRG neurons were exposed to two consecutive submaximally effective PS challenges (20μM) followed by a depolarisation by a high concentration of KCl, which allowed all neurons to be identified. The second PS challenge took place either in the presence or absence of the cannabinoid receptor agonist, WIN 55212-2 (1μM). In control experiments, PS evoked $[Ca^{2+}]_i$ responses which exhibited some desensitisation. On average PS-responsive neurons responded to the second PS challenge with a maximum response amplitude which was 62 ± 2% that of the first PS response amplitude (mean ± SEM; n= 356 neurons, 10, 6; Figure 4-18). However, in experiments where neurons were perfused with 1μM WIN 55212-2 for 2 minutes before and during the second PS challenge, the maximum response amplitude was reduced to 51 ± 3 % (% of the first PS response; mean ± SEM; $P<0.001$, Mann-Whitney U test; n= 213 neurons, 7, 3;Figure 4-18).

This finding suggested that application of WIN 55212-2 causes inhibition of PS-evoked responses in some DRG neurons. In order to test this, DRG neurons were exposed to three consecutive PS challenges (20μM). Following the protocol of previous experiments the first application of PS identified the PS-sensitive neurons and the second PS challenge was applied in the presence of 1μM WIN 55212-2, however the third PS challenge was applied in the presence of both 1μM WIN 55212-2 and 0.5μM AM251 (CB1 receptor antagonist). This experimental protocol allowed for detection of neurons whose responses were inhibited by co-application of PS with WIN 55212-2, and restored when a CB1 antagonist (AM251) was co-applied with WIN 55212-2 and PS. In these experiments, some neurons appeared to have a reduced PS response in the presence of WIN 55212-2 and in a small number of neurons (5%, n= 8/156 neurons, 4, 1) responses were increased (PS+WIN+AM251 amplitude/PS+WIN amplitude >250%) when WIN 55212-2 was

concomitantly applied with AM251 (see Figure 4-18b). These findings demonstrate that activation of natively expressed CB1 receptors might inhibit TRPM3 activity in a small number of DRG neurons.

a

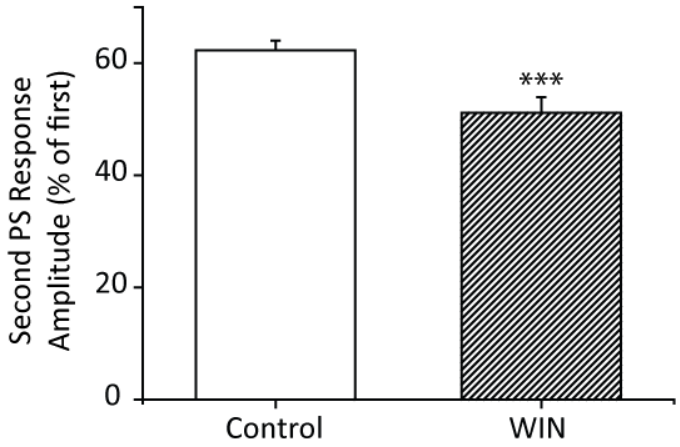
Second PS Response
Amplitude (% of first)
60
40
20
0
***
Control
WIN

b

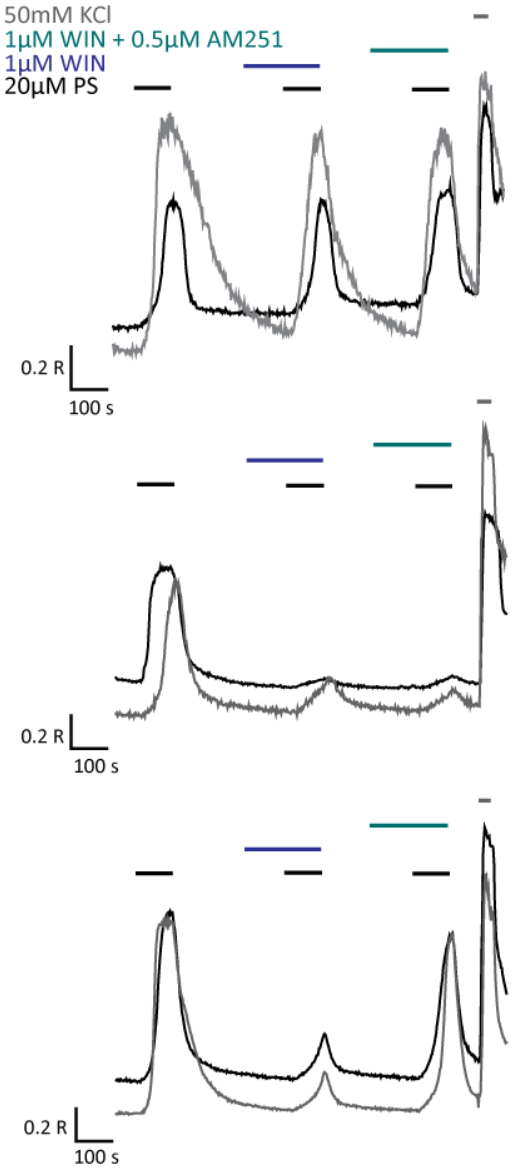
50mM KCl
1µM WIN + 0.5µM AM251
1µM WIN
20µM PS
0.2 R
100 s
0.2 R
100 s
0.2 R
100 s

Figure 4-18 CB1 modulates activation of TRPM3 expressed on sensory neurons

$[Ca^{2+}]_i$ responses were monitored by Fura-2 in PS-sensitive DRG neurons using microscope-based imaging. Neurons were exposed to two consecutive submaximal PS challenges (20μM), the second PS challenge took place either in the presence or absence of the cannabinoid receptor agonist WIN 55212-2 (1μM) (**a**) Column graph displaying average maximum response amplitudes for responses to the second PS challenge (as a % of the first PS response amplitude) for control experiments and experiments where neurons were perfused with 1μM WIN 55212-2. Columns represent mean ± SEM (***P<0.001, Mann-Whitney U test; control, n= 356 neurons, 10, 6; WIN, n= 213 neurons, 7, 3). (**b**) Representative traces displaying neuronal $[Ca^{2+}]_i$ responses to three sequential PS challenges (20μM) followed by depolarisation with high K^+ (50mM KCl). In some neurons (upper panel), PS-evoked increases in $[Ca^{2+}]_i$ were unaffected by application by of WIN 55212-2 and AM251. In other neurons PS evoked increases in $[Ca^{2+}]_i$ were inhibited by application of WIN 55212-2 (middle and bottom panels). This inhibition was prevented by concomitant AM251 application in some neurons (bottom panel) but not in all neurons (middle panel). R denotes Fura-2 ratio.

4.4.12 Morphine inhibits TRPM3 channels expressed in sensory neurons

Activation of opioid receptors expressed on sensory neurons causes inhibition of voltage-gated calcium channels, and has also been shown to inhibit capsaicin-induced TRPV1 currents; effects which are mediated by Gαi/o proteins (Endres-Becker et al., 2007; Stein et al., 2003).

There are three main subtypes of opioid receptors (μ, δ and κ), which are all expressed by sensory neurons and signal through Gαi/o proteins (Stein et al., 2003). In order to examine whether activation of opioid receptors expressed on sensory neurons can modulate natively expressed TRPM3 channels, the effects of the prototypical opioid receptor agonist morphine on the PS-evoked $[Ca^{2+}]_i$ responses of DRG neurons were investigated.

Isolated DRG neurons were exposed to two consecutive submaximally effective PS challenges (20μM) followed by a depolarising concentration of KCl. The second PS challenge took place either in the presence or absence of 10μM morphine. As mentioned previously, in control experiments double application of PS evoked $[Ca^{2+}]_i$ responses which were repeatable with some desensitisation. On average PS-responsive neurons responded to the second PS challenge with a response which was 62 ± 2% of the amplitude of the first PS response (mean ± SEM; n= 356 neurons, 10, 6; Figure 4-19). However, in experiments where neurons were perfused with 10μM morphine for 2 minutes before and during the second PS challenge, the response amplitude was strikingly reduced to 13 ± 1% of the first PS response (mean ± SEM; n= 641 neurons, 20, 6; significantly different to relative control amplitudes, $P<0.001$, Mann-Whitney U test). In the majority of neurons (57%) application of morphine completely abolished PS-evoked $[Ca^{2+}]_i$ responses (<5% of first PS response; n= 364/641; compared to 2%, n= 8/356 in control experiments).

In order to test whether morphine could still exert its inhibitory effects in the presence of an opioid receptor antagonist, the effects of morphine (10μM) concomitantly applied with naloxone (1μM) were investigated. Naloxone prevented the inhibitory effects of morphine as the response amplitude evoked by the second PS challenge was 59 ± 5% in the presence of naloxone (% of the first PS response; mean ± SEM; n= 39 neurons, 2, 2; not significantly different to relative control amplitudes, Kruskal-Wallis test; Figure 4-20) which is similar to the relative amplitude in controls (62 ± 2%). This confirmed that morphine was exerting its inhibitory effects by binding to an opioid receptor present on DRG neurons.

Next, the involvement of Gαi/o proteins was investigated using pertussis toxin (PTX). PTX is an exotoxin which prevents signalling of G proteins belonging to the Gi family by catalysing ADP-ribosylation of α subunits. Isolated DRG neurons were pre-treated with PTX (~ 2 ½ hours) and then exposed to two consecutive PS challenges, the first without and the second with morphine. The inhibitory effects of morphine were reduced by pre-treatment of neurons with PTX, however not to the same extent as concomitant treatment with naloxone. The response amplitude of neurons pre-treated with PTX and exposed to morphine was 44 ± 3% in comparison to 13 ± 1% with morphine (% of the first PS response; mean ± SEM; n= 150 neurons, 5, 2; significantly different to relative morphine amplitudes, $P<0.001$, Kruskal-Wallis test; Figure 4-20). These findings suggest that activation of a sensory-neuron expressed opioid receptor and subsequent Gαi/o protein signalling is able to modulate the activity of TRPM3 channels.

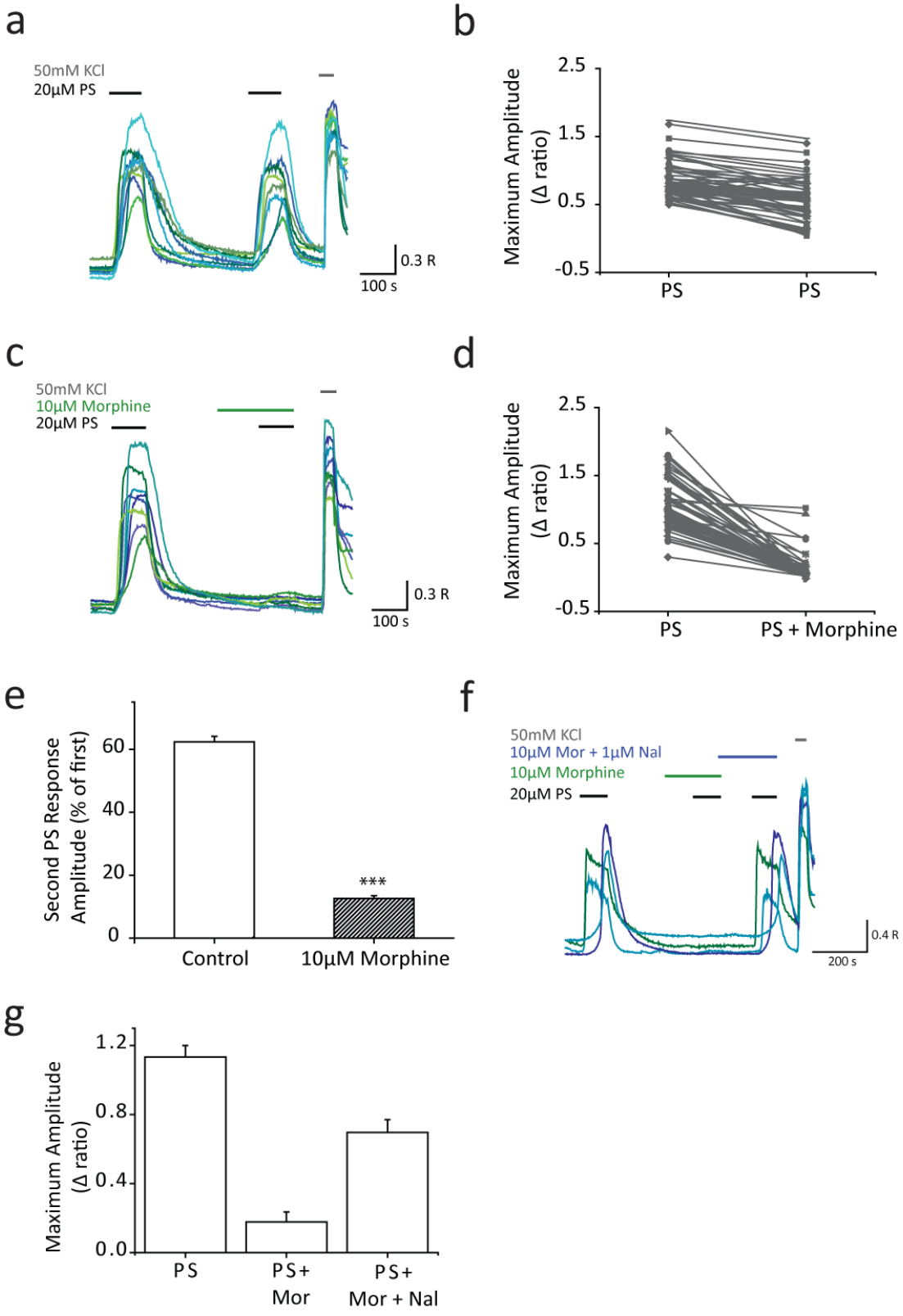
a
50mM KCl
20μM PS
0.3 R
100 s
b
Maximum Amplitude
(Δ ratio)
2.5
1.5
0.5
-0.5
PS
PS
c
50mM KCl
10μM Morphine
20μM PS
0.3 R
100 s
d
Maximum Amplitude
(Δ ratio)
2.5
1.5
0.5
-0.5
PS
PS + Morphine
e
Second PS Response
Amplitude (% of first)
60
40
20
0
***
Control
10μM Morphine
f
50mM KCl
10μM Mor + 1μM Nal
10μM Morphine
20μM PS
0.4 R
200 s
g
Maximum Amplitude
(Δ ratio)
1.2
0.8
0.4
0.0
PS
PS+
Mor
PS+
Mor + Nal

Figure 4-19 Morphine inhibits TRPM3 channels expressed on sensory neurons

$[Ca^{2+}]_i$ responses were monitored by Fura-2 in PS-sensitive DRG neurons using microscope-based imaging. Neurons were exposed to two consecutive submaximal PS challenges (20μM); the second PS challenge took place either in the presence or absence of the opioid receptor agonist morphine (10μM). (**a**) Representative traces displaying neuronal $[Ca^{2+}]_i$ responses to two sequential PS challenges (20μM) followed by depolarisation with high K^+ (50mM KCl) in a control experiment. R denotes Fura-2 ratio. (**b**) Scatter and line plot showing the relationship between maximum response amplitudes (Δ Fura-2 ratio) for the first and second PS responses in a representative control experiment. (**c**) Representative traces displaying neuronal $[Ca^{2+}]_i$ responses to two sequential PS challenges (20μM) followed by depolarisation with high K^+ (50mM KCl). Neurons were perfused with 10μM morphine 2 minutes before and during the second PS challenge. PS-evoked increases in $[Ca^{2+}]_i$ were inhibited by application of morphine. R denotes Fura-2 ratio. (**d**) Scatter and line plot showing the relationship between maximum response amplitudes (Δ Fura-2 ratio) for the first and second PS responses in a representative morphine experiment. (**e**) Column graph displaying average maximum response amplitudes for responses to the second PS challenge (as a % of the first PS response amplitude) for control experiments and experiments where neurons were perfused with 10μM morphine. Columns represent mean ± SEM; $P < 0.001$; Mann-Whitney U test (control, n= 356 neurons, 10, 6; morphine, n= 641 neurons, 20, 6). (**f**) Representative traces displaying neuronal $[Ca^{2+}]_i$ responses to three sequential PS challenges (20μM) followed by depolarisation with high K^+ (50mM KCl). PS-evoked increases in $[Ca^{2+}]_i$ are inhibited by application of morphine (10μM) but not by co-application of morphine with the opioid antagonist, naloxone (1μM). R denotes Fura-2 ratio. (**g**) Column graph displaying average maximum response amplitudes for responses for the first, second and third PS responses for the experiment shown in (f). Columns represent mean ± SEM (n= 37 neurons, 1, 1).

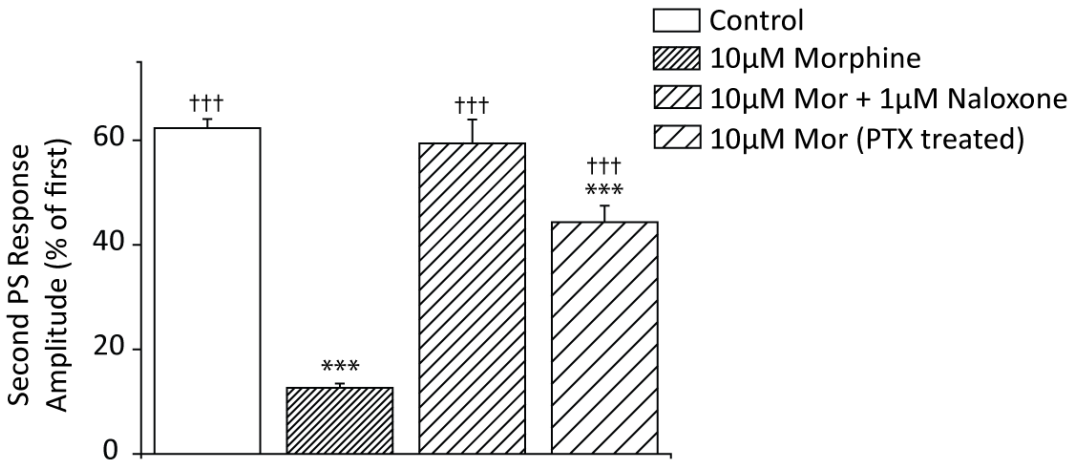

Figure 4-20 Morphine inhibits TRPM3 by binding to a sensory neuron expressed opioid receptor linked to Gαi/o proteins

$[Ca^{2+}]_i$ responses were monitored by Fura-2 in PS-sensitive DRG neurons using microscope-based imaging. Neurons were exposed to two consecutive submaximal PS challenges (20µM). Column graph displaying average maximum response amplitudes for responses to the second PS challenge (as a % of the first PS response amplitude). Application of 10µM morphine inhibited PS-evoked responses; this effect was abolished by concomitant application of the opioid receptor antagonist naloxone (1µM) and was reduced by pre-treatment of neurons with PTX. Columns represent mean ± SEM. *** P <0.001, P values represent comparison to control. ††† P <0.001, P values represent comparison to 10µM morphine. Kruskal-Wallis test (control, n= 356 neurons, 10, 6; morphine, n= 641 neurons, 20, 6; morphine + naloxone, n= 39 neurons, 2, 2; morphine PTX treated, n= 150 neurons, 5, 2).

4.4.13 Activation of μ-opioid receptors inhibits TRPM3

In order to examine which opioid receptor subtypes are important for morphine-induced inhibition of TRPM3, the effects of three selective opioid receptor agonists on the PS-evoked $[Ca^{2+}]_i$ responses of DRG neurons were investigated. Using the experimental format previously described, isolated DRG neurons were exposed to two consecutive submaximal PS challenges (20μM) followed by a depolarising concentration of KCl. The second PS challenge took place either in the presence or absence of 20nM U50488 (a κ opioid receptor agonist), 20nM SB205607 (a δ opioid receptor agonist) or 20nM DAMGO (a μ opioid receptor agonist).

Exposure of neurons to a κ opioid receptor agonist did not inhibit PS-induced responses. The average PS response amplitude of neurons perfused with U50488 was 72 ± 3% compared to a response amplitude of 62 ± 2% in control experiments (% of the first PS response; mean ± SEM; control, n= 356 neurons, 10, 6; U50488, n= 140 neurons, 4, 2; not significantly different to relative control amplitudes, Kruskal-Wallis test; Figure 4-21).

In contrast, neurons perfused with a δ opioid receptor agonist (SB205607) had a slightly reduced second response to PS in comparison to control experiments with a response amplitude of 52 ± 3% (% of the first PS response; mean ± SEM; n= 200 neurons, 5, 3; significantly different to relative control amplitudes, $p<0.05$, Kruskal-Wallis test; Figure 4-21). This finding suggests that the PS-induced responses of some DRG neurons are inhibited by activation of δ opioid receptors; therefore the δ opioid receptor subtype could be responsible for a small part of the inhibition seen with morphine.

Application of a μ opioid receptor agonist (DAMGO) produced an inhibition of PS-evoked responses which mimicked that of morphine, the average PS response amplitude was reduced to 18 ± 2% compared to 62 ± 2% in control experiments (% of the first PS response; mean ± SEM; control, n= 356 neurons, 10, 6; DAMGO, n= 184 neurons, 5, 3; significantly different to relative control amplitudes, $p<0.001$, Kruskal-Wallis test; Figure 4-21). Furthermore application of DAMGO caused complete inhibition of PS-induced $[Ca^{2+}]_i$ responses in 41% of neurons (<5% of first PS response; n= 76/184; compared to 2%, n= 8/356 in control experiments). These findings suggest that morphine exerts an inhibitory effect on TRPM3 channels predominantly by binding to and activating μ opioid receptors.

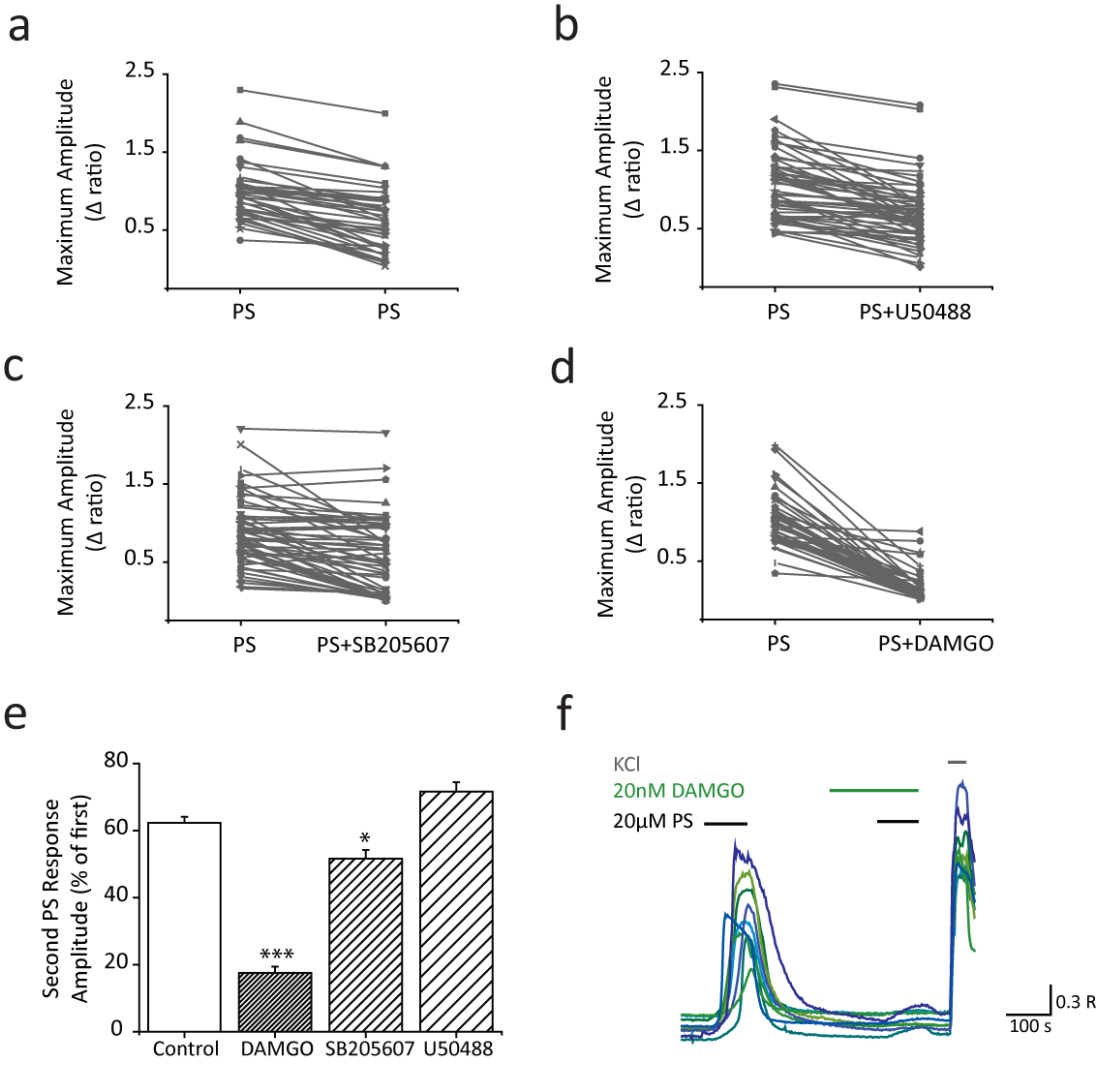

Figure 4-21 DAMGO inhibits TRPM3 channels expressed by sensory neurons

$[Ca^{2+}]_i$ responses were monitored by Fura-2 in PS-sensitive DRG neurons using microscope-based imaging. Neurons were exposed to two consecutive submaximal PS challenges (20μM); the second PS challenge took place either in the presence or absence of a selective opioid receptor agonist (DAMGO, μ opioid receptor agonist; SB205607, δ opioid receptor agonist; U50488, κ opioid receptor agonist) (**a**) Scatter and line plot showing the relationship between maximum response amplitudes (Δ Fura-2 ratio) for the first and second PS responses in a representative control experiment, (**b**) 20nM U50488 experiment, (**c**) 20nM SB205607 experiment and (**d**) 20nM DAMGO experiment. (**e**) Column graph displaying average maximum response amplitudes for responses to the second PS challenge (as a % of the first PS response amplitude) for control experiments and experiments where neurons were perfused with a selective opioid receptor agonist (20nM). Columns represent mean ± SEM. P values represent comparison to control. * $P < 0.05$, ** $P < 0.01$, *** $P < 0.001$; Kruskal-Wallis test (control, n= 356 neurons, 10, 6; DAMGO, n= 184 neurons, 5, 3; SB205607, n= 200 neurons, 5, 3; U50488, n= 140 neurons, 4, 2). (**f**) Representative traces displaying neuronal $[Ca^{2+}]_i$ responses to two sequential PS challenges (20μM) followed by depolarisation with high K^+ (50mM KCl). Neurons were perfused with 20nM DAMGO 2 minutes before and during the second PS challenge. PS-evoked increases in $[Ca^{2+}]_i$ were inhibited by application of DAMGO. R denotes Fura-2 ratio.

4.4.14 TRPM3 and Pain

4.4.14.1 Persistent Pain

Findings presented in this chapter have demonstrated that the absence of functional TRPM3 channels results in a reduced sensitivity to acute heat pain.

In order to examine whether TRPM3 is involved in sensing 'tonic' or more persistent pain, *Trpm3*$^{+/+}$ and *Trpm3*$^{-/-}$ mice were given an intraplantar injection of 2.5% formalin into their left hindpaw and their behavioural responses (time spent licking, shaking or biting the affected the paw) were measured and compared. This test characteristically induces two phases of pain, an immediate (~3 minutes after injection) initial phase which is followed by a period of inactivity, which leads into a later second phase (~20-30 minutes after injection) (Le Bars et al., 2001). *Trpm3*$^{-/-}$ mice exhibited similar behavioural responses to *Trpm3*$^{+/+}$ mice in the first phase of pain but displayed significantly reduced nocifensive behaviour during the later phase of the behavioural response (Figure 4-22a).

These results indicate that TRPM3 serves an important role in the detection of pain; in the absence of TRPM3, mice are less sensitive to both acute (see section 4.5.2.3) and persistent pain.

4.4.14.2 Visceral pain

In order to investigate whether TRPM3 is involved in other mechanisms of persistent pain, acetic acid induced-writhing was examined in *Trpm3*$^{+/+}$ and *Trpm3*$^{-/-}$ animals. Mice were given an intraperitoneal injection of acetic acid which induces a characteristic behavioural response composed of stereotyped body movements or 'writhing' (Le Bars et al., 2001). The number of writhes exhibited by *Trpm3*$^{+/+}$ and *Trpm3*$^{-/-}$ mice were measured and compared. Surprisingly, *Trpm3*$^{-/-}$ animals displayed more writhes on average than wildtype animals, suggesting an increased sensitivity of knockout animals although this effect was not significant (Figure 4-22b). These findings could indicate a divergence in the pain-sensing mechanisms of the somatosensory and visceral systems.

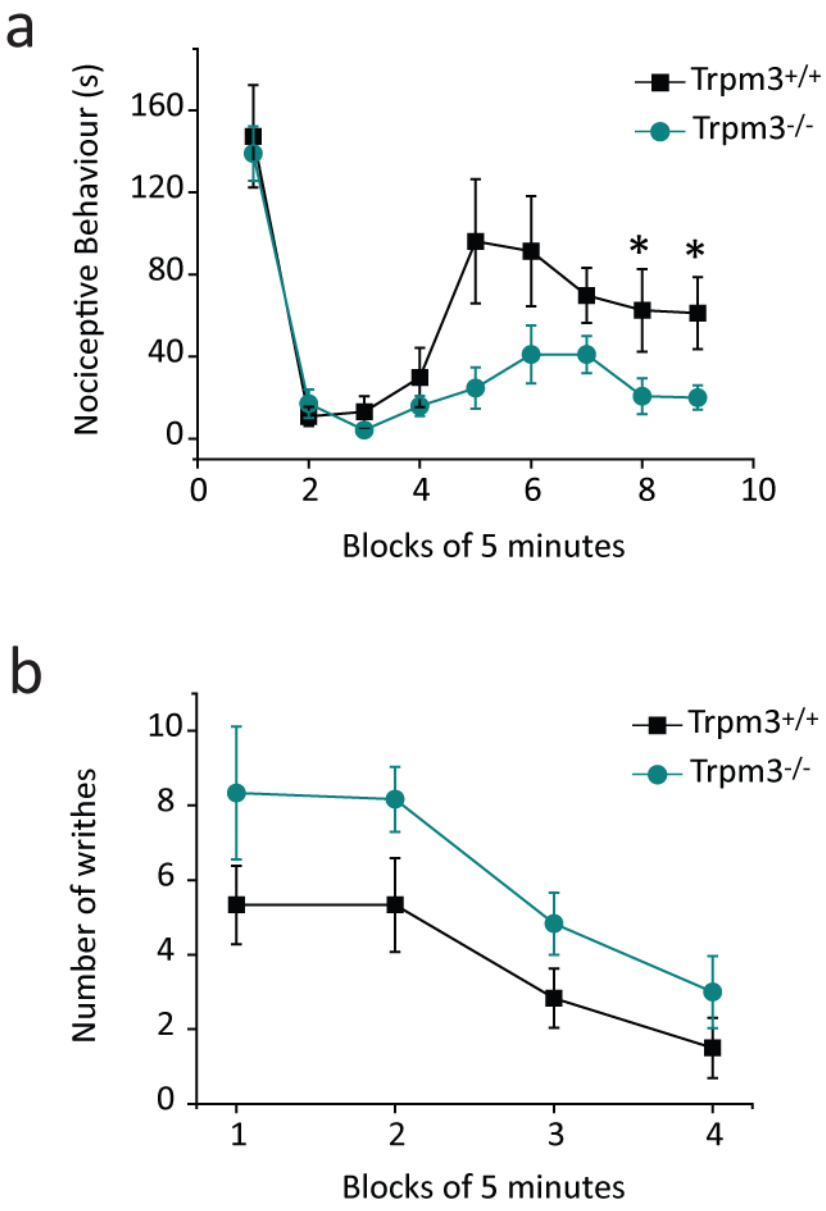

Figure 4-22 TRPM3 plays a role in persistent pain mechanisms

(**a**) *Trpm3*$^{+/+}$ and *Trpm3*$^{-/-}$ mice were given an intraplantar injection of 2.5% formalin into their left hindpaw and their nociceptive behaviour was measured in seconds. Nociceptive behaviour relates to licking, shaking or biting of the affected paw. *Trpm3*$^{-/-}$ mice exhibited significantly reduced nociceptive behaviour in response to injection of formalin in comparison to wildtype mice. Data points represent mean ± SEM (* $P < 0.05$; Mann-Whitney U test; n= 6 mice for both genotypes). (**b**) *Trpm3*$^{+/+}$ and *Trpm3*$^{-/-}$ mice were given an intraperitoneal injection of acetic acid and the number of writhes exhibited by each animal was measured. *Trpm3*$^{-/-}$ mice displayed more writhing behaviour than wildtype animals. Data points represent mean ± SEM (NS, t-test; n= 6 mice for both genotypes).

4.5 Discussion

The findings presented in this chapter have characterised mouse TRPM3 expressed in CHO cells and confirmed activation of TRPM3 channels by the endogenous neurosteroid pregnenolone sulphate and by heating. In addition, a role for TRPM3 in noxious heat sensing has been demonstrated, DRG neurons from *Trpm3*$^{-/-}$ mice had a smaller percentage of heat-sensitive neurons than wildtype DRG neurons and *Trpm3*$^{-/-}$ mice exhibited a reduced sensitivity to noxious heat in behavioural experiments. Moreover, the findings presented in this chapter have demonstrated that TRPM3 activity, like that of other sensory TRP channels, can be regulated by intracellular pathways downstream of Gq, Gs and Gi/o linked GPCR activation. Importantly, the results presented in this chapter have shown that the activity of TRPM3 is regulated by activation of μ-opioid receptors in a G_i-dependent manner. Finally, the findings presented here have provided evidence for a pro-nociceptive role of TRPM3 in acute and persistent pain.

4.5.1 Chemical activation and inhibition of TRPM3

Recombinantly expressed TRPM3 channels exhibited robust $[Ca^{2+}]_i$ responses to application of PS. Furthermore, PS-induced changes in $[Ca^{2+}]_i$ were not evident in untransfected CHO cells (up to 200μM) consistent with selective-activation of TRPM3. PS activated recombinantly expressed TRPM3 channels in a concentration-dependent manner with an EC_{50} value of ~10μM which is similar to the values reported by Wagner *et al* (2008). In addition, PS (50μM)-evoked increases in $[Ca^{2+}]_i$ were relatively absent in neurons from *Trpm3*$^{-/-}$ mice (evoked a response in 1% of *Trpm3*$^{-/-}$ neurons), demonstrating the utility of PS as a probe for TRPM3 expression and the presence of functional TRPM3 channels in a subset of sensory neurons, consistent with previous reports (Vriens et al., 2011). Measured plasma PS levels in adults lie within the mid to high (100-300) nanomolar range (Havlíková et al., 2002; de Peretti and Mappus, 1983) which is just below the threshold for TRPM3 activation measured here. It is therefore unlikely that circulating levels of PS are sufficient to cause activation of TRPM3. However, measured concentrations of PS are increased in maternal serum at the time of birth and are even at higher in the umbilical cord serum at the time of delivery (Bičíková et al., 2002; Klak et al., 2003). If during these events, raised levels of PS reach micromolar concentrations this could lead to activation of TRPM3 channels.

PS-induced responses were inhibited by both mefenamic acid and ononetin. Mefenamic acid inhibited responses in the TRPM3 CHO cell line with an IC_{50} value in the low micromolar range consistent with previous findings (Klose et al., 2011). Ononetin inhibited PS-induced responses with an IC_{50} value in the high nanomolar range which is consistent with the IC_{50} value reported in a previous study (Straub et al., 2013a). These compounds were the best available antagonists for inhibition of TRPM3.

4.5.2 TRPM3 and heat sensitivity

4.5.2.1 Recombinantly expressed TRPM3 channels are sensitive to heat

Recombinantly expressed TRPM3 channels displayed robust $[Ca^{2+}]_i$ responses to heating, consistent with previous findings (Vriens et al., 2011). Heat-evoked responses were inhibited, to the response level of untransfected cells, by both mefenamic acid and ononetin demonstrating the requirement of TRPM3 channels for these responses. These findings are consistent with the conclusion that TRPM3 is a thermosensitive channel which is opened by heating. Interestingly, recombinantly expressed TRPM3 channels responded to heat with an average threshold temperature of 44°C, which is almost identical to the activation threshold of TRPV1 and the threshold for heat pain in humans (Basbaum et al., 2009; Caterina et al., 1997; Tominaga et al., 1998).

4.5.2.2 Heat sensitivity of DRG neurons

The majority of heat-sensitive wildtype DRG neurons (74%) were sensitive to PS and due to the relative absence of PS-evoked $[Ca^{2+}]_i$ responses in neurons lacking functional TRPM3 channels these neurons can be considered TRPM3-expressing. The majority of TRPM3-expressing, heat-sensitive neurons co-expressed TRPV1 (86%) leaving only a small population of neurons which only expressed TRPM3 (14%). In the subpopulation of heat-sensitive neurons which co-express TRPV1 and TRPM3 it is difficult to ascertain whether TRPM3 plays a role in the transduction of heat as it is possible that TRPV1 is acting as a heat-sensor in these neurons.

The number of heat-sensitive neurons responding to both PS and capsaicin in the current study is similar to the number reported in an earlier study by Vriens and colleagues (2011). The same study reported that 41% of heat-sensitive neurons were sensitive to PS but not capsaicin; this differs from the findings presented in this chapter, where only 10% of heat-sensitive neurons were identified as responsive to PS only. This discrepancy could be explained by a difference in the initial proportion of DRG neurons displaying heat

sensitivity. Vriens and colleagues reported that 82% of DRG neurons tested displayed heat-evoked responses. This value is higher than the number found in both the study presented here (~44%) and previous studies (~34-51%) examining the heat sensitivity of cultured DRG neurons (Caterina et al., 2000; Noël et al., 2009).

Importantly, the findings presented in this chapter showed that not all PS-sensitive neurons were heat-sensitive: 43% of neurons which responded to PS did not display heat sensitivity. This suggests that expression of TRPM3 alone by sensory neurons does not confer sensitivity to heat over the temperature range studied. It is possible that TRPM3 requires the presence or absence of an additional biochemical factor or protein for heat sensitivity, which is only present/absent in a subpopulation of TRPM3-expressing nerves.

Notably, the temperature activation thresholds between different subpopulations of heat-sensitive neurons (PS- and capsaicin-sensitive, just PS-sensitive, just capsaicin-sensitive) were not dissimilar. This finding is consistent with similar temperature activation thresholds for TRPM3 and TRPV1.

Despite the majority of WT DRG neurons expressing TRPM3, neurons from mice lacking functional TRPM3 channels exhibited only a small reduction in heat-sensitivity. The number of heat-sensitive neurons was 10% lower in *Trpm3*$^{-/-}$ mice compared to *Trpm3*$^{+/+}$ mice ($p<0.001$, Pearson's Chi-Square test). It is possible that this reduction in heat-sensitivity represents the loss of the small subpopulation (10%) of heat-sensitive *Trpm3*$^{+/+}$ neurons which were responsive to PS but not capsaicin. In the other, larger subpopulation of heat-sensitive neurons (which responded to PS and capsaicin) the presence of TRPV1 could be masking any effect on heat sensitivity due to the loss of TRPM3.

However, these findings indicate that TRPM3 plays a small role in the heat-sensing mechanisms of sensory neurons and are in contrast to the findings by Vriens and colleagues (2011) which demonstrated a much larger loss of heat sensitivity in *Trpm3*$^{-/-}$ mice (23% reduction in heat-sensitive neurons). However, due to the large number of heat-sensitive WT neurons reported in Vriens e*t al*, the larger loss of heat sensitivity still results in 59% of DRG neurons which are responsive to heat in *Trpm3*$^{-/-}$ mice (Vriens et al., 2011). The large number of heat-sensitive neurons remaining in *Trpm3*$^{-/-}$ animals highlights that TRPM3 is not required for the heat sensitivity of all neurons.

In the current study, the temperature thresholds of wildtype and *Trpm3*$^{-/-}$ neurons were identical. Again, this finding is consistent with TRPM3 and TRPV1 having similar temperature activation thresholds.

4.5.2.3 TRPM3 is partly-responsible for noxious heat responses in vivo

Notably, *Trpm3*$^{-/-}$ mice displayed significantly longer latencies to withdrawal from a noxious heat stimulus (53°C) than their wildtype counterparts. This finding is consistent with a previous study examining heat pain thresholds in mice who lack functional TRPM3 channels and suggests that TRPM3 does contribute to noxious heat sensing *in vivo* (Vriens et al., 2011). Although the loss in heat sensitivity was modest in sensory neurons isolated from *Trpm3*$^{-/-}$ mice, this small reduction in the number of heat sensitive neurons could be significant for the sensation of noxious heat. Alternatively, expression of TRPM3 at other sites could contribute this behavioural effect. The results presented in this chapter have demonstrated expression of TRPM3 in the spinal cord as well as in multiple areas of the central nervous system.

4.5.2.4 Which proteins are responsible for transduction of heat stimuli in sensory neurons?

The current study suggests that deletion of TRPM3 channels has a small impact on the heat sensitivity of sensory neurons. TRPV1 is largely thought to be the molecular transducer for noxious heat however there is a discrepancy over the effects of TRPV1 deletion on sensory neuron heat sensitivity; some studies have argued that neurons lacking TRPV1 exhibit deficits in heat sensitivity (Caterina et al., 2000; Davis et al., 2000) whilst other studies have shown that *Trpv1*$^{-/-}$ neurons possess a residual heat-sensing ability around the temperature range which activates TRPV1 (Lawson et al., 2008; Vriens et al., 2011; Woodbury et al., 2004).

Moreover, one study has shown that whilst application of a TRPV1 antagonist was able to inhibit some of the remaining heat-evoked responses in *Trpm3*$^{-/-}$ mice, the heat-evoked responses of a large population of neurons (~50%) were unaffected by the antagonist (Vriens et al., 2011). Which raises the question, what is responsible for the TRPM3/TRPV1-independent component of heat sensation?

Anoctamin 1 (ANO1), a Ca^{2+} activated chloride channel (CaCC), expressed within the nociceptive subpopulation of sensory neurons has been implicated in sensory heat transduction mechanisms (Cho et al., 2012). The study reported that heating activates Cl^-

conductances in DRG neurons and that ANO1 is activated by heat with a threshold temperature of 44°C. Furthermore, it was noted that co-treatment of neurons with the TRPV1 antagonist, capsazepine and the CaCC blocker, mefloquine, results in complete inhibition of heat-evoked currents of WT DRG neurons whilst mefloquine blocks heat responses in *Trpv1*$^{-/-}$ neurons (Cho et al., 2012). It is possible that activation of ANO1 by heat leads to depolarisation of sensory neurons and opening of voltage gated calcium channels.

Heating results in clustering of STIM1 at ER-plasma membrane junctions leading to Orai1-mediated Ca^{2+} influx (Xiao et al., 2011). However, this temperature-dependent activation of Orai1 results in responses which function as 'heat-off' signals, as they occur during the cooling phase after heating (Xiao et al., 2011).

A rhodopsin encoded by the ninaE gene has also been implicated in temperature discrimination mechanisms in *Drosophila* (Shen et al., 2011). Temperature discrimination was impaired in *Drosophila* larvae when the ninaE gene was mutated. Mutant larvae did not show a preference for their ideal temperature (18°C) over other ambient temperatures (19-24°C) in a thermotaxis assay. This mechanism of temperature discrimination also requires the activity of PLC and TRPA1. Interestingly, thermotactic discrimination abilities were rescued by the introduction of the mammalian melanopsin receptor (Shen et al., 2011). This study highlights an alternative pathway by which an ion channel can be activated by heat which could also function in mammals. It is also possible that other thermo-sensitive ion channels still remain to be found.

4.5.3 Modulation of TRPM3 channel activation

4.5.3.1 TRPM3 is potentiated by cAMP- dependent mechanisms

Activation of heterologously-expressed TRPM3 channels by PS resulted in robust $[Ca^{2+}]_i$ responses which were potentiated by combined activation of adenylyl cyclase and inhibition of phosphodiesterase enzymes, and by application of a membrane permeable cAMP analogue. These findings demonstrate the existence of a cAMP-dependent mechanism for potentiation of TRPM3 channels.

Interestingly, the effects of the membrane-permeable cAMP analogue on PS-induced TRPM3 activation could not be reversed by a non-selective protein kinase inhibitor or a PKA-selective inhibitor suggesting that the sensitisation evoked by increases in cAMP levels is independent of PKA activation. This finding is surprising considering that the majority of

cAMP mediated-actions are executed by PKA and also considering the well-established role of PKA as a regulator of ion channels (Berridge, 2012).

4.5.3.2 How do increases in cAMP modulate TRPM3 channel activity?

It is important to note that whilst PKA is the main effector of cAMP-dependent mechanisms it is not the only one; exchange proteins activated by cAMP (Epac) are also targeted by cAMP (Berridge, 2012; Kawasaki et al., 1998; de Rooij et al., 1998). Epac are proteins encoded by the Epac1 and Epac2 genes, which function as guanine nucleotide exchange factors for two members of the ras-related protein (Rap) family, Rap1 and Rap2b (Kawasaki et al., 1998; de Rooij et al., 1998; Schmidt et al., 2001). Epac 1 is widely expressed in adult human tissues and has strong expression in the kidney, ovary, thyroid and spinal cord and lower expression levels in the brain (Kawasaki et al., 1998). Epac 2 is not as widely expressed as Epac 1 but has high expression levels in the brain (Kawasaki et al., 1998). Epac have been associated with cAMP signalling pathways which function independently from PKA. Activation of a Gs-linked GPCR has previously been shown to cause cAMP dependent activation of PLCε, mediated by Epac activation of Rap2b (Schmidt et al., 2001). Furthermore, Epac has also been implicated in the cAMP-induced, PLC/PLD-dependent translocation of PKCε to the plasma membrane of DRG neurons (Hucho et al., 2005). It is possible that the cAMP-dependent, PKA-independent, potentiation of TRPM3 activity is the result of Epac mediated actions.

4.5.3.3 PLC activation positively modulates TRPM3 activation

The majority of TRP channels are regulated in some way by actions downstream of PLC activation (Rohacs, 2013). The findings of the current study have demonstrated that TRPM3 channel activity is positively modulated by activation of PLC. The PS-induced $[Ca^{2+}]_i$ responses of heterologously-expressed TRPM3 channels were potentiated by the PLC-activating compound, *m*-3M3FBS, which stimulates the β2, β3, γ1, γ2, and δ1 isoforms of PLC (Bae et al., 2003). This effect was reversed by the presence of the PLC inhibitor U73122. Interestingly, U73122 (in the presence of *m*-3M3FBS) not only reversed the potentiating effects of *m*-3M3FBS but reduced PS-induced responses to lower amplitude levels than the responses of untreated cells. This finding suggests that in this experimental setting there is a resting level of PLC activity.

4.5.3.4 How does PLC activation modulate TRPM3?

As discussed earlier activation of PLC leads to the hydrolysis of the membrane phospholipid PIP_2, resulting in the release of the second messengers; DAG and IP_3 as hydrolysis products (Rohacs, 2013). IP_3 acts on receptors present on the membranes of intracellular calcium stores stimulating the liberation of Ca^{2+} and DAG activates PKC. The sensory neuron TRP channel, TRPV1, is sensitised by activation of PLCβ which occurs downstream of Gαq-linked GPCR activation (Rohacs, 2013). There are two possible pathways which are thought to be responsible for this PLC-mediated sensitisation; the first involves phosphorylation of the channel by the PKCε isoform and the second involves relief from tonic inhibition of the channel by PIP_2. The latter pathway is controversial due to conflicting experimental findings on the actions of PIP_2 on TRPV1 channel activity. PIP_2 has been shown to both activate and inhibit TRPV1 activity (Chuang et al., 2001; Klein et al., 2008; Lukacs et al., 2007; Prescott and Julius, 2003; Ufret-Vincenty et al., 2011; Yao and Qin, 2009)

2.2.3.1 PKC activation

The role played by DAG production and any consequent PKC activation in the observed potentiation of TRPM3 by PLC activation was investigated. Interestingly, direct activation of PKC by PMA or PDBu did not cause a potentiation of channel activity but resulted in an inhibition. Similarly, the broad-spectrum protein kinase inhibitor, staurosporine also inhibited PS-induced $[Ca^{2+}]_i$ responses. The effects of PMA and PDBu could be due to a direct effect of these compounds on the channel rather than an effect of PKC inhibition. Experiments investigating the effects of the inactive analogues of these compounds, 4α-PMA and 4α-PDBu, would be useful in determining whether these compounds directly interfere with TRPM3 channel activity independently of PKC activation. Staurosporine also inhibits PKA, p60v-Src tyrosine kinase and CaM kinase II in addition to PKC, within the same concentration range therefore its effects on TRPM3 cannot be interpreted entirely through its actions on PKC (Rüegg and Burgess, 1989).

2.2.3.2 PIP_2 hydrolysis

It is possible that PIP_2 exerts an inhibitory effect on the TRPM3 channel, which is relieved when it is hydrolysed by PLC thus causing a potentiation of channel activity. PIP_2 has been shown to inhibit the activity of TRPV3 and TRPA1 in addition to TRPV1, although the effects of PIP_2 on TRPA1 are similarly conflicting (Dai et al., 2007; Doerner et al., 2011).

4.5.3.5 Sensitisation of TRPM3 by inflammatory mediators which signal through a PLCβ-pathway

Regardless of how PLC-activation leads to an increased sensitivity of TRPM3 to ligand activation, these findings suggest that TRPM3 can be sensitised by mediators released during inflammation, such as bradykinin and prostaglandins, which activate sensory neuron Gq-coupled receptors leading to PLCβ activation. During inflammation, these mediators increase the sensitivity of peripheral sensory neurons by modulating the activity of ion channels resulting in pain hypersensitivity. Previous studies have already indicated a role for TRPM3 channels in the development of heat hyperalgesia, mice lacking functional TRPM3 channels do not develop the increased sensitivity to heat which is characteristic of inflammatory pain (Vriens et al., 2011).

Interestingly, the activity of the human $TRPM3_{1325}$ variant was not modulated by activation of the histamine H1 receptor or endogenously-expressed muscarinic receptors which can couple to Gαq proteins causing activation of PLCβ (Grimm et al., 2003). This finding is surprising due to the modulatory effects observed on mouse TRPM3 activation by PLC activation in the current study.

4.5.4 Activation of the CB1 receptor inhibits TRPM3 channel activity

Stimulation of the CB1-receptor co-expressed with TRPM3 in a CHO cell line resulted in decreased PS-induced responses in some cells. Moreover, inhibition of the CB1 receptor unmasked PS responses in a subpopulation of cells, suggesting a level of constitutive activity of the CB1 receptor. The main effectors of CB1 receptors are the Gαi/o proteins which inhibit adenylyl cyclase activity and consequently lead to decreased levels of cAMP (Turu and Hunyady, 2010). CB1-induced inhibition of recombinantly expressed TRPM3 responses are consistent with previous findings (discussed in section 4.5.3.1) showing the positive modulatory effect of elevating cAMP levels on TRPM3 channel activity.

The findings presented in this chapter, have also shown that activation of endogenously expressed, sensory neuron CB1 receptors can modulate the activity of native TRPM3 channels. A small subpopulation of PS-sensitive DRG neurons appeared to be inhibited by CB1 receptor stimulation, an effect which in some neurons (5%) was prevented in the presence of a CB1 receptor antagonist. Although these findings demonstrate that modulation of endogenously expressed TRPM3 channels by CB1 receptors can occur, the

modulatory effects were only evident in a very small number of PS-sensitive neurons; this could reflect a low co-expression level of CB1 with TRPM3.

4.5.5 Activation of the μ-opioid receptor inhibits TRPM3 channel activity

The opioid receptor agonist morphine caused a striking inhibition of PS-induced $[Ca^{2+}]_i$ responses of sensory neurons, the PS-evoked responses of ~57% of PS-sensitive neurons were completely inhibited by morphine. The effects observed with morphine were opioid receptor sub-type specific and were reliant on G proteins belonging to the Gαi family; this was demonstrated by the lack of effect displayed by morphine in the presence of an opioid-receptor antagonist and on cells pre-treated with PTX. These findings are consistent with the positive modulatory effects of cAMP on TRPM3 activity discussed previously and the inhibitory effects of CB1 receptor stimulation on TRPM3 activation (section 4.5.3.1, 4.5.4 and Figure 4-23).

The effects of morphine were mimicked by the μ-opioid receptor agonist, DAMGO which caused complete inhibition of PS-evoked responses in ~41% of PS-sensitive neurons. Activation of the δ-opioid receptor also had a small inhibitory effect on PS-evoked responses comparable to activation of the CB1 receptor; however stimulation of the κ-opioid receptor exerted no inhibitory effects on PS-evoked responses. These findings strongly suggest a high level of co-expression of μ-opioid receptors with TRPM3 channels in primary afferent sensory neurons. A study by Khasabova and colleagues (2004) investigating inhibition of depolarisation-induced $[Ca^{2+}]_i$ responses of DRG neurons by morphine, also noted an involvement of μ and δ but not κ receptors (Khasabova et al., 2004).

Notably, the effects of stimulating μ-opioid receptors on TRPM3 channel activation are similar to the effects reported for TRPV1 channels (Endres-Becker et al., 2007). Morphine inhibited capsaicin-induced currents in 79% of DRG neurons, effects which were mimicked by the μ-opioid receptor agonist DAMGO. This effect was also dependent on Gi proteins and could be reversed by application of a cAMP analogue or stimulation of adenylyl cyclase (Endres-Becker et al., 2007). Interestingly, the study by Endres-Becker *et al* reported that heat-evoked responses in 86% of DRG neurons were also inhibited by morphine. The findings presented here suggest that inhibition of heat-evoked responses by morphine could be due to inhibition of either TRPM3 or TRPV1.

4.5.6 CB1 and μ-opioid receptor-mediated modulation of TRPM3 during inflammation

Opioids are commonly used analgesics for the treatment of pain. Opioids inhibit pain transmission, in part, by reducing the excitability of primary afferent neurons (Stein and Machelska, 2011). Moreover, cannabinoids which are active at CB1 receptors have been shown to be analgesic in various models of pain hypersensitivity (Agarwal et al., 2007; McDougall, 2011).

A study examining mice with a specific deletion of the μ-opioid receptor in Nav1.8 positive neurons has shown that in an inflammatory pain model, opiate-induced analgesia is partly mediated by μ-opioid receptors expressed on sensory nerve endings (Weibel et al., 2013). Similar findings were reported in a study examining specific deletion of the CB1-receptor in Nav1.8 positive sensory neurons, which determined that CB1 receptors expressed on peripheral nerves are critical for a large part of cannabinoid agonist-induced analgesia (produced by systemic administration) in a model of inflammatory pain (Agarwal et al., 2007).

The findings presented in this chapter have already shown that the activity of TRPM3 can be sensitised by intracellular pathways downstream of Gs and Gq linked GPCR activation. Signalling through these pathways is increased during periods of inflammation leading to sensitisation of nociceptive afferents. If sensitisation of TRPM3 channels, expressed on sensory neurons, is involved in the generation of pain hypersensitivity, inhibition of TRPM3 channels by opiates which are active at μ-opioid receptors or cannabinoids which act on CB1 receptors could contribute to anti-hyperalgesia. However, modulation of TRPM3 channels via CB1 receptors in the periphery is probably less prevalent considering the small effect of CB1-receptor activation on the PS-induced responses of cultured sensory neurons.

4.5.7 TRPM3 contributes to the sensation of pain

As previously discussed (see section 4.5.2.3), the findings presented in this chapter have shown that *Trpm3*$^{-/-}$ mice exhibit a reduced sensitivity to noxious heat in comparison to their wildtype counterparts. In addition, other studies (performed by Clive Gentry, King's College London) have demonstrated that *Trpm3*$^{-/-}$ mice have normal behavioural responses to mechanical and cold (10°C) stimuli. These experimental findings demonstrate that TRPM3 channels are not essential for behavioural responses to stimulation with noxious cold or mechanical stimuli.

Interestingly, further studies (performed by Clive Gentry, King's College London) have shown that *Trpm3*$^{-/-}$ mice do not develop the cold or heat hypersensitivity normally associated with inflammatory (induced by complete Freund's adjuvant) or neuropathic (induced by partial sciatic nerve ligation) pain conditions (unpublished data, Clive Gentry). This is an intriguing finding as it suggests that TRPM3 is responsible for regulating sensitivity to both heat and cold in these pain states.

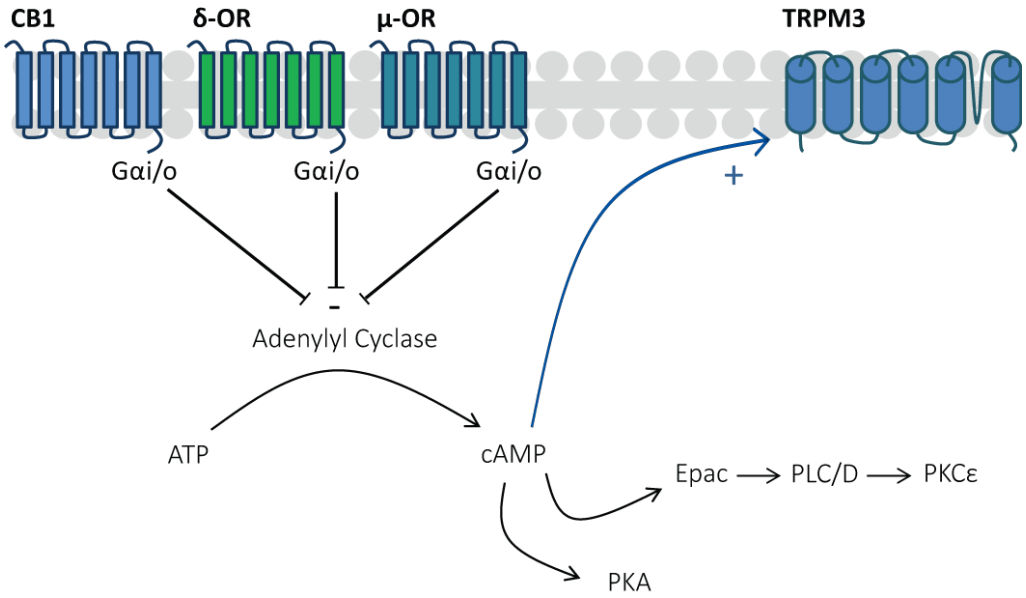

Figure 4-23 Schematic illustrating inhibition of TRPM3 channels by Gαi linked GPCR receptors

Activation of sensory neuron expressed CB1 receptors, δ-opioid receptors (δ-OR) and μ-opioid receptors (μ-OR) can lead to inhibition of adenylyl cyclase activity via activation of heterotrimeric G protein and release of a Gαi-GTP monomer (Stein et al., 2003; Turu and Hunyady, 2010). This inhibition of adenylyl cyclase activity results in decreased cAMP production and therefore lowers the cellular levels of cAMP; therefore preventing the cAMP-mediated activity which aids TRPM3 channel function. Effectors of cAMP mediated actions include PKA and Epac; Epac can couple to members of the Rap family leading to activation of PLC and PLD enzymes which can lead to increases in the activity of the PKCε isoform (Hucho et al., 2005; Schmidt et al., 2001).

The results of the current study have also implicated TRPM3 channels in behavioural sensitivity in a model of persistent pain. The formalin test of nociception induces two phases of behaviour, an immediate initial phase and a later second phase. The first phase of pain was unchanged in *Trpm3*$^{-/-}$ mice whereas nociceptive behaviour was reduced in the second phase. The first phase of formalin-induced pain is thought to be due to the direct activation of nociceptive neurons whereas the second phase is suggested to be driven by sensitisation mechanisms (Le Bars et al., 2001). There is debate over whether the

sensitisation represented by the second phase is peripherally or centrally located. One study argued that the second phase of the formalin test is due to redistribution of formaldehyde which results in a second phase of excitation (Fischer et al., 2014). This study also suggests that the 'interphase' of the formalin test is the result of neuronal hyperpolarisation driven by inhibition of sodium currents.

Interestingly many drugs including; NSAID drugs, NMDA antagonists, morphine and gabapentin are only analgesic in the second phase of pain (Le Bars et al., 2001; McNamara et al., 2007). The finding that animals lacking functional TRPM3 channels display less spontaneous pain behaviour in the second phase of formalin-induced pain could reflect an involvement of TRPM3 in peripheral or central sensitisation mechanisms, consistent with findings showing that *Trpm3*$^{-/-}$ mice fail to exhibit heat or cold hypersensitivity in CFA-induced inflammation and nerve ligation.

In contrast to the pro-nociceptive roles of TRPM3 indicated by the hot-plate test and the formalin test, the results of this chapter suggest an anti-nociceptive role for TRPM3 in abdominal pain-sensing mechanisms. *Trpm3*$^{-/-}$ mice appeared to display a greater number of 'writhing' movements compared to their wildtype counterparts after administration of an intraperitoneal injection of acetic acid however this finding was not statistically significant. These results could suggest that mice lacking functional TRPM3 channels are more sensitive to acetic-acid induced pain than mice with functional TRPM3 channels. The outer lining of the abdomen receives innervation from the somatosensory nervous system and therefore the pain could be either visceral or somatic in origin (Le Bars et al., 2001). TRPM3 channels expressed in visceral sensory neurons or even non-neuronal tissues could play roles which contribute to anti-nociception. However, further investigations will be required to determine whether TRPM3 channels do have an anti-nociceptive role in the acetic acid writhing test or whether the activity of TRPM3 is affected by pH.

4.5.8 The role played by TRPM3 in the spinal cord and brain

The findings presented in this chapter have examined modulation and activation of TRPM3 channels at the level of the DRG neurons. *Trpm3*$^{-/-}$ animals experience deficits in acute and tonic noxious pain sensing and also impaired development of some pain hypersensitivities. TRPM3 has been labelled as a noxious heat sensor however deletion of TRPM3 from the sensory neuron ganglia only causes a small effect on the heat sensing capabilities of sensory neurons and they retain significant heat sensitivity. It is possible that expression of TRPM3 channels in other areas of the nervous system is responsible for the nociceptive impairments observed in *Trpm3*$^{-/-}$ mice. TRPM3 was found at relatively high levels in the mouse dorsal spinal cord. Furthermore, TRPM3 was found to be expressed at levels comparable to the DRG, in the midbrain, cerebellum and olfactory bulb. These findings suggest the likelihood of varied and distinct physiological roles for TRPM3 channels which are yet to be discovered.

4.6 Conclusion

TRPM3 is a sensory neuron expressed, Ca^{2+} permeable channel which can be activated by the neurosteroid pregnenolone sulphate and by heat. Functional TRPM3 channels are required for sensitivity to noxious heat *in vivo* and are involved in nociceptive responses to tonic pain. Their activity is sensitised by intracellular signalling pathways which are downstream of increased cAMP levels and PLC activation. Interestingly, within a sensory neuron setting the activity of TRPM3 channels is inhibited by activation of μ-opioid receptors.

Chapter 5. A spinal cord synaptosome CGRP release assay for the study of TRPA1 channels

5.1 Introduction

The peripheral terminals of primary afferent neurons innervate peripheral tissues and function as transducers of local stimuli. Depolarisation of the peripheral sensory terminals generates action potentials, which are conducted along the peripheral axons to the central terminals, where they synapse with second-order neurons in the dorsal horn of the spinal cord (primary afferents of the DRG) or spinal trigeminal nucleus (primary afferents of the TG).

Sensory neuron TRP channels are expressed on the membranes of both peripheral and central terminals of primary afferent neurons and activation of TRP channels at both sites can lead to the release of the neuropeptides CGRP and SP (Eberhardt et al., 2014, 2012; Kessler et al., 1999; Kilo et al., 1997; Mogg et al., 2013; Pozsgai et al., 2012; Saria et al., 1986; Trevisani et al., 2007; Yan et al., 2006). Additionally, stimulation of TRP channels has been shown to evoke neuropeptide release from the axons of primary afferent nerves and from sensory ganglia (Boillat et al., 2014; Eberhardt et al., 2008; Kunkler et al., 2011; Nakamura et al., 2012; Spitzer et al., 2008; Weller et al., 2011). The release of CGRP and SP into the periphery by antidromic stimulation causes neurogenic inflammation (Brain and Cox, 2006). CGRP has potent vasodilator effects and SP increases vascular permeability (Brain et al., 1985; Yano et al., 1989). Moreover, the release of CGRP and SP from central terminals is implicated in pain (Brain and Cox, 2006).

5.1.1 Sensory neurotransmitters

Synaptic transmission of information relies upon transmitter release. Primary afferent neurons conveying information about innocuous stimuli release the excitatory neurotransmitter glutamate from their presynaptic terminals eliciting excitatory postsynaptic potentials (EPSPs) in second-order sensory neurons (Jahr and Jessell, 1985; Woolf and Ma, 2007). However, nociceptive nerve fibres, which are either unmyelinated (C) or thinly myelinated (Aδ) fibres, release CGRP and SP in addition to glutamate from their presynaptic terminals (Woolf and Ma, 2007). The current study focuses on the release of CGRP from central terminals.

5.1.2 CGRP

Two isoforms of CGRP exist, CGRPα and CGRPβ, which are formed from two different genes (Brain and Cox, 2006). The CGRPα isoform is widely expressed and is localised to C and Aδ

fibres of the DRG whereas the CGRPβ isoform is predominantly expressed in neurons of the enteric nervous system. Receptors for CGRP are expressed within the dorsal horn of the spinal cord and it is thought that release of CGRP at the first central synapse could contribute to pain hypersensitivity (Bennett et al., 2000; Chen et al., 2010; Cottrell et al., 2005; Kawamura et al., 1989; Yu et al., 1994; Zhang et al., 2001). CGRPα-expressing sensory nerves have been shown to be sensitive to agonists of TRPV1 and TRPA1, in addition to acidic pH, ATP and some pruritic substances (McCoy et al., 2012). Moreover, CGRPα neurons have been shown to be important for behavioural responses to heat and itch, and have been reported to suppress cold sensitivity (McCoy et al., 2013).

5.1.3 TRP Channels at Central Synapses

The role TRP channels play in sensing chemical, thermal and mechanical stimuli in the periphery is well characterised (Caterina et al., 1999; Damann et al., 2008; Peier et al., 2002b; Story et al., 2003b), yet the role TRP channels play when expressed at central terminals remains ambiguous. Sensory neuron TRP channels, notably TRPV1, TRPA1 and TRPM8, are expressed on the presynaptic, central terminals of primary afferent neurons, in addition to nerve terminals in the periphery, but are not expressed by spinal neurons (Andersson et al., 2011; Baccei et al., 2003; Dhaka et al., 2008; Kim et al., 2010; Mogg et al., 2013; Sikand and Premkumar, 2007; Takashima et al., 2007).

Activation of TRPV1 and TRPA1 channels expressed on central terminals has been shown to increase neurotransmitter release within the spinal cord (Li and Eisenach, 2001, 2005; Mogg et al., 2013; Puttfarcken et al., 2010; Saria et al., 1986; Trevisani et al., 2007) and activation of TRPV1, TRPA1 and TRPM8 channels has been shown to increase the frequency of spontaneous mEPSCs recorded in the dorsal horn of the spinal cord (Jeffry et al., 2009; Wrigley et al., 2009). Conversely, activation of these sensory neuron TRP channels at presynaptic central terminals has been shown to inhibit evoked EPSCs (Jeffry et al., 2009; Wrigley et al., 2009). This latter finding suggests that activation of TRP channels at central terminals can interrupt nociceptive transmission through a process of depolarisation block. Consistent with these findings, one study concluded that the intrathecal administration of compounds which activate TRPA1, such as cinnamaldehyde and the acetaminophen-metabolite, *N*-acetyl-*p*-benzoquinoneimine, can interrupt spinal nociceptive transmission by activation of TRPA1 and a consequent reduction in voltage-gated calcium and sodium currents (Andersson et al., 2011).

The function of TRP channels at the central synapse appears two-fold, when activated in the absence of depolarising stimuli they can increase the frequency of spontaneous mEPSCs. However, in the presence of a depolarising stimulus, TRP channels located on the presynaptic-membrane can diminish this incoming stimulus inhibiting eEPSCs; positioning these channels as novel therapeutic targets in nociceptive conditions.

5.1.4 Neurotransmitter Release 'in-vitro'

Neurotransmitter release can be used to profile functional TRP channels which are expressed at the central terminals of primary afferents. *In vivo,* microdialysis has commonly been used to measure transmitter release however it is impractical for investigating detailed concentration-response relationships of different compounds. Furthermore, accurate estimations of drug concentrations reaching receptors cannot be made. The aim of the current study was to develop and characterise a different approach, measuring CGRP release from tissue preparations *in vitro* using a medium-throughput (96-well format) enzyme-linked immunosorbent assay (ELISA).

5.2 Aim of the present study

The aim of the present study was to investigate whether activation of TRPA1 channels natively expressed on the central terminals of primary afferent neurons present in the dorsal horn of the spinal cord could evoke CGRP release. In addition it was to test whether depolarisation-induced CGRP release could be modulated by inhibition of VGCCs, or by opioid receptor activation. These experimental aims were investigated by measuring CGRP release from samples of homogenised rat spinal cord with an ELISA.

The initial studies in this chapter were carried out at the laboratories of Eli Lilly and Company (Erlwood, UK) under the supervision Drs Lisa Broad and Adrian Mogg.

5.3 Materials and Methods

5.3.1 Solutions and Reagents

Some experiments were completed with Tyrode's salts with HEPES buffer (Invitrogen; 041-95897M) + 10µM thiorphan (to prevent CGRP breakdown by endogenous proteases) but the majority of the experiments were conducted in HBTS (136mM NaCl, 2.7mM KCl, 1.8mM $CaCl_2$, 1.05mM $MgCl_2$, 5mM glucose, 10mM HEPES and 335µM NaH^2PO^4) + 10µM thiorphan buffered to pH 7.4 (NaOH). HBTS containing high extracellular potassium was made by iso-osmotic addition of 40mM KCl. For Ca^{2+}-free experiments $CaCl_2$ was omitted from the solution and 1mM EGTA was added.

Master stock solutions of AITC, cinnamaldehyde (Sigma-Aldrich; St Louis, MO), AP18 (Maybridge; Tintagel, Cornwall, UK) were made in DMSO (Calbiochem; Darmstadt, Germany). Master stock solutions of 4-HNE and 4-ONE (Cayman Chemical; Ann Arbour, MI) were made in EtOH. Stock solutions of nifedipine, mibefradil dihydrochloride, ω-conotoxin MVIIC (Tocris Bioscience; Bristol, UK) were made in HBTS. Master stock solutions of morphine and naloxone (Sigma-Aldrich; St Louis, MO) were made in H_2O. All master stock solutions were aliquotted and stored at -20°C. Dilutions from these aliquots into HBTS were made daily for their use in experiments.

5.3.2 Methodology for 96 well CGRP release assay

Adult, male, Sprague Dawley rats (~250-500g) were killed by exposure to a rising concentration of CO_2 or by cervical dislocation. The lumbar portion of the spinal cord was then dissected, weighed and placed in a Sterilin tube containing ice-cold HBTS buffer without thiorphan. The cord was homogenised using approximately 12-15 strokes of a glass-Teflon hand homogeniser. The homogenate was then centrifuged for 1 minute at 1000rpm in a bench-top centrifuge and the supernatant carefully removed and reconstituted at a final concentration of 4mg/ml in HBTS. 100µl of the homogenate solution was placed in each well of a 96-well filter plate (Millipore, type MSBVN1B50) using a multi-channel pipette. The use of filter plates in these experiments allowed the solutions bathing the synaptosomes to be easily removed. The filter plate containing the homogenate was incubated at 37°C in a humidified incubator gassed with 5% CO_2 in air for 20 minutes prior to compound addition.

Following the 20 minute incubation period, the filter plate containing the homogenate was removed from the incubator and the buffer in the wells filtered to waste using a vacuum manifold. Extracellular solutions either in the presence or absence of antagonists or modulators were added to the wells of the filter plate (100µl per well) and the filter plate was incubated for 10 minutes at 37°C. The contents of the filter plate were then filtered to waste using a vacuum manifold. Extracellular solutions containing agonists or KCl (either in the presence or absence of antagonists or modulators) were then added to the wells of the filter plate (100 µl per well) and incubated for a further 10 minutes at 37°C.

Following the stimulation period, solutions contained within the wells of the filter plate were rapidly transferred to the wells of an ELISA CGRP immunoplate (SPlbio, France) containing anti-CGRP-AChE tracer (100µl per well) by centrifugal force (200x *g*). The immunoplate was then covered with plastic film and incubated at 4°C for 16–20 hours. The following day, the immunoplate was washed four times and Ellman's reagent was added to the wells of the plate (200µl). The plate was left at room temperature to develop in the dark for 45 minutes. The absorbance of each well was then measured at 405 nm using a 96-well plate spectrophotometer (Molecular Devices, Sunnyvale, CA).

5.3.3 Data analysis

Raw absorbance values were imported into Excel (Microsoft) for further analysis and then into Origin (Origin Pro, version 9.1) for graphical representation of the results. The amount of CGRP released was reported as a percentage over basal release (the amount of CGRP released upon addition of HBTS) or 40mM KCl-induced release. Release stimulated in the presence of an antagonist or modulator is normalised to an appropriate antagonist/modulator basal release where possible. Where stated, *n* refers to the number of independent experiments performed using spinal cord tissue from different animals. In each individual experiment a minimum of 4 replicate samples per treatment were used.

5.3.4 Statistics

Normality of data was tested using the Shapiro-Wilk Test and homogeneity of variances tested using Levene's test. Differences in means between two groups were analysed using an independent samples t-test. Differences in means between three groups or more were analysed using a one-way ANOVA, followed by a Tukey's HSD post-hoc test (for datasets with equal variances) or a Dunnett's T3 post-hoc test (for datasets with unequal variances). All statistical analyses were made using IBM SPSS statistics, version 22.

5.4 Results

5.4.1 Activation of TRPA1 evokes CGRP Release from spinal cord homogenate

In order to examine whether activation of TRPA1 evokes CGRP release from rat spinal cord synaptosomes, spinal cord homogenate was stimulated with TRPA1 agonists and the resulting CGRP release examined by ELISA. Stimulation of rat spinal cord homogenate by the pungent TRPA1 agonist, cinnamaldehyde, evoked a concentration-dependent increase in CGRP release with a mean EC_{50} value of 54.79 ± 5.84μM (mean ± SEM; n= 10 experiments; Figure 5-1a). Activation by allyl-isothiocyanate (AITC) also evoked CGRP release with an EC_{50} value of 17.08 ± 0.77μM (mean ± SEM; n= 3 experiments; Figure 5-1b). CGRP release was also evoked by electrophilic, endogenous agonists of TRPA1. 4-HNE and 4-ONE evoked CGRP release from spinal cord homogenate with EC_{50} values of 17.39 ± 0.68μM and 63.80 ± 4.26μM, respectively (mean ± SEM; n= 3 experiments; Figure 5-1).

In order to examine whether the CGRP release induced by the TRPA1 agonists is dependent on the influx of Ca^{2+} ions, the effect of removing external Ca^{2+} was examined using cinnamaldehyde-induced CGRP release. In the presence of extracellular Ca^{2+}, cinnamaldehyde induced robust increases in CGRP release and in the absence of extracellular Ca^{2+}, cinnamaldehyde-induced CGRP release was attenuated. The average response to 1000μM cinnamaldehyde in Ca^{2+} free solutions was decreased to 18 ± 6% of the response in Ca^{2+} containing solutions (mean ± SEM; n = 3 experiments; Figure 5-2). This finding suggests that influx of extracellular Ca^{2+} ions is required for TRPA1 agonist-induced CGRP release.

5.4.2 TRPA1-induced CGRP release requires synaptosomes which originate from the dorsal spinal cord

TRPA1 is thought to be expressed on the primary afferent nerve terminals of the dorsal root ganglia which enter the spinal cord via the dorsal roots and typically terminate within layers I-V of the dorsal horn (Story et al., 2003b). In order to investigate whether the CGRP release evoked by TRPA1 agonists occurs due to stimulation of dorsal spinal cord synaptosomes, separate homogenates were prepared from the dorsal and ventral spinal cord and stimulation by cinnamaldehyde (100μM) and KCl (40mM) was examined. Stimulation of dorsal spinal cord homogenate by cinnamaldehyde evoked CGRP release which was on average 14 ± 5% above the basal levels of release (mean ± SEM; n= 3 experiments). However, stimulation of ventral spinal cord homogenate by cinnamaldehyde

(100µM) failed to evoke CGRP release above basal levels (0 ± 1% over basal release; mean ± SEM; n= 3 experiments; Figure 5-3).

Stimulation of dorsal spinal cord homogenate by KCl (40mM) evoked large increases in CGRP release which were on average 67 ± 9% over the basal level of release (mean ± SEM; n= 3 experiments). However, stimulation of ventral spinal cord homogenate by KCl (40mM) only evoked a small increase in CGRP release which was significantly lower than the release evoked by dorsal spinal cord homogenate (6 ± 4% over basal release; $p<0.01$; t-test; n= 3 experiments; Figure 5-3).

These findings suggest that cinnamaldehyde-evoked CGRP release is dependent on synaptosomes which originate from the dorsal spinal cord. Furthermore, these findings suggest that depolarisation-induced CGRP release relies primarily on the release of CGRP from dorsal spinal cord synaptosomes but also indicate that a small amount of CGRP can be released by depolarisation of synaptosomes originating from the ventral spinal cord.

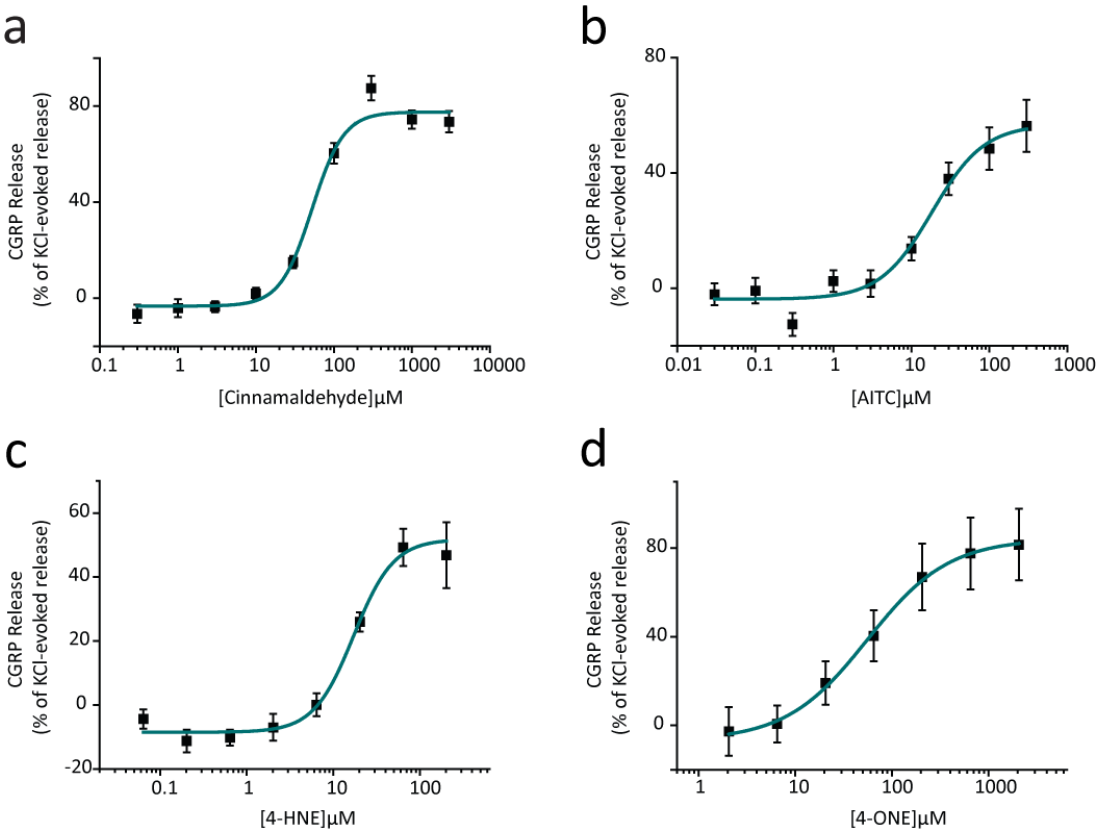

Figure 5-1 Activation of TRPA1 evokes CGRP release

The release of CGRP from rat spinal cord homogenate was measured by ELISA. Application of TRPA1 agonists evoked concentration-dependent increases in CGRP release from spinal cord homogenate. (**a**) Cinnamaldehyde induced CGRP release with an EC_{50} value of 54.78 ± 5.84µM (mean ± SEM; n= 10). (**b**) AITC evoked CGRP release with an EC_{50} value of 17.08 ± 0.77µM (mean ± SEM; n= 3). (**c**) The endogenous TRPA1 agonist 4-HNE stimulated CGRP release with an EC_{50} value of 17.39 ± 0.68µM (mean ± SEM; n= 3). (**d**) Another endogenous TRPA1 agonist, 4-ONE, also induced CGRP release with an EC_{50} value of 63.80 ± 4.26µM (mean ± SEM; n= 3). Representative plots shown, data points are the mean normalised release (% of 40mM KCl-induced release) of quadruplicate wells ± SEM.

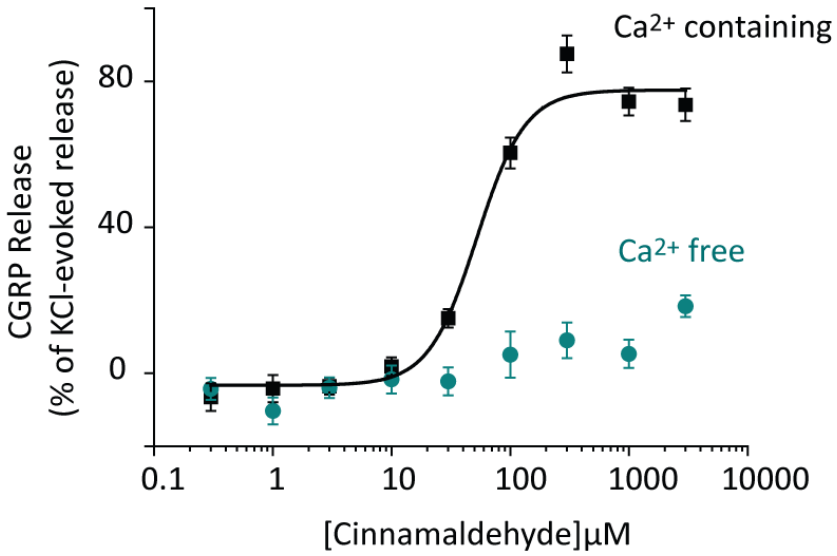

Figure 5-2 Cinnamaldehyde-induced CGRP release is dependent on extracellular Ca^{2+}

Cinnamaldehyde-induced CGRP release from rat spinal cord homogenate was measured by ELISA in the presence and absence of external Ca^{2+}. In the absence of external Ca^{2+} ions cinnamaldehyde-induced CGRP release was attenuated. Representative plot shown, data points are the mean normalised (% of 40mM KCl-induced release) release of quadruplicate wells ± SEM.

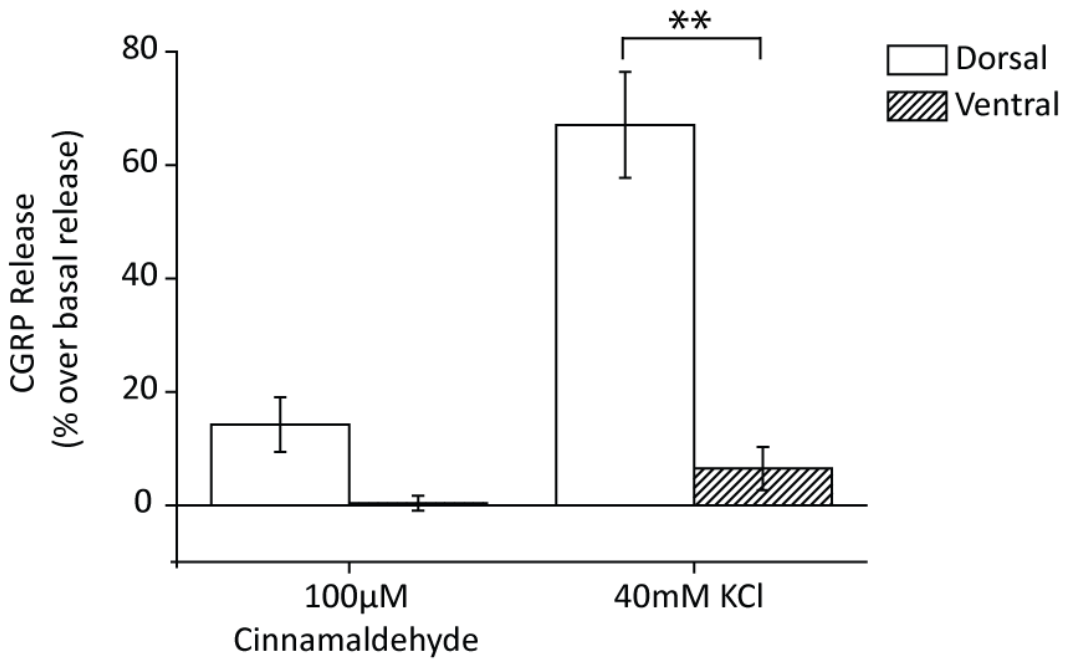

Figure 5-3 Cinnamaldehyde induces CGRP release from dorsal but not ventral spinal cord synaptosomes

CGRP release from dorsal and ventral spinal cord homogenate was measured by ELISA. Cinnamaldehyde (100µM) induced CGRP release from dorsal spinal cord homogenate (14 ± 5% over basal release; mean ± SEM; n = 3 experiments) but did not evoke release from synaptosomal preparations from the ventral spinal cord (0 ± 1% over basal release; mean ± SEM; n = 3 experiments). KCl (40mM) evoked a large increase in CGRP release from dorsal spinal cord homogenate (67 ± 9% over basal release; mean ± SEM; n = 3 experiments). The CGRP release evoked by KCl in ventral spinal cord homogenate was significantly lower (6 ± 4% over basal release; mean ± SEM; n = 3 experiments). Columns represent mean ± SEM (** $P < 0.01$; t-test n= 3 experiments).

5.4.3 Cinnamaldehyde- and AITC-evoked CGRP release is mediated through activation of TRPA1

In order to test whether the CGRP release evoked by TRPA1 agonists is mediated through activation of TRPA1, the effect of a TRPA1 antagonist (AP18) on cinnamaldehyde- and AITC-induced CGRP release was examined. Dorsal spinal cord homogenate was stimulated with 100µM cinnamaldehyde and 100µM AITC in the presence and the absence of 50µM AP18. In the absence of AP18, both cinnamaldehyde and AITC evoked notable increases in CGRP release. Cinnamaldehyde evoked CGRP release (39 ± 8% of 40mM KCl-evoked release, mean ± SEM; n= 3 experiments) was completely inhibited in the presence of AP18 (average release reduced to -1 ± 3% of 40mM KCl-evoked release, mean ± SEM; $p< 0.05$; t-test; n= 3 experiments; Figure 5-4). Similar to cinnamaldehyde-evoked release, AITC-induced CGRP release was also significantly inhibited in the presence of AP18, where the average release was reduced from 42 ± 11% to 8 ± 5% of the amount released by 40mM KCl (mean ± SEM; $p< 0.05$; t-test; n= 3 experiments; Figure 5-4). These findings demonstrate that both cinnamaldehyde and AITC evoke CGRP release in this preparation by activating TRPA1.

5.4.4 VGCC blockade does not affect TRPA1-induced CGRP release

TRPA1 channel opening leads to an influx of Na^+ and Ca^{2+} ions, an event which causes membrane depolarisation. The depolarisation may, in turn, result in the opening of voltage-gated ion channels. To investigate whether Ca^{2+} influx through voltage-gated calcium channels (VGCCs) contributes to the CGRP release evoked by TRPA1 activation, the effect of VGCC inhibitors on cinnamaldehyde-induced CGRP release from dorsal spinal cord homogenate was investigated.

Dorsal spinal cord homogenate was stimulated with 100µM cinnamaldehyde in the presence and absence of the L-type VGCC inhibitor nifedipine (5µM), the T-type VGCC inhibitor mibefradil dihydrochloride (10µM), a low concentration of ω-conotoxin MVIIC (200nM) to inhibit P/Q-type VGCCs or a high concentration of ω-conotoxin MVIIC to inhibit N and P/Q-type VGCCs (1µM). The CGRP release evoked by 100µM cinnamaldehyde was not significantly altered in the presence of the VGCC inhibitors (NS; ANOVA; n= 3-4 experiments; Figure 5-5). However, a trend for increased CGRP release was evident when homogenate was stimulated by cinnamaldehyde in the presence of nifedipine (5µM) where release was increased from 32 ± 6% to 50 ± 9% of 40mM KCl-evoked release (mean ± SEM; n= 4 experiments; Figure 5-5).

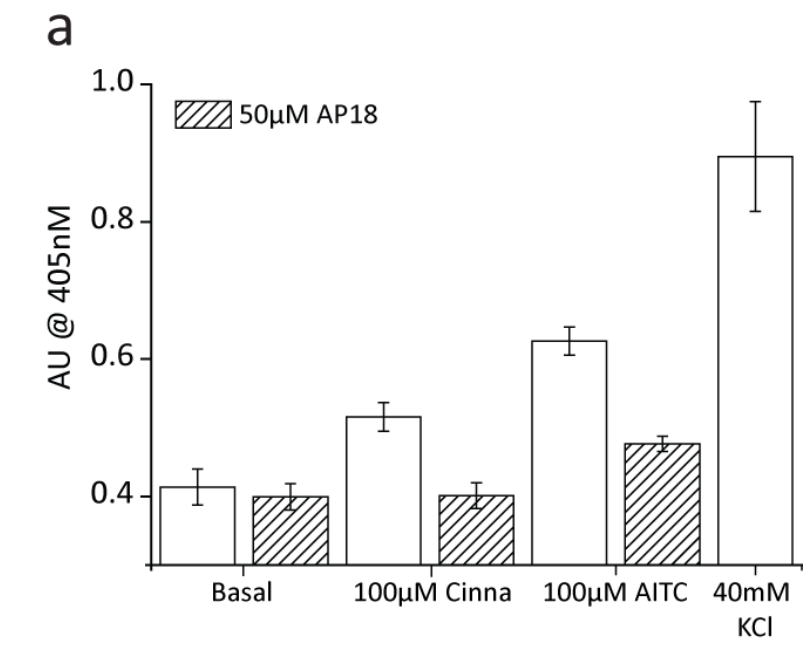
a
1.0
0.8
0.6
0.4
AU @ 405nM
50µM AP18
Basal
100µM Cinna
100µM AITC
40mM KCl

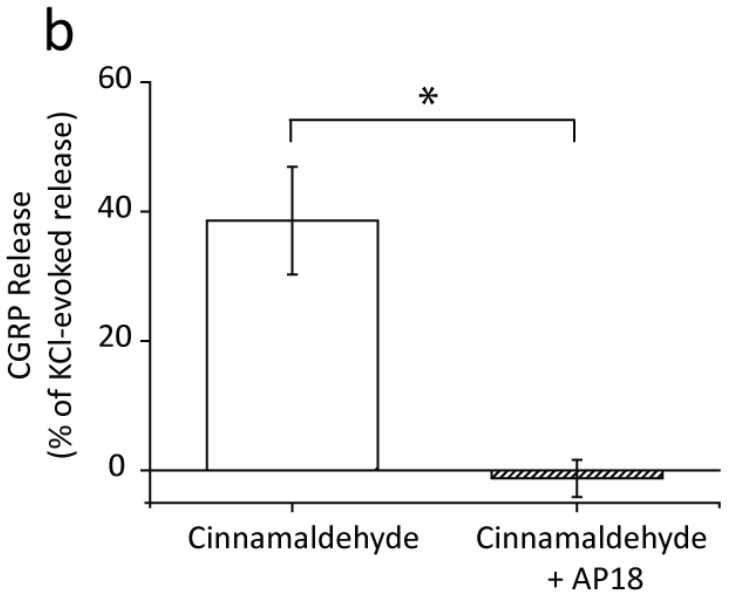
b
60
40
20
0
CGRP Release
(% of KCl-evoked release)
*
Cinnamaldehyde
Cinnamaldehyde + AP18

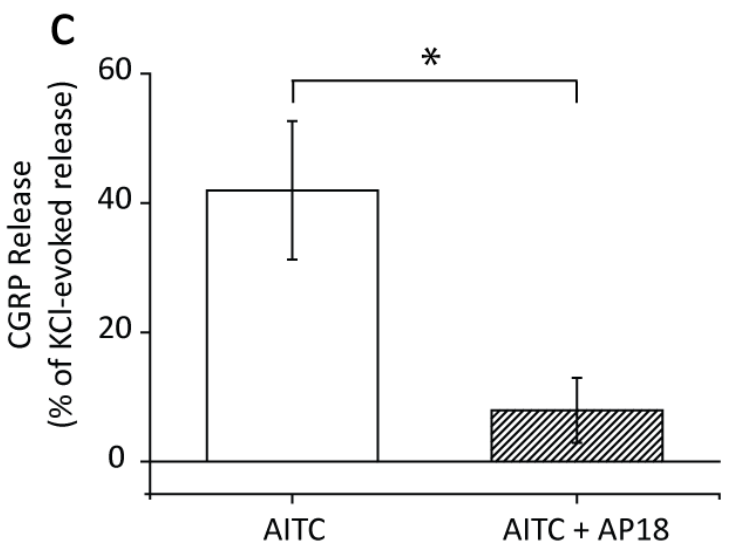
c
60
40
20
0
CGRP Release
(% of KCl-evoked release)
*
AITC
AITC + AP18

Figure 5-4 AITC and cinnamaldehyde-induced CGRP release is inhibited by a TRPA1 antagonist

The effect of a TRPA1 antagonist, AP18 (50µM), on cinnamaldehyde (100µM) and AITC (100µM) evoked CGRP release (measured by ELISA) from rat dorsal spinal cord homogenate was examined. (**a**) Graph displaying CGRP release (as measured by absorbance at 405 nM) evoked by 100µM AITC and 100µM cinnamaldehyde in the presence and absence of 50µM AP18 in a representative experiment. Also shown are the levels of CGRP release evoked by negative (basal) and positive (40mM KCl) controls. Columns represent mean ± SEM of quadruplicate wells. (**b**) Cinnamaldehyde-induced CGRP release was significantly inhibited by AP18, release was reduced from 39 ± 8% of 40mM KCl-evoked release in the absence of AP18, to -1 ± 3% of 40mM-KCl evoked release in the presence of AP18. Columns represent mean ± SEM (* $P < 0.05$; t-test; n= 4 experiments). (**c**) AITC-induced CGRP release was also significantly inhibited by AP18, AITC-induced release was reduced from 42 ± 11% of 40mM KCl-evoked release to 8 ± 5% of 40mM KCl-evoked release in the presence of AP18. Columns represent mean ± SEM (* $P < 0.05$; t-test; n= 4 experiments).

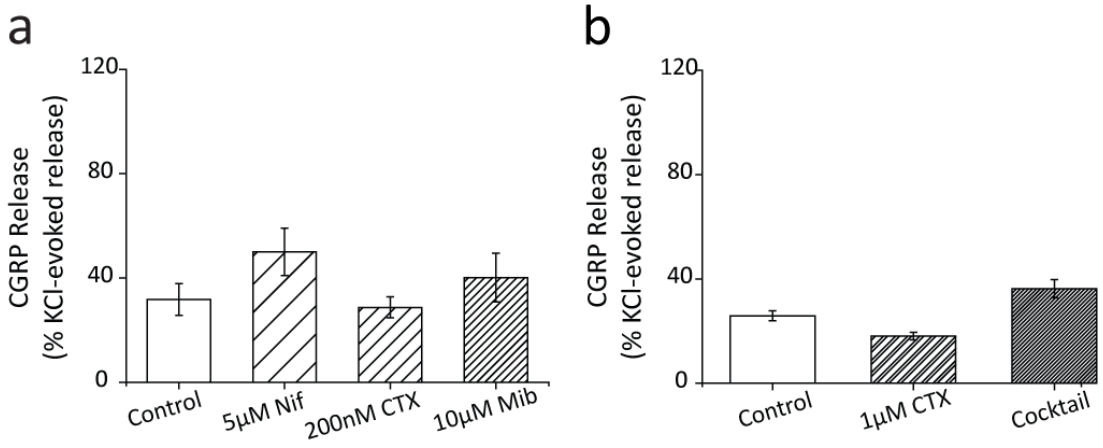

Figure 5-5 Blocking VGCCs does not affect cinnamaldehyde-induced CGRP release

The effect of VGCC-blockade on 100µM cinnamaldehyde-induced CGRP release (measured by ELISA) from rat dorsal spinal cord homogenate was examined. (**a**) 100µM cinnamaldehyde-induced CGRP release (control) was not significantly affected in the presence of 5µM nifedipine, 200nM ω-conotoxin MVIIC (CTX) or 10µM mibefradil dihydrochloride. Columns represent mean ± SEM (ANOVA; n= 4 experiments). (**b**) 100µM cinnamaldehyde-induced CGRP release (control) was not significantly altered in the presence of 1µM ω-conotoxin MVIIC (CTX) or a cocktail of VGCC blockers (containing 5µM nifidepine, 1µM ω-conotoxin MVIIC and 10µM mibefradil dihydrochloride). Data is normalised to 40mM KCl-induced release. Columns represent mean ± SEM (ANOVA; n= 3 experiments).

5.4.5 T-type VGCCs are required for CGRP release induced by depolarisation

CGRP release is evoked by high concentrations of KCl which lead to depolarisation and opening of VGCCs. In order to study the differential contribution of VGCC subtypes to depolarisation-induced CGRP release, the effect of VGCC inhibitors on KCl-induced CGRP release from dorsal spinal cord homogenate was investigated.

Dorsal spinal cord homogenate was stimulated with 40mM KCl in the presence and absence of individual VGCC inhibitors; nifedipine (5µM), mibefradil dihydrochloride (10µM), ω-conotoxin MVIIC (200nM), ω-conotoxin MVIIC (1µM).

Depolarisation-induced CGRP release was not affected by the presence of 5µM nifedipine or 200nM ω-conotoxin MVIIC. Block of N and P/Q type VGCCs by 1µM ω-conotoxin MVIIC lead to a small reduction in depolarisation-induced CGRP release, however this effect was not significant (73 ± 8% of 40mM KCl-evoked release; mean ± SEM; NS; ANOVA followed by Tukey's HSD test; n= 4 experiments; Figure 5-6). Interestingly, depolarisation evoked CGRP release was significantly inhibited in the presence of the T-type VGCC inhibitor, mibefradil dihydrochloride (10µM) (48 ± 6% of 40mM KCl-evoked release, mean ± SEM; $p<0.001$; ANOVA followed by Tukey's HSD test; n= 5 experiments; Figure 5-6). Furthermore, depolarisation-induced CGRP release was profoundly inhibited in the presence a VGCC inhibitor cocktail (containing 5µM nifidepine, 1µM ω-conotoxin MVIIC and 10µM mibefradil dihydrochloride), where CGRP release was reduced to 28 ± 9% of 40mM KCl-evoked release (mean ± SEM; $p<0.001$; ANOVA followed by Tukey's HSD test; n= 4 experiments; Figure 5-6). These findings suggest an importance of T- and to a lesser extent N-type VGCCs for depolarisation-induced CGRP release.

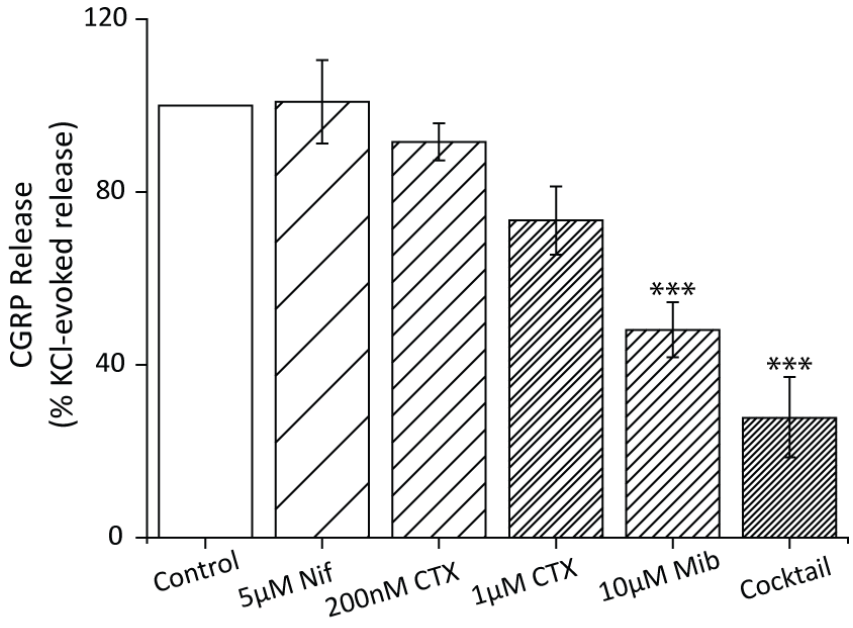

Figure 5-6 Depolarisation-evoked CGRP release is inhibited by VGCC blockade

The effect of VGCC-blockade on depolarisation-induced (40mM KCl) CGRP release (measured by ELISA) from rat dorsal spinal cord homogenate was examined. 40mM KCl evoked CGRP release which was significantly decreased in the presence of the t-type VGCC blocker, mibefradil dihydrochloride (10µM) and a cocktail of VGCC inhibitors (containing 5µM nifidepine, 1µM ω-conotoxin MVIIC and 10µM mibefradil dihydrochloride). There was a trend for homogenate treated with 1µM ω-conotoxin MVIIC (CTX) to exhibit a reduced release to 40mM KCl although this was not significant. Treatment with 5µM nifedipine and 200nM ω-conotoxin MVIIC had no effect on KCl-induced release. Data is normalised to 40mM KCl-induced release (control). Columns represent mean ± SEM (*** P <0.001; ANOVA followed by Tukey's HSD test; nifedipine, 200nM CTX, 10µM Mib, n= 5 experiments; 1µM CTX and cocktail, n= 4).

5.4.6 Modulation of depolarisation-induced CGRP release by morphine

Activation of opioid receptors expressed on sensory neurons causes inhibition of voltage-gated calcium channels. In order to examine whether depolarisation-induced CGRP release could be inhibited by opioid receptor activation, the effects of the prototypical opioid receptor agonist, morphine, on KCl-induced CGRP release was investigated.

Dorsal spinal cord homogenate was stimulated with KCl (5-60mM) in the presence and absence of 10µM morphine. The concentration dependent KCl-evoked CGRP release was suppressed in the presence of 10µM morphine; the largest effects were on CGRP release evoked by 40 and 60mM KCl (Figure 5-7a).

An inhibitory trend of morphine (10µM) on CGRP release was observed, CGRP release evoked by 40mM KCl was reduced from 77 ± 7% to 62 ± 5% over basal release in the presence of morphine (mean ± SEM; NS; ANOVA; n= 4 experiments). Furthermore, CGRP release evoked by 60mM KCl was reduced from 131 ± 17% to 103 ± 6% over basal release (mean ± SEM; NS; ANOVA; n= 4 experiments). In order to examine whether the inhibitory effects of morphine on CGRP release were mediated by opioid receptors, dorsal spinal cord homogenate was stimulated with KCl (40 and 60mM) in the presence of morphine (10µM) and the opioid receptor antagonist naloxone (1µM). The inhibitory effects of morphine were reduced by naloxone indicating that the release of CGRP can be modulated by opioid receptor activation (Figure 5-7b).

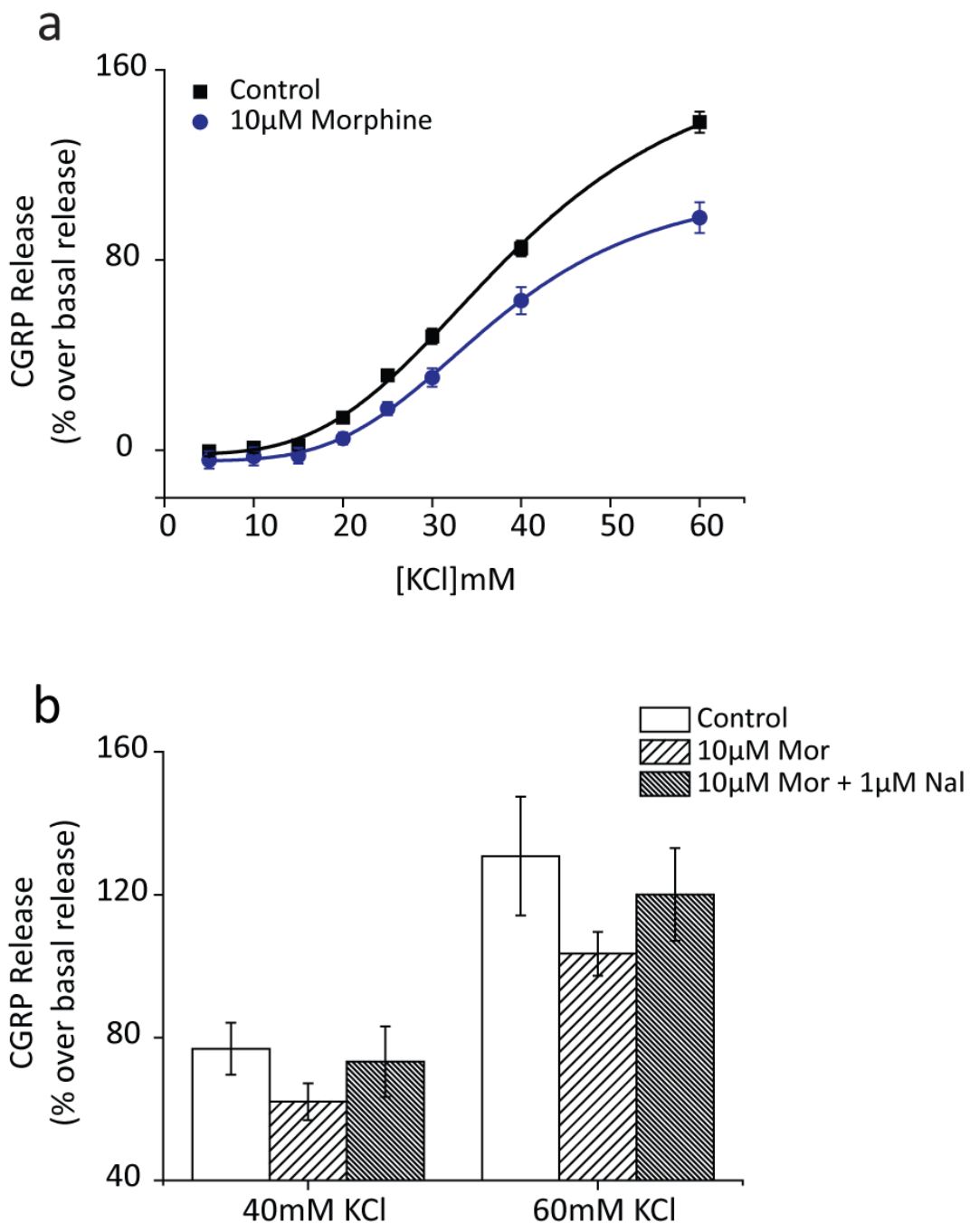

Figure 5-7 The effect of morphine on depolarisation-induced CGRP release

(**a**) The effect of morphine on depolarisation-induced CGRP release (measured by ELISA) from rat dorsal spinal cord homogenate was examined. KCl evoked CGRP release in a concentration dependent manner which was inhibited by morphine (10µM). Representative plot shown, data points are the mean normalised (% over basal) release of quadruplicate wells ± SEM. (**b**) There was a trend for homogenate treated with morphine to exhibit a reduced CGRP release in response to 40mM and 60mM KCl. This effect was reversed in the presence of naloxone. Data is normalised to basal release. Columns represent mean ± SEM (NS; ANOVA followed by Tukey's HSD test; n= 4 experiments).

5.5 Discussion

The results presented in this chapter describe a medium-throughput methodology for examining stimulation of spinal cord synaptosomes and have shown that activation of TRPA1 by pungent food compounds and products of lipid peroxidation evokes CGRP release from this preparation. The results of this study suggest that TRPA1 mediated CGRP release does not require opening of VGCCs. Additionally, the results have demonstrated an involvement of low-threshold T-type VGCCs and to a lesser extent, N-type VGCCs, in the depolarisation-evoked release of CGRP within the spinal cord.

5.5.1 CGRP release is evoked by TRPA1 agonists

The CGRP release assay allowed full concentration response curves to be constructed for cinnamaldehyde, AITC, 4-HNE and 4-ONE. Concentrations of cinnamaldehyde, AITC and 4-HNE required to evoke CGRP release from synaptosomes were within the same range as those needed to activate TRPA1 channels expressed in recombinant cell systems (Macpherson et al. 2007; Taylor-Clark et al. 2008; Bandell et al. 2004). However the concentration of 4-ONE required for half-maximal release of CGRP reported in the current study (~64μM) is higher than the EC_{50} value (~2μM) reported for recombinant TRPA1 channels in other studies (Taylor-Clark et al., 2008b). Cinnamaldehyde-induced CGRP release was dependent on extracellular calcium. Moreover, cinnamaldehyde- and AITC-evoked CGRP release was inhibited by the TRPA1-selective inhibitor, AP18, confirming that the release is mediated by the TRPA1 channel.

5.5.2 CGRP release occurs predominantly from the dorsal spinal cord

CGRP release induced by activation of TRPA1 was restricted to dorsal spinal cord homogenate. Stimulation of ventral spinal cord homogenate with the TRPA1 agonist, cinnamaldehyde, failed to release CGRP above basal levels. In light of the findings that TRPA1 expression in the dorsal spinal cord is abolished with dorsal rhizotomy (Kim et al., 2010), these findings are consistent with TRPA1-induced CGRP release from the central terminals of TRPA1-expressing primary afferent neurons which terminate in the superficial layers of the dorsal horn (Kim et al., 2010).

CGRP release evoked by high potassium was significantly higher in homogenate samples from the dorsal spinal cord in comparison to samples from the ventral spinal cord. However, a small release of CGRP in response to high potassium was evident in ventral

spinal cord homogenate; this suggests that depolarisation of some motor neuron terminals could lead to the release of CGRP. This finding is consistent with reports of CGRP expression within motor neuron cell bodies of the ventral spinal cord where it is suggested to be involved in repair mechanisms following nerve injury (Chen et al., 2010; McCoy et al., 2012).

5.5.3 TRPA1-induced CGRP release is largely independent of VGCCs

Interestingly, inhibition of L-type, T-type, P/Q-type and N-type VGCCs did not significantly alter the levels of CGRP released by a sub-maximal concentration of cinnamaldehyde. This finding suggests that Ca^{2+} influx through the TRPA1 channel itself is sufficient to evoke release and is consistent with reports of a high Ca^{2+} permeability of TRPA1 (see Zygmunt and Högestätt, 2014 for review). Similar findings were reported for TRPV1 in a study examining CGRP release from rat sciatic nerve axons which found that capsaicin-induced CGRP release was unaffected by blockade of L-type and T-type VGCCs both of which were important for high potassium-induced CGRP release (Spitzer et al., 2008).

A trend was observed for potentiation of cinnamaldehyde-induced release by nifedipine; release was increased from 32 ± 6% to 50 ± 9% (of KCl-evoked release) in the presence of 5µM nifedipine. The 1,4-dihydropyridines have been demonstrated to be TRPA1 agonists and nifedipine has been shown to activate recombinantly-expressed TRPA1 channels with an EC_{50} value of ~0.4µM (Fajardo et al., 2008b). An increased release of CGRP could therefore be due to the synergistic activation of TRPA1 by cinnamaldehyde and nifedipine, resulting in increased Ca^{2+} influx and CGRP release (Fajardo et al., 2008b). Moreover, nifedipine has also been identified as an activator of the sensory neuron-expressed channel, TRPM3, with an EC_{50} value of ~30µM (Wagner et al., 2008). Activation of TRPM3 channels could also contribute to the release of CGRP, although it has not yet been identified whether these channels are expressed on peptidergic nerve terminals. Confounding activation of TRPA1 or TRPM3 by the L-type VGCC inhibitor and consequent CGRP release could mask any inhibition and makes assessing the role of L-type VGCCs in cinnamaldehyde-induced release difficult. However inhibition of other VGCCs present on sensory nerves had no effect on TRPA1-induced release, suggesting that TRPA1-induced CGRP release is largely independent of VGCCs.

5.5.4 Depolarisation-induced CGRP release requires low-threshold T-type VGCCs

In the current study, the contribution of VGCC subtypes to depolarisation-induced CGRP release was also examined. Studies examining CGRP release evoked by high extracellular potassium from isolated lung and skin have identified a reliance upon N and L-type high VGCC subtypes (Kress et al., 2001; Lou et al., 1992). However, the importance of T-type low VGCCs was not investigated in these studies. In the current study, high potassium (40mM) induced CGRP release which was significantly decreased by inhibition of T-type VGCCs. Mibefradil dihydrochloride, decreased high potassium induced-CGRP release by ~50%. Consistent with this finding, a dependence on T-type VGCCs has also been demonstrated for nitric oxide-induced CGRP release from cultured trigeminal ganglion neurons and high potassium-induced CGRP release from sciatic nerve axons (Bellamy et al., 2006; Spitzer et al., 2008). Moreover, inhibition of T-type VGCCs has been shown to decrease mEPSC frequency in the dorsal horn of the spinal cord (Bao et al., 1998). It is important to note that mibefradil dihydrochloride also has a small effect on high threshold L-type VGCC, however it has a 12-13 fold greater affinity for T-type VGCCs and the concentration used in this study (10μM) should act predominantly to inhibit T-type VGCCs (Martin et al., 2000). Interestingly, T-type calcium channels are implicated in nociception. Thermal and mechanical hypersensitivity induced by peripheral nerve injury and diabetic neuropathy has been shown to be alleviated by T-type channel blockers (Dogrul et al., 2003; Latham et al., 2009; Lee et al., 2010b; Pathirathna et al., 2005) and oligodeoxynucleotide antisense knockdown of Cav3.2 (Bourinet et al., 2005).

In contrast to other studies investigating CGRP release (Kress et al., 2001; Lou et al., 1992; Spitzer et al., 2008), pharmacological blockade of L-type VGCCs had no effect on high potassium-induced CGRP release. However, as discussed in section 5.5.3, the 1,4-dihydropyridine drug, nifedipine (5μM) used to investigate L-type VGCC involvement can activate TRPA1 within this concentration range and could also activate TRPM3. Such an effect could be masking any potential inhibition of release achieved by block of L-type VGCCs (Fajardo et al., 2008b; Wagner et al., 2008). Interestingly, some studies have used another 1,4-dihydropyridine compound, nimodipine, which is also an agonist of TRPA1, to test the involvement of L-type VGCC but reported inhibition of high potassium-induced CGRP release (Kress et al., 2001; Spitzer et al., 2008).

In the current study, pharmacological blockade of P/Q-type VGCCs alone by a low concentration of ω-conotoxin MVIIC (200nM) did not significantly alter CGRP release

evoked by high potassium. However, block of both N and P/Q type VGCCs by a higher concentration of ω-conotoxin MVIIC (1μM) lead to a reduction in high potassium-evoked CGRP release, although this was not a significant effect. This result suggests that N-type VGCCs could contribute to depolarisation-induced CGRP release. Consistent with this possibility, application of a VGCC inhibitor cocktail reduced high-potassium evoked release by ~72%, which is a greater inhibition than achieved by mibefradil dihydrochloride alone indicating that other VGCC subtypes are also required for CGRP release.

5.5.5 Modulation of depolarisation-evoked release

Opioid receptors are expressed on the peripheral and central terminals of sensory neurons. Activation of opioid receptors causes a decrease in cAMP levels and inhibition of VGCCs (Stein et al., 2003). Consistent with this, morphine inhibited high potassium-induced CGRP release and this effect could be reversed using the opioid antagonist naloxone. These data are consistent with an anti-nociceptive effect of morphine in the dorsal horn by presynaptic inhibition of CGRP expressing primary afferent nerve fibres. Similar findings have been demonstrated by a study examining CGRP release from the rat brainstem, which reported that morphine inhibited high-potassium evoked CGRP release which could be reversed by naloxone (Greco et al., 2014).

5.6 Conclusion

Activation of TRPA1 channels natively expressed in the rat dorsal spinal cord induces release of the neuropeptide transmitter, CGRP. TRPA1-dependent CGRP release does not require activation of T-type, N-type or P/Q-type VGCCs. However, CGRP release evoked by depolarisation is predominantly dependent on activation of low-threshold T-type VGCCs and can be inhibited by activation of natively-expressed opioid receptors.

In summary, the findings of this results chapter have demonstrated the use of a dorsal spinal cord homogenate assay for investigation of natively-expressed TRPA1 channels and for modulation of depolarising stimuli at the level of the dorsal spinal cord.

References

Abeele, F.V., Zholos, A., Bidaux, G., Shuba, Y., Thebault, S., Beck, B., Flourakis, M., Panchin, Y., Skryma, R., and Prevarskaya, N. (2006). Ca2+-independent Phospholipase A2-dependent Gating of TRPM8 by Lysophospholipids. J. Biol. Chem. *281*, 40174–40182.

Agarwal, N., Pacher, P., Tegeder, I., Amaya, F., Constantin, C.E., Brenner, G.J., Rubino, T., Michalski, C.W., Marsicano, G., Monory, K., et al. (2007). Cannabinoids mediate analgesia largely via peripheral type 1 cannabinoid receptors in nociceptors. Nat. Neurosci. *10*, 870–879.

Ahluwalia, J., Urban, L., Capogna, M., Bevan, S., and Nagy, I. (2000). Cannabinoid 1 receptors are expressed in nociceptive primary sensory neurons. Neuroscience *100*, 685–688.

Alessandri-Haber, N., Yeh, J.J., Boyd, A.E., Parada, C.A., Chen, X., Reichling, D.B., and Levine, J.D. (2003). Hypotonicity Induces TRPV4-Mediated Nociception in Rat. Neuron *39*, 497–511.

Alessandri-Haber, N., Joseph, E., Dina, O.A., Liedtke, W., and Levine, J.D. (2005). TRPV4 mediates pain-related behavior induced by mild hypertonic stimuli in the presence of inflammatory mediator. Pain *118*, 70–79.

Almaraz, L., Manenschijn, J.-A., de la Peña, E., and Viana, F. (2014). Trpm8. Handb. Exp. Pharmacol. *222*, 547–579.

Andersson, D.A., Nash, M., and Bevan, S. (2007). Modulation of the Cold-Activated Channel TRPM8 by Lysophospholipids and Polyunsaturated Fatty Acids. J. Neurosci. *27*, 3347–3355.

Andersson, D.A., Gentry, C., Moss, S., and Bevan, S. (2008). Transient Receptor Potential A1 Is a Sensory Receptor for Multiple Products of Oxidative Stress. J. Neurosci. *28*, 2485–2494.

Andersson, D.A., Gentry, C., Alenmyr, L., Killander, D., Lewis, S.E., Andersson, A., Bucher, B., Galzi, J.-L., Sterner, O., Bevan, S., et al. (2011). TRPA1 mediates spinal antinociception induced by acetaminophen and the cannabinoid Δ(9)-tetrahydrocannabiorcol. Nat. Commun. *2*, 551.

Andersson, D.A., Gentry, C., and Bevan, S. (2012). TRPA1 Has a Key Role in the Somatic Pro-Nociceptive Actions of Hydrogen Sulfide. PLoS ONE *7*.

Baccei, M.L., Bardoni, R., and Fitzgerald, M. (2003). Development of nociceptive synaptic inputs to the neonatal rat dorsal horn: glutamate release by capsaicin and menthol. J. Physiol. *549*, 231–242.

Bae, Y.-S., Lee, T.G., Park, J.C., Hur, J.H., Kim, Y., Heo, K., Kwak, J.-Y., Suh, P.-G., and Ryu, S.H. (2003). Identification of a Compound That Directly Stimulates Phospholipase C Activity. Mol. Pharmacol. *63*, 1043–1050.

Balsinde, J., and Balboa, M.A. (2005). Cellular regulation and proposed biological functions of group VIA calcium-independent phospholipase A2 in activated cells. Cell. Signal. *17*, 1052–1062.

Bandell, M., Story, G.M., Hwang, S.W., Viswanath, V., Eid, S.R., Petrus, M.J., Earley, T.J., and Patapoutian, A. (2004). Noxious cold ion channel TRPA1 is activated by pungent compounds and bradykinin. Neuron *41*, 849–857.

Bao, J., Li, J.J., and Perl, E.R. (1998). Differences in Ca2+ Channels Governing Generation of Miniature and Evoked Excitatory Synaptic Currents in Spinal Laminae I and II. J. Neurosci. *18*, 8740–8750.

Le Bars, D., Gozariu, M., and Cadden, S.W. (2001). Animal models of nociception. Pharmacol. Rev. *53*, 597–652.

Basbaum, A.I., Bautista, D.M., Scherrer, G., and Julius, D. (2009). Cellular and Molecular Mechanisms of Pain. Cell *139*, 267–284.

Bautista, D.M., Jordt, S.-E., Nikai, T., Tsuruda, P.R., Read, A.J., Poblete, J., Yamoah, E.N., Basbaum, A.I., and Julius, D. (2006). TRPA1 Mediates the Inflammatory Actions of Environmental Irritants and Proalgesic Agents. Cell *124*, 1269–1282.

Bautista, D.M., Siemens, J., Glazer, J.M., Tsuruda, P.R., Basbaum, A.I., Stucky, C.L., Jordt, S.-E., and Julius, D. (2007). The menthol receptor TRPM8 is the principal detector of environmental cold. Nature *448*, 204–208.

Beavo, J.A., Rogers, N.L., Crofford, O.B., Baird, C.E., Hardman, J.G., Sutherland, E.W., and Newman, E.V. (1971). Effects of Phosphodiesterase Inhibitors on Cyclic Amp Levels and on Lipolysis*. Ann. N. Y. Acad. Sci. *185*, 129–136.

Bellamy, J., Bowen, E.J., Russo, A.F., and Durham, P.L. (2006). Nitric oxide regulation of calcitonin gene-related peptide gene expression in rat trigeminal ganglia neurons. Eur. J. Neurosci. *23*, 2057–2066.

Bennett, A.D., Chastain, K.M., and Hulsebosch, C.E. (2000). Alleviation of mechanical and thermal allodynia by CGRP8-37 in a rodent model of chronic central pain. PAINÂ® *86*, 163–175.

Bennett, D.L., Averill, S., Clary, D.O., Priestley, J.V., and McMahon, S.B. (1996). Postnatal changes in the expression of the trkA high-affinity NGF receptor in primary sensory neurons. Eur. J. Neurosci. *8*, 2204–2208.

Berridge, M.J. (2012). Cell Signalling Biology: Module 2 - Cell signalling pathways. Biochem. J.

Bessou, P., and Perl, E.R. (1969). Response of cutaneous sensory units with unmyelinated fibers to noxious stimuli. J. Neurophysiol. *32*, 1025–1043.

Bevan, S., Quallo, T., and Andersson, D.A. (2014). TRPV1. In Mammalian Transient Receptor Potential (TRP) Cation Channels, B. Nilius, and V. Flockerzi, eds. (Springer Berlin Heidelberg), pp. 207–245.

Bičíková, M., Klak, J., Hill, M., Žižka, Z., Hampl, R., and Calda, P. (2002). Two neuroactive steroids in midpregnancy as measured in maternal and fetal sera and in amniotic fluid. Steroids *67*, 399–402.

Binzen, U., Greffrath, W., Hennessy, S., Bausen, M., Saaler-Reinhardt, S., and Treede, R.-D. (2006). Co-expression of the voltage-gated potassium channel Kv1.4 with transient receptor potential channels (TRPV1 and TRPV2) and the cannabinoid receptor CB1 in rat dorsal root ganglion neurons. Neuroscience *142*, 527–539.

Boillat, A., Alijevic, O., and Kellenberger, S. (2014). Calcium entry via TRPV1 but not ASICs induces neuropeptide release from sensory neurons. Mol. Cell. Neurosci. *61*, 13–22.

Bourinet, E., Alloui, A., Monteil, A., Barrère, C., Couette, B., Poirot, O., Pages, A., McRory, J., Snutch, T.P., Eschalier, A., et al. (2005). Silencing of the Cav3.2 T-type calcium channel gene in sensory neurons demonstrates its major role in nociception. EMBO J. *24*, 315–324.

Bourque, C.W. (2008). Central mechanisms of osmosensation and systemic osmoregulation. Nat. Rev. Neurosci. *9*, 519–531.

Brain, S.D., and Cox, H.M. (2006). Neuropeptides and their receptors: innovative science providing novel therapeutic targets. Br. J. Pharmacol. *147 Suppl 1*, S202–S211.

Brain, S.D., Williams, T.J., Tippins, J.R., Morris, H.R., and MacIntyre, I. (1985). Calcitonin gene-related peptide is a potent vasodilator. Nature *313*, 54–56.

Brierley, S.M., Castro, J., Harrington, A.M., Hughes, P.A., Page, A.J., Rychkov, G.Y., and Blackshaw, L.A. (2011). TRPA1 contributes to specific mechanically activated currents and sensory neuron mechanical hypersensitivity. J. Physiol. *589*, 3575–3593.

Burgess, P.R., and Perl, E.R. (1967). Myelinated afferent fibres responding specifically to noxious stimulation of the skin. J. Physiol. *190*, 541–562.

Burnstock, G. (2000). P2X receptors in sensory neurones. Br. J. Anaesth. *84*, 476–488.

Burnstock, G. (2001). Purine-mediated signalling in pain and visceral perception. Trends Pharmacol. Sci. *22*, 182–188.

Burnstock, G. (2009). Purines and sensory nerves. Handb. Exp. Pharmacol. 333–392.

Calixto, J.B., Kassuya, C.A.L., André, E., and Ferreira, J. (2005). Contribution of natural products to the discovery of the transient receptor potential (TRP) channels family and their functions. Pharmacol. Ther. *106*, 179–208.

Del Camino, D., Murphy, S., Heiry, M., Barrett, L.B., Earley, T.J., Cook, C.A., Petrus, M.J., Zhao, M., D'Amours, M., Deering, N., et al. (2010). TRPA1 contributes to cold hypersensitivity. J. Neurosci. Off. J. Soc. Neurosci. *30*, 15165–15174.

Carlton, S.M., and Hargett, G.L. (2007). Colocalization of metabotropic glutamate receptors in rat dorsal root ganglion cells. J. Comp. Neurol. *501*, 780–789.

Caterina, M.J., Schumacher, M.A., Tominaga, M., Rosen, T.A., Levine, J.D., and Julius, D. (1997). The capsaicin receptor: a heat-activated ion channel in the pain pathway. Nature *389*, 816–824.

Caterina, M.J., Rosen, T.A., Tominaga, M., Brake, A.J., and Julius, D. (1999). A capsaicin-receptor homologue with a high threshold for noxious heat. Nature *398*, 436–441.

Caterina, M.J., Leffler, A., Malmberg, A.B., Martin, W.J., Trafton, J., Petersen-Zeitz, K.R., Koltzenburg, M., Basbaum, A.I., and Julius, D. (2000). Impaired Nociception and Pain Sensation in Mice Lacking the Capsaicin Receptor. Science *288*, 306–313.

Cavanaugh, D.J., Lee, H., Lo, L., Shields, S.D., Zylka, M.J., Basbaum, A.I., and Anderson, D.J. (2009). Distinct subsets of unmyelinated primary sensory fibers mediate behavioral responses to noxious thermal and mechanical stimuli. Proc. Natl. Acad. Sci. U. S. A. *106*, 9075–9080.

Chao, M.V. (2003). Neurotrophins and their receptors: A convergence point for many signalling pathways. Nat. Rev. Neurosci. *4*, 299–309.

Chen, C.C., Akopian, A.N., Sivilotti, L., Colquhoun, D., Burnstock, G., and Wood, J.N. (1995). A P2X purinoceptor expressed by a subset of sensory neurons. Nature *377*, 428–431.

Chen, L.-J., Zhang, F.-G., Li, J., Song, H.-X., Zhou, L.-B., Yao, B.-C., Li, F., and Li, W.-C. (2010). Expression of calcitonin gene-related peptide in anterior and posterior horns of the spinal cord after brachial plexus injury. J. Clin. Neurosci. *17*, 87–91.

Cho, H., Yang, Y.D., Lee, J., Lee, B., Kim, T., Jang, Y., Back, S.K., Na, H.S., Harfe, B.D., Wang, F., et al. (2012). The calcium-activated chloride channel anoctamin 1 acts as a heat sensor in nociceptive neurons. Nat. Neurosci. *15*, 1015–1021.

Chuang, H., Prescott, E.D., Kong, H., Shields, S., Jordt, S.-E., Basbaum, A.I., Chao, M.V., and Julius, D. (2001). Bradykinin and nerve growth factor release the capsaicin receptor from PtdIns(4,5)P2-mediated inhibition. Nature *411*, 957–962.

Chuang, H., Neuhausser, W.M., and Julius, D. (2004). The Super-Cooling Agent Icilin Reveals a Mechanism of Coincidence Detection by a Temperature-Sensitive TRP Channel. Neuron *43*, 859–869.

Chubanov, V., and Gudermann, T. (2014). TRPM6. In Mammalian Transient Receptor Potential (TRP) Cation Channels, B. Nilius, and V. Flockerzi, eds. (Springer Berlin Heidelberg), pp. 503–520.

Chung, M.-K., Lee, H., Mizuno, A., Suzuki, M., and Caterina, M.J. (2004). TRPV3 and TRPV4 mediate warmth-evoked currents in primary mouse keratinocytes. J. Biol. Chem. *279*, 21569–21575.

Ciura, S., and Bourque, C.W. (2006). Transient Receptor Potential Vanilloid 1 Is Required for Intrinsic Osmoreception in Organum Vasculosum Lamina Terminalis Neurons and for Normal Thirst Responses to Systemic Hyperosmolality. J. Neurosci. *26*, 9069–9075.

Ciurtin, C., Majeed, Y., Naylor, J., Sukumar, P., English, A.A., Emery, P., and Beech, D.J. (2010). TRPM3 channel stimulated by pregnenolone sulphate in synovial fibroblasts and negatively coupled to hyaluronan. BMC Musculoskelet. Disord. *11*, 111.

Clapham, D.E. (2003). TRP channels as cellular sensors. Nature *426*, 517–524.

Cockayne, D.A., Dunn, P.M., Zhong, Y., Rong, W., Hamilton, S.G., Knight, G.E., Ruan, H.-Z., Ma, B., Yip, P., Nunn, P., et al. (2005). P2X2 knockout mice and P2X2/P2X3 double knockout mice reveal a role for the P2X2 receptor subunit in mediating multiple sensory effects of ATP. J. Physiol. *567*, 621–639.

Cohen, D.M. (2005). SRC family kinases in cell volume regulation. Am. J. Physiol. - Cell Physiol. *288*, C483–C493.

Colbert, H.A., Smith, T.L., and Bargmann, C.I. (1997). OSM-9, A Novel Protein with Structural Similarity to Channels, Is Required for Olfaction, Mechanosensation, and Olfactory Adaptation inCaenorhabditis elegans. J. Neurosci. *17*, 8259–8269.

Colburn, R.W., Lubin, M.L., Stone, D.J., Wang, Y., Lawrence, D., D'Andrea, M.R., Brandt, M.R., Liu, Y., Flores, C.M., and Qin, N. (2007). Attenuated Cold Sensitivity in TRPM8 Null Mice. Neuron *54*, 379–386.

Corey, D.P., García-Añoveros, J., Holt, J.R., Kwan, K.Y., Lin, S.-Y., Vollrath, M.A., Amalfitano, A., Cheung, E.L.-M., Derfler, B.H., Duggan, A., et al. (2004). TRPA1 is a candidate for the mechanosensitive transduction channel of vertebrate hair cells. Nature *432*, 723–730.

Cosens, D.J., and Manning, A. (1969). Abnormal electroretinogram from a Drosophila mutant. Nature *224*, 285–287.

Coste, B., Mathur, J., Schmidt, M., Earley, T.J., Ranade, S., Petrus, M.J., Dubin, A.E., and Patapoutian, A. (2010). Piezo1 and Piezo2 are essential components of distinct mechanically-activated cation channels. Science *330*, 55–60.

Coste, B., Xiao, B., Santos, J.S., Syeda, R., Grandl, J., Spencer, K.S., Kim, S.E., Schmidt, M., Mathur, J., Dubin, A.E., et al. (2012). Piezo proteins are pore-forming subunits of mechanically activated channels. Nature *483*, 176–181.

Cottrell, G.S., Roosterman, D., Marvizon, J.-C., Song, B., Wick, E., Pikios, S., Wong, H., Berthelier, C., Tang, Y., Sternini, C., et al. (2005). Localization of calcitonin receptor-like receptor and receptor activity modifying protein 1 in enteric neurons, dorsal root ganglia, and the spinal cord of the rat. J. Comp. Neurol. *490*, 239–255.

Dai, Y., Wang, S., Tominaga, M., Yamamoto, S., Fukuoka, T., Higashi, T., Kobayashi, K., Obata, K., Yamanaka, H., and Noguchi, K. (2007). Sensitization of TRPA1 by PAR2 contributes to the sensation of inflammatory pain. J. Clin. Invest. *117*, 1979–1987.

Damann, N., Voets, T., and Nilius, B. (2008). TRPs in Our Senses. Curr. Biol. *18*, R880–R889.

Davis, J.B., Gray, J., Gunthorpe, M.J., Hatcher, J.P., Davey, P.T., Overend, P., Harries, M.H., Latcham, J., Clapham, C., Atkinson, K., et al. (2000). Vanilloid receptor-1 is essential for inflammatory thermal hyperalgesia. Nature *405*, 183–187.

Dawes, J.M., Andersson, D.A., Bennett, D.L.H., Bevan, S., and McMahon, S.B. (2013). Inflammatory mediators and modulators of pain. In Wall & Melzack's Textbook of Pain, (Elsevier Health Sciences), pp. 48–67.

Den Dekker, E., Hoenderop, J.G.J., Nilius, B., and Bindels, R.J.M. (2003). The epithelial calcium channels, TRPV5 & TRPV6: from identification towards regulation. Cell Calcium *33*, 497–507.

Delmas, P., Hao, J., and Rodat-Despoix, L. (2011). Molecular mechanisms of mechanotransduction in mammalian sensory neurons. Nat. Rev. Neurosci. *12*, 139–153.

Dhaka, A., Murray, A.N., Mathur, J., Earley, T.J., Petrus, M.J., and Patapoutian, A. (2007). TRPM8 Is Required for Cold Sensation in Mice. Neuron *54*, 371–378.

Dhaka, A., Earley, T.J., Watson, J., and Patapoutian, A. (2008). Visualizing Cold Spots: TRPM8-Expressing Sensory Neurons and Their Projections. J. Neurosci. *28*, 566–575.

Doerner, J.F., Hatt, H., and Ramsey, I.S. (2011). Voltage- and temperature-dependent activation of TRPV3 channels is potentiated by receptor-mediated PI(4,5)P2 hydrolysis. J. Gen. Physiol. *137*, 271–288.

Dogrul, A., Gardell, L.R., Ossipov, M.H., Tulunay, F.C., Lai, J., and Porreca, F. (2003). Reversal of experimental neuropathic pain by T-type calcium channel blockers. Pain *105*, 159–168.

Dong, X., Han, S., Zylka, M.J., Simon, M.I., and Anderson, D.J. (2001). A diverse family of GPCRs expressed in specific subsets of nociceptive sensory neurons. Cell *106*, 619–632.

Drew, L.J., Rohrer, D.K., Price, M.P., Blaver, K.E., Cockayne, D.A., Cesare, P., and Wood, J.N. (2004). Acid-sensing ion channels ASIC2 and ASIC3 do not contribute to mechanically activated currents in mammalian sensory neurones. J. Physiol. *556*, 691–710.

Drews, A., Mohr, F., Rizun, O., Wagner, T.F.J., Dembla, S., Rudolph, S., Lambert, S., Konrad, M., Philipp, S.E., Behrendt, M., et al. (2014). Structural requirements of steroidal agonists of transient receptor potential melastatin 3 (TRPM3) cation channels. Br. J. Pharmacol. *171*, 1019–1032.

Dubin, A.E., and Patapoutian, A. (2010). Nociceptors: the sensors of the pain pathway. J. Clin. Invest. *120*, 3760–3772.

Duncan, L.M., Deeds, J., Hunter, J., Shao, J., Holmgren, L.M., Woolf, E.A., Tepper, R.I., and Shyjan, A.W. (1998). Down-Regulation of the Novel Gene Melastatin Correlates with Potential for Melanoma Metastasis. Cancer Res. *58*, 1515–1520.

Eberhardt, M., Hoffmann, T., Sauer, S.K., Messlinger, K., Reeh, P.W., and Fischer, M.J.M. (2008). Calcitonin gene-related peptide release from intact isolated dorsal root and trigeminal ganglia. Neuropeptides *42*, 311–317.

Eberhardt, M., Dux, M., Namer, B., Miljkovic, J., Cordasic, N., Will, C., Kichko, T.I., de la Roche, J., Fischer, M., Suárez, S.A., et al. (2014). H2S and NO cooperatively regulate vascular tone by activating a neuroendocrine HNO–TRPA1–CGRP signalling pathway. Nat. Commun. *5*.

Eberhardt, M.J., Filipovic, M.R., Leffler, A., de la Roche, J., Kistner, K., Fischer, M.J., Fleming, T., Zimmermann, K., Ivanovic-Burmazovic, I., Nawroth, P.P., et al. (2012). Methylglyoxal

activates nociceptors through transient receptor potential channel A1 (TRPA1): a possible mechanism of metabolic neuropathies. J. Biol. Chem. *287*, 28291–28306.

Eijkelkamp, N., Quick, K., and Wood, J.N. (2013). Transient Receptor Potential Channels and Mechanosensation. Annu. Rev. Neurosci. *36*, 519–546.

Eilers, H., Lee, S.-Y., Hau, C.W., Logvinova, A., and Schumacher, M.A. (2007). The rat vanilloid receptor splice variant VR.5'sv blocks TRPV1 activation. Neuroreport *18*, 969–973.

Emery, E.C., Young, G.T., Berrocoso, E.M., Chen, L., and McNaughton, P.A. (2011). HCN2 ion channels play a central role in inflammatory and neuropathic pain. Science *333*, 1462–1466.

Endres-Becker, J., Heppenstall, P.A., Mousa, S.A., Labuz, D., Oksche, A., Schäfer, M., Stein, C., and Zöllner, C. (2007). μ-Opioid Receptor Activation Modulates Transient Receptor Potential Vanilloid 1 (TRPV1) Currents in Sensory Neurons in A Model of Inflammatory Pain. Mol. Pharmacol. *71*, 12–18.

Erpelding, N., Moayedi, M., and Davis, K.D. (2012). Cortical thickness correlates of pain and temperature sensitivity. PAIN *153*, 1602–1609.

Evans, D.H. (2008). Osmotic and Ionic Regulation: Cells and Animals (CRC Press).

Fajardo, O., Meseguer, V., Belmonte, C., and Viana, F. (2008a). TRPA1 Channels Mediate Cold Temperature Sensing in Mammalian Vagal Sensory Neurons: Pharmacological and Genetic Evidence. J. Neurosci. *28*, 7863–7875.

Fajardo, O., Meseguer, V., Belmonte, C., and Viana, F. (2008b). TRPA1 channels: novel targets of 1,4-dihydropyridines. Channels Austin Tex *2*, 429–438.

Faouzi, M., and Penner, R. (2014). TRPM2. In Mammalian Transient Receptor Potential (TRP) Cation Channels, B. Nilius, and V. Flockerzi, eds. (Springer Berlin Heidelberg), pp. 403–426.

Fischer, M., Carli, G., Raboisson, P., and Reeh, P. (2014). The interphase of the formalin test. Pain *155*, 511–521.

Fleig, A., and Chubanov, V. (2014). TRPM7. In Mammalian Transient Receptor Potential (TRP) Cation Channels, B. Nilius, and V. Flockerzi, eds. (Springer Berlin Heidelberg), pp. 521–546.

Fonfria, E., Murdock, P.R., Cusdin, F.S., Benham, C.D., Kelsell, R.E., and McNulty, S. (2006). Tissue distribution profiles of the human TRPM cation channel family. J. Recept. Signal Transduct. Res. *26*, 159–178.

Fox, A.J., Barnes, P.J., and Dray, A. (1995). Stimulation of guinea-pig tracheal afferent fibres by non-isosmotic and low-chloride stimuli and the effect of frusemide. J. Physiol. *482*, 179–187.

Freichel, M., Tsvilovskyy, V., and Camacho-Londoño, J.E. (2014). TRPC4- and TRPC4-Containing Channels. In Mammalian Transient Receptor Potential (TRP) Cation Channels, B. Nilius, and V. Flockerzi, eds. (Springer Berlin Heidelberg), pp. 85–128.

García-Añoveros, J., and Wiwatpanit, T. (2014). TRPML2 and Mucolipin Evolution. In Mammalian Transient Receptor Potential (TRP) Cation Channels, B. Nilius, and V. Flockerzi, eds. (Springer Berlin Heidelberg), pp. 647–658.

Garrison, S.R., Dietrich, A., and Stucky, C.L. (2012). TRPC1 contributes to light-touch sensation and mechanical responses in low-threshold cutaneous sensory neurons. J. Neurophysiol. *107*, 913–922.

Genzen, J.R., Cleve, W.V., and McGehee, D.S. (2001). Dorsal Root Ganglion Neurons Express Multiple Nicotinic Acetylcholine Receptor Subtypes. J. Neurophysiol. *86*, 1773–1782.

Gilman, A.G. (1987). G proteins: transducers of receptor-generated signals. Annu. Rev. Biochem. *56*, 615–649.

Gomis, A., Soriano, S., Belmonte, C., and Viana, F. (2008). Hypoosmotic- and pressure-induced membrane stretch activate TRPC5 channels. J. Physiol. *586*, 5633–5649.

Greco, M.C., Lisi, L., Currò, D., Navarra, P., and Tringali, G. (2014). Tapentadol inhibits calcitonin gene-related peptide release from rat brainstem in vitro. Peptides *56*, 8–13.

Grimm, C., Kraft, R., Sauerbruch, S., Schultz, G., and Harteneck, C. (2003). Molecular and Functional Characterization of the Melastatin-related Cation Channel TRPM3. J. Biol. Chem. *278*, 21493–21501.

Grimm, C., Kraft, R., Schultz, G., and Harteneck, C. (2005). Activation of the melastatin-related cation channel TRPM3 by D-erythro-sphingosine [corrected]. Mol. Pharmacol. *67*, 798–805.

Grimm, C., Barthmes, M., and Wahl-Schott, C. (2014). TRPML3. In Mammalian Transient Receptor Potential (TRP) Cation Channels, B. Nilius, and V. Flockerzi, eds. (Springer Berlin Heidelberg), pp. 659–674.

Guinamard, R., Sallé, L., and Simard, C. (2011). The non-selective monovalent cationic channels TRPM4 and TRPM5. Adv. Exp. Med. Biol. *704*, 147–171.

Güler, A.D., Lee, H., Iida, T., Shimizu, I., Tominaga, M., and Caterina, M. (2002). Heat-Evoked Activation of the Ion Channel, TRPV4. J. Neurosci. *22*, 6408–6414.

Hanke, J.H., Gardner, J.P., Dow, R.L., Changelian, P.S., Brissette, W.H., Weringer, E.J., Pollok, B.A., and Connelly, P.A. (1996). Discovery of a Novel, Potent, and Src Family-selective Tyrosine Kinase Inhibitor STUDY OF Lck- AND FynT-DEPENDENT T CELL ACTIVATION. J. Biol. Chem. *271*, 695–701.

Havlíková, H., Hill, M., Hampl, R., and Stárka, L. (2002). Sex- and age-related changes in epitestosterone in relation to pregnenolone sulfate and testosterone in normal subjects. J. Clin. Endocrinol. Metab. *87*, 2225–2231.

Hellmich, U.A., and Gaudet, R. (2014). Structural Biology of TRP Channels. In Mammalian Transient Receptor Potential (TRP) Cation Channels, B. Nilius, and V. Flockerzi, eds. (Springer International Publishing), pp. 963–990.

Hirata, H., and Meng, I.D. (2010). Cold-Sensitive Corneal Afferents Respond to a Variety of Ocular Stimuli Central to Tear Production: Implications for Dry Eye Disease. Invest. Ophthalmol. Vis. Sci. *51*, 3969–3976.

Hirata, H., and Oshinsky, M.L. (2012). Ocular dryness excites two classes of corneal afferent neurons implicated in basal tearing in rats: involvement of transient receptor potential channels. J. Neurophysiol. *107*, 1199–1209.

Hoffmann, A., Grimm, C., Kraft, R., Goldbaum, O., Wrede, A., Nolte, C., Hanisch, U.-K., Richter-Landsberg, C., Brück, W., Kettenmann, H., et al. (2010). TRPM3 is expressed in sphingosine-responsive myelinating oligodendrocytes. J. Neurochem. *114*, 654–665.

Huang, S.M., Li, X., Yu, Y., Wang, J., and Caterina, M.J. (2011). TRPV3 and TRPV4 ion channels are not major contributors to mouse heat sensation. Mol. Pain *7*, 37.

Hucho, T.B., Dina, O.A., and Levine, J.D. (2005). Epac Mediates a cAMP-to-PKC Signaling in Inflammatory Pain: An Isolectin B4(+) Neuron-Specific Mechanism. J. Neurosci. *25*, 6119–6126.

Irie, S., and Furukawa, T. (2014). TRPM1. In Mammalian Transient Receptor Potential (TRP) Cation Channels, B. Nilius, and V. Flockerzi, eds. (Springer Berlin Heidelberg), pp. 387–402.

Jahr, C.E., and Jessell, T.M. (1985). Synaptic transmission between dorsal root ganglion and dorsal horn neurons in culture: antagonism of monosynaptic excitatory postsynaptic potentials and glutamate excitation by kynurenate. J. Neurosci. Off. J. Soc. Neurosci. *5*, 2281–2289.

Jang, Y., Lee, Y., Kim, S.M., Yang, Y.D., Jung, J., and Oh, U. (2012). Quantitative analysis of TRP channel genes in mouse organs. Arch. Pharm. Res. *35*, 1823–1830.

Jeffry, J.A., Yu, S.-Q., Sikand, P., Parihar, A., Evans, M.S., and Premkumar, L.S. (2009). Selective targeting of TRPV1 expressing sensory nerve terminals in the spinal cord for long lasting analgesia. PloS One *4*, e7021.

Ji, R.-R., Xu, Z.-Z., and Gao, Y.-J. (2014). Emerging targets in neuroinflammation-driven chronic pain. Nat. Rev. Drug Discov. *13*, 533–548.

Jordt, S.-E., Bautista, D.M., Chuang, H., McKemy, D.D., Zygmunt, P.M., Högestätt, E.D., Meng, I.D., and Julius, D. (2004). Mustard oils and cannabinoids excite sensory nerve fibres through the TRP channel ANKTM1. Nature *427*, 260–265.

Julius, D., and Basbaum, A.I. (2001). Molecular mechanisms of nociception. Nature *413*, 203–210.

Junger, W.G., Hoyt, D.B., Hamreus, M., Liu, F.C., Herdon-Remelius, C., Junger, W., and Altman, A. (1997). Hypertonic saline activates protein tyrosine kinases and mitogen-activated protein kinase p38 in T-cells. J. Trauma *42*, 437–443; discussion 443–445.

Karashima, Y., Talavera, K., Everaerts, W., Janssens, A., Kwan, K.Y., Vennekens, R., Nilius, B., and Voets, T. (2009). TRPA1 acts as a cold sensor in vitro and in vivo. Proc. Natl. Acad. Sci. U. S. A. *106*, 1273–1278.

Kawamura, M., Kuraishi, Y., Minami, M., and Satoh, M. (1989). Antinociceptive effect of intrathecally administered antiserum against calcitonin gene-related peptide on thermal and mechanical noxious stimuli in experimental hyperalgesic rats. Brain Res. *497*, 199–203.

Kawasaki, H., Springett, G.M., Mochizuki, N., Toki, S., Nakaya, M., Matsuda, M., Housman, D.E., and Graybiel, A.M. (1998). A Family of cAMP-Binding Proteins That Directly Activate Rap1. Science *282*, 2275–2279.

Kessler, F., Habelt, C., Averbeck, B., Reeh, P.W., and Kress, M. (1999). Heat-induced release of CGRP from isolated rat skin and effects of bradykinin and the protein kinase C activator PMA. Pain *83*, 289–295.

Khasabova, I.A., Simone, D.A., and Seybold, V.S. (2002). Cannabinoids attenuate depolarization-dependent Ca2+ influx in intermediate-size primary afferent neurons of adult rats. Neuroscience *115*, 613–625.

Khasabova, I.A., Harding-Rose, C., Simone, D.A., and Seybold, V.S. (2004). Differential effects of CB1 and opioid agonists on two populations of adult rat dorsal root ganglion neurons. J. Neurosci. Off. J. Soc. Neurosci. *24*, 1744–1753.

Kilo, S., Harding-Rose, C., Hargreaves, K.M., and Flores, C.M. (1997). Peripheral CGRP release as a marker for neurogenic inflammation: a model system for the study of neuropeptide secretion in rat paw skin. Pain *73*, 201–207.

Kim, Y.S., Son, J.Y., Kim, T.H., Paik, S.K., Dai, Y., Noguchi, K., Ahn, D.K., and Bae, Y.C. (2010). Expression of transient receptor potential ankyrin 1 (TRPA1) in the rat trigeminal sensory afferents and spinal dorsal horn. J. Comp. Neurol. *518*, 687–698.

Kinsman, B., Cowles, J., Lay, J., Simmonds, S.S., Browning, K.N., and Stocker, S.D. (2014). Osmoregulatory thirst in mice lacking the transient receptor potential vanilloid type 1 (TRPV1) and/or type 4 (TRPV4) receptor. Am. J. Physiol. - Regul. Integr. Comp. Physiol. ajpregu.00102.2014.

Klak, J., Hill, M., Parízek, A., Havlíková, H., Bicíková, M., Hampl, R., Fait, T., Sulcová, J., Pouzar, V., Kancheva, R., et al. (2003). Pregnanolone isomers, pregnenolone and their polar conjugates around parturition. Physiol. Res. Acad. Sci. Bohemoslov. *52*, 211–221.

Klein, R.M., Ufret-Vincenty, C.A., Hua, L., and Gordon, S.E. (2008). Determinants of molecular specificity in phosphoinositide regulation. Phosphatidylinositol (4,5)-bisphosphate (PI(4,5)P2) is the endogenous lipid regulating TRPV1. J. Biol. Chem. *283*, 26208–26216.

Klein, R.R., Bourdon, D.M., Costales, C.L., Wagner, C.D., White, W.L., Williams, J.D., Hicks, S.N., Sondek, J., and Thakker, D.R. (2011). Direct Activation of Human Phospholipase C by Its Well Known Inhibitor U73122. J. Biol. Chem. *286*, 12407–12416.

Klose, C., Straub, I., Riehle, M., Ranta, F., Krautwurst, D., Ullrich, S., Meyerhof, W., and Harteneck, C. (2011). Fenamates as TRP channel blockers: mefenamic acid selectively blocks TRPM3. Br. J. Pharmacol. *162*, 1757–1769.

Knowlton, W.M., Palkar, R., Lippoldt, E.K., McCoy, D.D., Baluch, F., Chen, J., and McKemy, D.D. (2013). A sensory labeled-line for cold: TRPM8-expressing sensory neurons define the cellular basis for cold, cold pain, and cooling-mediated analgesia. J. Neurosci. Off. J. Soc. Neurosci. *33*, 2837–2848.

Kobayashi, K., Fukuoka, T., Obata, K., Yamanaka, H., Dai, Y., Tokunaga, A., and Noguchi, K. (2005). Distinct expression of TRPM8, TRPA1, and TRPV1 mRNAs in rat primary afferent neurons with aδ/c-fibers and colocalization with trk receptors. J. Comp. Neurol. *493*, 596–606.

Kraft, R., Grimm, C., Frenzel, H., and Harteneck, C. (2006). Inhibition of TRPM2 cation channels by N-(p-amylcinnamoyl)anthranilic acid. Br. J. Pharmacol. *148*, 264–273.

Kress, M., Izydorczyk, I., and Kuhn, A. (2001). N- and L- but not P/Q-type calcium channels contribute to neuropeptide release from rat skin in vitro. Neuroreport *12*, 867–870.

Kruger, L. (1996). Pain and Touch (Academic Press).

Kunert-Keil, C., Bisping, F., Krüger, J., and Brinkmeier, H. (2006). Tissue-specific expression of TRP channel genes in the mouse and its variation in three different mouse strains. BMC Genomics *7*, 159.

Kunkler, P.E., Ballard, C.J., Oxford, G.S., and Hurley, J.H. (2011). TRPA1 receptors mediate environmental irritant-induced meningeal vasodilatation. Pain *152*, 38–44.

Kwan, K.Y., Allchorne, A.J., Vollrath, M.A., Christensen, A.P., Zhang, D.-S., Woolf, C.J., and Corey, D.P. (2006). TRPA1 Contributes to Cold, Mechanical, and Chemical Nociception but Is Not Essential for Hair-Cell Transduction. Neuron *50*, 277–289.

Kwan, K.Y., Glazer, J.M., Corey, D.P., Rice, F.L., and Stucky, C.L. (2009). TRPA1 modulates mechanotransduction in cutaneous sensory neurons. J. Neurosci. Off. J. Soc. Neurosci. *29*, 4808–4819.

Lambert, S., Drews, A., Rizun, O., Wagner, T.F.J., Lis, A., Mannebach, S., Plant, S., Portz, M., Meissner, M., Philipp, S.E., et al. (2011). Transient Receptor Potential Melastatin 1 (TRPM1) Is an Ion-conducting Plasma Membrane Channel Inhibited by Zinc Ions. J. Biol. Chem. *286*, 12221–12233.

Latham, J.R., Pathirathna, S., Jagodic, M.M., Choe, W.J., Levin, M.E., Nelson, M.T., Lee, W.Y., Krishnan, K., Covey, D.F., Todorovic, S.M., et al. (2009). Selective T-type calcium channel blockade alleviates hyperalgesia in ob/ob mice. Diabetes *58*, 2656–2665.

Lawson, J.J., McIlwrath, S.L., Woodbury, C.J., Davis, B.M., and Koerber, H.R. (2008). TRPV1 Unlike TRPV2 Is Restricted to a Subset of Mechanically Insensitive Cutaneous Nociceptors Responding to Heat. J. Pain *9*, 298–308.

Lechner, S.G., Markworth, S., Poole, K., Smith, E.S.J., Lapatsina, L., Frahm, S., May, M., Pischke, S., Suzuki, M., Ibañez-Tallon, I., et al. (2011). The Molecular and Cellular Identity of Peripheral Osmoreceptors. Neuron *69*, 332–344.

Lee, J., Cha, S.-K., Sun, T.-J., and Huang, C.-L. (2005). PIP2 Activates TRPV5 and Releases Its Inhibition by Intracellular Mg2+. J. Gen. Physiol. *126*, 439–451.

Lee, J., Moon, S., Cha, Y., and Chung, Y.D. (2010a). Drosophila TRPN(=NOMPC) channel localizes to the distal end of mechanosensory cilia. PloS One *5*, e11012.

Lee, M.J., Shin, T.J., Lee, J.E., Choo, H., Koh, H.Y., Chung, H.J., Pae, A.N., Lee, S.C., and Kim, H.J. (2010b). KST5468, a new T-type calcium channel antagonist, has an antinociceptive effect on inflammatory and neuropathic pain models. Pharmacol. Biochem. Behav. *97*, 198–204.

Lee, N., Chen, J., Sun, L., Wu, S., Gray, K.R., Rich, A., Huang, M., Lin, J.-H., Feder, J.N., Janovitz, E.B., et al. (2003). Expression and Characterization of Human Transient Receptor Potential Melastatin 3 (hTRPM3). J. Biol. Chem. *278*, 20890–20897.

Lewin, G.R., and Moshourab, R. (2004). Mechanosensation and pain. J. Neurobiol. *61*, 30–44.

Li, X., and Eisenach, J.C. (2001). alpha2A-adrenoceptor stimulation reduces capsaicin-induced glutamate release from spinal cord synaptosomes. J. Pharmacol. Exp. Ther. *299*, 939–944.

Li, X., and Eisenach, J.C. (2005). Adenosine reduces glutamate release in rat spinal synaptosomes. Anesthesiology *103*, 1060–1065.

Li, W., Feng, Z., Sternberg, P.W., and Xu, X.Z.S. (2006). A C. elegans stretch receptor neuron revealed by a mechanosensitive TRP channel homologue. Nature *440*, 684–687.

Liedtke, W., and Friedman, J.M. (2003). Abnormal osmotic regulation in trpv4-/- mice. Proc. Natl. Acad. Sci. *100*, 13698–13703.

Liedtke, W., Choe, Y., Martí-Renom, M.A., Bell, A.M., Denis, C.S., AndrejŠali, Hudspeth, A.J., Friedman, J.M., and Heller, S. (2000). Vanilloid Receptor–Related Osmotically Activated Channel (VR-OAC), a Candidate Vertebrate Osmoreceptor. Cell *103*, 525–535.

Liedtke, W., Tobin, D.M., Bargmann, C.I., and Friedman, J.M. (2003). Mammalian TRPV4 (VR-OAC) directs behavioral responses to osmotic and mechanical stimuli in Caenorhabditis elegans. Proc. Natl. Acad. Sci. *100*, 14531–14536.

Liman, E.R. (2014). TRPM5. In Mammalian Transient Receptor Potential (TRP) Cation Channels, B. Nilius, and V. Flockerzi, eds. (Springer Berlin Heidelberg), pp. 489–502.

Liu, B., and Qin, F. (2005). Functional control of cold- and menthol-sensitive TRPM8 ion channels by phosphatidylinositol 4,5-bisphosphate. J. Neurosci. Off. J. Soc. Neurosci. *25*, 1674–1681.

Liu, D., and Liman, E.R. (2003). Intracellular Ca2+ and the phospholipid PIP2 regulate the taste transduction ion channel TRPM5. Proc. Natl. Acad. Sci. U. S. A. *100*, 15160–15165.

Liu, L., Li, Y., Wang, R., Yin, C., Dong, Q., Hing, H., Kim, C., and Welsh, M.J. (2007). Drosophila hygrosensation requires the TRP channels water witch and nanchung. Nature *450*, 294–298.

Liu, Q., Tang, Z., Surdenikova, L., Kim, S., Patel, K.N., Kim, A., Ru, F., Guan, Y., Weng, H.-J., Geng, Y., et al. (2009). Sensory neuron-specific GPCRs Mrgprs are itch receptors mediating chloroquine-induced pruritus. Cell *139*, 1353–1365.

Liu, Q., Weng, H.-J., Patel, K.N., Tang, Z., Bai, H., Steinhoff, M., and Dong, X. (2011). The Distinct Roles of Two GPCRs, MrgprC11 and PAR2, in Itch and Hyperalgesia. Sci. Signal. *4*, ra45.

Livak, K.J., and Schmittgen, T.D. (2001). Analysis of relative gene expression data using real-time quantitative PCR and the 2(-Delta Delta C(T)) Method. Methods San Diego Calif *25*, 402–408.

Lou, Y.P., Franco-Cereceda, A., and Lundberg, J.M. (1992). Different ion channel mechanisms between low concentrations of capsaicin and high concentrations of capsaicin and nicotine regarding peptide release from pulmonary afferents. Acta Physiol. Scand. *146*, 119–127.

Lukacs, V., Thyagarajan, B., Varnai, P., Balla, A., Balla, T., and Rohacs, T. (2007). Dual Regulation of TRPV1 by Phosphoinositides. J. Neurosci. *27*, 7070–7080.

Majeed, Y., Agarwal, A., Naylor, J., Seymour, V., Jiang, S., Muraki, K., Fishwick, C., and Beech, D. (2010). Cis-isomerism and other chemical requirements of steroidal agonists and partial agonists acting at TRPM3 channels. Br. J. Pharmacol. *161*, 430–441.

Majeed, Y., Bahnasi, Y., Seymour, V.A.L., Wilson, L.A., Milligan, C.J., Agarwal, A.K., Sukumar, P., Naylor, J., and Beech, D.J. (2011). Rapid and Contrasting Effects of Rosiglitazone on Transient Receptor Potential TRPM3 and TRPC5 Channels. Mol. Pharmacol. *79*, 1023–1030.

Majeed, Y., Tumova, S., Green, B.L., Seymour, V.A.L., Woods, D.M., Agarwal, A.K., Naylor, J., Jiang, S., Picton, H.M., Porter, K.E., et al. (2012). Pregnenolone sulphate-independent inhibition of TRPM3 channels by progesterone. Cell Calcium *51*, 1–11.

Mantyh, P.W. (2006). Cancer pain and its impact on diagnosis, survival and quality of life. Nat. Rev. Neurosci. *7*, 797–809.

Maroto, R., Raso, A., Wood, T.G., Kurosky, A., Martinac, B., and Hamill, O.P. (2005). TRPC1 forms the stretch-activated cation channel in vertebrate cells. Nat. Cell Biol. *7*, 179–185.

Martin, R.L., Lee, J.H., Cribbs, L.L., Perez-Reyes, E., and Hanck, D.A. (2000). Mibefradil block of cloned T-type calcium channels. J. Pharmacol. Exp. Ther. *295*, 302–308.

Mathar, I., Jacobs, G., Kecskes, M., Menigoz, A., Philippaert, K., and Vennekens, R. (2014). TRPM4. In Mammalian Transient Receptor Potential (TRP) Cation Channels, B. Nilius, and V. Flockerzi, eds. (Springer Berlin Heidelberg), pp. 461–487.

McCoy, E.S., Taylor-Blake, B., and Zylka, M.J. (2012). CGRPα-expressing sensory neurons respond to stimuli that evoke sensations of pain and itch. PloS One *7*, e36355.

McCoy, E.S., Taylor-Blake, B., Street, S.E., Pribisko, A.L., Zheng, J., and Zylka, M.J. (2013). Peptidergic CGRPα primary sensory neurons encode heat and itch and tonically suppress sensitivity to cold. Neuron *78*, 138–151.

McDougall, J.J. (2011). Peripheral analgesia: Hitting pain where it hurts. Biochim. Biophys. Acta BBA - Mol. Basis Dis. *1812*, 459–467.

McKemy, D.D. (2005). How cold is it? TRPM8 and TRPA1 in the molecular logic of cold sensation. Mol. Pain *1*, 16.

McKemy, D.D. (2013). The Molecular and Cellular Basis of Cold Sensation. ACS Chem. Neurosci. *4*, 238–247.

McKemy, D.D., Neuhausser, W.M., and Julius, D. (2002). Identification of a cold receptor reveals a general role for TRP channels in thermosensation. Nature *416*, 52–58.

McNamara, C.R., Mandel-Brehm, J., Bautista, D.M., Siemens, J., Deranian, K.L., Zhao, M., Hayward, N.J., Chong, J.A., Julius, D., Moran, M.M., et al. (2007). TRPA1 mediates formalin-induced pain. Proc. Natl. Acad. Sci. *104*, 13525–13530.

McNamara, F.N., Randall, A., and Gunthorpe, M.J. (2005). Effects of piperine, the pungent component of black pepper, at the human vanilloid receptor (TRPV1). Br. J. Pharmacol. *144*, 781–790.

McNeil, B., and Dong, X. (2014). Mrgprs as Itch Receptors. In Itch: Mechanisms and Treatment, E. Carstens, and T. Akiyama, eds. (Boca Raton (FL): CRC Press),.

Mederos y Schnitzler, M., Storch, U., Meibers, S., Nurwakagari, P., Breit, A., Essin, K., Gollasch, M., and Gudermann, T. (2008). Gq-coupled receptors as mechanosensors mediating myogenic vasoconstriction. EMBO J. *27*, 3092–3103.

Mennerick, S., Lamberta, M., Shu, H.-J., Hogins, J., Wang, C., Covey, D.F., Eisenman, L.N., and Zorumski, C.F. (2008). Effects on Membrane Capacitance of Steroids with Antagonist Properties at GABAA Receptors. Biophys. J. *95*, 176–185.

Mizuno, A., Matsumoto, N., Imai, M., and Suzuki, M. (2003). Impaired osmotic sensation in mice lacking TRPV4. Am. J. Physiol. - Cell Physiol. *285*, C96–C101.

Mogg, A., Mill, C., Folly, E., Beattie, R., Blanco, M., Beck, J., and Broad, L. (2013). Altered pharmacology of native rodent spinal cord TRPV1 after phosphorylation. Br. J. Pharmacol. *168*, 1015–1029.

Molliver, D.C., Wright, D.E., Leitner, M.L., Parsadanian, A.S., Doster, K., Wen, D., Yan, Q., and Snider, W.D. (1997). IB4-Binding DRG Neurons Switch from NGF to GDNF Dependence in Early Postnatal Life. Neuron *19*, 849–861.

Montell, C., and Rubin, G.M. (1989). Molecular characterization of the Drosophila trp locus: a putative integral membrane protein required for phototransduction. Neuron *2*, 1313–1323.

Moqrich, A., Hwang, S.W., Earley, T.J., Petrus, M.J., Murray, A.N., Spencer, K.S.R., Andahazy, M., Story, G.M., and Patapoutian, A. (2005). Impaired Thermosensation in Mice Lacking TRPV3, a Heat and Camphor Sensor in the Skin. Science *307*, 1468–1472.

Morgan, K., Sadofsky, L.R., Crow, C., and Morice, A.H. (2014). Human TRPM8 and TRPA1 pain channels, including a gene variant with increased sensitivity to agonists (TRPA1 R797T), exhibit differential regulation by SRC-tyrosine kinase inhibitor. Biosci. Rep. *34*, 469–478.

Mosso, J.A., and Kruger, L. (1973). Receptor categories represented in spinal trigeminal nucleus caudalis. J. Neurophysiol. *36*, 472–488.

Muraki, K., Iwata, Y., Katanosaka, Y., Ito, T., Ohya, S., Shigekawa, M., and Imaizumi, Y. (2003). TRPV2 Is a Component of Osmotically Sensitive Cation Channels in Murine Aortic Myocytes. Circ. Res. *93*, 829–838.

Naeini, R.S., Witty, M.-F., Séguéla, P., and Bourque, C.W. (2006). An N-terminal variant of Trpv1 channel is required for osmosensory transduction. Nat. Neurosci. *9*, 93–98.

Nakamura, Y., Une, Y., Miyano, K., Abe, H., Hisaoka, K., Morioka, N., and Nakata, Y. (2012). Activation of transient receptor potential ankyrin 1 evokes nociception through substance P release from primary sensory neurons. J. Neurochem. *120*, 1036–1047.

Nandigama, R., Bonitz, M., Papadakis, T., Schwantes, U., Bschleipfer, T., and Kummer, W. (2010). Muscarinic acetylcholine receptor subtypes expressed by mouse bladder afferent neurons. Neuroscience *168*, 842–850.

Naylor, J., Li, J., Milligan, C.J., Zeng, F., Sukumar, P., Hou, B., Sedo, A., Yuldasheva, N., Majeed, Y., Beri, D., et al. (2010). Pregnenolone Sulphate- and Cholesterol-Regulated TRPM3 Channels Coupled to Vascular Smooth Muscle Secretion and Contraction. Circ. Res. *106*, 1507–1515.

Nealen, M.L., Gold, M.S., Thut, P.D., and Caterina, M.J. (2003). TRPM8 mRNA Is Expressed in a Subset of Cold-Responsive Trigeminal Neurons From Rat. J. Neurophysiol. *90*, 515–520.

Nilius, B., and Owsianik, G. (2011). The transient receptor potential family of ion channels. Genome Biol. *12*, 218.

Nilius, B., Mahieu, F., Prenen, J., Janssens, A., Owsianik, G., Vennekens, R., and Voets, T. (2006). The Ca2+-activated cation channel TRPM4 is regulated by phosphatidylinositol 4,5-biphosphate. EMBO J. *25*, 467–478.

Nishihara, E., Hiyama, T.Y., and Noda, M. (2011). Osmosensitivity of Transient Receptor Potential Vanilloid 1 Is Synergistically Enhanced by Distinct Activating Stimuli Such as Temperature and Protons. PLoS ONE *6*, e22246.

Noël, J., Zimmermann, K., Busserolles, J., Deval, E., Alloui, A., Diochot, S., Guy, N., Borsotto, M., Reeh, P., Eschalier, A., et al. (2009). The mechano-activated K+ channels TRAAK and TREK-1 control both warm and cold perception. EMBO J. *28*, 1308–1318.

Norrsell, U., Finger, S., and Lajonchere, C. (1999). Cutaneous sensory spots and the “law of specific nerve energies”: history and development of ideas. Brain Res. Bull. *48*, 457–465.

North, A.R. (1996). P2X purinoceptor plethora. Semin. Neurosci. *8*, 187–194.

Oberwinkler, J., and Philipp, S.E. (2014). Trpm3. Handb. Exp. Pharmacol. *222*, 427–459.

Oberwinkler, J., Lis, A., Giehl, K.M., Flockerzi, V., and Philipp, S.E. (2005). Alternative Splicing Switches the Divalent Cation Selectivity of TRPM3 Channels. J. Biol. Chem. *280*, 22540–22548.

Olausson, H., Cole, J., Rylander, K., McGlone, F., Lamarre, Y., Wallin, B.G., Krämer, H., Wessberg, J., Elam, M., Bushnell, M.C., et al. (2008). Functional role of unmyelinated tactile afferents in human hairy skin: sympathetic response and perceptual localization. Exp. Brain Res. *184*, 135–140.

Page, A.J., Brierley, S.M., Martin, C.M., Martinez-Salgado, C., Wemmie, J.A., Brennan, T.J., Symonds, E., Omari, T., Lewin, G.R., Welsh, M.J., et al. (2004). The ion channel ASIC1 contributes to visceral but not cutaneous mechanoreceptor function. Gastroenterology *127*, 1739–1747.

Page, A.J., Brierley, S.M., Martin, C.M., Price, M.P., Symonds, E., Butler, R., Wemmie, J.A., and Blackshaw, L.A. (2005). Different contributions of ASIC channels 1a, 2, and 3 in gastrointestinal mechanosensory function. Gut *54*, 1408–1415.

Park, U., Vastani, N., Guan, Y., Raja, S.N., Koltzenburg, M., and Caterina, M.J. (2011). TRP vanilloid 2 knock-out mice are susceptible to perinatal lethality but display normal thermal and mechanical nociception. J. Neurosci. Off. J. Soc. Neurosci. *31*, 11425–11436.

Parra, A., Madrid, R., Echevarria, D., del Olmo, S., Morenilla-Palao, C., Acosta, M.C., Gallar, J., Dhaka, A., Viana, F., and Belmonte, C. (2010). Ocular surface wetness is regulated by TRPM8-dependent cold thermoreceptors of the cornea. Nat. Med. *16*, 1396–1399.

Pathirathna, S., Todorovic, S.M., Covey, D.F., and Jevtovic-Todorovic, V. (2005). 5α-reduced neuroactive steroids alleviate thermal and mechanical hyperalgesia in rats with neuropathic pain. Pain *117*, 326–339.

Pedersen, K.E., Meeker, S.N., Riccio, M.M., and Undem, B.J. (1998). Selective stimulation of jugular ganglion afferent neurons in guinea pig airways by hypertonic saline. J. Appl. Physiol. *84*, 499–506.

Pedersen, S.F., Owsianik, G., and Nilius, B. (2005). TRP channels: an overview. Cell Calcium *38*, 233–252.

Peier, A.M., Reeve, A.J., Andersson, D.A., Moqrich, A., Earley, T.J., Hergarden, A.C., Story, G.M., Colley, S., Hogenesch, J.B., McIntyre, P., et al. (2002a). A heat-sensitive TRP channel expressed in keratinocytes. Science *296*, 2046–2049.

Peier, A.M., Moqrich, A., Hergarden, A.C., Reeve, A.J., Andersson, D.A., Story, G.M., Earley, T.J., Dragoni, I., McIntyre, P., Bevan, S., et al. (2002b). A TRP Channel that Senses Cold Stimuli and Menthol. Cell *108*, 705–715.

De Peretti, E., and Mappus, E. (1983). Pattern of plasma pregnenolone sulfate levels in humans from birth to adulthood. J. Clin. Endocrinol. Metab. *57*, 550–556.

Perl, E.R. (1968). Myelinated afferent fibres innervating the primate skin and their response to noxious stimuli. J. Physiol. *197*, 593–615.

Perraud, A.L., Fleig, A., Dunn, C.A., Bagley, L.A., Launay, P., Schmitz, C., Stokes, A.J., Zhu, Q., Bessman, M.J., Penner, R., et al. (2001). ADP-ribose gating of the calcium-permeable LTRPC2 channel revealed by Nudix motif homology. Nature *411*, 595–599.

Petersen, C.C., Berridge, M.J., Borgese, M.F., and Bennett, D.L. (1995). Putative capacitative calcium entry channels: expression of Drosophila trp and evidence for the existence of vertebrate homologues. Biochem. J. *311 (Pt 1)*, 41–44.

De Petrocellis, L., Vellani, V., Schiano-Moriello, A., Marini, P., Magherini, P.C., Orlando, P., and Di Marzo, V. (2008). Plant-derived cannabinoids modulate the activity of transient receptor potential channels of ankyrin type-1 and melastatin type-8. J. Pharmacol. Exp. Ther. *325*, 1007–1015.

Pierau, F.-K., Torrey, P., and Carpenter, D.O. (1974). Mammalian cold receptor afferents: role of an electrogenic sodium pump in sensory transduction. Brain Res. *73*, 156–160.

Pozsgai, G., Hajna, Z., Bagoly, T., Boros, M., Kemény, Á., Materazzi, S., Nassini, R., Helyes, Z., Szolcsányi, J., and Pintér, E. (2012). The role of transient receptor potential ankyrin 1 (TRPA1) receptor activation in hydrogen-sulphide-induced CGRP-release and vasodilation. Eur. J. Pharmacol. *689*, 56–64.

Prager-Khoutorsky, M., Khoutorsky, A., and Bourque, C.W. (2014). Unique Interweaved Microtubule Scaffold Mediates Osmosensory Transduction via Physical Interaction with TRPV1. Neuron *83*, 866–878.

Prescott, E.D., and Julius, D. (2003). A modular PIP2 binding site as a determinant of capsaicin receptor sensitivity. Science *300*, 1284–1288.

Price, M.P., McIlwrath, S.L., Xie, J., Cheng, C., Qiao, J., Tarr, D.E., Sluka, K.A., Brennan, T.J., Lewin, G.R., and Welsh, M.J. (2001). The DRASIC Cation Channel Contributes to the Detection of Cutaneous Touch and Acid Stimuli in Mice. Neuron *32*, 1071–1083.

Puttfarcken, P.S., Han, P., Joshi, S.K., Neelands, T.R., Gauvin, D.M., Baker, S.J., Lewis, L.G.R., Bianchi, B.R., Mikusa, J.P., Koenig, J.R., et al. (2010). A-995662 [(R)-8-(4-methyl-5-(4-(trifluoromethyl)phenyl)oxazol-2-ylamino)-1,2,3,4-tetrahydronaphthalen-2-ol], a novel, selective TRPV1 receptor antagonist, reduces spinal release of glutamate and CGRP in a rat knee joint pain model. Pain *150*, 319–326.

Quick, K., Zhao, J., Eijkelkamp, N., Linley, J.E., Rugiero, F., Cox, J.J., Raouf, R., Gringhuis, M., Sexton, J.E., Abramowitz, J., et al. (2012). TRPC3 and TRPC6 are essential for normal mechanotransduction in subsets of sensory neurons and cochlear hair cells. Open Biol. *2*.

Reid, G., and Flonta, M.-L. (2001a). Cold transduction by inhibition of a background potassium conductance in rat primary sensory neurones. Neurosci. Lett. *297*, 171–174.

Reid, G., and Flonta, M.-L. (2001b). Physiology: Cold current in thermoreceptive neurons. Nature *413*, 480–480.

Robertson, B., and Bevan, S. (1991). Properties of 5-hydroxytryptamine3 receptor-gated currents in adult rat dorsal root ganglion neurones. Br. J. Pharmacol. *102*, 272–276.

Rohacs, T. (2007). Regulation of TRP channels by PIP2. Pflüg. Arch. - Eur. J. Physiol. *453*, 753–762.

Rohacs, T. (2009). Phosphoinositide regulation of non-canonical Transient Receptor Potential channels. Cell Calcium *45*, 554–565.

Rohacs, T. (2013). Regulation of transient receptor potential channels by the phospholipase C pathway. Adv. Biol. Regul. *53*, 341–355.

Rohács, T., Lopes, C.M.B., Michailidis, I., and Logothetis, D.E. (2005). PI(4,5)P2 regulates the activation and desensitization of TRPM8 channels through the TRP domain. Nat. Neurosci. *8*, 626–634.

Romanovsky, A.A., Almeida, M.C., Garami, A., Steiner, A.A., Norman, M.H., Morrison, S.F., Nakamura, K., Burmeister, J.J., and Nucci, T.B. (2009). The transient receptor potential vanilloid-1 channel in thermoregulation: a thermosensor it is not. Pharmacol. Rev. *61*, 228–261.

De Rooij, J., Zwartkruis, F.J.T., Verheijen, M.H.G., Cool, R.H., Nijman, S.M.B., Wittinghofer, A., and Bos, J.L. (1998). Epac is a Rap1 guanine-nucleotide-exchange factor directly activated by cyclic AMP. Nature *396*, 474–477.

Roza, C., Puel, J.-L., Kress, M., Baron, A., Diochot, S., Lazdunski, M., and Waldmann, R. (2004). Knockout of the ASIC2 channel in mice does not impair cutaneous mechanosensation, visceral mechanonociception and hearing. J. Physiol. *558*, 659–669.

Rüegg, U.T., and Burgess, G.M. (1989). Staurosporine, K-252 and UCN-01: potent but nonspecific inhibitors of protein kinases. Trends Pharmacol. Sci. *10*, 218–220.

Runnels, L.W., Yue, L., and Clapham, D.E. (2001). TRP-PLIK, a bifunctional protein with kinase and ion channel activities. Science *291*, 1043–1047.

Runnels, L.W., Yue, L., and Clapham, D.E. (2002). The TRPM7 channel is inactivated by PIP(2) hydrolysis. Nat. Cell Biol. *4*, 329–336.

Saria, A., Gamse, R., Petermann, J., Fischer, J.A., Theodorsson-Norheim, E., and Lundberg, J.M. (1986). Simultaneous release of several tachykinins and calcitonin gene-related peptide from rat spinal cord slices. Neurosci. Lett. *63*, 310–314.

Sato, K., Kiyama, H., Park, H.T., and Tohyama, M. (1993). AMPA, KA and NMDA receptors are expressed in the rat DRG neurones. Neuroreport *4*, 1263–1265.

Schaible, H.G. (2007). Peripheral and central mechanisms of pain generation. Handb. Exp. Pharmacol. 3–28.

Schlingmann, K.P., Weber, S., Peters, M., Niemann Nejsum, L., Vitzthum, H., Klingel, K., Kratz, M., Haddad, E., Ristoff, E., Dinour, D., et al. (2002). Hypomagnesemia with secondary hypocalcemia is caused by mutations in TRPM6, a new member of the TRPM gene family. Nat. Genet. *31*, 166–170.

Schmidt, M., Evellin, S., Weernink, P.A., von Dorp, F., Rehmann, H., Lomasney, J.W., and Jakobs, K.H. (2001). A new phospholipase-C-calcium signalling pathway mediated by cyclic AMP and a Rap GTPase. Nat. Cell Biol. *3*, 1020–1024.

Schnorr, S., Eberhardt, M., Kistner, K., Rajab, H., Käßer, J., Hess, A., Reeh, P., Ludwig, A., and Herrmann, S. (2014). HCN2 channels account for mechanical (but not heat) hyperalgesia during long-standing inflammation. Pain *155*, 1079–1090.

Semmo, M., Köttgen, M., and Hofherr, A. (2014). The TRPP Subfamily and Polycystin-1 Proteins. In Mammalian Transient Receptor Potential (TRP) Cation Channels, B. Nilius, and V. Flockerzi, eds. (Springer Berlin Heidelberg), pp. 675–711.

Sexton, J.E., Vernon, J., and Wood, J.N. (2014). TRPs and Pain. In Mammalian Transient Receptor Potential (TRP) Cation Channels, B. Nilius, and V. Flockerzi, eds. (Springer International Publishing), pp. 873–897.

Sharif-Naeini, R., Ciura, S., Zhang, Z., and Bourque, C.W. (2008). Contribution of TRPV channels to osmosensory transduction, thirst, and vasopressin release. Kidney Int. *73*, 811–815.

Shen, W.L., Kwon, Y., Adegbola, A.A., Luo, J., Chess, A., and Montell, C. (2011). Function of Rhodopsin in Temperature Discrimination in Drosophila. Science *331*, 1333–1336.

Shibasaki, K., Murayama, N., Ono, K., Ishizaki, Y., and Tominaga, M. (2010). TRPV2 Enhances Axon Outgrowth through Its Activation by Membrane Stretch in Developing Sensory and Motor Neurons. J. Neurosci. *30*, 4601–4612.

Sidi, S., Friedrich, R.W., and Nicolson, T. (2003). NompC TRP channel required for vertebrate sensory hair cell mechanotransduction. Science *301*, 96–99.

Sikand, P., and Premkumar, L.S. (2007). Potentiation of glutamatergic synaptic transmission by protein kinase C-mediated sensitization of TRPV1 at the first sensory synapse. J. Physiol. *581*, 631–647.

Six, D.A., and Dennis, E.A. (2000). The expanding superfamily of phospholipase A2 enzymes: classification and characterization. Biochim. Biophys. Acta BBA - Mol. Cell Biol. Lipids *1488*, 1–19.

Smith, G.D., Gunthorpe, M.J., Kelsell, R.E., Hayes, P.D., Reilly, P., Facer, P., Wright, J.E., Jerman, J.C., Walhin, J.-P., Ooi, L., et al. (2002). TRPV3 is a temperature-sensitive vanilloid receptor-like protein. Nature *418*, 186–190.

Smith, N.J., Hone, A.J., Memon, T., Bossi, S., Smith, T.E., McIntosh, J.M., Olivera, B.M., and Teichert, R.W. (2013). Comparative functional expression of nAChR subtypes in rodent DRG neurons. Front. Cell. Neurosci. *7*.

Snider, W.D., and McMahon, S.B. (1998). Tackling Pain at the Source: New Ideas about Nociceptors. Neuron *20*, 629–632.

Spitzer, M.J.S., Reeh, P.W., and Sauer, S.K. (2008). Mechanisms of potassium- and capsaicin-induced axonal calcitonin gene-related peptide release: involvement of L- and T-type calcium channels and TRPV1 but not sodium channels. Neuroscience *151*, 836–842.

Squire, L., Berg, D., Bloom, F.E., Lac, S. du, Ghosh, A., Squire, L.R., Spitzer, N.C., McConnell, S.K., Roberts, J.L., and Zigmond, M.J. (2002). Fundamental Neuroscience (Academic Press).

Staaf, S., Franck, M.C.M., Marmigère, F., Mattsson, J.P., and Ernfors, P. (2010). Dynamic expression of the TRPM subgroup of ion channels in developing mouse sensory neurons. Gene Expr. Patterns *10*, 65–74.

Steen, K.H., and Reeh, P.W. (1993). Actions of cholinergic agonists and antagonists on sensory nerve endings in rat skin, in vitro. J. Neurophysiol. *70*, 397–405.

Stein, C., and Machelska, H. (2011). Modulation of Peripheral Sensory Neurons by the Immune System: Implications for Pain Therapy. Pharmacol. Rev. *63*, 860–881.

Stein, C., Schäfer, M., and Machelska, H. (2003). Attacking pain at its source: new perspectives on opioids. Nat. Med. *9*, 1003–1008.

Story, G.M., Peier, A.M., Reeve, A.J., Eid, S.R., Mosbacher, J., Hricik, T.R., Earley, T.J., Hergarden, A.C., Andersson, D.A., Hwang, S.W., et al. (2003a). ANKTM1, a TRP-like channel expressed in nociceptive neurons, is activated by cold temperatures. Cell *112*, 819–829.

Story, G.M., Peier, A.M., Reeve, A.J., Eid, S.R., Mosbacher, J., Hricik, T.R., Earley, T.J., Hergarden, A.C., Andersson, D.A., Hwang, S.W., et al. (2003b). ANKTM1, a TRP-like channel expressed in nociceptive neurons, is activated by cold temperatures. Cell *112*, 819–829.

Straub, I., Mohr, F., Stab, J., Konrad, M., Philipp, S., Oberwinkler, J., and Schaefer, M. (2013a). Citrus fruit and fabacea secondary metabolites potently and selectively block TRPM3. Br. J. Pharmacol. *168*, 1835–1850.

Straub, I., Krügel, U., Mohr, F., Teichert, J., Rizun, O., Konrad, M., Oberwinkler, J., and Schaefer, M. (2013b). Flavanones That Selectively Inhibit TRPM3 Attenuate Thermal Nociception In Vivo. Mol. Pharmacol. *84*, 736–750.

Suto, K., and Gotoh, H. (1999). Calcium signaling in cold cells studied in cultured dorsal root ganglion neurons. Neuroscience *92*, 1131–1135.

Szolcsányi, J. (1977). A pharmacological approach to elucidation of the role of different nerve fibres and receptor endings in mediation of pain. J. Physiol. (Paris) *73*, 251–259.

Takahashi, N., Kozai, D., and Mori, Y. (2012). TRP channels: sensors and transducers of gasotransmitter signals. Membr. Physiol. Membr. Biophys. *3*, 324.

Takashima, Y., Daniels, R.L., Knowlton, W., Teng, J., Liman, E.R., and McKemy, D.D. (2007). Diversity in the Neural Circuitry of Cold Sensing Revealed by Genetic Axonal Labeling of Transient Receptor Potential Melastatin 8 Neurons. J. Neurosci. *27*, 14147–14157.

Taylor, A.C., McCarthy, J.J., and Stocker, S.D. (2008). Mice Lacking the Transient Receptor Vanilloid Potential 1 (TRPV1) Channel Display Normal Thirst Responses and Central Fos Activation to Hypernatremia. Am. J. Physiol. - Regul. Integr. Comp. Physiol.

Taylor-Clark, T.E., Undem, B.J., MacGlashan, D.W., Ghatta, S., Carr, M.J., and McAlexander, M.A. (2008a). Prostaglandin-Induced Activation of Nociceptive Neurons via Direct Interaction with Transient Receptor Potential A1 (TRPA1). Mol. Pharmacol. *73*, 274–281.

Taylor-Clark, T.E., McAlexander, M.A., Nassenstein, C., Sheardown, S.A., Wilson, S., Thornton, J., Carr, M.J., and Undem, B.J. (2008b). Relative contributions of TRPA1 and TRPV1 channels in the activation of vagal bronchopulmonary C-fibres by the endogenous autacoid 4-oxononenal. J. Physiol. *586*, 3447–3459.

Tominaga, M. (2007). The Role of TRP Channels in Thermosensation. In TRP Ion Channel Function in Sensory Transduction and Cellular Signaling Cascades, W.B. Liedtke, and S. Heller, eds. (Boca Raton (FL): CRC Press),.

Tominaga, M., Caterina, M.J., Malmberg, A.B., Rosen, T.A., Gilbert, H., Skinner, K., Raumann, B.E., Basbaum, A.I., and Julius, D. (1998). The cloned capsaicin receptor integrates multiple pain-producing stimuli. Neuron *21*, 531–543.

Trevisani, M., Siemens, J., Materazzi, S., Bautista, D.M., Nassini, R., Campi, B., Imamachi, N., Andrè, E., Patacchini, R., Cottrell, G.S., et al. (2007). 4-Hydroxynonenal, an endogenous aldehyde, causes pain and neurogenic inflammation through activation of the irritant receptor TRPA1. Proc. Natl. Acad. Sci. U. S. A. *104*, 13519–13524.

Tsavaler, L., Shapero, M.H., Morkowski, S., and Laus, R. (2001). Trp-p8, a novel prostate-specific gene, is up-regulated in prostate cancer and other malignancies and shares high homology with transient receptor potential calcium channel proteins. Cancer Res. *61*, 3760–3769.

Tsuruda, P.R., Julius, D., and Minor, D.L. (2006). Coiled coils direct assembly of a cold-activated TRP channel. Neuron *51*, 201–212.

Turu, G., and Hunyady, L. (2010). Signal transduction of the CB1 cannabinoid receptor. J. Mol. Endocrinol. *44*, 75–85.

Ufret-Vincenty, C.A., Klein, R.M., Hua, L., Angueyra, J., and Gordon, S.E. (2011). Localization of the PIP2 sensor of TRPV1 ion channels. J. Biol. Chem. *286*, 9688–9698.

Vandewauw, I., Owsianik, G., and Voets, T. (2013). Systematic and quantitative mRNA expression analysis of TRP channel genes at the single trigeminal and dorsal root ganglion level in mouse. BMC Neurosci. *14*, 21.

Viana, F., de la Peña, E., and Belmonte, C. (2002). Specificity of cold thermotransduction is determined by differential ionic channel expression. Nat. Neurosci. *5*, 254–260.

Volkers, L., Mechioukhi, Y., and Coste, B. (2014). Piezo channels: from structure to function. Pflüg. Arch. - Eur. J. Physiol. 1–5.

Vriens, J., Watanabe, H., Janssens, A., Droogmans, G., Voets, T., and Nilius, B. (2004). Cell swelling, heat, and chemical agonists use distinct pathways for the activation of the cation channel TRPV4. Proc. Natl. Acad. Sci. U. S. A. *101*, 396–401.

Vriens, J., Owsianik, G., Hofmann, T., Philipp, S.E., Stab, J., Chen, X., Benoit, M., Xue, F., Janssens, A., Kerselaers, S., et al. (2011). TRPM3 Is a Nociceptor Channel Involved in the Detection of Noxious Heat. Neuron *70*, 482–494.

Vriens, J., Nilius, B., and Voets, T. (2014a). Peripheral thermosensation in mammals. Nat. Rev. Neurosci. *15*, 573–589.

Vriens, J., Held, K., Janssens, A., Tóth, B.I., Kerselaers, S., Nilius, B., Vennekens, R., and Voets, T. (2014b). Opening of an alternative ion permeation pathway in a nociceptor TRP channel. Nat. Chem. Biol. *10*, 188–195.

Wagner, T.F.J., Loch, S., Lambert, S., Straub, I., Mannebach, S., Mathar, I., Düfer, M., Lis, A., Flockerzi, V., Philipp, S.E., et al. (2008). Transient receptor potential M3 channels are ionotropic steroid receptors in pancreatic β cells. Nat. Cell Biol. *10*, 1421–1430.

Wagner, T.F.J., Drews, A., Loch, S., Mohr, F., Philipp, S.E., Lambert, S., and Oberwinkler, J. (2010). TRPM3 channels provide a regulated influx pathway for zinc in pancreatic beta cells. Pflüg. Arch. Eur. J. Physiol. *460*, 755–765.

Walker, R.G., Willingham, A.T., and Zuker, C.S. (2000). A Drosophila mechanosensory transduction channel. Science *287*, 2229–2234.

Wall, P.D. (1967). The laminar organization of dorsal horn and effects of descending impulses. J. Physiol. *188*, 403–423.

Wang, H., and Woolf, C.J. (2005). Pain TRPs. Neuron *46*, 9–12.

Wang, W., Zhang, X., Gao, Q., and Xu, H. (2014). TRPML1: An Ion Channel in the Lysosome. In Mammalian Transient Receptor Potential (TRP) Cation Channels, B. Nilius, and V. Flockerzi, eds. (Springer Berlin Heidelberg), pp. 631–645.

Watanabe, H., Vriens, J., Suh, S.H., Benham, C.D., Droogmans, G., and Nilius, B. (2002). Heat-evoked Activation of TRPV4 Channels in a HEK293 Cell Expression System and in Native Mouse Aorta Endothelial Cells. J. Biol. Chem. *277*, 47044–47051.

Watanabe, H., Vriens, J., Prenen, J., Droogmans, G., Voets, T., and Nilius, B. (2003). Anandamide and arachidonic acid use epoxyeicosatrienoic acids to activate TRPV4 channels. Nature *424*, 434–438.

Weibel, R., Reiss, D., Karchewski, L., Gardon, O., Matifas, A., Filliol, D., Becker, J.A.J., Wood, J.N., Kieffer, B.L., and Gaveriaux-Ruff, C. (2013). Mu opioid receptors on primary afferent nav1.8 neurons contribute to opiate-induced analgesia: insight from conditional knockout mice. PloS One *8*, e74706.

Weller, K., Reeh, P.W., and Sauer, S.K. (2011). TRPV1, TRPA1, and CB1 in the isolated vagus nerve – Axonal chemosensitivity and control of neuropeptide release. Neuropeptides *45*, 391–400.

Wes, P.D., Chevesich, J., Jeromin, A., Rosenberg, C., Stetten, G., and Montell, C. (1995). TRPC1, a human homolog of a Drosophila store-operated channel. Proc. Natl. Acad. Sci. U. S. A. *92*, 9652–9656.

Willcockson, H., and Valtschanoff, J. (2008). AMPA and NMDA glutamate receptors are found in both peptidergic and non-peptidergic primary afferent neurons in the rat. Cell Tissue Res. *334*, 17–23.

Wilsher, N.E., Court, W.J., Ruddle, R., Newbatt, Y.M., Aherne, W., Sheldrake, P.W., Jones, N.P., Katan, M., Eccles, S.A., and Raynaud, F.I. (2007). The Phosphoinositide-Specific Phospholipase C Inhibitor U73122 (1-(6-((17β-3-Methoxyestra-1,3,5(10)-trien-17-yl)amino)hexyl)-1H-pyrrole-2,5-dione) Spontaneously Forms Conjugates with Common Components of Cell Culture Medium. Drug Metab. Dispos. *35*, 1017–1022.

Woo, S.-H., Ranade, S., Weyer, A.D., Dubin, A.E., Baba, Y., Qiu, Z., Petrus, M., Miyamoto, T., Reddy, K., Lumpkin, E.A., et al. (2014). Piezo2 is required for Merkel-cell mechanotransduction. Nature *509*, 622–626.

Wood, J.N., and Docherty, R. (1997). Chemical activators of sensory neurons. Annu. Rev. Physiol. *59*, 457–482.

Woodbury, C.J., Zwick, M., Wang, S., Lawson, J.J., Caterina, M.J., Koltzenburg, M., Albers, K.M., Koerber, H.R., and Davis, B.M. (2004). Nociceptors lacking TRPV1 and TRPV2 have normal heat responses. J. Neurosci. Off. J. Soc. Neurosci. *24*, 6410–6415.

Woolf, C.J., and Ma, Q. (2007). Nociceptors--noxious stimulus detectors. Neuron *55*, 353–364.

Wrigley, P.J., Jeong, H.-J., and Vaughan, C.W. (2009). Primary afferents with TRPM8 and TRPA1 profiles target distinct subpopulations of rat superficial dorsal horn neurones. Br. J. Pharmacol. *157*, 371–380.

Xiao, B., Coste, B., Mathur, J., and Patapoutian, A. (2011). Temperature-dependent STIM1 activation induces Ca2+ influx and modulates gene expression. Nat. Chem. Biol. *7*, 351–358.

Xiao, R., Tang, J., Wang, C., Colton, C.K., Tian, J., and Zhu, M.X. (2008). Calcium plays a central role in the sensitization of TRPV3 channel to repetitive stimulations. J. Biol. Chem. *283*, 6162–6174.

Xu, H., Ramsey, I.S., Kotecha, S.A., Moran, M.M., Chong, J.A., Lawson, D., Ge, P., Lilly, J., Silos-Santiago, I., Xie, Y., et al. (2002). TRPV3 is a calcium-permeable temperature-sensitive cation channel. Nature *418*, 181–186.

Xu, H., Zhao, H., Tian, W., Yoshida, K., Roullet, J.-B., and Cohen, D.M. (2003). Regulation of a Transient Receptor Potential (TRP) Channel by Tyrosine Phosphorylation SRC FAMILY KINASE-DEPENDENT TYROSINE PHOSPHORYLATION OF TRPV4 ON TYR-253 MEDIATES ITS RESPONSE TO HYPOTONIC STRESS. J. Biol. Chem. *278*, 11520–11527.

Xu, S.-Z., Zeng, F., Boulay, G., Grimm, C., Harteneck, C., and Beech, D.J. (2005). Block of TRPC5 channels by 2-aminoethoxydiphenyl borate: a differential, extracellular and voltage-dependent effect. Br. J. Pharmacol. *145*, 405–414.

Yamamoto, M., Chen, M.Z., Wang, Y.-J., Sun, H.-Q., Wei, Y., Martinez, M., and Yin, H.L. (2006). Hypertonic stress increases phosphatidylinositol 4,5-bisphosphate levels by activating PIP5KIbeta. J. Biol. Chem. *281*, 32630–32638.

Yan, J.-Y., Sun, R.-Q., Hughes, M.G., McAdoo, D.J., and Willis, W.D. (2006). Intradermal injection of capsaicin induces acute substance P release from rat spinal cord dorsal horn. Neurosci. Lett. *410*, 183–186.

Yang, X.-R., Lin, M.-J., McIntosh, L.S., and Sham, J.S.K. (2006). Functional expression of transient receptor potential melastatin- and vanilloid-related channels in pulmonary arterial and aortic smooth muscle. Am. J. Physiol. - Lung Cell. Mol. Physiol. *290*, L1267–L1276.

Yano, H., Wershil, B.K., Arizono, N., and Galli, S.J. (1989). Substance P-induced augmentation of cutaneous vascular permeability and granulocyte infiltration in mice is mast cell dependent. J. Clin. Invest. *84*, 1276–1286.

Yao, J., and Qin, F. (2009). Interaction with Phosphoinositides Confers Adaptation onto the TRPV1 Pain Receptor. PLoS Biol *7*, e1000046.

Yu, L.-C., Hansson, P., and Lundeberg, T. (1994). The calcitonin gene-related peptide antagonist CGRP8–37 increases the latency to withdrawal responses in rats. Brain Res. *653*, 223–230.

Zamudio-Bulcock, P.A., Everett, J., Harteneck, C., and Valenzuela, C.F. (2011). Activation of steroid-sensitive TRPM3 channels potentiates glutamatergic transmission at cerebellar Purkinje neurons from developing rats. J. Neurochem. *119*, 474–485.

Zhang, Z., and Bourque, C.W. (2003). Osmometry in osmosensory neurons. Nat. Neurosci. *6*, 1021–1022.

Zhang, L., Hoff, A.O., Wimalawansa, S.J., Cote, G.J., Gagel, R.F., and Westlund, K.N. (2001). Arthritic calcitonin/α calcitonin gene-related peptide knockout mice have reduced nociceptive hypersensitivity. PAINÂ® *89*, 265–273.

Zhang, X., Mak, S., Li, L., Parra, A., Denlinger, B., Belmonte, C., and McNaughton, P.A. (2012). Direct inhibition of the cold-activated TRPM8 ion channel by Gαq. Nat. Cell Biol. *14*, 851–858.

Zhang, X.-F., Chen, J., Faltynek, C.R., Moreland, R.B., and Neelands, T.R. (2008). Transient receptor potential A1 mediates an osmotically activated ion channel. Eur. J. Neurosci. *27*, 605–611.

Zhang, Y., Hoon, M.A., Chandrashekar, J., Mueller, K.L., Cook, B., Wu, D., Zuker, C.S., and Ryba, N.J.P. (2003). Coding of sweet, bitter, and umami tastes: Different receptor cells sharing similar signaling pathways. Cell *112*, 293–301.

Zhang, Z., Okawa, H., Wang, Y., and Liman, E.R. (2005). Phosphatidylinositol 4,5-bisphosphate rescues TRPM4 channels from desensitization. J. Biol. Chem. *280*, 39185–39192.

Zhang, Z., Kindrat, A.N., Sharif-Naeini, R., and Bourque, C.W. (2007). Actin Filaments Mediate Mechanical Gating during Osmosensory Transduction in Rat Supraoptic Nucleus Neurons. J. Neurosci. *27*, 4008–4013.

Zhu, J.X., Wu, X.Y., Owyang, C., and Li, Y. (2001). Intestinal serotonin acts as a paracrine substance to mediate vagal signal transmission evoked by luminal factors in the rat. J. Physiol. *530*, 431–442.

Zimmermann, K., Lennerz, J.K., Hein, A., Link, A.S., Kaczmarek, J.S., Delling, M., Uysal, S., Pfeifer, J.D., Riccio, A., and Clapham, D.E. (2011). Transient receptor potential cation channel, subfamily C, member 5 (TRPC5) is a cold-transducer in the peripheral nervous system. Proc. Natl. Acad. Sci. U. S. A. *108*, 18114–18119.

Zygmunt, P.M., and Högestätt, E.D. (2014). TRPA1. In Mammalian Transient Receptor Potential (TRP) Cation Channels, B. Nilius, and V. Flockerzi, eds. (Springer Berlin Heidelberg), pp. 583–630.

Zygmunt, P.M., Petersson, J., Andersson, D.A., Chuang, H., Sørgård, M., Di Marzo, V., Julius, D., and Högestätt, E.D. (1999). Vanilloid receptors on sensory nerves mediate the vasodilator action of anandamide. Nature *400*, 452–457.

Zygmunt, P.M., Andersson, D.A., and Hogestatt, E.D. (2002). Delta 9-tetrahydrocannabinol and cannabinol activate capsaicin-sensitive sensory nerves via a CB1 and CB2 cannabinoid receptor-independent mechanism. J. Neurosci. Off. J. Soc. Neurosci. *22*, 4720–4727.

Zygmunt, P.M., Ermund, A., Movahed, P., Andersson, D.A., Simonsen, C., Jönsson, B.A.G., Blomgren, A., Birnir, B., Bevan, S., Eschalier, A., et al. (2013). Monoacylglycerols activate TRPV1--a link between phospholipase C and TRPV1. PloS One *8*, e81618.